Pharmacological modelling to investigate antimalarial drug treatment

Thesis submitted in accordance with the requirements of the University of Liverpool for the degree of Doctor of Philosophy

by

Katherine Kay

July, 2013

Contents

Abstract

Malaria remains a major public health concern for billions of people worldwide. Achieving the ambitious goal of malaria eradication requires co-ordination of control strategies dealing with a range of parasite, vector, human, social and environmental factors. Availability of effective antimalarial treatment is a key component in malaria control. However the number of drugs available is limited and drug resistance, particularly in *Plasmodium falciparum*, has now been reported for all currently available antimalarials. Mathematical models provide the opportunity to explore key features underlying antimalarial drug action, effectiveness and resistance. They further allow investigation into questions that cannot otherwise be easily addressed, either because they are too expensive, unethical or logistically too complex. This thesis aims to develop pharmacological models to investigate antimalarial drug treatment.

In Chapter 2 we develop a pharmacokinetic-pharmacodynamic (PK/PD) model of antimalarial drug treatment (calibrated using published data) and use it to investigate the efficacy of artemisinin combination therapies (ACTs).

Chapter 3 addresses two assumptions built into the methodology that limit the models future application. The model now allows for (i) time lags and drug concentration profiles for drugs absorbed across the gut wall and, if necessary, converted to another active form (ii) multiple drugs within a treatment regimen (iii) differing modes of drug action in combinations (iv) modelling drugs converted to an active metabolite with similar modes of action.

In Chapter 4 we extend the methodology to allow for i) the presence of more than one clone when treatment begins (ii) the acquisition of new clones during treatment follow-up (iii) the tracking of individual clones using molecular markers. We then use

these extensions to simulate clinical trial data to determine the best methods of analysis.

Chapter 5 details how the drug action components of the extended PK/PD model were incorporated into OpenMalaria; a mathematical model of malaria epidemiology allowing investigation of the effects of various intervention strategies including malaria vaccines, vector control strategies and antimalarial drug treatment.

In Chapter 6 we investigate the ability of clinical trials to accurately estimate (WoS) using the extended PK/PD model. Windows of selection (WoS) are often used to quantify the genetic process whereby parasites evolve increasing tolerance to antimalarial drugs.

We noted a conspicuous lack of comprehensive, good-quality PK datasets currently available in the literature. Despite this, the models produced results highly consistent with field data. They were applied to investigate the potential implications of drug resistance and to make predications about the future effectiveness of antimalarials. We emphasise the value of mathematical models by simulating 'field data' to assess the best methods of analysing clinical trials and to investigate the predictive ability of WoS. While we do not suggest models can replace the information gained in clinical trials, this work does demonstrate the importance of mathematical models capable of generating results consistent with field data.

Publications

The content of one chapter of this thesis has already been published in a scientific journal

Chapter 2: Winter, K., and I. M. Hastings. 2011. Development, evaluation and application of an *in silico* model for antimalarial drug treatment failure. Antimicrob Agents 55:3380-3392.

A modified version of Chapter 3 has been published

Chapter 3: Kay, K., and I. M. Hastings. 2013. Predicting the impact of artemisinin resistance on antimalarial drug effectiveness. PLoS Comput Biol. 9:e1003151

I generated the data (details in Chapter 4) and wrote the appendix for a second published manuscript, the paper can be found in the Appendix to Chapter 4

Chapter 4: Jaki, T., A. Parry, K. Winter, and I. Hastings. 2012. Analysing malaria drug trials on a per-individual or per-clone basis: a comparison of methods. Stat Med:doi: 10.1002/sim.5706.

I also contributed as a minor author to the poster presented at the Challenges in Malaria Meeting (Basel, Switzerland)

Chapter *7*: Staehli Hodel, E., K. Kay, D. Hayes, A. Terlouw, and I. Hastings. 2012. An *in silico* drug treatment model to assess the robustness of regional age-based dosing regimens for artemisinin-based combination therapies. Malar J 11:P91

Due to the editorial difference of scientific journals, the chapter's structure and language varies slightly.

Contributors Statement

In accordance with the University of Liverpool's rules on PhD these, I hereby present the contributions to all chapters:

Chapter 1. K Kay wrote the introduction and I Hastings supervised the writing.

Chapter 2. K Kay wrote the model, analysed the results, wrote the first draft of the paper and adapted the paper to a thesis chapter. I Hastings supervised the analysis and the writing. Three anonymous referees contributed suggestions to improve the manuscript.

Chapter 3. K Kay wrote the model, analysed the results, wrote the first draft of the paper and adapted the paper to a thesis chapter. I Hastings supervised the analysis and the writing.

Chapter 4. K Kay wrote the model, simulated the data, wrote the first draft of the paper's appendix, adapted the appendix to a thesis chapter and contributed to editing the manuscript. A Parry and T Jaki analysed the data and wrote the first draft of the manuscript. I Hastings supervised the analysis and the writing of the paper and Chapter.

Chapter 5. K Kay implemented the methodology (described in Chapters 2 and 3) and wrote the Chapter. I Hastings supervised the implementation and writing. The model structure was originally written by T Antao and subsequently edited by D Hardy.

Chapter 6. K Kay wrote the model, analysed the results, wrote the first draft of the paper and adapted the paper to a thesis chapter. I Hastings supervised the analysis and the writing.

Chapter 7. K Kay wrote the discussion and I Hastings supervised the writing.

Presentations and conferences

Oral Presentations

10/2012	Challenges in Malaria, Basel, Switzerland
07/2012	Technical Advisory Group (TAG) Meeting, Swiss Tropical Institute, Basel, Switzerland
08/2011	TAG Meeting, Swiss Tropical Institute, Basel, Switzerland
06/2010	TAG Meeting, Swiss Tropical Institute, Basel, Switzerland
07/2010	Molecular and Biochemical Parasitology Group Meeting, Liverpool School of Tropical Medicine, UK
06/2009	TAG Meeting, Swiss Tropical Institute, Basel, Switzerland

Poster Presentations

11/2012	American Society of Tropical Medicine and Hygiene (ASTMH), Atlanta, USA
10/2012	Challenges in Malaria, Basel, Switzerland
04/2012	British Society for Parasitology Conference, Glasgow, UK
05/2011	Postgraduate Research Day, Liverpool School of Tropical Medicine, UK
03/2011	Postgraduate Research Day, University of Liverpool, UK
05/2010	Postgraduate Research Day, Liverpool School of Tropical Medicine, UK

Conferences Attended

11/2012	American Society of Tropical Medicine and Hygiene (ASTMH), Atlanta, USA
10/2012	Challenges in Malaria, Basel, Switzerland
04/2012	British Society for Parasitology Conference, Edinburgh, UK
04/2010	British Society for Parasitology Conference, Cardiff, UK
11/2009	Multilateral Initiative on Malaria (MIM) Conference, Nairobi, Kenya
04/2009	British Society for Parasitology Conference, Glasgow, UK

Acknowledgements

I have been overwhelmed by the support I have received from my supervisors, colleagues, friends and family while completing this PhD. I would like to begin with a special thank you to my supervisor, Ian Hastings. I cannot express how much I appreciate the patient guidance, support and encouragement you have provided. To my co-supervisor, Anja Terlouw, thank you for all your valuable help and advice over the years. There are numerous staff and students based both here at the Liverpool School of Tropical Medicine and at the Swiss Tropical and Public Health Institute who I would like to thank for their friendly help and support throughout. I would particularly like to thank Mary Creegan for her continual assistance with all administrative tasks. Thank you to Tiago Antao for patiently helping me negotiate the daunting world of computer programming and for always being available to answer questions. This work was supported by the Bill and Melinda Gates Foundation, grant 37999.01.

To my friends, I want to say a huge thank you for always being there. Your enthusiastic support and endless cups of coffee have helped keep me going. I am especially gratefully to my parents for their support throughout all my studies at University and the countless times they helped move my vast collection of "stuff" across most of Liverpool and Preston. Finally, I want to thank my husband, Chris, your endless encouragement, support and love have made this possible.

Abbreviations

ACT	Artemisinin combination therapies
AIDS	Acquired immunodeficiency syndrome
ANC	Antenatal care
AQ	Amodiaquine
AR	Artemether
ARC3	Artemisinin Resistance Confirmation, Characterisation and Containment project
ARDS	Acute respiratory distress syndrome
AS	Artesunate
BMGF	Bill and Melinda Gates Foundation
CL	Clearance (drug)
CQ	Chloroquine
DDT	Dichlorodiphenyltrichloroethane
DHA	Dihydroartemisinin
dhfr	Dihydrofolate reductase gene
dhps	Dihydropteroate synthase gene
F	Absorption rate
FSaT	Focussed Screen and Treat
GMAP	Global malaria action program
GMEP	Global Malaria Eradication Program
GPARC	Global Plan for Artemisinin Resistance Containment
GSK	GlaxoSmithKline
GUI	Graphic User Interface
HIV	Human Immunodeficiency Virus
IPT	Intermittent preventive treatment
IPTc	Intermittent preventive treatment for children
IPTi	Intermittent preventive treatment for infants

IPTp	Intermittent preventive treatment for pregnant women
IRS	Indoor residual spraying
ITN	Insecticide treated net
LF	Lumefantrine
LLIN	Long-lasting insecticide treated net
MVM	Malaria vaccine model
MSAT	Mass screen and treat
MQ	Mefloquine
PATH MVI	Program for appropriate technology in health malaria vaccine initiative
PD	Pharmacodynamics
pfcrt	*Plasmodium falciparum* chloroquine resistance transporter gene
PfCRT	*Plasmodium falciparum* chloroquine resistance transporter protein
pfcyt b	*Plasmodium falciparum* cytochrome b gene
pfdhfr	*Plasmodium falciparum* dihydrofolate reductase gene
pfdhps	*Plasmodium falciparum* dihydropteroate synthase gene
pfmdr1	*Plasmodium falciparum* multidrug resistance 1 gene
pfnhe-1	*Plasmodium falciparum* Na^+/H^+ exchanger gene
PK	Pharmacokinetics
PQ	Piperaquine
QN	Quinine
RBM	Roll back malaria partnership
RDT	Rapid diagnostic test
ROC	Receiver operating curve
RTS,S	Malaria vaccine candidate
SCM	Seasonal Malaria Chemoprevention
SP	Sulfadoxine-pyrimethamine
Vd	Volume of distribution
WHO	World Health Organisation
x	Absorption rate constant
XML	Extensible Markup Language

Chapter 1

Introduction

1. Malaria

1.1. The disease and its treatment

Malaria is a devastating tropical disease transmitted by certain species of *Anopheles* mosquitoes. It presents a major public health concern for an estimated 3.3 billion people across 106 malaria endemic countries (395). With the burden of disease concentrated in sub-Saharan Africa (accounting for approximately 81% of cases and 91% of deaths) it claims more human lives each year than any other infectious disease except AIDS and tuberculosis (372). The World Malaria report, published in 2011, states that in 2010 there were an estimated 216 million cases of malaria and an estimated 655,000 deaths (395). The groups most at risk include children under five (86% of deaths occurring globally) and pregnant women.

Malaria in humans is caused by one of five species of *Plasmodium* parasites (*P.falciparum*, *P.vivax*, *P.ovale* (including two sub-species *P.ovale curtisi* and *P.ovale wallikeri*), *P.malariae* and *P.knowlesi*) of which *P.falciparum* is generally regarded as the most deadly. However it is important to note that the general perception that infections by *P.vivax* are 'benign' is changing and the significant risk posed by *P.vivax* recognised (20, 21, 217, 266). The natural life cycle of the malaria parasite requires infection of two successive hosts, humans and the *Anopheles* mosquito. The female mosquito ingests the malaria parasites while taking a blood

meal from an infected host. The parasites develop from gametocytes to sporozoites in the intestines and midgut of the mosquito. The sporozoites then migrate to the mosquito salivary glands where they are passed back to a human host during the mosquito's next blood meal. Once in the human, parasites travel via the blood to the liver where they replicate and mature, eventually releasing merozoites into the blood. These merozoites invade the erythrocytes and undergo asexual replication; ring stage trophozoites mature into schizonts that eventually rupture the red blood cell and release more merozoites. This asexual cycle continues with merozoites periodically released into the blood stream and it is these blood stage parasites that are responsible for the clinical manifestations of the disease. Occasionally, the merozoites differentiate into gametocytes (the sexual erythrocytic stage) and it is these gametocytes that are taken up by the mosquito during a blood meal, perpetuating the malaria life cycle.

Malaria infections result in a wide variety of symptoms with disease severity ranging from absent or very mild symptoms to severe disease. Early symptoms typically include fever, headache and vomiting with onset usually occuring 10-15 days after the mosquito bite. Because flu-like symptoms of any origin are often mistaken for early malaria infections this can lead to an over-diagnosis of the disease. However, a significant delay in treatment (particularly in *P.falciparum* infections) is likely to be fatal and so prompt treatment with an effective antimalarial is crucial. Therefore, WHO recommends to presumptively treat suspected malaria cases (particularly in children) (379), however this can lead to overuse of antimalarial drugs. Infections are typically classified as either uncomplicated or severe (complicated). Severe malaria occurs most commonly if uncomplicated infections are not promptly treated or in patients with little to no immunity. Low immunity levels characteristically occur in people living in areas of low or no malaria transmission and/or in young children and pregnant women. The clinical manifestations of severe infections can include cerebral malaria (coma), severe anaemia due to haemolysis (destruction of the red blood cells), hypoglycaemia, acute renal failure, acute pulmonary oedema (fluid build up in the lungs) or acute respiratory distress syndrome (ARDS) (380).

Clinical diagnosis of malaria, based on symptoms alone, is known to be inaccurate resulting in over-diagnosis of malaria incidence and hence over-administration of

antimalarials (187, 194, 246). For example, Nwanyanwu *et al.* (246) have shown malaria diagnosis based on clinical signs and symptoms over-estimates malaria cases; of the 248 of adult males with a reported fever (in Malawi, 1994), only 15% of the fevers were due to malaria yet 22% of patients received antimalarials. The WHO now recommends that every suspected cause of malaria be confirmed first by either using a rapid diagnostic test (RDT) or by microscopy (380). This improves upon the previous assumption that all fever cases in malaria endemic countries are due to malaria (and presumptively treated). It allows patients deemed to be parasite-negative to be correctly diagnosed and treated while avoiding unnecessary use of antimalarials thereby reducing patient side-effects, drug-interactions and selection pressure for drug resistance (395). Positive diagnosis should be followed by prompt treatment with an effective antimalarial (380); a step crucial to both patient survival and malaria control. Despite the obvious benefits, confirmation of parasitaemia is not always feasible in resource poor settings, usually due to a lack of functioning microscopes or RDTs.

1.2. Antimalarial drug resistance

1.2.1. Definition

The WHO originally defined 'antimalarial drug resistance' in 1967 as "the ability of a parasite strain to survive or multiply despite the administration and absorption of a drug given in doses equal to or higher than those usually recommended but within the tolerance of the subject" (369). This was modified in 1986 to include the sentence: "the form of the drug active against the parasite must be able to gain access to the parasite or the infected erythrocyte for the duration of the time necessary for its normal action" (45). However, given the mechanism of action of the artemisinin parent drugs and their active metabolite this definition may require further discussion and clarification (378).

1.2.2. Origins of drug resistance

To date, drug resistance has been documented in three of the five malaria species infecting humans, namely *P.falciparum, P.vivax* and *P.malariae* (378) (note only *P.falciparum* drug resistance will be discussed here). Many factors contribute to the development and spread of drug resistance. It is usually the result of complex interactions between the drug-deployment pattern, drug characteristics (including the drug pharmacokinetics (PK), dosing regimen and cross-resistance), parasite characteristics (including genetic mutations and transmission level), human host factors (such as immunity) and vector and environmental factors (133, 157, 222, 302, 354, 366). Resistance is encoded by genetic mutations in, or changes to the number of copies of genes that determine the drug's target or that affect pumps regulating the concentration of drug within the parasite (378). This may be the result of a single genetic change (for example, atovaquone resistance is the result of a single mutation in the cytochrome *b* gene) or multiple independent changes (342). The latter is more common for drug resistance in malaria (131), for example, the acquisition of sulfadoxine-pyrimethamine (SP) resistance in *P.falciparum* is the result of an accumulation of sequential mutations in the *dhfr* (dihydrofolate reductase) gene (163, 186). The evolution of resistance is arguably a two-stage process in which mutations encoding drug resistance are preceded by those encoding drug tolerance (131). Increased drug tolerance allows parasites to persist in the presence of sub-therapeutic drug levels (as opposed to resistant parasites that can persist despite therapeutic drug levels) and given the frequency with which antimalarials are used in malaria endemic areas, a large proportion of the population have residual drug levels resulting from previous treatments (141, 142, 325). This results in a strong selection pressure, which drives tolerant parasites through the population (352). Resistance is complicated by cross-resistance occurring among drugs that belong to the same chemical family or have similar modes of action (157, 378).

1.2.3 Measuring Drug Resistance

Clinical treatment failures and/or increased parasite clearance times for *P.falciparum*, resulting from confirmed *in vivo* parasite resistance, have now been documented for

all current antimalarials including early evidence of resistance to the most recent class of drugs, the artemisinins (22, 52, 151, 152, 195). Susceptibility of *P.falciparum* to antimalarials can be determined in one of four ways.

i. Clinical Trials

Therapeutic efficacy studies are generally considered the gold standard capable of detecting subtle differences in treatment outcomes. They allow measurement of clinical and parasitological efficacy and are the primary reference for ministries of health in updating treatment strategies and policies. WHO (387) originally defined the therapeutic response in terms of sensitivity and resistance (with three levels of resistance); in 2001 this was updated and based on clinical outcomes defined as either adequate clinical response, early treatment failure or late treatment failure (34). These studies provide a good indication as to drug efficacy, but additional studies are required to confirm and characterise the genetic basis of drug resistance (378).

ii. *In vitro* assays

Changes in the *P.falciparum* phenotype are determined using *in vitro* assays; parasites are exposed to a precise drug concentration and the inhibition of intrinsic growth or schizont maturation (25, 33, 34) measured. However, this method removes the effects of host factors such as PK and immunity.

iii. Molecular markers

It is also important that the genetic changes associated with resistance are identified. The use of molecular markers to detect early treatment failures in malaria was suggested by Wellems & Plowe (353) and most recently implemented by the WHO (386). To date there are currently only six genes known (or suspected) to be associated with drug resistance in *P.falciparum*

⇒ dihydrofolate reductase (*pfdhfr*) (29, 104, 106, 155, 156)

Point mutations in the *pfdhfr* gene confer resistance to pyrimethamine in a step-wise manner with resistance levels increasing as mutations accumulate (beginning with Ser108Asn then either Asn51Ile or Cys59Arg and Ile164Leu) (28, 157) while the double mutation Ser108Thr and Ala16Val

appear to be associated with cycloguanil (the active metabolite of proguanil) resistance (26, 156).

⇒ dihydropteroate synthase (*pfdhps*) (18, 30, 93, 204)

Resistance to sulfadoxine has been associated with five point mutations of the *pfdhps* gene. Resistance begins with the Ala437Gly and Lys540Glu mutations and increases with the Ser436Ala/Phe, Ala581Gly and Ala613Thr/Ser mutations (156)

⇒ chloroquine (CQ) resistance transporter (*pfcrt*) (91)

The *pfcrt* gene is a key gene associated with CQ resistance beginning when lysine is replaced at codon 76 with threonine (103, 378). This change is associated with different sets of mutations at different codons, including Cys72Ser, Met74Ile, Asn75Glu, Ala220Ser, Gln271Glu, Asn326Ser, Ile356Thr and Arg371Ile although the specific changes depend on the geographic setting (378). Combinations of artesunate-amodiaquine (AS-AQ) appear to select for mutant forms of *pfcrt* in field isolates (76) (thereby increasing CQ resistance) while artemether-lumefantrine (AR-LF) selects for the wild-type *pfcrt* (confirmed *in vitro* (306)). Mutations in *pfcrt* have also been shown to affect the dose-responses of mefloquine, halofantrine and artemisinin (42, 187). A review of the functional and evolutionary basis of the *pfcrt* resistance gene can be found in Cooper *et al*. (69) and Ecker *et al.* (91).

⇒ multidrug resistance 1 gene (*pfmdr1*) (encoding P-glycoprotein homolog 1; Pgh1 proteins) (150, 165, 166, 169, 188, 219)

The specific role of *pfmdr1* in the CQ response is unclear (69), however, mutations of interest include Asn86Tyr, Tyr184Phe, Ser1034Cys, Asn1042Asp and Asp1246Tyr (378). Linkage disequilibrium between the Lys76Thr mutation on the *pfcrt* gene and the Asp86Tyr mutation on the *pfmdr1* gene has been observed in field studies (378). The interactions between *pfcrt* and *pfmdr1* alleles result in varying levels of CQ and AQ with *pfmdr1* mutations appearing to modulate drug effect (273, 282). Mutations in *pfmdr1* have also been associated with resistance to the amino-alcohols (i.e. mefloquine (MQ), halofantrine (HF), lumefantrine (LF) and quinine (QN)) and the artemisinins (302, 346, 378, 390). Increases in *pfmdr1* copy number were found to be responsible for MQ resistance in

the Cambodia-Thailand region alongside an increased risk of treatment failures following AR-LF and AS-MQ therapies (note that a four-dose regimen was used in these studies) (165, 169). Field studies have shown the wild-type Asn86 allele is a potential marker for reduced LF susceptibility with repeated AR-LF treatments appearing to select for the allele in recurrent infections (51, 74, 192). Amplification of the *pfmdr1* gene *in vitro* has also been associated with small but significant reductions in parasite sensitivity which could explain the cross-resistance between amino-alcohols and artemisinins *in vitro* (54, 267) Reductions in *pfmdr1* copy number and gene mutations were found to reduce sensitivity to MQ, QN, HF and the artemisinins *in vitro* (150, 188).

⇒ Na^+/H^+ exchanger (*pfnhe-1*)

It is difficult to demonstrate resistance to QN and like CQ it is influence by mutations in several genes (*pfcrt*, *pfmdr1* and *pfnhe-1*) (93). While studies of laboratory strains and field isolates indicate a number of mutations which maybe associated with decreased parasite susceptibility to QN (5, 84, 158). Further studies are needed (378).

⇒ cytochrome *b* (*pfcyt b*) (32, 177, 227)

Resistance to atovaquone is linked to a single mutation at position 268 in the *cyt b* gene, most frequently Tyr268Ser but also Tyr268Asn or Tyr268Cys (32, 177, 227)

Research into the genes responsible for artemisinin resistance is ongoing. Recent studies have shown drug response maybe associated with the ABC transporters, for example, Anderson *et al.* (8) observed an association between ABC transporter G7 and AS. As yet however, there is no conclusive evidence supporting this theory

iv. Pharmacokinetic (PK) studies

Clinical PK studies are performed to understand the relationship between drug dosage regimens and the drugs concentration time profiles. They provide crucial information about the absorption, distribution, metabolism and elimination of a drug within the body. PK studies are conducted throughout drug development with different aims. Studies performed during the early stages of drug development typically include healthy volunteers and are conducted under controlled conditions

to determine the safety and PK of a drug. During the later stages of drug development and after a drug has been approved, PK studies are conducted in patients who have the target disease (in this case malaria) to investigate patient PK profiles. They show the relationship between drug dosage and concentrations in the blood, and between drug concentrations in the blood and therapeutic effects. PK studies can also be used to further investigate the influence of factors such as age, gender, body weight, genetic factors, severity of disease, complications, meals, and concomitant drugs.

1.2.4. History of drug use and resistance

QN, extracted from the bark of the cinchona tree, was the first and only known antimalarial agent at the beginning of the 19th century. Today, QN is a highly effective antimalarial (including against CQ-resistant malaria) but the high frequency of adverse effects has inevitably lead to poor patient compliance so, QN is generally reserved for the treatment of severe malaria (19, 154). However, since the development of artemisinins the use of QN in cases of severe malaria is now often replaced with artemisinin monotherapy (380). Possibly as a result of it's limited use, resistance to quinine has been slow to emerge and only reported sporadically in parts of South East Asia and South America (14, 215, 220).

Introduced in 1934, chloroquine quickly became one of the most successful drugs deployed against malaria and the drug of choice in the Global Malaria Eradication Program (GMAP) launched by WHO in 1955 (373). CQ is characterised by its rapid efficacy, low toxicity and affordability (91, 353). It accumulates in the parasite food vacuole and works by inhibiting heme polymerisation (324). Although GMAP was discontinued in 1969 the widespread use of CQ throughout the program lead to the emergence and spread of CQ resistance worldwide. Resistance is associated with copy number changes and point mutations in the genes encoding the parasite *PfCRT* protein (for a review see (29, 56, 214)) and *pfmdr1* (although the specific role of *pfmdr1* is unclear (69)). The mutated form of *PfCRT* is able to reduce CQ accumulation in the digestive vacuole. Despite the global presence of CQ-resistant

P.falciparum, it has been suggested that CQ-resistance is the result of at least six independent emergences (91). Beginning in Colombia (223) and the Cambodia-Thailand border (124) during the late 1950s, resistance spread steadily throughout the 1960s and 1970s to South America, Southeast Asia and India eventually reaching Africa in the late 1970s (91, 258). However, it is highly probable that CQ-resistant parasites incur a fitness cost when compared to the wild-type sensitive parasites. An *in vitro* study by Hayward *et al.* (137) used transfected *P.falciparum* strains (described in Reed *et al*. (271)) to demonstrate that in the absence of drug pressure, parasites with the *pfmdr1* mutation (associated with enhanced CQ resistance) incur a 25% fitness cost relative to the wild-type parasites. Epidemiological studies have similarly shown that, in the absence of drug pressure, it is possible for parasite sensitivity to be recovered. For example, in a region of Malawi known for highly prevalent CQ-resistance, drug-sensitive parasites repopulated the region approximately ten years after CQ treatment was stopped (184). Hastings & Donnelly (127) estimated the fitness effect in Malawi as 5%. Similar CQ recovery has subsequently been observed in parasite in Kenya (229), Vietnam (152, 238, 334) and China (190, 349).

SP was gradually introduced in the 1960s (33) as an effective, affordable, well tolerated and easy to administer (388) single-dose replacement (second-line) for CQ-resistant malaria. It's a drug combination that acts synergistically to inhibit folate synthesis in the parasite (by targeting the dihydropteroate synthase (*dhps*) and dihydrofolate reductase (*dhfr*) enzymes). Resistance to SP developed rapidly in South East Asia (84, 153) but remained low in Africa until the 1990s (247) when resistance was imported from South East Asia. In recent years resistance has developed and been reported in Africa, Asia, Indonesia and South America (14, 60, 96, 106, 142, 144, 199) prompting concern about the potential public health impact (35, 164, 228), particularly given their role in IPT (see below).

MQ was developed in the 1970s and emerged as the successor to CQ in the 1980s. It is a synthetic analogue of QN and like CQ, it is believed to target the digestive vacuole and heme polymerisation (324, 340). First introduced as a monotherapy in Thailand in 1977, MQ is now primarily administered in combination with AS (379, 380). Resistance to MQ appeared soon after its introduction and in the late 1980s and

was reported along the Thai-Cambodian and Thai-Myanmar (Thai-Burmese) borders (297, 367), marking the emergence of multidrug resistant *P.falciparum* (defined as resistance to three or more classes of antimalarial drugs (366)). Despite this early emergence of resistance, reports of MQ resistance in other areas are sporadic. Case-reports suggest some MQ resistance from the Amazon Basin (366) but the level of resistance in South America is far below that in South East Asia. Similarly, *in vitro* studies suggest the presence of *P.falciparum* strains with low MQ sensitivity in Africa (43, 160). The rapid emergence of MQ resistance along the Thai-Cambodian and Thai-Myanmar borders is possibly due to the previously widespread use of the structurally related antimalarial quinine (366).

Lumefantrine (LF), originally known as benflumetol, was originally synthesised by the Chinese Academy of Military Medical Sciences in the 1970s. As with CQ and MQ, LF works within the parasite food vacuole where it is thought to interfere with the haem polymerisation process (358). LF has rarely been used as a monotherapy outside China and there is almost no published data on the *in vivo* efficacy of the monotherapy. Instead it was administered through the late 1980s in combination with AR. In 1990, the Chinese government and Novartis (then Ciba-Geigy) launched a joint venture to manufacture the AR-LF combination (under the name Coartem®). This combination was registered as an antimalarial in the early-2000s and was adopted as a first line treatment for uncomplicated malaria by many African countries throughout the mid-2000s. Early studies of drug efficacy indicated the use of AR-LF selected quickly for LF-tolerant parasites (125, 192) leading to concern about its therapeutic lifespan, particularly in high transmission areas (130). It is approximately seven years since the first emergences of LF-tolerance and the phenotype has now been confirmed in other areas (for a review see (248)). However, it is important to note that despite earlier concerns of emerging drug tolerance, the combination of AR-LF is still effective and resistance has not yet been observed.

Piperaquine (PQ) was originally synthesised in France (then called compound 13228 RP) in the 1950's but it was not until 1966, when the Shanghi Research Institute of Pharmacological Industry began work on the drug (56) that's it potential as an antimalarial was realised. In 1978, it replaced CQ as the first-line monotherapy for malaria treatment throughout China. Despite decades of clinical use the exact

mechanism of action for PQ is unknown but given its close structural resemblance to CQ it is assumed they are assumed to have similar modes of action (328). However, PQ remains effective against CQ-resistant isolates (27) indicating the despite their structural similarities, resistance is controlled by different mechanisms (90). As with all drugs, the potential development of PQ resistance is concerning although to date reports of PQ resistance both in the field (98, 396) and *in vitro* (90) are limited.

Artemisinin was originally isolated from the sweet woodworm plant *Artemisia annua* in the 1970s (219) and it, or its semi-synthetic derivatives, including AS, AR and DHA (an *in vivo* active metabolite of AS and AR), are the most recent class of antimalarials and a main constitute of current first-line therapies in 84 countries (i.e. ACTs) (395). With the broadest parasite stage specificity, the artemisinins are highly potent against both the erythrocytic stages and the early stage gametocytes (332) resulting in the fastest drug killing rate (measured as parasite reduction ratio (360)) of the currently available antimalarials. However, while the artemisinins produce a swift and powerful antimalarial effect (including against multidrug resistant strains of *P.falciparum*) they are rapidly eliminated from the body and so recrudescence can be a particular problem. This is usually overcome by combining the artemisinins with a longer-lasting partner drug (with a different mode of action) (379, 380) thus maximising their effectiveness and protecting them against the development of resistance. Alternatively, the duration of the monotherapy has been extended in some countries (39, 208) but use of artemisinin monotherapies are strongly discouraged (295, 391, 393). If used as a monotherapy, a full 7-day treatment course is required to completely eliminate the parasite. However, the rapid parasite clearance and hence resolution of symptoms associated with the artemisinins inevitably results in poor patient compliance with few patients taking the full 7-days required to produce adequate cure rates. One of the most important features of the ACTs is their potential ability to delay the spread of resistance, particularly to the partner drug. For example, wide-scale use of AS plus MQ decreased the rate MQ resistance spread in northwest Thailand (243). The reason for this is two-fold, first the use two drugs (with different modes of action) prevents further selection for resistance while the presence of an artemisinin (in this case AS) results in higher cure rates (24). ACTs typically decrease the transmission advantage of the resistant parasites over sensitive parasites by

reducing the gametocyte carriage ratio from 4:1 (resistant: sensitive) for monotherapies to a ratio of 1:1 for ACTs (265).

Given its widespread use as a first-line treatment, emerging (or the potential emergence of) artemisinin resistance to ACTs threatens global control and elimination strategies. Resistance to the artemisinins first became a concern in 2005 with the four most affected countries including Cambodia, Thailand, Viet Nam and Myanmar. The first confirmed cases of artemisinin resistance were reported (in late 2006) in western Cambodia, along the Cambodia-Thailand border (241) leading to the development of the Artemisinin Resistance Confirmation, Characterisation and Containment project (ARC3) (funded by the BMGF) in early 2007. To date, incidences of artemisinin resistance (matching WHO's working definition of drug resistance (45)) have been confirmed in western Cambodia (Pailin and Tasanh) (22, 52, 151, 152, 195) and western Thailand (Wang Pha/Mae Sot) (260) while resistance is suspected in Myanmar, Viet Nam and along the Myanmar-China border (150) and changes in parasite clearance rates noted on the Kenyan coast (38). To date, artemisinin resistance has manifested through delayed clearance times (52, 151, 196) and while still clinically effective, a molecular marker for artemisinin resistance is yet to be identified and so it is unclear whether the drug resistant-parasites identified most recently in western Thailand have emerged independently, or have spread from western Cambodia. In 2010, WHO embarked on the development of the Global Plan for Artemisinin Resistance Containment (GPARC). Launched in 2011, GPARC called for urgent action to protect the efficacy of ACTs, contain artemisinin resistance in existing 'hotspots' and to stop its spread around the world (377).

1.2.5. Current status of drug treatment

There are a limited number of antimalarials available for effective chemotherapy; currently these include the 4-aminoquinolines (CQ, AQ), the arylaminoalcohols (MQ, halofantrine, LF), antifolates (SP), atovaquone and artemisinin and its derivatives (AS, AR, DHA). Of these, most target the pathogenic blood stages (77) responsible for patients symptoms. The only drugs found to be effective at reducing gametocyte carriage include primaquine (298) and the artemisinins (42, 319). Several classes of

antibiotic have been shown to exert antimalarial effects (74) but their relatively slow activity makes them unsuitable for chemotherapy. Despite this some antibiotics, particularly doxycycline, are used for antimalarial prophylaxis (30, 249). Since 2001 WHO has recommended treating uncomplicated malaria infections with combinations of two or more unrelated drugs (379), preferably artemisinin combination therapies (ACTs). The ACTs including a fast-acting artemisinin derivative and a slower acting partner drug with five ACT combinations currently recommended for treatment of *P.falciparum*: AR-LF, AS-AQ, AS-MQ, AS-SP and DHA-PQ (380). The specific drug choice for first- and second-line antimalarial therapy is made at a country level and is based not only on the efficacy of the drugs against the parasite (which should be monitored at least once every two years, as recommended in the WHO standard protocol) but also the cost and availability of the drugs within each country (378). By the end of 2010 the national policies of 84 countries included an ACT as the first-line treatment with AR-LF accounting for approximately 70% of the ACTs in the public sector (395).

2. Epidemiology and control of malaria (excluding drugs)

2.1. Control strategies

Antimalarial drugs are just one of the many methods currently employed in the bid to combat malaria. While the drugs are primarily used to treat patients with an existing infection they also affect malaria transmission by reducing the population of infected hosts. It is therefore impossible to examine drug resistance isolated from the general context of malaria control and so I here present a brief summary of the current control measures. Given the complexity of malaria epidemiology, which varies even over small distances, it is difficult to develop a universal malaria control policy that is appropriate to all situations in all countries. Instead, a range of control strategies are typically employed with specific control program details determined at a national and sub-national level with the aim to achieving the basic elements of the Global Malaria Control Strategy (GMAP) (375): (i) providing effective antimalarials to those infected with malaria (ii) implementing sustainable and effective preventative measures to

avert or detect and contain epidemics in high-risk areas (iii) strengthening of local research and development.

Vector control is an effective preventative measure designed to reduce malaria morbidity and mortality through the reduction of vector transmission. It includes a range of strategies including indoor residual spraying (IRS), insecticide treated nets (ITN), larval control and/or environmental control. By far the most extensively used are the long-lasting insecticide treated nets (LLINs) and IRS (395) both working to reduce the human-vector contact by reducing the lifespan of the female mosquitoes. The protection provided by ITNs (including LLINs) is two-fold affording both personal protection to the individual sleeping under the net (by preventing mosquito contact) and a wider community level protection through the reduction of the vector population (the mosquito is killed upon contact with the net) and hence a reduction in transmission intensity of the targeted area. IRS involves spraying a residual insecticide on to the interior walls of buildings, where many species of Anopheles mosquitoes rest following a blood meal (381). Again it is an effective way of controlling malaria transmission in the targeted area thus reducing the local burden of morbidity and mortality. Both IRS and ITNs require high coverage levels to be achieved for effective control, IRS for example requires >80% of houses in the target area to be sprayed if it is to be an effective control measure (383). Note, there are currently four classes of insecticides available for IRS including pyrethroids, organochlorides, organophosphates and carbonates but only one class of insecticide (the pyrethroids) available for ITNs. The largest threat to vector control is insecticide resistance, particularly to pyrethroids, but the scope of this problem lies outside the remit of this thesis.

Intermittent preventive treatment (IPT) is a public health intervention aimed at treating and preventing malaria episodes in the most at risk groups i.e. infants (IPTi), children (ITPc) and pregnant women (IPTp). It involves administering an single dose of a long-acting, effective antimalarial at predefined times to a specific at risk population, regardless of the individuals infectious status (51). Initially recommended by WHO (389) for pregnant women in 1998 (390) because of its safety and efficacy during pregnancy, IPTp is administered under supervision at antenatal care (ANC) twice during pregnancy (390) as part of national control policies in 35 high-burden

countries in sub-Saharan Africa and Papua New Guinea (395). It has been shown to be highly efficacious (compared to a placebo or CQ prophylaxis) at reducing the risk of placental infection, low birth weights and/or severe maternal anaemia (1, 32, 97, 99, 149, 159, 172, 208). Since 2009, WHO has also recommended IPTi with SP in countries with moderate to high malaria transmission (382, 394). The delivery of IPTi occurs alongside routine childhood vaccinations (57, 156, 182) and its efficacy rates in the prevention of malaria episodes (33, 67, 103, 121, 126, 136, 183) range from 22.6% (202) to 63.2% (290). However, despite its positive impact no country has yet adopted it as a national policy (395). Most recently IPT has been extended to children with studies in Senegal (using AS-SP; (65)), Mali (SP; (79)), Ghana (AS-AQ or SP; (179)) and Kenya (AQ-SP; (66)) demonstrating the protective efficacy of IPTc. This approach of chemoprevention has been extended to programs such as Focussed Screen and Treat (FSaT) or Seasonal Malaria Chemoprevention (SCM). For example, FSaT is a variation of mass screen and treat (MSAT) in which all individuals in a population are tested and, if necessary, treated for malaria. However, FSaT focuses on a much smaller geographic area, such as a household, village or hotspot.

A malaria vaccine, deployed alongside current control methods, could play a crucial role in the future control and eventual elimination of malaria (205). Vaccines have historically contributed to a reduction in the spread and burden of infectious diseases and have played a major part in elimination programs (for example smallpox and the ongoing polio and measles campaigns (102, 370, 376)). Research towards this end is ongoing for malaria but despite the potential health benefits, there is currently no licensed vaccine. The progress and life cycle stages of *P.falciparum* currently being targeted by vaccine development programs were recently reviewed by Crompton *et al.* (71). The most clinically advanced malaria vaccine candidate to date is RTS,S; originally synthesised by GlaxoSmithKline (GSK) in 1987, it has since been developed by GSK Biological and PATH MVI, with funding from the BMGF (since 2001). RTS,S is currently at least 5-10 years ahead of approximately 20 other potential vaccines in either phase 1 or 2 of clinical trials under development (395) and entered phase 3 clinical trials in 2009 (347). Targeting the pre-erythrocytic phases of *P.falciparum*, RTS,S is a fusion protein consisting of a malaria antigen with hepatitis B surface antigen, and includes a new potent adjuvant (to boost the immune system response) (323). By definition the pre-erythrocytic vaccines target either the

sporozoites stage that are inoculated by the mosquito, or the liver stage that immediately follows and aims to trigger the immune system to prevent infections (85, 170, 209). These stages are particularly attractive as vaccine targets because parasite numbers are still low (274), infections are asymptomatic and they provide a relatively large window of opportunity for an effective immune response (approximately 6 days for *P.falciparum*) (118). Initial results from the phase 3 clinical trials of RTS,S are positive with the RTS,S/AS01 vaccine reducing the number of clinical malaria episodes by approximately half during the first 12 months following vaccination (338). This is consistent with the results seen in children and infants during phase 2 trials.

2.2. Current Status of malaria control

Malaria specific mortality rates have fallen by 25% and the estimated incidence of malaria by 17% globally between 2000 and 2010 (395). This considerable reduction follows the recent shift in malaria control targets to encompass the ultimate goal of malaria eradication (337). However elimination/eradication is not simple, programs must be implemented in a diverse range of epidemiological settings and deal with differences in parasite, vector, human, social and environmental factors (5). Malaria endemic-countries also contain some of the most operationally challenging areas typically with under-performing health services, insufficient financial, social and human resources and political instability. Current expert views on the likelihood and feasibility of malaria eradication vary and it is unclear what the future will hold. However, scaling up of current control strategies will further reduce the burden of disease while research and development of new antimalarials, insecticides, diagnostics and vaccines will assist in the eventual elimination of malaria.

3. Modelling malaria

3.1. Models of general malaria epidemiology

Mathematic models of malaria can be traced back to Ronald Ross; the first person to discover that the Anopheles mosquitoes transmits malaria. Throughout his life, Ross made many important contributions to the epidemiology of malaria though perhaps his greatest was the development of mathematical models for the study of malaria. In 1905, Ross developed a mathematical description of malaria transmission relating mosquito flight distances and initial densities to the changing mosquito densities that result from larval control measures (279). Further study of malaria in Mauritius resulted in his early models of malaria transmission (281), which were later developed to include a new differential equation model (191, 280). His work on mosquito density showed that to eradicate malaria mosquito densities needed to be driven below a particular threshold density or longevity rather than eradicated completely. This work provided a quantitative framework and justification that dominated the first 50 years of malaria control.

Despite the pioneering mathematical work conducted throughout his life, Ross's work was largely ignored until the 1950's when George Macdonald began to test Ross's theory with epidemiological (196) and entomological (197) field data. He extended the basic model to demonstrate the importance of vector control and interruption of transmission in malaria elimination (198, 200, 201). Throughout his career he placed particular emphasis on defining and measuring quantities relevant to malaria eradication, for example, the stability index (the expected number of human bites by a mosquito over its lifetime) (197) and the basic reproductive number (denoted R_0; the expected number of human cases that would arise from each human case in a population with no previous exposure to malaria and no malaria control) (198). Macdonald's analysis also helped explain how contact pesticides (such as DDT) worked by severely reducing the number of mosquitoes that would live long enough to survive sporogony and transmit malaria (199). These models were published around the same time as the World Health Organisation (WHO) launched the Global Malaria Eradication Program (GMEP). One of the aims of the GMEP was to use DDT

to target the adult *Anopheles* mosquito and so, unsurprising, Macdonald was recruited to the cause. His influence within GMEP is evidenced by his election to chair the committee that wrote the first technical report on malaria eradication (371).

By the 1970's it was clear that Macdonald's model could be greatly improved by adding explicit considerations of human immunity (215) and so, as part of the Garki project in Nigeria, Dietz and Molineaux developed a more sophisticated model (81). The model incorporated a number of novel concepts including the possibility of super-infection (previously explored mathematically (195, 348)) and considered the development of immunity (previously modelled by Bailey (18)). It had two primary objectives, the first, to explore the epidemiology of malaria and second, to predict the effects of specific control measures (including larvicide, adulticide and mass drug action), alone and in combination (49, 127, 190). The model provided significant advances to the work of previous models however, although it achieved its first aim reasonably well, it was unable to accurately reproduce the effect of control measures. Ultimately, the project encountered difficulties in accurately quantifying the input parameters and suffered from oversimplified assumptions (207), particularly those regarding the immunity of the patient and the biology of the mosquitoes (235). Despite the disappointingly poor predictive ability of the Garki model, the techniques used and ideas described within the project inspired much of the theoretical work throughout the 1980s.

In the years since the publication of the Garki project there have been many scientific and technological advancements that have driven, both directly and indirectly, the development of mathematical models. Foremost amongst these is the availability of high-speed computers which have made previously time-consuming calculations and simulations commonplace. The result of this has been a massive upsurge in malaria models over the last few decades, with extensions of the basic malaria models expanding to include:

- Compartmental models with dynamics similar to a viral infection (i.e. susceptible-infected-recovered-susceptible (SIRS)) (13, 14) that were later developed to allow for semi-immune individuals (58, 239, 240) within the population.

- The transmission dynamics (78) and epidemiology of serial infection and immunity to infection with multiple parasite "strains" (120, 123).
- The processes driving the acquisition of immunity (105)
- The full dynamics of super infection (13, 113, 210) assuming both an infinite (18) and finite number of genotypes (234).
- Heterogeneity of mosquito biting behaviour, survival, human demography, immunity development in humans and the within-host dynamics of the parasite (3, 54, 71, 76, 128, 133, 193, 194).
- The effects of mosquito biting behaviour on disease transmission (48, 53, 76).
- The seasonality of malaria transmission (14, 59, 146, 192, 214).
- The dynamics of mosquito and malaria transmission (289) including the effects of various control measures, for example zooprophylaxis (170, 288), genetically modified mosquitoes (36, 188), larvicides (119), ITNs (61, 169, 170, 186), combinations of ITNs with IRS (60), use of antimalarials (185, 250), IPTi (278) and vaccines (122, 123, 160).
- The blood-stage asexual cycle of parasites described in terms of changes to the proportion of infected erythrocytes, uninfected erythrocytes and merozoites (6, 145)
- Individual-based models, such as those by Smith *et al*. (309, 311) follow the course of infections within the human (4, 129, 137, 138, 179) and are based upon the within-host dynamics (80, 92, 213). These simulations allow for superinfection within individuals, where multiple infections develop and run their own course while interacting with each other through the immune system.
- Geospatial statistical models that use data from survey sites to produce transmission, prevalence or disease maps across broad geographical sites (113, 134, 135, 173) and the distribution of malaria vectors (62-64).
- Insecticide resistance, specifically pyrethroid resistance (74).
- Antimalarial drug resistance (see section 3.2.)

A review of the historical development of mathematical models of malaria epidemiology can be found in Mandal *et al.* (206).

3.2. Models of antimalarial drug resistance

Mathematical models of infectious diseases have helped underpin our understanding of disease transmission dynamics both within and between hosts and parasites and are typically classified as either deterministic or stochastic. Deterministic models assume that a system follows a fixed and defined set of rules with no random variation or noise; they consider only the average or mean behaviour of a system and assume the randomness has a negligible effect (384). In contrast, stochastic models assume this randomness is important and explicitly include it within the model system (384). While both modelling approaches provide valuable insights into disease dynamics the models described herein are deterministic. The natural variation in drug metabolism within humans and drug effect on parasites was included in the model parameters thereby allowing us to capture the complexities of the malaria parasite life cycle while modelling the effects of antimalarials and the potential evolution of drug resistance.

There are a large number of mathematical models investigating antimicrobial drug effects available in the published literature (Mideo *et al.* (218) review models of malaria pathogenesis). Models detailing the acquisition and spread of antimalarial drug resistance are numerous:

- Aneke (9) examined transmission of sensitive and resistant parasites assuming that if all treated individuals respond to treatment then there are no gametocytes and that all infective individuals become immediately symptomatic.
- Antao & Hastings (10) investigated how epistasis, inbreeding, selection heterogeneity and multiple simultaneous drug deployments interact to influence the spread of drug resistance.
- Antia *et al*. (11), model the within-host dynamics of an antigenically varying parasite and host immunity
- Bacaër & Sokhna (17) make the assumption that immune infected humans are not infectious and present a model focused on the diffusion of resistance due to mosquito mobility.
- Chiyaka *et al.* (62) describe the influence of treatment and drug resistant parasites on the transmission of malaria. Their model takes into account treated humans that might still be infectious to mosquitoes and partially immune humans who are

also infectious but have a low gametocyte count as compared to their non-immune counterparts.

- Dye & Williams (89) investigated the conditions under which out-crossing could delay the evolution of drug resistance and whether the conditions are met by know multigenic resistance mechanisms.
- Gupta & Hill (122) discuss the co-evolutionary consequences of heterogeneity in host resistance and diversity in parasite virulence. The model assumes host heterogeneity can be described by one locus with two alleles are coded as either resistance or sensitive
- Gupta *et al*. (121) model of malaria epidemiology concentrating on patterns of infection and strain selection
- Hastings (128) used parasite population genetics (with parasites coded as susceptible, tolerant or fully-resistant) to investigate the evolution of drug resistance.
- Koella & Anita (174) extended the basic Ross-Macdonald model to explore the consequences of changing the level of drug use on the frequency of resistant malaria parasites. They assumed those who acquired immunity were no longer infectious and the infectious population recovers into the immune class.
- Pongtavornpinyo *et al.* (262) develop a model combining malaria transmission with the evolution of drug resistance to investigate questions of treatment strategies in different transmission settings.
- White (355) – Study of within host dynamics with humans either treated with drugs or untreated

3.3. Pharmacological models of antimalarial drug resistance

3.3.1. Importance of PK/PD models

Czock & Keller (73) provide a comprehensive review "mechanism-based" PK/PD modelling of antimicrobial drugs, including their specific application to malaria.

3.3.2. Pharmacology

Pharmacology is the study of drugs including their origin, composition, properties, therapeutic use, and toxicology. It also includes the development of new drugs that are first tested *in vitro* for biochemical activity and then *in vivo* for safety, effectiveness, side effects and interactions with other drugs to find the best dosing regimens. The relationship between drug dose and effect can be separated into pharmacokinetic (dose-concentration) and pharmacodynamic (concentration-effect) components (Figure 1). Pharmacokinetics (PK) defines the fate of drugs in the body. It uses mathematics to quantify the time course (i.e. absorption, distribution, metabolism and elimination) of the drug and metabolite concentrations in the body. The time course of orally administered drugs can be described using the standard Michaelis-Menten equation with just a few basic PK parameters (figure 1A) including: bioavailability (F), absorption rate constant (x), clearance (CL) and volume of distribution (Vd). However there is large inter-individual variability in these PK parameters which can be the result of numerous factors including variations in how the patient absorbs the drug, how it is distributed, metabolised and finally eliminated from the body. These factors can be further affected by the patient's disease state (e.g. pregnancy or co-infections with either HIV/AIDS or TB etc.), physiological state (e.g. those at the extremes of age or weight) and/or via interactions with other drugs present. Pharmacodynamics (PD) defines the relationship between the drug concentration (at the site of action) and the time course of the resulting effect. In the context of this thesis it refers to the parasite's response to the administered drug (Figure 1B). The PD were based upon the Michaelis-Menten dynamics in which the population increased according to a parasite growth rate constant and decreased according to the drug dependent killing, determined from the Michaelis-Menten equation.

3.3.2. PK/PD modelling

Pharmacokinetic-pharmacodynamic (PK/PD) modelling combines a PK model component that describes the time course of drug in the plasma (Figure 1A) and a PD model component that relates the plasma concentration to the drug effect (Figure 1B)

A.

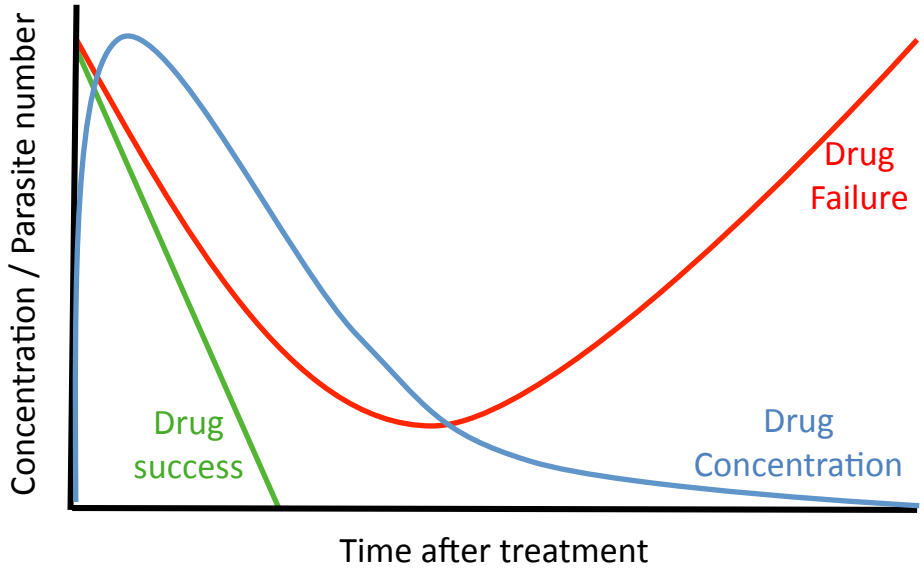

B.

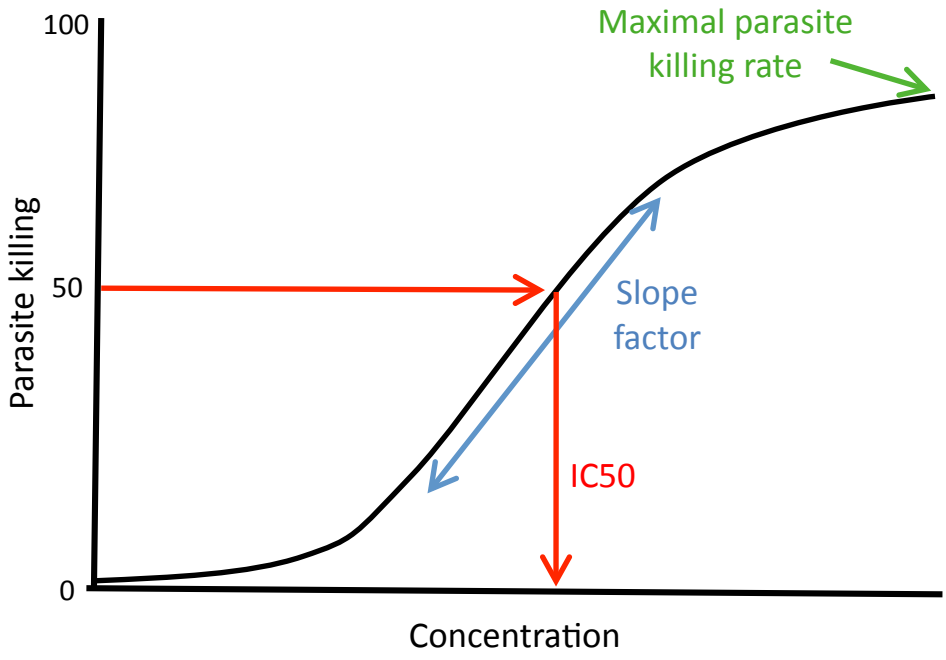

Figure 1. Pharmacokinetic-pharmacodynamic (PK/PD) modelling combines a PK model component that describes the time course of drug in the plasma (Graph A, blue line) and a PD model component that relates the plasma concentration to the drug effect (Graph B, black line) to determine the time course of drug effect after treatment. Antimalarials either successfully clear parasites (Graph A, green line) or initially reduce the parasite burden but do not fully clear the infection (Graph B, red line). Parasite pharmacodynamics are derived from the concentration-effect curve as shown in Graph B.

to determine the time course of drug effect after treatment. The models use differential equations to describe the dynamics of a parasite population in the presence of antimalarial drug treatment. Historically, PK/PD models have been used by

- Austin *et al.* (16) identify the optimal pattern of drug administration to clear an infection.
- Hoshen *et al.* (143) develop a stage-specific PK/PD model for AR including a period of drug-induced 'dormancy' during which the parasite's life cycle is temporarily suspended.
- Hoshen *et al.* (144) present a PK/PD model of CQ monotherapy designed to investigate whether CQ treatment could be improved in patients with different levels of immunity.
- Hoshen *et al.* (148) describe a PK/PD model designed to simulate the effect of AS and MQ combination therapy and match their simulated results to field data.
- Hoshen *et al*. (149) adapt the PK model developed in Hoshen *et al*. (144) to investigate the optimal dosing regimen of MQ monotherapy in different settings of transmission and immunity.
- Saralamba *et al*. (285) develop a intrahost PK/PD model describing the parasites stage-specific response to artesunate therapy to investigate the hypothesis that artemisinin resistance is the result of decreased ring-stage drug sensitivity.
- Simpson *et al.* (302) adapt the PK model developed in Hoshen *et al*. (144) to explore the development of resistance after the *de novo* use of 2 of the most widely used MQ doses.
- Zaloumis *et al*. (399) extend the stage-specific within host model developed by Saralamba *et al*. (285) to account for the action of two or more antimalarial treatments.

While clinical trials provide the gold standard method guiding drug deployment policies, PK/PD models conducted *in silico* have the potential to provide valuable insights into the effectiveness of drug treatments and thus guide policy decisions. Accurate simulations can, for example, rapidly investigate the consequences of varied drug deployment strategies to identify optimal dosage levels, frequency and duration. Moreover, they can be used to investigate real-life situations that cannot be ethically addressed in the field, for example the impact of poor patient compliance on

a treatment regimen, or to investigate situations which cannot be addressed until it is too late, an obvious example includes the consequences of developing drug tolerance / resistance and its subsequent spread through the population. However, despite decades of work modelling malaria the application of PK/PD models to investigate antimalarial drug treatment has been limited to the eight accounts describe above. To date the methods have largely been confined to the investigation of monotherapies with only two notable exceptions. First, Hoshen *et al.* (148) investigated the AS-MQ combination modelling the action of AR through the MQ Michaelis-Menten equation thus ignoring the specific action of the artemisinin and it's absorption, conversion and elimination phases (148). While Zaloumis *et al*. (399) describe a parasite stage-specific PK/PD model for antimalarial drugs and use it to investigate the optimal dosing regimen of combination therapies however where not able to reliably replicate the results of clinical trials. It should be noted that the Zaloumis *et al*. (399) paper was only recently published and so not considered while developing the model described in this thesis; the main methodological differences and model results are discussed further in Chapter 7. Given the widespread use of combination therapies and with the recent, massive shift towards using ACTs as first-line antimalarial therapy in malaria endemic countries, the inability of mathematical models to accurately predict treatment outcome severely reduces the value of such models. This thesis concentrates specifically on the development of PK/PD methodology to study the effectiveness of antimalarials, with particular focus on the evolution of drug resistance. Historically, drug resistance has been modelled assuming resistance is a dichotomous characteristic in which parasites are either fully sensitive or fully resistant to drugs (72, 89, 128). Here, resistance was modelled as a continuous process with parasite drug tolerance increasing progressively until parasites are no longer effected by the drug.

4. Aims of this thesis

The general aim of this thesis was to develop the basic pharmacokinetic-pharmacodynamic model for antimalarial drug treatment and to use this model to investigate key features of drug action and effectiveness.

The specific aims include

1. developing the methodology of the PK/PD model including model calibration and validation (Chapters 2 and 3)
2. simulate field data to optimise clinical trial analysis (Chapter 4 and 6)
3. implement the methodology into OpenMalaria (Chapter 5)

Chapter 2 details the development, calibration and validation of an *in silico* model of antimalarial drug treatment. This model was then extended to make results more compelling for specific ACTs (Chapter 3), address key questions about the analysis of field data (Chapter 4) and to allow for intravenous drug administration (Chapter 5). The drug action components of this PK-PD model were integrated into an open source C++ program (OpenMalaria) simulating malaria epidemiology and the impact of interventions (Chapter 5). Finally, the extended PK/PD model was used to investigate the ability of clinical trials to estimate windows of selection for antimalarial drugs (Chapter 6).

Chapter 2

Development, evaluation and application of an *in silico* model for antimalarial drug treatment and failure

ABSTRACT

Pharmacological 'mechanism based' modelling is refined and used to develop an *in silico* model of antimalarial drug treatment validated against clinical and field data. We used this approach to investigate key features of antimalarial drug action and effectiveness, with emphasis on the current generation of artemisinin combination therapies. We conclude: (i) The development of artemisinin tolerance and resistance will, unless checked, have an immediate, large impact on the protection afforded to its partner drug, and on likely clinical efficacy of artemisinin combination therapies. (ii) Long follow-up periods are required in clinical trials to detect all drug failures; follow-up periods of 28 days recommended by the World Health Organization are likely to miss at least 50% of drug failures and we confirm recent suggestions that 63 days would be a more appropriate follow-up period. (iii) Day seven serum drug concentrations are a significant risk factor of failure. Although, paradoxically, receiver operating characteristic curve analysis reveals their predictive power is relatively poor. (iv) The pharmacokinetic properties of the partner drugs in ACTs are the most important determinant of treatment outcome, particularly it's maximum killing rate. We discuss the assumptions made in such modelling approaches and how similar approaches may be refined in future work.

1. Introduction

Malaria remains an important public health problem in malaria endemic countries and prompt treatments with effective antimalarials is crucial to patient survival. Correctly dosing patients with malaria is however a constant problem and standard dosage regimens are usually based on information from adults with uncomplicated malaria. This neglects the differences seen in patient's age, weight, use of concomitant medication, genetic variation in pharmacokinetics especially in the groups most at risk (pregnant women, children and patients with severe malaria) and natural variation in parasite drug susceptibility. Furthermore, dosing regimens are determined during efficacy trials in which exact doses are calculated according to weight and taken under supervision, with strict adherence to dose timings. In real life, effectiveness is more important than efficacy. Drug effectiveness in the field is invariably less than the efficacy seen during trials for several reasons:

i. Drug regimens consisting of more than one dose are vulnerable to the effects of patient compliance. Some treatments such as artemether-lumefantrine require up to 6 doses per course so compliance may be much worse than single-dosage therapies such as sulfadoxine-pyrimethamine (SP).
ii. Drug trials tend to be small and may not capture the full natural variation in pharmacokinetics (PK) and pharmacodynamics (PD) within a population. Inter-individual variation in PK/PD may result in patients with sub-therapeutic drugs concentrations.
iii. Health systems in malaria endemic countries are not equipped to treat patients according to their weight which poses a particular problem when dosing children. A child's dose is determined according to an age band and whilst more practical this inevitably leads to a large proportion of dosages either above or below those recommended (330).

Clinical trials are expensive, relatively small and cannot ethically measure effects of factors such as poor compliance and under dosing. Subsequent field studies on effectiveness may infer the impact of factors such as compliance (293) but these can only be done after the drugs are deployed. Neither type of study can determine how robust the regimens are to small changes in parasite drug sensitivity nor how

vulnerable the regimens are to the evolution of drug resistance. In this paper, we investigate whether we can develop pharmacological models of antimalarial drug treatment that are sufficiently compelling that these questions can be usefully addressed *in silico*. The consensus method of modelling the effect of drug treatment on an infection is to track the change in total number of parasites in the body over time following treatment. A review of this "mechanism-based" pharmacokinetic/pharmacodynamic (PK/PD) modelling of antimicrobial drugs by Czock and Keller (73) lists 28 papers that have used (with modifications) this model, including application to malaria by Austin *et al.* (16) to identify the optimal pattern of drug administration to clear an infection, by Hoshen et *al*. (144, 149) to determine whether simulated treatment outcomes are improved with a split chloroquine dose and Simpson *et al.* (302) to compare the development of resistance after the *de novo* use of 2 of the most widely used antimalarial doses of MQ. We investigate four drugs: chloroquine (CQ), lumefantrine (LF), mefloquine (MQ) and piperaquine (PQ) given as monotherapies and as components of artemisinin-containing combination therapies (ACTs) with artesunate (AS), artemether (AR) or dihydroartemisinin (DHA) as appropriate. Chloroquine is no longer officially deployed for *P.falciparum* malaria through the formal health sector for treatment of *P. falciparum* (with the interesting exception of Guinea Bissau (138, 176, 341)). It is included here is for historical comparison and because it results in higher failure rates (see later) than the ACTs allowing us to compare the different dynamics of drug failure. Following convention, CQ, LF, MQ and PQ are collectively known as the 'partner' drugs within these ACTs. We demonstrate that this modelling approach generates results consistent with field data and try to identify the most important factors that determine drug treatment success and failure.

2. Methods

2.1. Basic Model

The rate of change in the total number of parasites present in a single patient over time depends on the parasite multiplication rate discounted by the proportions killed

by antimalarial drugs and cleared by host defences such as immunity. The methodology is based on a standard differential equation:

$$\frac{dP}{dt} = P\left[a - f(C) - f(I)\right] \qquad [1]$$

where P is the number of parasites in the infection, t is time after treatment (days in these simulations), a is the parasite growth rate (per day), $f(C)$ represents drug killing rate of parasites which depends on the drug concentration C, and $f(I)$ represents the host's background immunity to the infection. The drug killing function $f(C)$ is given by:

$$f(C) = \frac{V \bullet C^n}{C^n + K^n}, \qquad [2]$$

where C is the drug concentration (mg/l), V is the maximal parasite-killing rate constant (per day), K is the concentration at which 50% of the maximal killing rate occurs (mg/l) and n is the slope of the dose-response curve. Drug concentration decays over time, as

$$C = C_0 \bullet e^{-kt} \qquad [3]$$

where k is the terminal elimination rate constant (obtained from the drug half-life) and C_0 is the drug concentration at time zero i.e. immediately after treatment (drug absorption and conversion is assumed to be instantaneous in this methodology; see later discussion). The immunity function ($f(I)$) is assumed to be time-independent (i.e. immunity is not acquired over the course of treatment) and is a constant value depending on age and transmission settings as described later (Appendix 2).

Combining equations 1, 2 and 3 and integrating allows us to predict the number of parasites at any given time point *t* after treatment as:

$$P_t = P_0 \bullet e^{(a-f(I))\bullet t} \bullet \left[\frac{K^n + \left(C_0 \bullet e^{-kt}\right)^n}{K^n + C_0{}^n} \right]^{\frac{V}{k \bullet n}}$$

[4]

where P_0 is the initial number of parasites present in the body at time zero when treatment time commences. It is assumed that if and when P_t falls below one, an infection has been cleared. Note that this methodology tracks the total number of parasites in the body whereas clinical observations are on percentage of infected red blood cells; simple arithmetic using the number of RBC appropriate for patient age and weight allows conversion between the scales.

2.2. Extension of the basic methodology for malaria

Antimalarial regimens typically contain several doses spread over 3 days (Table 1). The concentration at time zero (C_0) is dependent on the existing drug concentration in the blood, augmented by any new drug dosage administered i.e.

$$C_0 = C' + \left[\frac{D}{V_d \bullet W} \right]$$

[5]

the drug concentration at the immediate end of the previous time step is represented by C' (C'=0 if first dosage), D is the drug dosage (mg) given, Vd is the volume of distribution (l/kg) and W is the weight of the patient (kg). The new dosage is converted to the concentration in the blood assuming instantaneous absorption and distribution; the dosage can be reduced to reflect drug bioavailability less than 100%.

Table 1. Standard adult dosages recommended by WHO (2006) and mean antimalarial drug parameters for artemether, artesunate, DHA, chloroquine, lumefantrine, mefloquine and piperaquine.

Variable	Default value						
	Artemether	Artesunate	DHA	Chloroquine	Lumefantrine	Mefloquine	Piperaquine
Dose (mg/kg)	1.6mg/kg given twice daily for 3 days	4mg/kg given once daily for 3 days	4 mg/kg once a day for 3 days	10mg/kg given once on days 1 and 2, 5mg/kg given once on day 3.	19.2mg/kg given twice daily for 3 days.	25mg/kg given once.	18 mg/kg once a day for 3 days
Volume of distribution (*Vd*)	17.4[110]	2.75[301]	8[57, 237]	300[359, 397]	21[68]	20.8[359]	150[57]
Elimination rate constant (*k*)	3.96 [a]	16.6 [212, 321]	19.8[57, 237]	0.0231[359]	0.16[110, 212, 350]	0.053[350]	0.03[151, 350]
Conc. required to produce half the desired effect (IC_{50})	0.0023 [a]	0.001[44, 211]	0.009[210]	0.02 [211, 225]	0.032[44, 321]	0.027 [44]	0.088 [237]
Maximal parasite-killing rate constant (*V*)	4[355]	4.6[355]	4.6 [b]	3.45[355]	3.45[355]	3.45[355]	3.45 [c]
Slope factor (*n*)	4 [b]	4[321]	4[321]	1.6 [a]	4[321]	5[321]	6 [60]

[a] Unpublished data from the Liverpool School of Tropical Medicine
[b] Assumed to be like artesunate
[c] Assumed to be like chloroquine, mefloquine and lumefantrine

Equations 4 and 5 are applied to each separate time interval in the drug regimen. For example in a 3-day regimen of CQ (Table 1) there would be 3 intervals i.e. day1, day2, day3 onwards; for artemether-lumefantrine there would be 5 half-day periods followed by dosage 6 onwards.

Antimalarials are now invariably deployed as combination therapies to improve therapeutic efficacy and to delay the development of drug resistance although we do recognize that many other drugs including monotherapies are still available through the informal health services. We also note that the use of quinine, particularly via continuous intravenous infusion in the case of severe malaria is still frequently administered. However, this model focuses on the treatment of uncomplicated malaria with orally administered drugs. It is assumed that two drugs act independently of each other in the combination (see discussion) and we simply expand Equation [1]:

$$\frac{dP}{dt} = P\left[a - f\left(C_1\right) - f\left(C_2\right) - f\left(I\right)\right] \qquad [6]$$

Integrating this gives

$$P_t = P_0 \bullet e^{(a-f(I))\bullet t} \bullet \left[\frac{K_1^{n_1} + \left(C_{0,1} \bullet e^{-k_1 t}\right)^{n_1}}{K_1^{n_1} + C_{0,1}^{n_1}}\right]^{\frac{V_1}{k_1 \bullet n_1}} \bullet \left[\frac{K_2^{n_2} + \left(C_{0,2} \bullet e^{-k_2 t}\right)^{n_2}}{K_2^{n_2} + C_{0,2}^{n_2}}\right]^{\frac{V_2}{k_2 \bullet n_2}} \qquad [7]$$

In Equation 7, the subscripts 1 and 2 for parameters K, C_0, n, k, and V, indicate whether the parameter value refers to drug 1 or 2. This equation can be used to find the change in parasite number between any two given time points, in this model it is used along side Equation 3 to update the parasite load and drug concentration daily. For clarity K will subsequently be referred to as IC50 in the text, figures and tables.

Acquired immunity was incorporated using the data of Pongtavornpinyo *et al.* (262) who identified three possible measures of acquired immunity for use in modelling based on parasite biomass, the incidence of severe malaria and the proportion of

symptomatic infections. For the purposes of this model the equations are standardized to return a minimum value of 0 (when age=0 and EIR=0) and a maximum of 1 and then scaled by a factor *ø* to produce *f(I)* used in equations 1 and 6; see Appendix 2 for details. We use immunity only briefly here (to simulate clinical trials) but include it as a proof-of-principal.

The dosing regimens of the drugs investigated, and estimates of the PK/PD parameters employed to model treatment are given in Table 1 and discussed in Appendix 1. This model has been implemented in R (version 2.9.2) (270), although earlier versions were run in Excel and Maple 12. All packages generated the same results and the results presented here were generated in R. The model runs in half-day time steps using Equation 7 for the first seven days to allow for multiple-dose regimens and one-day time steps thereafter to speed up simulations. It is possible to use Equation 4 to find treatment outcome algebraically after the final dose (144) but this approach of single daytime steps is more explicit and allows easy calculation of factors such as parasite clearance time, period of chemoprophylaxis and allows easy incorporation of factors such as stochastic variation in predicted parasite numbers. The discrete time step and algebraic analysis do, of course, give the same result.

2.3. Model Validation and analysis

The first step in model validation is to check that the outputs match observations made in the field. The chief criteria are that the regimens give a reliable cure rate (except in the case of short-term artemisinin monotherapies), that parasite clearance times (PCT) are plausible and that times until new infections are noted (PoC) are reasonable. The first term is self-explanatory: PCT is the time taken for the infection to fall below the limit of microscopic detection that we assume is 10^8. The period of chemoprophylaxis (PoC) describes the length of time a drug treatment suppresses the appearance of new infections, this is often reported in clinical trials. We assume drugs do not affect parasites during the liver phase as is believed to be the case for those drugs considered here (75). The earliest parasites able to cause a patent re-infection emerge from the liver at precisely the time when drug concentration from previous

treatments has declined sufficiently that parasite reduction turns into increase i.e. when *dP/dt* becomes positive. Successful re-infection can occur before this point (i.e. when *dP/dt* <0) but the number of parasites will initially fall, hence re-infection will occur fastest if parasites emerge on the day *dP/dt* first becomes positive. The time when *dP/dt* becomes greater than zero is found by evaluating Equation 4 to obtain P_t at the end of each daily time-step and finding when $P_t > P_{t-1}$. Only the partner drug is considered in calculating PoC because we assume the artemisinin in an ACT has disappeared by the time the first drug becomes permissive for parasite growth. We assume 10,000 merozoites emerge from the liver and become detectable when their numbers exceed 10^8, the time taken for this to occur can be estimated by solving Equation 4 with respect to *t*, where $P_0 = 10^5$, $P_t = 10^8$ and C_0 is the drug concentration on the day *dP/dt* >0 first becomes true. The PoC is then found by adding together the time taken for *dP/dt* to become positive and time required for a new infection to become patent. To get a rough estimate of when new infections may reasonably be observed we increased the PD parameters and parasite growth rate by 1 standard deviation (assuming CV =0.3, see later) to represent parasites that are slightly above average in their ability to resist the drug. The PoC will vary from person to person depending on variation in human PK, parasite drug sensitivity and growth rates. We later allow variation in all the PK and PD parameters resulting in PoC being different for each person; in this case the 5th centile value of PoC is reported as being indicative of when new infections may plausibly first start to be observed in high-transmission setting.

The initial analysis simply involved varying each individual parameter value in turn (while keeping other values constant) to find the size of change that resulted in treatment failure. This gave an initial indication of the relative importance of each parameter in determining treatment success or failure. In reality all parameter values vary simultaneously. This was incorporated by adding variation to seven different model parameters: the five PK/PD parameters listed on Table 1, the maximal parasite growth rate *a* and the number of parasites present at time of treatment P_0. With the exception of the initial parasite number, all variables were assumed to be normally distributed with a coefficient of variation (CV) of 30%; the mean values are given on Table 1. Values must be positive, so the program checked this was true; if less than zero, the model generated another random number in the same way until a positive

number was chosen. The number of parasites present at the start of treatment was chosen randomly from a uniform distribution between 10^{10} and 10^{12}. Populations of 10,000 patients were simulated for the following drug regimens: CQ, LF, MQ and PQ monotherapies and CQ+AS, MQ+AS, LF+AS, LF+AR, and PQ+DHA as ACTs. The results were analyzed by logistic regression (LR) with treatment failure as the outcome using the PASW Statistics 18 package. The independent variables included the initial parasitaemia (P_0), parasite growth rate (a), drug elimination rate constant (k), slope factor (n), IC50, volume of distribution (Vd) and the maximal parasite-killing rate (V). LR analyzed the effect of a one-unit change in the value of each parameter but the scales of the parameter values were so diverse that it made comparisons impossible (for example a one unit change in IC50 is proportionally much larger than a one unit increase in volume of distribution, see Table 1). The parameter values were therefore converted to z-scores because the odds ratio statistic on this scale indicates the increased or decreased risk of failure associated with a one standard deviation increase in the parameter value allowing easy comparison between variables. The changes in log-likelihood (LL) and Wald statistics measured the reduction in model fit when individual parameters are omitted: the larger the value, the worse the fit and hence the more important the parameter. Thus Wald and LL measured the relative importance of each parameter's variation on drug failure.

There is considerable interest in how the evolution of resistance to the artemisinin component may compromise the long-term effectiveness of ACTs. We investigated two aspects of this process. Firstly, we measured how increasing IC50 to the artemisinin component would reduce the protection afforded to its partner drug. This was achieved by increasing artemisinin IC50 values above their default values and measuring how much of a change in the partner drug IC50 would be required for drug failure to occur. Secondly, we measured how increasing IC50 to artemisinins would increase ACT failure rates if resistance to the partner drug were already present. As before, we allowed 30% CV in the default parameter values and measured failure rates while increasing IC50 to the artemisinin component (and still allowing a CV of 0.3 around this new artemisinin IC50 value). Both these measures (change in partner drug IC50 and drug failure rates) were standardized to allow direct comparison between different ACTs by constructing a standardized "protection index" so that a value of 1 indicates the 'basal' value at the original artemisinin IC50 value and a

value of 0 means the artemisinin component is useless and that the measure has become 'maximal', i.e. identical to that of the partner drug monotherapy: for example, if 'f' is the failure rate then its standardized protection index is 1-[(f-basal)/(maximal-basal)].

"Clinical trial" simulations were run to compare model outputs to field data. The data recorded were those typically measured in trials and available to investigators i.e. outcome (success/failure), number of parasites present at time of treatment, age of patient, place of residence and day 7 serum level. Place of residence and age of subjects was included to demonstrate the effects of immunity (Appendix 2) with a scaling factor of the immune function, Φ, set to 0.8: village A had an EIR of 10 and village B an EIR of 100. The clinical trial simulations included 400 individuals, 200 from village A and 200 from village B (aged 6 months to 15 years), all were treated with artesunate-mefloquine using the default parameters on Table 1 except the mean IC50 of mefloquine was increased to 0.8 to allow a proportion of failures more typical of clinical trials where a drug is failing. These parameters were varied with a CV of 0.3 to allow treatment failures (see above; there was no point analyzing a clinical trial where everyone is cured). The results were analyzed using logistic regression with treatment outcome as the dependent variable; independent variables were age (≤5 years or >5 years), location, low day 7 drug serum levels (defined as values below the 15th centile) and initial parasitaemia.

Low drug serum levels on day 7 have been shown to be a significant risk factor for treatment failure (see later discussion), so we (arbitrarily) defined low levels as being below the 15th centile and determined the risk associated with low day-7 serum levels by the odds ratio and population attributable risk percentage (PAR%) a measure of the percentage of treatment failures that could be avoided if adequate drug levels were achieved throughout the population. The diagnostic accuracy of the day-7 serum concentration was further explored using PASW Statistics 18.0 to generate receiver operating characteristic (ROC) curves. The correlation between drug serum concentrations on days 3, 5, 7 and 10 and area under the drug concentration curve (AUC) between days 0-25, 0-50, 0-100 and 0-∞ was investigated. The AUC between

any two time points was found using equation 9 whilst $AUC_{0-\infty}$ was found using equation 10,

$$AUC_{0-t} = C_0 \bullet \left(\frac{1 - e^{-k \bullet t}}{k} \right) \quad [9]$$

$$AUC_{0-\infty} = \frac{C_0}{k} \quad [10]$$

3. Results

Using the default parameter values without variation resulted in CQ, LF, MQ and PQ monotherapies reliably clearing malaria infections when the drug dosage schedules simulated were those recommended by the WHO (379) (Table 2), assuming initial parasite numbers were below 10^{12}. The use of artemisinins (AS, AR or DHA) as monotherapies over three days failed to clear infections (Table 2) although they did cure as monotherapies if given over seven days (data not shown). When initial parasite number was 10^{10} the parasite clearance times for LF, MQ and PQ began at three days and increased by approximately one day with each 10-fold increase in initial parasite number. The parasite clearance time for CQ began at four days when initial parasitaemia was set to 10^{10} and increased to six and seven days with increasing initial parasite number. For all partner drugs the addition of either AS or DHA reduced PCT by one to two days whilst the addition of AR to LF reduced the PCT by up to three days. Estimates of PoC when using the non-varied default parameters (Table 2) were always longer than expected (see later discussion).

The percentage change that can be tolerated in a given drug parameter before treatment fails is shown in Table 3 assuming an initial parasitaemia of 10^{10} to crudely illustrate how sensitive a drug regimen was to the natural variation between individuals (recall that the partner drugs are able to clear parasites as a monotherapy so it was pointless varying individual parameter values of the artemisinin component).

Table 2. Percentages of individuals predicted to be cured using drugs with and without artemisinins according to the dosing regimens detailed in Table 1, parasite clearance times, and periods of chemoprophylaxis [a]

Output	Drug					
	Artemether	Artesunate	Chloroquine (plus artesunate)	Lumefantrine (plus artesunate, artemether)	Mefloquine (plus artesunate)	Piperaquine (plus DHA)
% Cured	0	0	100 (100)	100 (100, 100)	100 (100)	100 (100)
PCT (days) with $P_0 = 10^{10}$	0	0	4 (2)	3 (2, 1)	3 (2)	3 (2)
PCT (days) with $P_0 = 10^{11}$	0	0	6 (3)	4 (2, 2)	4 (2)	4 (2)
PCT (days) with $P_0 = 10^{12}$	0	0	7 (4)	5 (3, 2)	5 (3)	5 (3)
PoC (days)	9	9	87	41	80	57
Apparent cure rate after 28 days (%)	0	0	92 (96)	96 (98, 99)	97 (98)	96 (97)
Apparent cure rate after 63 days (%)	0	0	91 (93)	90 (93, 96)	97 (99)	91 (92)
True cure rate (%)	0	0	85 (88)	90 (93, 95)	96 (97)	90 (91)
Mean PCT (days) ± sd	-	-	6.4 ± 4.5 (3.4 ± 2.64)	4.98 ± 3.915 (2.76 ± 2.1, 1.98 ± 0.65)	5.3 ± 4.7 (2.9 ± 2.7)	5.3 ± 3.95 (3.4 ± 2.5)
PoC (5th centile) (days)	-	-	52	31	59	40

[a] Note that the artemisinins have no effect on PoC because of its short half-lives, so PoC values are identical for all ACTs and their partner drug monotherapies.

Table 3. Percentages that drugs must deviate from the default values (see Table 1) to result in treatment failure in naïve patients with no immunity [a]

Drug	Variable					
	Dose (mg/kg)	Parasite growth rate, *a* (/day)	Elimination rate constant, *k* (/day)	IC50 (mg/l)	Volume of distribution, *Vd* (l/kg)	Maximal parasite killing rate constant, *V* (/day)
Mefloquine	-95.6	169.6	598.1	2122.2	2082.7	-56.5
Mefloquine + Artesunate	-98.4	178.3	805.7	2418.5	2404.8	-59.4
Chloroquine	-66.5	100.0	332.9	160.0	160.0	-40.3
Chloroquine + Artesunate	-85.0	108.7	462.8	191.0	191.0	-44.6
Lumefantrine	-96.9	134.8	262.5	2993.7	2971.4	-47.8
Lumefantrine + Artemether	-99.0	169.6	837.5	5868.0	5852.0	-56.5
Lumefantrine + Artesunate	-98.4	152.2	462.5	4275.0	4171.4	-50.7
Piperaquine	-61.1	143.5	366.7	161.4	154.7	-48.7
Piperaquine + DHA	-62.2	145.2	433.3	172.7	154.5	-50.4

[a] Positive values indicate that parameters must be increased for failure to occur, and negative values indicate that they must be decreases. Only partner drug PK/PD parameters are reported. The slope factor *n* did not influence treatment failure.

Studying the parameters without variation suggested chloroquine and piperaquine regimens are most sensitive to change whilst mefloquine and lumefantrine regimens are most robust. All regimens appeared to be particularly sensitive to changes in the parasite-killing rate constant, *V*; for example, a reduction of only 40% resulted in treatment failure for CQ monotherapy. The slope of the concentration effect curve had little or no effect on drug treatment outcome.

More realistically, allowing a 30% CV in parameter values reduced overall true cure rates to 85% (CQ), 90% (LF), 96% (MF) and 90% (PQ) for monotherapies (Table 2). The addition of artemisinins increased these to 88% (AS-CQ), 93% (AS-LF), 95% (AR-LF), 97% (AS-MQ) and 91% (DHA-PQ). The apparent cure rates at 28 and 63 days were recorded to investigate the effects of differing periods of follow-up in clinical trails (Table 2). The cure rates were over estimated at both time points but the apparent cure on day 63 gave a closer approximation of the true cure rate than the day 28 estimates. Apparent CQ cure rate on day 63 was 6% higher than the true cure rates; all other day 63 cure rates were within 2% of the true cure rate (Table 2). The parasite clearance times found in the presence of variation were all reduced with the addition of an artemisinin to the partner drug (Table 2). The range of PoC estimates were normally distributed (see Appendix 3) with the 5^{th} centile values presented in Table 2.

Allowing a CV of 30% in PK/PD parameters allowed the most important parameters to be identified and ranked using the Wald statistic from logistic regression (Table 4, noting that overall cure rates were given on Table 2) and compared to the results obtained by varying each parameter individually (Table 3). All model variables in monotherapies (except MQ initial parasite number) were found to be significant factors determining treatment outcome. For CQ, LF, MQ and PQ the Wald and log-likelihood statistics identified the maximal parasite-killing rate (*V*) to be the most important and the slope factor (*n*) to be the least important variables. The volume of distribution (*Vd*), IC50 and slope factor (*n*) of the artemisinin component in combinations (with the exception of AS IC50 in the AS+LF combination) were not found to be significant determining factors of treatment success/failure. Additionally when using the AS+MQ combination both the initial parasite number and the artesunate maximal parasite-killing rate constant (*V*) were not significant. The most important variable in all combination therapies was the rate of parasite killing (*V*) of

the partner drug closely followed in all cases by the rate of parasite growth (*a*). Where significant, the number of parasites present when treatment began was found to be the least influential factor in combination therapies.

The impact of increasing artemisinin IC50 values is shown on Figure 1 in terms of reduced protection afforded to the partner drug (Figure 1A) and in terms of likely increased failure rate of the ACT (Figure 1B). Both results suggest increasing resistance to artemisinin causes a rapid decline in protection.

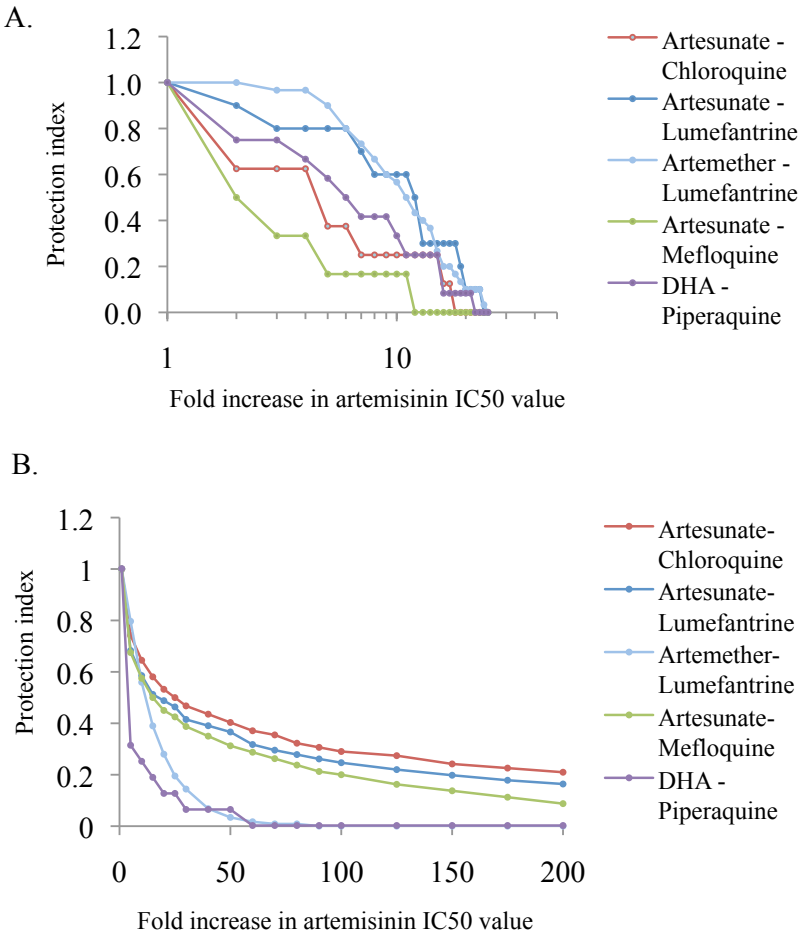

Figure 1. The consequences of resistance evolving to artemisinins through increasing IC50 values. A) Protection afforded to partner drug, quantified as the reduction in the partner drug IC50 value that can occur before drug failure occurs. (B) Clinical protection, quantified as changes in ACT failure rate as the artemisinin IC50 increases. These protection indices are standardized so that a value of 1 indicates values obtained using original artemisinin IC50 values (Table 2) and value of 0 indicates values equivalent to the partner drug monotherapies.

Table 4. Relative importance of variable parameters ranked for the nine treatment regimens, using Wald, log likelihood, and odds ratio statistics in logistic regression, with drug failure as the outcome [a]

Drug	Variables[b]	Rank	Wald Statistic	Change in -2 Log Likelihood	Significance (*P* value)	Odds ratio (95% CI)
Chloroquine	P_0	7	7.029	7.112	0.008	1.122 (1.031-1.223)
	a	2	478.113	2358.325	0.000	264.216 (160.274-435.566)
	k	5	324.825	640.959	0.000	10.762 (8.311-13.935)
	n	6	274.542	487.471	0.000	0.134 (0.105-0.169)
	IC50	3	394.607	1075.476	0.000	25.467 (18.504-35.052)
	Vd	4	387.435	1046.712	0.000	24.438 (17.777-33.595)
	V	1	508.018	5903.412	0.000	0.000 (0.000-0.000)
	Constant		522.451			0.000
Chloroquine plus Artesunate	P_0	9	17.670	18.283	0.000	1.227 (1.116-1.350)
	a	2	388.052	2044.336	0.000	321.885 (181.216-571.748)
	CQ *k*	5	231.727	420.421	0.000	8.185 (6.244-10.729)
	CQ *n*	6	221.282	386.808	0.000	0.145 (0.113-0.188)
	CQ IC50	3	321.878	827.574	0.000	21.178 (15.172-29.562)
	CQ *Vd*	4	316.659	788.882	0.000	19.629 (14.142-27.246)
	CQ *V*	1	417.353	5279.992	0.000	0.000 (0.000-0.000)
	AS *k*	7	43.178	46.965	0.000	1.812 (1.518-2.164)
	AS *n*	12	0.002	0.002	0.965	1.004 (0.842-1.196)
	AS IC50	10	2.786	2.804	0.094	1.162 (0.974-1.385)
	AS *Vd*	11	0.842	0.842	0.359	1.085 (0.911-1.292)
	AS *V*	8	40.981	44.564	0.000	0.555 (0.464-0.665)
	Constant		430.377			0.000
Lumefantrine	P_0	7	19.198	20.130	0.000	1.293 (1.152-1.450)
	a	2	267.100	1461.201	0.000	415.911 (201.797-857.206)
	k	3	243.528	821.347	0.000	56.223 (33.895-93.259)
	n	6	27.154	29.445	0.000	0.546 (0.435-0.686)
	IC50	5	77.610	96.781	0.000	2.955 (2.322-3.760)
	Vd	4	82.145	101.599	0.000	2.957 (2.339-3.739)
	V	1	289.468	5334.075	0.000	0.000 (0.000-0.000)
	Constant		295.124			0.000
Lumefantrine plus Artesunate	P_0	9	19.811	21.134	0.000	1.331 (1.173-1.509)
	a	2	232.508	1150.943	0.000	251.521 (123.598-511.845)
	LF *k*	3	186.486	485.514	0.000	22.058 (14.149-34.388)
	LF *n*	8	24.768	27.014	0.000	0.535 (0.418-0.684)
	LF IC50	7	28.178	31.114	0.000	1.977 (1.537-2.543)
	LF *Vd*	6	39.783	44.971	0.000	2.317 (1.784-3.008)
	LF *V*	1	257.517	4257.815	0.000	0.000 (0.000-0.000)
	AS *k*	4	62.142	75.273	0.000	2.872 (2.209-3.733)
	AS *n*	11	0.596	0.598	0.440	0.908 (0.712-1.159)
	AS IC50	10	8.165	8.342	0.004	1.387 (1.108-1.735)
	AS *Vd*	12	0.351	0.352	0.553	1.070 (0.855-1.340)
	AS *V*	5	52.110	62.342	0.000	0.398 (0.310-0.511)
	Constant		263.643			0.000
Lumefantrine plus Artemether	P_0	9	17.670	18.283	0.000	1.227 (1.116-1.350)
	a	2	388.052	2044.336	0.000	321.885 (181.216-571.748)
	LF *k*	5	231.727	420.421	0.000	8.185 (6.244-10.729)
	LF *n*	6	221.282	386.808	0.000	0.145 (0.113-0.188)
	LF IC50	3	321.878	827.574	0.000	21.178 (15.172-29.562)
	LF *Vd*	4	316.659	788.882	0.000	19.629 (14.142-27.246)
	LF *V*	1	417.353	5279.992	0.000	0.000 (0.000-0.000)
	AR *k*	7	43.178	46.965	0.000	1.812 (1.518-2.164)
	AR *n*	12	0.002	0.002	0.965	1.004 (0.842-1.196)
	AR IC50	10	2.786	2.804	0.094	1.162 (0.974-1.385)
	AR *Vd*	11	0.842	0.842	0.359	1.085 (0.911-1.292)
	AR *V*	8	40.981	44.564	0.000	0.555 (0.464-0.665)
	Constant		430.377			0.000

Continued on following page

Table 4. *Continued*

Drug	Variables[b]	Rank	Wald Statistic	Change in -2 Log Likelihood	Significance (*P* value)	Odds ratio (95% CI)
Mefloquine	P_0	7	1.469	1.477	0.224	1.083 (0.952-1.232)
	a	2	176.479	761.123	0.000	110.263 (55.093-220.680)
	k	3	80.146	116.012	0.000	4.264 (3.104-5.858)
	n	6	12.501	13.263	0.000	0.613 (0.468-0.804)
	IC50	5	13.256	13.883	0.000	1.581 (1.236-2.023)
	Vd	4	17.108	18.392	0.000	1.840 (1.378-2.456)
	V	1	202.508	3128.261	0.000	0.000 (0.000-0.000)
	Constant		206.623			0.000
Mefloquine plus Artesunate	P_0	9	1.538	1.548	0.213	1.093 (0.950-1.258)
	a	2	159.869	668.108	0.000	87.176 (43.613-174.254)
	MQ *k*	3	45.487	55.621	0.000	2.867 (2.111-3.894)
	MQ *n*	8	3.920	3.971	0.046	0.750 (0.564-0.997)
	MQ IC50	5	12.613	13.441	0.000	1.633 (1.246-2.142)
	MQ *Vd*	7	6.892	7.086	0.008	1.480 (1.104-1.983)
	MQ *V*	1	187.344	2676.097	0.000	0.000 (0.000-0.000)
	AS *k*	4	22.465	25.146	0.000	2.006 (1.504-2.675)
	AS *n*	11	0.088	0.088	0.767	0.959 (0.726-1.266)
	AS IC50	10	0.646	0.647	0.421	0.896 (0.686-1.171)
	AS *Vd*	12	0.020	0.020	0.887	0.980 (0.744-1.292)
	AS *V*	6	11.547	12.206	0.000	0.625 (0.476-0.819)
	Constant		192.601			0.000
Piperaquine	P_0	7	12.093	12.306	0.000	1.163 (1.068-1.266)
	a	2	405.719	1147.304	0.000	27.102 (19.659-37.363)
	k	5	268.650	446.987	0.000	6.565 (5.242-8.222)
	n	6	96.420	111.102	0.000	0.416 (0.349-0.495)
	IC50	4	324.886	666.386	0.000	11.141 (8.572-14.480)
	Vd	3	331.315	667.546	0.000	10.928 (8.447-14.138)
	V	1	514.197	4464.531	0.000	0.000 (0.000-0.000)
	Constant		543.153			0.000
Piperaquine plus DHA	P_0	8	13.759	14.059	0.000	1.181 (1.082-1.290)
	a	2	374.163	1074.747	0.000	28.157 (20.077-39.488)
	PQ *k*	5	231.611	376.353	0.000	5.928 (4.714-7.455)
	PQ *n*	6	90.066	104.273	0.000	0.411 (0.342-0.494)
	PQ IC50	4	283.653	533.022	0.000	8.900 (6.901-11.479)
	PQ *Vd*	3	298.725	566.776	0.000	9.691 (7.491-12.539)
	PQ *V*	1	470.841	4087.798	0.000	0.000 (0.000-0.000)
	DHA *k*	9	13.447	13.705	0.000	1.364 (1.155-1.609)
	DHA *n*	12	0.000	0.000	0.988	0.999 (0.844-1.181)
	DHA IC50	11	0.077	0.078	0.781	0.977 (0.828-1.152)
	DHA *Vd*	10	1.920	1.928	0.165	1.123 (0.953-1.322)
	DHA *V*	7	19.808	20.370	0.000	0.693 (0.590-0.815)
	Constant		499.203			0.000

[a] Chloroquine, mefloquine, and lumefantrine were all given alone and with artesunate, in addition to artemether-lumefantrine. Dosages are in accordance with WHO guidelines (Table 1). The sample size for each drug regimen was 10,000 patients, and overall failure rates are given in Table 2.

[b] P_0, parasite number at time of treatment; *a*, parasite growth rate; *k*, terminal elimination rate constant; *n*, slope of the dose-response curve, IC50, concentration at which 50% of maximal killing occurs; V_d, volume of distribution; *V*, maximal drug killing rate.

The "clinical trial" simulations examined the importance of four variables typically measured in the field, initial parasite number, location, patient age and day-7 serum level. Results for artesunate-mefloquine are shown on Table 5. People from a high transmission village are more immune and, as expected, were less likely to fail treatment; interestingly, this effect was always associated with very small confidence intervals. Young age was associated with increased risk of failure although this was not significant in our simulation. Several different field studies have reported day-7 serum concentration as a predictor of treatment failures (55, 97, 354); our results confirm that individuals with a low day-7 serum level have a three-fold higher risk of treatment failure than those with normal levels.

Table 5. Relative importance of each risk factor measured during a simulated clinical trial of AS-MQ, determined using Wald and odds ratio statistics [a]

Risk factors	Output		
	Wald statistic	Odds ratio (95% CI)	*P* value
log (Po)	0.000	0.977 (0.509-1.951)	0.992
Location (high EIR)	7.505	0.991 (0.985-0.997)	0.006
Age (under 5 years)	3.217	1.704 (0.952-0.3051)	0.073
Day 7 serum (<15th centile)	10.102	2.939 (1.512-5.713)	0.001
Constant	0.155	0.209	0.694

[a] The overall failure rate was 15.57%, and the results came from logistic regression analysis with treatment failure as the outcome

Individuals were categorized as having either normal or low day-7 serum levels using the 15th centile value and its effect on treatment success/failure reported on Table 6. These 15th centile values were found to be <0.056 (mg/L) for CQ, <1.647 for LF, <0.637 for MQ and <0.232 for PQ. The increased risk of treatment failing in those with low day-7 serum levels was largest when treating with DHA+PQ (OR=2.62) and smallest when treating with AS+MQ (OR=1.24) (note that we disregard the OR value on Table 5 because this was obtained after inflating the MQ IC50 value, see methods). The PAR% results suggest that increasing drug levels sufficiently to achieve normal day-7 serum levels in all individuals could reduced failure rates by as much as 17% when treating with DHA+PQ but by only 3% when using AS+MQ. The area under the ROC curve (AUROC) found low day-7 serum

levels to be a poor predictor of treatment outcome with AUROC values ranging from 0.538 for AS+MQ to 0.646 for PQ (a AUROC value of 0.5 indicates no predictive power, AUROC of 1 indicates perfect sensitivity and specificity). These poor predictive values occurred despite strong correlation between AUROC and AUC (Appendix 3). The estimates of OR were not noticeably affected by our choice of the 15th centile as the definition of 'low' serum levels: the same ORs were obtained when the cut-off was defined as the 10th, 20th or 30th centile (Appendix 3).

Table 6. Effects of low day 7 serum levels (<15th centile) on predicted outcomes of treatments

Drug	Output [a]				
	OR	Sensitivity	Specificity	AUROC	PAR %
Chloroquine	2.153 (1.883-2.462)	0.248 (0.229-0.268)	0.867 (0.864-0.870)	0.632 (0.617-0.647)	11.584
Chloroquine plus Artesunate	2.086 (1.805-2.411)	0.248 (0.227-0.271)	0.863 (0.860-0.866)	0.627 (0.610-0.643)	11.567
Lumefantrine	1.934 (1.654-2.262)	0.240 (0.216-0.265)	0.860 (0.857-0.863)	0.615 (0.596-0.633)	10.532
Lumefantrine plus Artesunate	1.919 (1.605-2.295)	0.242 (0.214-0.273)	0.857 (0.855-0.860)	0.603 (0.582-0.624)	10.839
Lumefantrine plus Artemether	1.354 (1.067-1.719)	0.190 (0.158-0.227)	0.852 (0.850-0.854)	0.557 (0.530-0.583)	4.762
Mefloquine	1.393 (1.104-1.759)	0.195 (0.162-0.231)	0.852 (0.851-0.854)	0.554 (0.528-0.580)	5.242
Mefloquine plus Artesunate	1.243 (0.955-1.619)	0.179 (0.144-0.218)	0.851 (0.850-0.853)	0.538 (0.509-0.567)	3.361
Piperaquine	2.557 (2.199-2.973)	0.286 (0.260-0.312)	0.865 (0.862-0.868)	0.646 (0.628-0.665)	15.949
Piperaquine plus DHA	2.618 (2.236-3.066)	0.293 (0.265-0.321)	0.864 (0.861-0.866)	0.645 (0.626-0.664)	16.780

[a] OR, odds ratio; AUROC, area under the ROC curve; PAR%, population attributable risk percentage. Data are means with 95% confidence intervals.

4. Discussion

All models need to make simplifications to make them tractable. We therefore explicitly identify and discuss the key simplifications and assumptions that underlie these analyses before moving on to discuss how well the model predictions fit with clinical data, and what the models results imply for the current generations of antimalarial drugs.

The mechanism–based modelling approach (73) assumes drugs are instantaneously absorbed (across the gut wall for most antimalarials) and instantaneously converted, if necessary, to their active metabolite. This is probably reasonable for CQ, LF, MF and PQ because their long half-life dominates the time taken for relatively rapid absorption and conversion, but this approach is less satisfactory for artemisinins where the half-life is so short that time lags in absorption and conversion may arguably become important. It would be possible to remodel this component using a standard PK compartment model as will be discussed later.

Within a human, drug bioavailability and the extent of absorption are important contributors to the variability of drug outcomes. Lumefantrine oral bioavailability is particularly variable and highly dependent on food intake; it is consequently poor in acute malaria cases but improves markedly with recovery (97). By assuming all patients modelled had uncomplicated malaria and followed the dosing recommendations, we ignored complications caused by bioavailability absorption. We also ignored any toxic effects resulting from high concentrations and any impact that might have on PK/PD parameters.

We investigated two modifications of the basic methodology. We first examined the effects of assuming density-dependent growth in *P.falciparum* (73) (see Appendix 1 for details) and then the effects of adding stochastic variation to *Pt* at the end of each day by choosing the value from a Poisson distribution. Neither modification had a significant effect on the outcome and both were subsequently removed; all results presented use a constant growth rate *a*, detailed in Appendix 1.

The effects of acquired immunity have been largely ignored and introduced only briefly during the simulation of clinical trials. The development and action of human immunity

against malaria is a vast topic of current research and, as far as we know, there is no consensus mathematical description of its acquisition. Hence we used proxies to illustrate its basic effect and await more sophisticated descriptions to incorporate its effect (Appendix 2). Its omission can be justified because it is important that drugs act effectively in all humans irrespective of immune status. Most malaria mortality is in non- or poorly-immune African children so the results presented here are most appropriate to this group.

The assumptions described above concern the structure of the model. The interpretation of the results requires a secondary assumption: that we have properly calibrated the PK/PD values of each drug (Appendix 1). Differences in drug assay sensitivity and reproducibility combined with natural PK variation between people resulted in a range of PK estimates. We incorporated natural variation in the model parameters to reflect inter-individual variation by simply assuming each parameter was normally distributed with a CV of 0.3. Ninety-five percent of parameter values will lie within 2 standard deviations of the mean i.e. from 0.4 to 1.6 assuming a standard mean of one, a roughly 4-fold range of inter-individual variability. More sophisticated calibrations could be made: for example lumefantrine bioavailability depends critically on its ingestion with fatty food so may vary widely depending on diet, drug IC50 values typically vary 10 fold (225), and so on. At this stage, we were less concerned with exact calibration of the model, compared to its construction and evaluation, and leave it to readers to calibrate the equations as they see fit. We do assert that PK/PD parameter values are known to vary widely so our approach of setting CV=0.3 seems a reasonable first approach for investigating the general properties and robustness of the drug regimens.

Despite these assumptions made during model construction and calibration it is gratifying to note that the results presented above closely match observations made in the field. In particular:

- CQ, LF, MQ and PQ monotherapies gave reliable cure rates when modelling infections of drug sensitive parasites.
- Calibrating the CQ model with IC50 values typical of resistant parasites gave high treatment failure rates. Doubling the CQ dosage (as was done in Guinea-Bissau (138, 176, 341)) restored the efficacy of CQ against these ‘resistant’ parasites (data not shown).
- Artemisinin monotherapies over three days were unable to clear an infection but extending treatment time to 7 days does reliably clear parasites (1).

- Adding an artemisinin to a failing drug did not completely prevent treatment failure, but it did reduce failure rate by around 50% (Table 2) in line with field observations (1). The addition of an artemisinin derivative also appeared to increase the robustness of the partner drug to inter-individual variability (Table 3).
- Estimates of parasite clearance times for ACTs were in the region of two to four days (Table 2) which closely match field estimates for AL (101, 163, 167, 283, 306, 343), CQ+AS (238), DHA+PQ (114, 151, 163, 237) and MQ+AS (101, 283).
- The predictions of PoC were similarly consistent with field data when allowing variation in PK/PD parameters (Table 2). The model predicted a PoC of 32 days for LF which is very close to the reported range in fully sensitive parasites of 24 to 30 days (305, 307) although we do note PoC is reduced as resistance spreads (130). The PoC for CQ was longer than expected at 52 days but this maybe due to the long terminal elimination half-life values reported for CQ (110, 269) which may not properly reflect elimination rates at higher, physiologically active concentrations (88). As MQ or PQ are not yet regularly deployed in areas of high transmission we were unable to find published estimates of PoC for either drug, we did however find papers comparing reinfection rates between two different drug regimens used in the same setting. Grande *et al.* (114) found the incidence of re-infections in their study site in Mali was higher in the DHA-PQ group than in the AS-MQ group and tentatively attribute this to the shorter post-treatment prophylactic effect seen in PQ compared to MQ. Our model predicts a similar relationship between the prophylactic effect of PQ and MQ, with reinfections occurring up to 19 days earlier following treatment with PQ compared to MQ, despite the longer half-life of PQ. This is possible because the PoC and hence time to reinfection depends not just on the drug half-life but also on its dosage (increasing dosage increases the protection time) and on parasite sensitivity to the drug (305, 307). Our model predictions of a longer PoC after MQ treatments compared with LF implies reinfections will occur sooner following LF treatment. This is in agreement with the findings of Sagara *et al.* (283) who found reinfections in Peru to occur more frequently following AR-LF treatment than AS-MQ. Finally, a study comparing the safety, efficacy and tolerability of AR-LF and DHA-PQ in Zambian children (233) observed more new infections during the follow up of patients receiving AR-LF than those receiving DHA-PQ which is consistent with our model predictions.

In summary, the model provides good qualitative and quantitative fit to clinical observation so, with the caveats noted above, it seems reasonable to ask what the modelling implies for current drug regimes.

All drugs achieved reliable cure under the default PK/PD parameters with, as expected, the additional of artemisinins rapidly reducing patient parasitaemia (PCT, Table 2) and hence helping resolution of symptoms. Monotherapy drug failures occur at rates between 4% (MQ) and 10% (LF and PQ) when variation in PK/PD is introduced, but these are within the 10% limit suggested by WHO to indicate a need to change the drug regimen. The failure rate of CQ 'sensitive' parasites is relatively high at 15%. We believe this arose because good quality parameter estimates are only readily available from fairly recent studies where some degree of CQ resistance had already evolved. We are comfortable with this failure rate because we wanted to investigate at least one situation where resistance had already arisen naturally (rather than by our manipulation of PD parameters) and to compare this with patterns noted in highly effective drugs such as the ACTs. Adding artemisinins improved cure rates, but did not eliminate all drug failures, again in line with field observations (1)**.**

Efficacy is measured in the field using clinical trials where continued patient follow-up is operationally challenging and problematic in most endemic areas. How this may affect trial results is addressed in Table 2, which reports 'apparent cure rate' at days 28 and 63 (the proportion of patients with no detectable parasites which may include patients with sub-patent infections that will later recrudesce) as well as true cure rate. It is generally accepted that 14 days is the minimum follow up period although current WHO guidelines mandate at least 28 days (321, 380) and there have been suggestions that the long half-lives of partner drugs in ACTs make it necessary to follow patients for up to 63 days (321). The magnitude of errors likely to be caused by short follow-up periods was not quantified by these authors and field data is difficult to assess: in principle drug failures can be distinguished from new infections during the follow-up period using molecular typing (386), but in practice this process is hampered by poor detection of 'minor' parasite clones present at the time of treatment (284) which, combined with technical limitations, generates ambiguous results (e.g. (116)). The results presented in Table 2 add quantification to the argument about appropriate length of patient follow-up. There was little difference between apparent cure rate at days 28 and 63 for chloroquine and mefloquine (although, interestingly, many failures occurred after day 63 for CQ) but the results from LF and PQ suggest that following patients for only 28

days would detect less than 50% of drug failures and that, consequently, a 63 day follow would be extremely beneficial in obtaining good estimates of clinical efficacy.

The robustness of drug regimes to changes in individual parameter values are shown in Table 3 and suggest that both CQ and PQ regimens are most sensitive to changes in PK/PD parameters, followed by MQ and finally LF; typically LF could tolerate variation up to 10 fold higher than that of CQ or PQ implying it is a much more robust and 'forgiving' drug regimen. It also implies that mutation(s) would have to encode very large effects to produce a LF drug-resistant phenotype. The addition of artemisinins to these monotherapies increases their power to tolerate variation in PK/PD parameters helping to protect against the rise and spread of resistance. The size of the protective effect could be large (for example adding AR to LF more than doubled the LF IC50 value at which drug failure occurred; Table 3) but in general was relatively modest in allowing increases more in the order of 20-30% over the monotherapy value.

Tables 3 and 4 can be used to identify parameters having the largest effect on treatment outcome. The maximal parasite-killing rate, V, of the partner drug was consistently ranked as the most important. Unfortunately, it is probably the parameter that is least well estimated (Appendix 1) so better estimates of its magnitude and variance would be valuable data for investigating antimalarial drug action. The parasite intrinsic growth rate constant a was almost as important as V for most treatment regimens modelled. This supports recent suggestions that faster growing, more 'virulent' parasites may be better able to survive drug treatment (292); interestingly, our results suggest that it is 'virulence' caused by increased parasite growth rate rather than 'virulence' attributable to high parasitaemia that is likely to affect drug sensitivity (see later discussion about the role of parasite number present at time of treatment). The relatively low rank of artemisinin PK/PD parameters in logistic regression analysis (Table 4) are consistent with their stated role as providing protection against resistance to the partner and increasing speed of resolution of symptoms (reducing PCT) rather than being the primary determinate of treatment outcome.

The analyses shown on Table 3 and 4 consistently show that the slope of the concentration-effect curve had little effect on treatment outcome. When plotting the concentration-effect curve, the point of inflection is the point on a curve at which the curvature changes sign, this occurs where drug levels have decayed to the IC50 value. At drug levels greater than the

IC50 the drug effect increases with increasing values of *n*, at levels less than the IC50 drug effect decreases with increasing values of *n*. The results suggest that the two effects cancel out so that the slope has little effect on treatment outcome (we assume this could be shown algebraically from the above equations but are forced to leave this to researchers more mathematically gifted than us). This observation is important: an influential paper by Shen *et al.* (299) on HIV treatment argued that drugs with a high value of slope parameter would be much more effective. Our results suggest this cannot be extrapolated to antimalarials. The underlying reason is presumably because antiretroviral drugs are taken daily and maintained at high concentrations (when high values of *n* are beneficial) so the penalty paid by high *n* at low drug concentrations is never incurred. It should be noted that higher values of *n* will increase kill rates at higher concentrations so may therefore be important in rapidly clearing parasites following treatment and hence rapidly alleviating symptoms. We are aware of unpublished suggestions that changes in the value of *n* have been associated with increased resistance and our analysis suggest that these changes may be indirect consequence of structural alteration changing IC50 and/or V rather than being directly driven by selection on *n*.

An unexpected result from the simulations was the small apparent effect of initial parasitaemia on treatment outcome. It was consistently ranked as one of the least important factors influencing outcome (Table 4) and had no significant effect in the clinical trial simulation (Table 5). In contrast, most real clinical trials identify high parasitaemia as a strong risk factor for failure. Intuitively we might also expect an infection of 10^{11} parasites to be about 10 times more difficult to eradicate than an infection of 10^{10} parasites. First note that the odds ratio (OR) associated with initial parasitaemia is generally around 1.1 to 1.3 (Table 4) and highly significant, so it does have an effect, it is simply not one of the more important ones; its non-significance in Table 5 can be explained by the simulated clinical trial having only 400 subjects, thereby lacking statistical power to detect the effect. These results suggests that patients generating high drug concentrations and/or infected with more sensitive parasites can reliably clear infections irrespective of initial parasitaemia, whereas patients with low drug concentrations and/or more resistant parasites are unable to clear infections with any more than 10^{10} parasites. This argument implies there is only a small number of patients where drug concentrations and parasite drug sensitivity are sufficiently well balanced that initial parasitaemia becomes the decisive factor determining outcome. This raises the interesting possibility that the importance of initial parasitaemia in clinical trials may not be a

direct effect, but be due to confounding with other factor(s). Initial parasitaemia is such a good indicator of immunity that we used it as a surrogate for immune status in our simulations (Appendix 2; noting that we allowed immune status and parasite number to be independent variables in the simulations) so it may be that the significance of initial parasitaemia is due to its inverse correlation with host immunity. The other plausible confounding factor is that high parasitaemia at treatment is often associated with clinical symptoms which may affect drug absorption and metabolism (e.g. (178, 237, 356, 357, 359)).

The "clinical trial" simulations allowed us to assess whether the models produce results consistent with field data obtained in clinical trials. It also allowed us to interrogate the simulated field data to assess the usefulness of output measurements in typical clinical trial analysis because, unlike in real trials, we had access to all the parameter values that determine outcome. Using four variables commonly measured in the field we found both the effects of acquired immunity and the concentration of drug in the patient's serum on day-7 to be significant factors affecting the likelihood of treatment failures. A patient's age and the transmission intensity at time of treatment were both used as an indication of the effects of immunity on treatment outcome: transmission intensity was invariably associated with treatment outcome and the effect of age was also sometime significant. We ran numerous simulations of these clinical trials and although the basic patterns were consistent, there were large differences in parameter estimates between simulations (data not shown) even though they were based on random variables taken from the same parameter distributions and this effect may become more pronounced in real clinical trials that typically have fewer patients and lower failure rates. There have been suggestions that day 7 serum drug levels be collected as routine part of antimalarial drug effectiveness trials (362). Again, the detailed data produced by our simulations allow this suggestion to be quantified and examined in more detail. The simulations confirmed that low drug levels (here defined as below the 15th centile) are associated with increased odds of failing treatment (Table 6) but that, somewhat counter-intuitively, their predictive ability measured as sensitivity, specificity and area under the ROC curve was generally poor. The reason becomes obvious by considering the case of DHA+PQ drug. Failure rates in patients with low drug levels were 16.99% and with normal drug levels was 7.22%, giving an OR of 2.62. However, many people with normal levels failed treatment, while many people with low levels were successfully treated. Hence sensitivity and specificity were both fairly poor at 29% and 86% respectively. A practical use of day 7 serum levels is for drug effectiveness surveillance: if low levels are associated with

increased risk of failure then consideration should be given to increasing the drug dosage. Table 6 presents the population attributable risk percentage associated with low drug levels; in principle this predicts the reduction in failure rates that would occur if drug levels were increased so that no one was subsequently exposed to 'low' levels. However this is a crude method and underestimates the true effect. Increasing drug levels would not just prevent people from receiving 'low' levels, but would also increase every patient's drug levels thereby increasing cure rates among patients receiving 'normal' levels (and the possibility that some patients may develop high drug levels with potential risks of adverse events). It is impossible to quantify this effect from analysis of failure rates in clinical trials and is another instance where quantitative modelling of the type described here can contribute to predicting the benefits of increasing drug dosage rate.

The receiver operating characteristic (ROC) curve is a graphical representation of the trade-offs between sensitivity and specificity whose area under the curve (AUROC) quantifies the predictive power of the variable with a value of 1 indicating perfect predictive capability and a value of 0.5 indicating no predictive ability. The AUROC values given in Table 6 and the ROC curves presented in Appendix 3 suggest the day-7 serum to be at best a moderate predictor of treatment outcome. Our analysis allowed both human PK variation and differential levels of drug sensitivity in parasites. We conjecture that area under the ROC curve may even provide a clue as to why treatments may be failing. If they are failing due to under-dosing the AUROC should be high (low drug level is a good predictor of failure) while if parasite drug resistance is the main factor causing failure then drug levels should be less important determinants of treatment failure and the AUROC should be corresponding low (as in our simulations). Future work on the simulations will explicitly investigate how much information ROC curves may provide on the etiology of drug failure. In summary, we therefore recommend that clinical trials report not just the odds ratio of failure associated with low drug levels, but also present a ROC curve analysis.

Increasing tolerance, and possible resistance, to artemisinins has recently been observed (86, 241, 365) leading to intense speculation about how this will affect the overall effectiveness of ACTs (e.g. (47, 94)). An obvious question is how the protection afforded by artemisinins to its partner drugs changes as resistance evolves to artemisinins: is there likely to be 'safety margin' associated with artemisinins whereby large increases in its IC50 can be tolerated before its protective values falls, or is a linear fall in protection likely, or as a worst-case

scenario is a rapid decline in protective effective likely to occur? The results shown on Figure 1 suggest the latter scenario, supporting assertions that measures are urgently required to prevent the evolution and spread of artemisinin resistance (50, 87).

Two issues not directly addressed above are those of synergism and cross-resistance between drugs in a combination (note that the two factors are distinct). Modelling the effect of combination therapies on parasite numbers was achieved by assuming that the two drugs act independently (Equation 7). This is likely to be the case for most combinations with ACTs but other combinations, such as SP and atovaquone-proguanil, may well show synergy. Unfortunately, there is no universally accepted approach for determining synergism and antagonism, and the topic is fraught with controversy and confusion. Greco *et al.* (115) list no less than 13 different methods to determine synergism and, in a comprehensive review, Chou (64) says, "it is hard to find any other field in biomedical science that has more controversy and confusion than drug combinations"; he then cites Goldin & Mantel (111) as giving seven different definitions for synergism, none of them supporting the others. There appears to be no concise mathematical way of describing synergisms. The best way to incorporate synergism is likely to be the empirical approach taken by Gatton *et al.* (109) for SP who simply use isobolograms to predict the kill rate for any given concentration combination of the constituent drugs. In summary, incorporating synergy into these models is likely to be problematic, both philosophically and practically, so we do not attempt it here. We do note that this precludes use of this methodology to investigate combinations such as SP and atovaquone-proguanil. Cross-resistance may occur between drugs in a combination even though they act independently; for example there are concerns that parasites show cross-resistance to mefloquine and artemisinins (8, 225). This effect can be readily included using covariance terms between the IC50 (and/or max kill rates) values to each drug. This was not addressed here in the interests of simplicity and to avoid adding additional covariance terms, but it is important to recognize the assumption that PD parameters are independent can be easily relaxed.

Incorporation of the artemisinin component was the most simplified part of the simulation. The mechanism-based modelling assumes instant absorption and conversion of artemether and artesunate into its active form DHA. As noted above, this can be incorporated using a compartmental model where the compartments are the gut, artesunate/artemether unconverted in the serum and DHA in the serum after conversion. The different rates of these

processes may explain why the PK/PD parameter estimates differed for the three forms of artemisinins (fuller discussion of the time course and conversion of artemisinins can be found in Giao & de Vries (110)). We decided against incorporating an explicit compartment model at this stage to minimize model complexity and because calibration of the transfer rates between compartments would be problematic and probably contentious. Instead, we chose to calibrate models separately for each artemisinin variant (Table 1) and to present the results for the partner drugs with alternative artemisinin variants to demonstrate that the results are robust. A second limitation of the model for artemisinins was that it ignored the possibility that parasites enter a drug-induced dormancy stage in which they are unaffected by the drug, as has been suggested to occur for artemisinin (143, 182, 333) and, more recently, for atovaquone (253). Intuitively, it seems unlikely that this will affect the results: artemisinins in 3 day regimens do not clear all parasites so a small residue persisting in a dormancy stage may be negligible, especially as they are likely to 'recover' in a time scale where they are likely to encounter high residual levels of the partner drug. Furthermore, ignoring dormancy leads to overestimating the impact of the artemisinin component in clearing infection and the results shown above suggest that even an overestimated impact is secondary to the role played by the partner drugs (Table 4). We note that our approach of daily updating the parasite load and drug level was explicitly designed to make the calculations highly flexible and, in principle, we could incorporate the effects of dormancy by augmenting the parasites present each day by those predicted to be exiting the dormancy stage. In summary it would be possible to make the extension into compartmental models and dormancy but we leave this to future work.

A second way in which this mechanism-based modelling approach could be usefully developed in malaria is to make the simulations more specific to drugs and their human subjects. Drug absorption, distribution, metabolism and excretion can differ substantially in young children or infants, pregnant women, patients with severe disease and those with a HIV/AIDS co-infection (22). Most clinical trials are performed on non-pregnant adults with uncomplicated malaria and no co-morbidities for ethical reasons so it seems likely that, at least in the first instance, the impact of these factors on treatment outcome may be initially addressed by well-constructed and calibrated PK/PD model. Similarly we incorporated variation in PK/PD by assuming a CV of 30% across all parameters. Some parameters are likely to be much more variable (for example Mu *et al.* (225) reported IC50s over a 100 fold range) while others (possibly V?) may be much less variable. Incorporating parameter values

and associated distributions specific to individual drugs would give us confidence to extend the results into the quantitative domain useful for policy makers. One notable example is the use of fixed treatment dosages based on age or height bands where there will be considerable variation in drug concentrations within groups as a consequence of variation in body weight: dosages have to reliably cure all people within the band (while avoiding toxic concentrations) and it is not immediately obvious how to indentify the appropriate dosage for each band nor, consequently, how many bands would be required.

We do not suggest that pharmacological modelling of antimalarial treatment will ever replace the gold standard of clinical trials but it does appear capable of generating results that are entirely consistent with field observations. It has key advantages in speed, the ability to generate large data sets, the ability to rapidly compare different scenarios, and freedom from ethical restrictions on investigating factors such as poor compliance. The value of modelling is that it can take arguments that are predominantly verbal into a more explicit, quantitative domain; our objectives here were to improve our understanding of how antimalarial drugs act in general, what conclusions could be drawn about, for example, the impact of increasing levels of artemisinin resistance, and what data collected in the field may reveal about ACTs. It seemed reasonable to apply mechanism based PK/PD modelling to this problem. Future work will develop the methodology in more specific directions. In particular we will incorporate the absorption, conversion and distribution phases of the drugs. These are important in artemisinins where absorption lag times may be significant compared to their half-lives, and where conversion of artesunate and artemether to DHA may be relatively rapid. The absorption and distribution phases also determine peak serum concentrations of the partner drugs that may be important determinants of potential toxicity; this becomes important when designing fixed-dose regimens based on age, weight or height bands because dosages per Kg may vary widely within a band. We have also extended the mathematics to investigate drugs given as infusions (such as intravenous quinine) but have not presented this methodology in the interest of brevity. Finally, it would be informative to include the possibility that parasites may enter dormant stages where they are unaffected by drugs such as the artemisinins (143, 182, 333) and atovaquone (253). Meanwhile, we conclude that initial analyses of antimalarial PK/PD models are encouraging, qualitatively improve our understanding of how antimalarial PK/PD factors combine to determine treatment outcome and await future developments with interest.

Appendix 1

Calibration of models

The intrinsic growth rate *a*, was defined as growth rate in the absence of host immunity and drug effects (Equation 1 of the main text). Empirical studies differ in their estimates for the rate of parasite growth during the asexual stage in the blood. Kitchen (171, 172) suggested that in non-immune subjects, the multiplication averages 6-fold but can reach 20-fold every 2 day cycle. Later estimates by Kwiatkowski & Nowak (180) gave a maximal value of 16-fold for uninhibited parasite growth (such as in non-immune infants or naïve infected adults). Simpson *et al.* (302) used the estimates provided by Kitchen (171, 172) and assumed a single asexual parasite multiplies 10-fold every two days giving its instantaneous growth rate, *a*, as ln (√10)=1.15. Simpson *et al.* (302) utilized a PK/PD modelling approach analogous to ours, for this reason we chose their same estimate of *a* equal to 1.15.

The intrinsic growth rate *a* can be linked to parasite density using a model of logistic growth:

$$a_t = a \bullet \left(1 - \frac{P_t}{P_0}\right) \qquad [A1.1]$$

here a_t is the parasite growth rate at time *t* and *a* is the intrinsic growth rate; we assume that an infection has reached its logistic "carrying capacity" (P_0) at time of treatment. Note that Equation 7 assumes growth rate is a constant however if, as implied in Equation A1.1, growth rate is dependent on time, the integration of Equation 6 to Equation 7 is invalidated. We overcame this by using a constant growth rate within each half- or one-day time steps

calculated from the parasite number (P_t in Equation 8) at the end of the previous time step. As this modification had no significant effect on the outcome it was subsequently removed.

The maximal parasite-killing rate constants (V) came from clinical observations following treatment. The underlying assumption was that drug killing is maximal immediately after treatment (note the implicit assumption that drug concentration is effectively saturated and that higher killing rates would not occur at higher concentrations) so that the observed drop in parasite numbers reflects this maximal kill rate. Assuming the decline in parasitaemia is first order, the parasite count (P_t) at any given time (t) is given by

$$P_t = P_0 e^{-Vt} \qquad \text{[A1.2]}$$

where V is the maximal parasite-killing rate constant. It is often convenient to use the parasite reduction ratio (PPR) over a 2 day time step (reflecting a single parasite growth cycle) where PPR= P_0/P_2; consequently t = 2 days, $P_2 = P_0\ e^{-2V}$ so that PPR=$P_0/P_2 = 1/e^{-2V}$ giving the relationship between PRR and parasite-killing rate (V) as (355):

$$V = -0.5 \bullet \ln\left(\frac{1}{PRR}\right) \qquad \text{[A1.3]}$$

Values of IC50 and the drug dose/response slope factor came from *in vitro* assays. Both Nyugen *et al.* (237) and Dondorp *et al.* (86) used *in vitro* testing of drug sensitivity to assess the *ex vivo* antimalarial activity using parasite isolates obtained from infected individuals. The 50% inhibitory concentration (IC50) was determined using the log-probit approximation, to fit the concentration inhibition data (86). Earlier work by Brockman *et al.* (44) and Mayxay *et al.* (210) used the program WinNonlin to calculate the IC50 and slope value parameters of the concentration-response curve by fitting data to an inhibitory E-max model.

Human PK parameters, the elimination rate and volume of distribution, came from clinical studies. A problem was that estimates could vary widely depending on factors such as whether whole blood or serum was analyzed and laboratory methodology. Estimation of PK parameters for artemisinins is confounded by the hydrolysis of artemether and artesunate to

DHA that may occur *ex vivo* at ambient temperature if blood samples are not separated and stored rapidly (358). The selected values came from recent studies made in laboratories conforming to good laboratory practice and where we could be sure that samples had been properly taken, stored and prepared. In each study the blood sample was centrifuged immediately after sampling and the separated plasma was stored at between -25 (237) and -80ºC (57) until analysis. For each drug, the PK parameters were then derived from the plasma concentration-time profile using standard non-compartmental analysis.

The model parameters were analyzed as mean values and variation was added by using CV=0.3 to reflect the inter-individual variation. 95% of the values lie within two standard deviations (σ) of the mean so if CV =30%, then95% of the variable values lie within 40-160% of the mean, approximately a 4-fold range in the PK/PD parameters. This choice of CV was arbitrary but was intended to reflect the general belief that PK parameters in humans typically vary over a 3 to 4 fold range (although we cannot find a formal reference for this generally accepted rule of thumb).

Appendix 2

Incorporation of immunity into the calculations

There are several relatively sophisticated models for the acquisition of immunity to malaria infections incorporating non-specific immunity, strain-specific immunity and immunity to a repertoire of *var* antigenic profiles (e.g. (108, 221, 252)). These all run on two-day time steps so it would be relatively simple, but time consuming, to incorporate them into the PK/PD modelling. We have avoided doing so, partly because of the resources and time required, partly because these models are difficult to calibrate and make compelling and require more parameters that would obscure the main results of the PK/PD modelling, and partly because the stand-alone models described in the main text are explicitly designed to be integrated into OpenMalaria (311) which already has a sophisticate intrahost component that tracks immunity (Smith and Penny, personal communication).

The effects of immunity were briefly introduced using the surrogates of immunity presented by Pongtavornpinyo and colleagues (261, 262) and used in their modelling. These surrogates were as follows: parasite density in patent infections, probability of clinical symptoms in people with a patent infection and incidence of severe malaria. Pongtavornpinyo *et al*. (261) calibrated this relationship with field data relating each of the measures to age and annual entomological inoculation rate (EIR) (305). The immunity equations presented by Pongtavornpinyo *et al.* (261) were transformed to lie on a scale of 0 to 1 as follows:

1. The outcomes are inversely related to immunity, so the equations were multiplied by -1 to get a measure of immunity:

$$f(i) = f(P) \bullet (-1) \qquad [A2.1]$$

where f(i) is the newly transformed immunity equation and f(P) represents the original function derived by Pongtavornpinyo (261).

2. The minimum value of this function was assumed to occur when age and EIR are zero. The minimum number is negative (because the original equation has been multiplied by -1) so subtracting a negative number is equivalent to adding a number of that magnitude:

$$f(i) = \left(f(P) \bullet (-1)\right) - \left(-\min\right) \qquad [A2.2]$$

3. The maximum value of this new function was assumed to occur in people aged 25 living in an area with an EIR of 1000. Dividing through by the maximum should make all values lie between 0 and 1,

$$f(i) = \frac{\left(f(P) \bullet (-1)\right) - \left(-\min\right)}{\max} \qquad [A2.3]$$

Note that Pongtavornpinyo *et al.* (262) fitted polynomial curves to their data so minimum immunity value may not occur at exactly age=EIR=0 nor the maximum at age=25, EIR=1000 (although maximum and minimum did occur very close to these values). The calculations involving immunity therefore made a check that the immunity scale was not <0 (and if this occurred reset it to 0) and was <1 (any value >1 were reset to one)

These standardized relationships are shown on Figure A2.1. The function derived using the parasite density per person (Figure A2.1.A) gives a more gradual acquisition of immunity that we feel is more realistic (Pongtavornpinyo (261) also came to this conclusion although we recognize that this is purely subjective). Its standardized value as a function of age and EIR is

$$f(i) = -5.937e^{-0.001age + 0.000003EIR - 0.000002ageEIR} - 0.588e^{0.011age + 0.003EIR - 0.0045ageEIR} + 6.524 \qquad [A2.4]$$

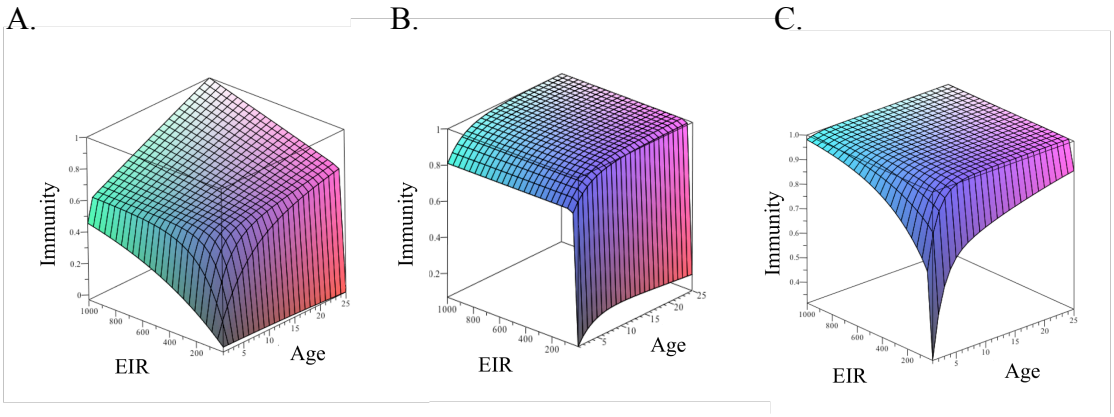

Figure A2.1. A graphical representation of Pongtavornpinyo's (2006) immunity functions after standardizing to lie between 0 and 1. A) Function derived using parasite density. B) Function based on incidence of severe malaria hospital admissions. C) Function based on the incidence of clinical malaria.

These values are standardized to lie between 0 and 1. We scale their impact by a parameter Φ to get the final immune killing function f(I) i.e.

$$f(I) = f(i) \bullet \phi$$

[A2.5]

We selected a value of Φ=0.8 on completely arbitrary grounds: it meant immunity was able to offset a parasites growth rate by almost two thirds (because a=1.15; Appendix 1) and gave an overall drug failure rate of around 16% in our clinical trail simulations. Note that immunity is only incorporated once into our simulations (to produce the simulated clinical trial data shown on Table 5) as a proof-of-concept and that all validation against field data was done assuming patients were non-immune. We included immunity here primarily for illustration and note that future researchers can easily fit and use other functions within the current framework.

Appendix 3

Miscellaneous outputs from the model

We use this Appendix to include data that support and expand some of the interpretations and conclusions drawn in the main text, but whose inclusion would detract from the main argument.

Logistic regression assumes the logit of the outcome changes linearly with the independent variables; this was checked by splitting the range of each variable into 10 evenly sized groups and plotting the percentage of successful treatments for each group (see Figure A3.1).

The correlation matrix (Table A3.1) for CQ, MQ and LF show AUC for days 0-25, days 0-50, days 0-100 and 0-∞ to be highly correlated to the day-7 serum concentration. PQ day-7 serum level was similarly highly correlated with AUC for days 0-25, days 0-50 and days 0-100 but, unusually, not strongly correlated with AUC for 0-∞.

The ROC curves used to determine the predictive ability of the day-7 serum level are shown in Figure A3.2; in each case the AUROC showed day-7 serum level to be a poor predictor of treatment outcome. The effects of low day-7 serum level remained consistent when different cut-off values, in this case the 10^{th}, 15^{th}, 20^{th} and 30^{th} centile values, were used to define low normal day-7 serum levels (Table A3.2). Table A3.3 gives the AUROC curve values for other potential diagnostic predictors of treatment outcome including serum levels on days 3, 5, 7 and 10 and the AUC between days 0-25, 0-50, 0-100 and 0-∞.

The period of chemoprophylaxis for the four partner drugs examined here showed a large amount of variation when model parameters were chosen assuming CV =0.3. We present the 5^{th} centile value in Table 2 but also include histograms showing the range of values in Figure

A3.3. Note that these values indicate times of drug protection afforded to re-infection by a moderately resistant parasite clone (1SD above the mean for parasite PD parameters and growth rate) so it is entirely plausible that, for example, a person predicted to have a PoC of 100 days would be re-infected much sooner by a more resistant or faster growing parasites clone

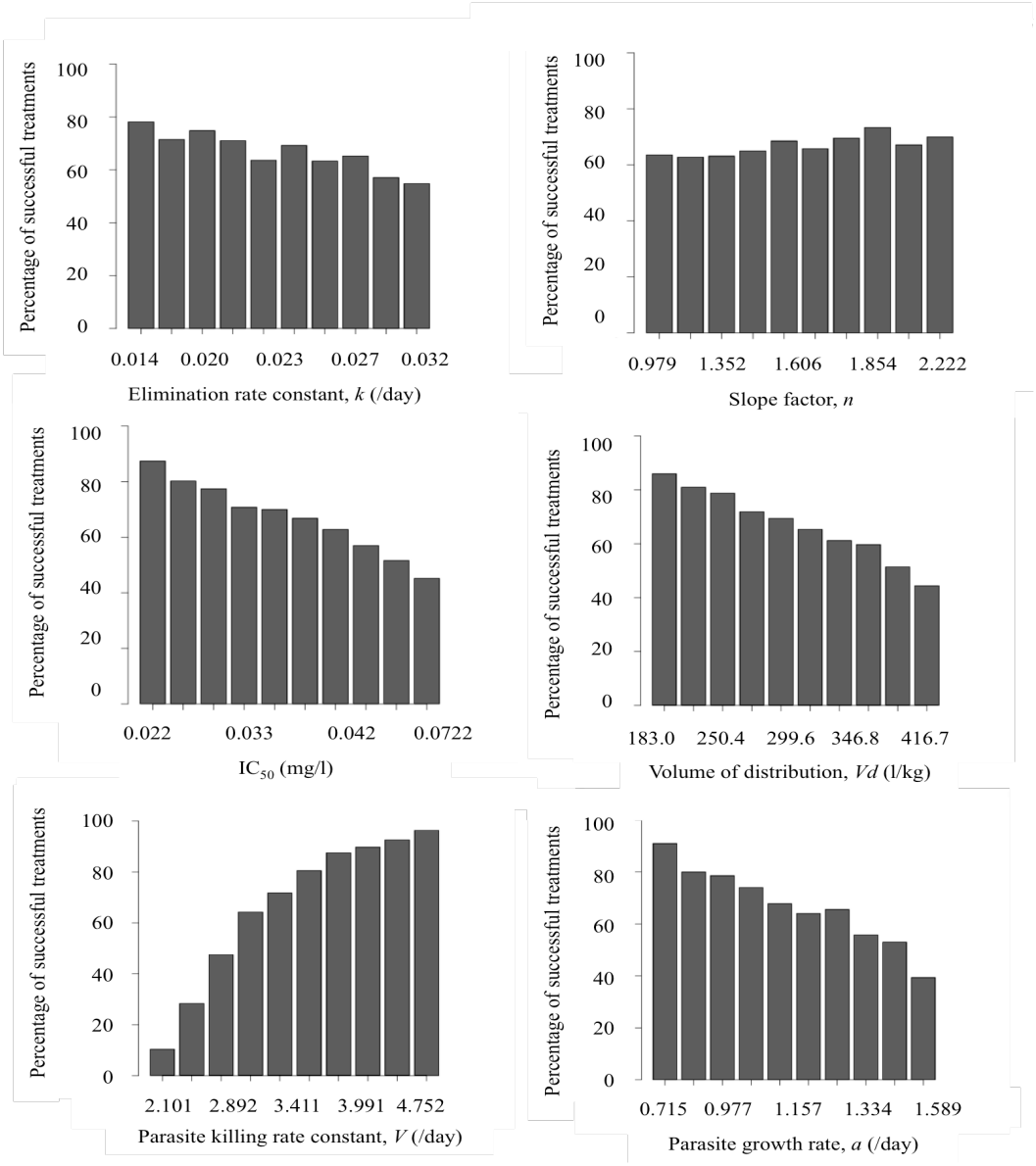

Figure A3.1. The risks associated with factors included in logistic regression analysis are assumed to be on a linear scale. The plot confirms this assumption is reasonable.

Table A3.1. Correlation matrix showing the high correlation between the diagnosis predictors for treatment outcome.

Chloroquine

Lumefantrine

	Day 3 serum concentration	Day 5 serum concentration	Day 7 serum concentration	Day 10 serum concentration	AUC 0-25	AUC 0-50	AUC 0-100	AUC 0-inf
Day 3 serum concentration	-	1.000	0.998	0.996	0.992	0.969	0.918	0.561
Day 5 serum concentration	0.998	-	1.000	0.998	0.995	0.975	0.929	0.572
Day 7 serum concentration	0.992	0.998	-	0.999	0.997	0.981	0.939	0.584
Day 10 serum concentration	0.979	0.989	0.996	-	0.999	0.987	0.950	0.597
AUC 0-25	0.985	0.993	0.998	0.999	-	0.993	0.961	0.613
AUC 0-50	0.969	0.980	0.989	0.996	0.996	-	0.987	0.657
AUC 0-100	0.954	0.967	0.977	0.987	0.988	0.997	-	0.709
AUC 0-inf	0.932	0.945	0.956	0.968	0.969	0.984	0.993	-

Mefloquine

Piperaquine

	Day 3 serum concentration	Day 5 serum concentration	Day 7 serum concentration	Day 10 serum concentration	AUC 0-25	AUC 0-50	AUC 0-100	AUC 0-inf
Day 3 serum concentration	-	0.998	0.992	0.981	0.974	0.927	0.866	0.584
Day 5 serum concentration	0.999	-	0.998	0.991	0.987	0.948	0.893	0.608
Day 7 serum concentration	0.997	0.999	-	0.997	0.995	0.965	0.917	0.630
Day 10 serum concentration	0.993	0.997	0.999	-	0.999	0.981	0.941	0.654
AUC 0-25	0.987	0.992	0.996	0.999	-	0.987	0.951	0.668
AUC 0-50	0.955	0.965	0.974	0.983	0.990	-	0.988	0.721
AUC 0-100	0.895	0.910	0.924	0.940	0.954	0.986	-	0.774
AUC 0-inf	0.562	0.577	0.592	0.609	0.627	0.676	0.729	-

TABLE A3.2. The effects of 'low' day-7 serum levels on the predicted outcome of treatments. 'Low' was defined as either <10th, <15th, <20th and <30th centile.

Drug	Output*					
	Centile	OR	Sensitivity	Specificity	AUROC	PAR %
Chloroquine	10th	2.34 (2.01-2.73)	0.18 (0.16-0.12)	0.91 (0.91-0.92)		8.99
	15th	2.15 (1.88-2.46)	0.25 (0.23-0.27)	0.87 (0.86-0.87)	0.63	11.58
	20th	2.16 (1.91-2.45)	0.32 (0.30-0.34)	0.82 (0.82-0.82)	(0.62-0.65)	15.10
	30th	2.19 (1.96-2.46)	0.45 (0.43-0.48)	0.73 (0.72-0.73)		21.79
Chloroquine plus Artesunate	10th	2.22 (1.88-2.62)	0.18 (0.16-0.20)	0.91 (0.91-0.91)		8.74
	15th	2.09 (1.81-2.41)	0.25 (0.23-0.27)	0.86 (0.86-0.87)	0.63	11.57
	20th	2.10 (1.84-2.39)	0.32 (0.20-0.35)	0.82 (0.81-0.82)	(0.61-0.64)	15.06
	30th	2.16 (1.91-2.45)	0.46 (0.43-0.48)	0.72 (0.17-0.19)		22.22
Lumefantrine	10th	2.24 (1.88-2.67)	0.18 (0.16-0.21)	0.91 (0.91-0.91)		9.18
	15th	1.93 (1.65-2.26)	0.24 (0.22-0.27)	0.86 (0.86-0.86)	0.62	10.53
	20th	1.99 (1.72-2.30)	0.31 (0.29-0.34)	0.81 (0.81-0.82)	(0.60-0.63)	14.30
	30th	1.95 (1.71-2.23)	0.44 (0.41-0.47)	0.72 (0.71-0.72)		19.59
Lumefantrine plus Artesunate	10th	2.20 (1.80-2.69)	0.19 (0.16-0.21)	0.91 (0.91-0.91)		9.41
	15th	1.92 (1.61-2.30)	0.24 (0.21-0.27)	0.86 (0.86-0.86)	0.60	10.84
	20th	1.76 (1.49-2.08)	0.30 (0.27-0.33)	0.81 (0.81-0.81)	(0.58-0.62)	11.94
	30th	1.89 (1.62-2.20)	0.44 (0.40-0.47)	0.71 (0.71-0.71)		19.29
Lumefantrine plus Artemether	10th	1.34 (1.01-1.77)	0.13 (0.10-0.16)	0.90 (0.90-0.90)		3.08
	15th	1.35 (1.07-1.72)	0.19 (0.16-0.23)	0.85 (0.85-0.85)	0.56	4.76
	20th	1.40 (1.13-1.73)	0.26 (0.22-0.30)	0.80 (0.80-0.81)	(0.53-0.58)	6.93
	30th	1.37 (1.13-1.66)	0.37 (0.32-0.41)	0.70 (0.70-0.71)		9.40
Mefloquine	10th	1.47 (1.13-1.93)	0.14 (0.11-0.17)	0.90 (0.90-0.90)		4.23
	15th	1.39 (1.10-1.76)	0.20 (0.16-0.23)	0.85 (0.85-0.85)	0.55	5.24
	20th	1.56 (1.27-1.92)	0.28 (0.24-0.32)	0.80 (0.80-0.81)	(0.53-0.58)	9.52
	30th	1.42 (1.18-1.72)	0.37 (0.33-0.42)	0.70 (0.70-0.71)		10.64
Mefloquine plus Artesunate	10th	1.24 (0.91-1.69)	0.12 (0.09-0.16)	0.90 (0.90-0.90)		2.21
	15th	1.24 (0.96-1.62)	0.18 (0.14-0.22)	0.85 (0.85-0.85)	0.54	3.36
	20th	1.47 (1.17-1.85)	0.27 (0.23-0.31)	0.80 (0.80-0.80)	(0.51-0.57)	8.16
	30th	1.30 (1.05-1.60)	0.36 (0.31-0.40)	0.70 (0.70-0.70)		7.80
Piperaquine	10th	2.87 (2.42-3.39)	0.22 (0.19-0.24)	0.91 (0.91-0.92)		12.83
	15th	2.56 (2.20-2.97)	0.29 (0.26-0.31)	0.87 (0.86-0.87)	0.65	15.95
	20th	2.50 (2.17-2.88)	0.36 (0.33-0.39)	0.82 (0.81-0.82)	(0.63-0.67)	19.84
	30th	2.58 (2.26-2.95)	0.50 (0.47-0.53)	0.72 (0.72-0.73)		28.43
Piperaquine plus DHA	10th	2.86 (2.39-3.41)	0.22 (0.19-0.24)	0.91 (0.91-0.91)		13.08
	15th	2.62 (2.24-3.07)	0.29 (0.27-0.32)	0.86 (0.86-0.87)	0.65	16.78
	20th	2.58 (2.22-2.99)	0.37 (0.34-0.40)	0.82 (0.81-0.82)	(0.63-0.66)	20.94
	30th	2.60 (2.26-2.30)	0.50 (0.47-0.54)	0.72 (0.72-0.72)		29.07

Table A3.3. Area under the ROC curve for various diagnostic predictors of treatment outcome, obtained for several drug monotherapies and combination therapies [a]

Drug	Variable								
	Day 3 serum level	Day 5 serum level	Day 7 serum level	Day 10 serum level	AUC_{0-25}	AUC_{0-50}	AUC_{0-100}	$AUC_{0-\infty}$	Treatment success (%)
Chloroquine	0.626	0.629	0.632	0.636	0.639	0.647	0.649	0.647	85.36
Chloroquine plus Artesunate	0.621	0.624	0.627	0.630	0.633	0.639	0.640	0.637	88.09
Lumefantrine	0.531	0.554	0.569	0.580	0.571	0.574	0.575	0.575	89.59
Lumefantrine plus Artesunate	0.525	0.542	0.554	0.562	0.555	0.557	0.557	0.557	92.63
Lumefantrine plus Artemether	0.498	0.503	0.508	0.513	0.508	0.508	0.508	0.508	95.43
Mefloquine	0.544	0.549	0.554	0.559	0.560	0.566	0.568	0.568	95.22
Mefloquine plus Artesunate	0.531	0.535	0.538	0.542	0.543	0.548	0.549	0.549	96.08
Piperaquine	0.637	0.637	0.642	0.652	0.657	0.664	0.665	0.664	90.18
Piperaquine plus DHA	0.636	0.641	0.645	0.650	0.654	0.661	0.663	0.661	91.33

[a] The 10,000 patients included in the analysis were simulated as described in the main text

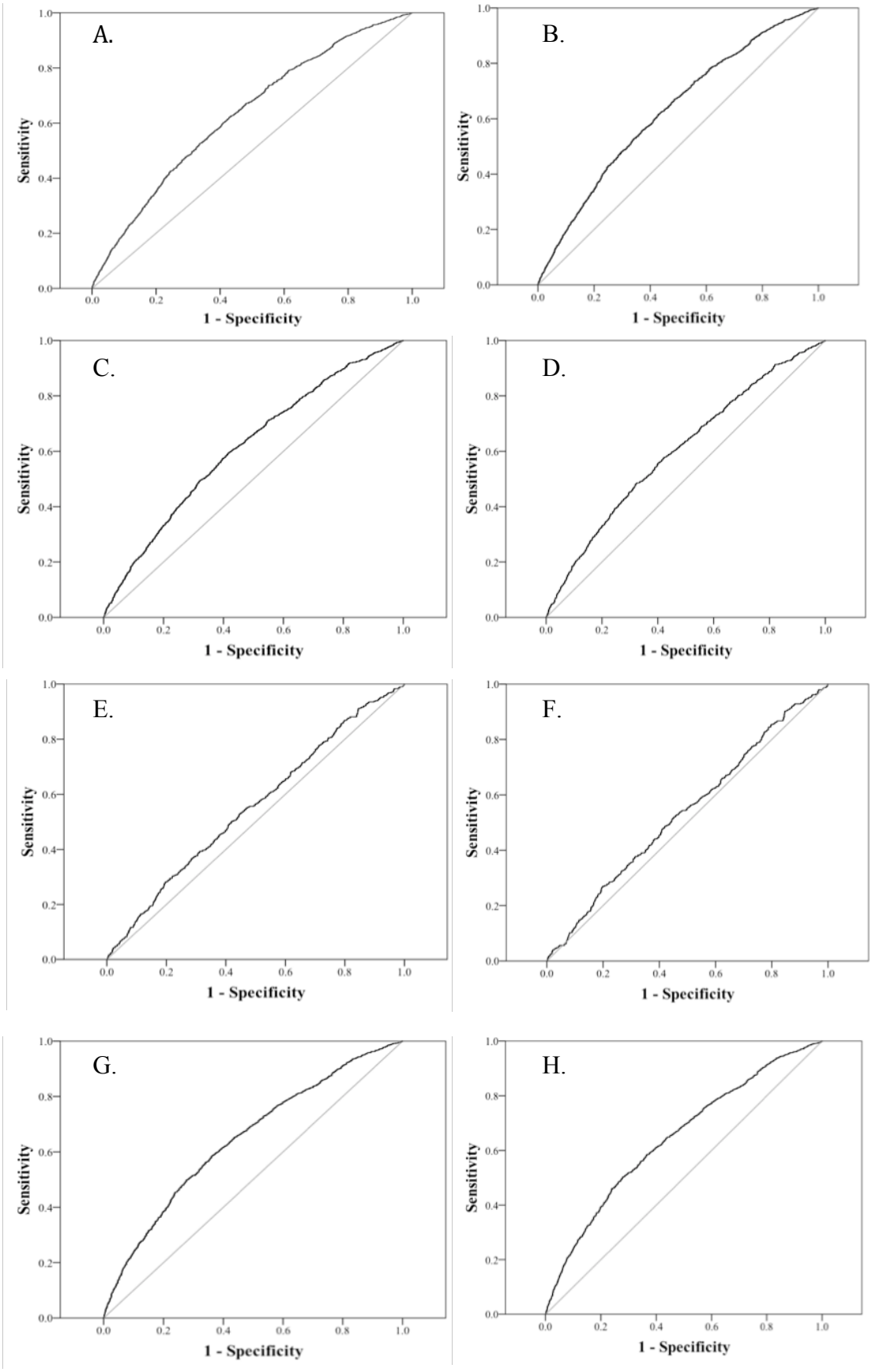

Figure A3.2. The ability of day-7 serum concentrations to predict treatment success or failure was examined using ROC curves for 8 drug regimens; (A) CQ, (B) AS-CQ, (C) LF, (D) AS-LF, (E) MQ, (F) AS-MQ, (G) PQ, (H) DHA-PQ

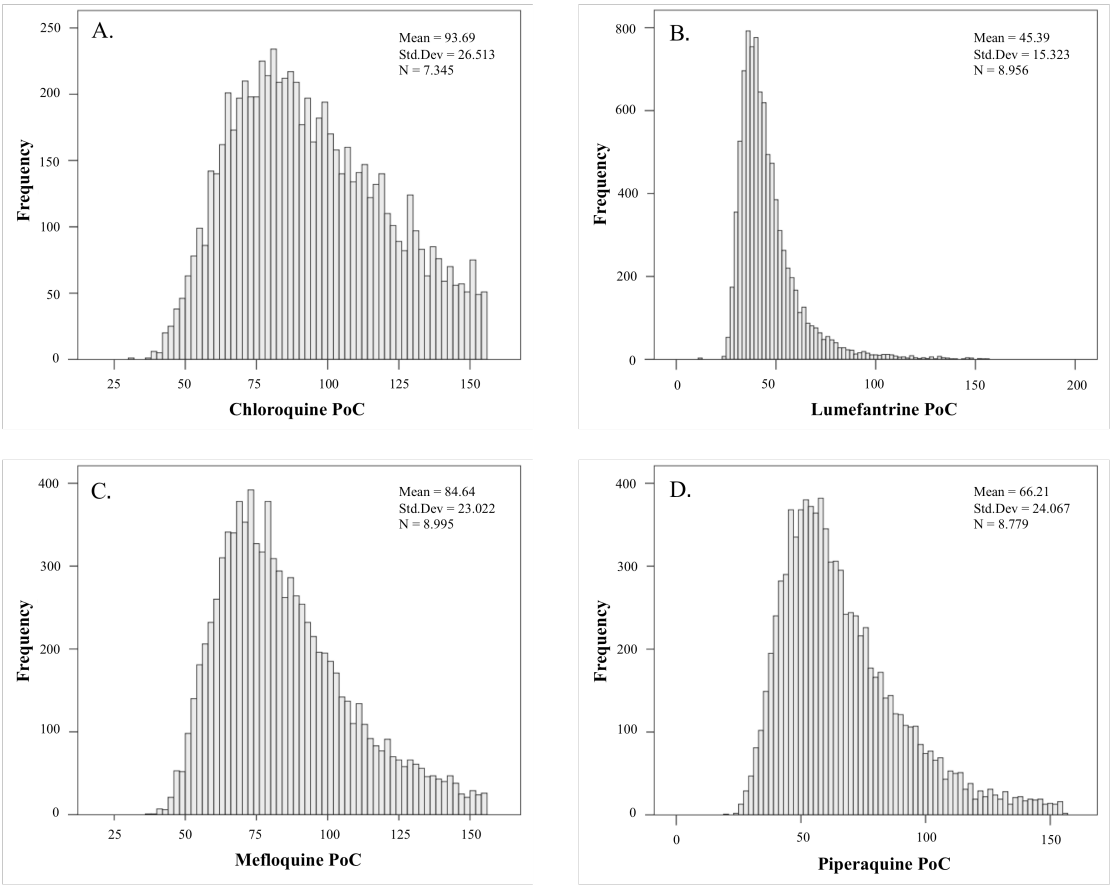

Figure A3.3. The period of chemoprophylaxis (PoC) of the four partner drugs (A) chloroquine, (B) lumefantrine, (C) mefloquine, (D) piperaquine. Using only data from patients who were successfully treated.

Chapter 3

Improving pharmacokinetic-pharmacodynamic modeling to investigate anti-infective chemotherapy with application to the current generation of antimalarial drugs

ABSTRACT

Mechanism-based pharmacokinetic-pharmacodynamic (PK/PD) modelling is the standard computational technique for simulating the drug treatment of infectious diseases with the potential to enhance our understanding of drug treatment outcomes, drug deployment strategies and dosing regimens. Standard methodology has assumed that only a single drug is used, which acts only in its unconverted form, and that oral drugs are instantaneously absorbed across the gut wall to their site of action. Treatment of infectious diseases often uses combination therapies so we show how the PK/PD methodologies can be refined and substantially extended to incorporate (i) the time lags and drug concentration profiles resulting from absorption across the gut wall and, if required, conversion to another active form (ii) multiple drugs within a treatment combination (iii) differing modes of action of drugs in the combination: additive, synergistic, antagonistic (iv) modelling drugs converted to an active metabolite with a similar mode of action. This methodology was applied to a case study of two first-line treatments of malaria based on artemisinin combination therapies (ACTs, artemether-lumefantrine and artesunate-mefloquine) where the likelihood of increased artemisinin tolerance / resistance has lead to speculation on their continued long-term effectiveness. We note previous estimates of artemisinin kill rate were underestimated

by a factor of seven and that the extended PK/PD methodology produced result consistent with field observations. The simulations predict that a potentially rapid decline in ACT effectiveness is likely to occur as artemisinin resistance spreads, emphasising the importance of containing the spread of artemisinin resistance before it results in widespread drug failure. We found that PK/PD data is generally very poorly reported in the malaria literature, severely reducing its value for subsequent re-application, and make specific recommendations to improve this situation.

1. Introduction

Most human infections are currently treatable by drugs. Clinical trials remain the gold standard, empirical approach guiding drug deployment policy and practical issues such as dosing regimes. However *in silico* simulations based on computational predictions of drug treatment outcome have the potential to play a vital ancillary role in designing and guiding these deployment practices. Accurate simulations can rapidly investigate the consequences of putative changes in deployment practices such as changes in regimen (dosage level, frequency and duration of treatment) and can investigate and potentially quantify the threat posed by the evolution of drug resistance. The methodology used to investigate such factors *in silico* is mechanism-based PK/PD modelling, whose basic methodology and range of applications was recently reviewed by Czock and Keller (73). In essence, this approach uses differential equations to calculate the decline in drug concentration after treatment, converts this into a pathogen killing rate, to find how pathogen number declines after treatment and whether the infection is eventually cleared. The PK/PD methodology assumes a single drug is instantaneously present in the patient after treatment (drug absorption and conversion processes are ignored) and that pathogens are killed by the drug in its unaltered form. In practice, drug combinations are now mandatory for the treatment of many infections, including the 'big three' infective killers HIV, TB and malaria so the single-drug PK/PD methodology needs to be updated to reflect these policies. Many drugs also have short half-lives so the time taken for their absorption (across the gut in the case of oral regimens) may be a significant period relative to half-life and needs to be incorporated into the methodology. Finally, many drugs undergo conversion in the human (often in the liver) to other active

forms that also kill the pathogens. This manuscript describes the computational extensions required to update the standard mechanistic-based modelling approach to allow for multiple drugs within a combination, and their absorption/conversion phases. We then illustrate their application to the current batch of first line antimalarial drugs, the artemisinin-based combination therapies (ACTs).

Malaria caused by *Plasmodium falciparum*, is one of the top three infective killers of humans with an estimated 0.75 to 1.5 million deaths per annum. ACTs are now the WHO recommended first-line treatment for uncomplicated malaria (380). The deployment of these combination therapies was designed to slow or even prevent the evolution of drug resistance which has, historically, been a potent threat to successful malaria treatment; delays in changing policy led to the widespread retention of ineffective drugs and acrimonious accusations of 'medical malpractice' aimed at such august institutions as the World Health Organisation (15) and the malaria community must prevent any similar situation ever arising. However, the policy of deploying ACTs worldwide has lead to increasing levels of artemisinin-tolerance and possibly artemisinin-resistance in *Plasmodium falciparum* being reported on the Cambodia-Thailand border (52, 86, 87, 241, 365) leading to intense speculation about how this will affect the current and future effectiveness of ACTs (e.g. (47, 94)). It is not possible to directly observe the consequences of antimalarial drug resistance until it is too late, so the best approach is to develop the best possible *in silico* models to help guide deployment policies aimed at maintaining long-term effectiveness of these key anti-infective drugs. We therefore apply our updated *in silico* PK/PD modelling methodology to explicitly investigate two front-line ACTs and the public health consequences of increasing tolerance and resistance. Accurate PK/PD modelling has two further important applications. Firstly, it can generate accurate simulations of field data upon which methods of analysis can be developed and refined (158); the underlying parameters of interest are often unknown in field data but are easily recovered from simulated data enabling the performance of statistical tests to be gauged. Secondly, they can be used to investigate real-life situation that cannot be ethically addressed in the field, an obvious example being poor adherence to a treatment regimen.

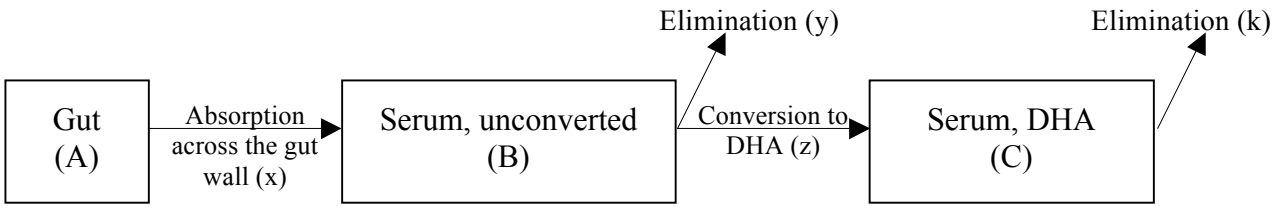

Figure 1. A standard PK one-compartment model allowing for absorption of a drug from the gut (component A) at rate x, into the unconverted form in the serum (component B) where it is eliminated at a rate y and converted into an active form (DHA in this example; component C) at rate z. DHA is then eliminated at rate k.

2. Methods

Mathematical extensions of the basic model

We use mechanistic PK/PD modelling (73) as previously described in Winter & Hastings (364) with the four key extensions outlined below.

2.1. Pharmacokinetics – incorporating the absorption, conversion and elimination of drugs

Standard PK/PD models (73) and their subsequent application to malaria (16, 144, 149, 302, 364) have previously assumed the drugs are instantaneously present in the serum at time t=0, are not converted to any other form and decay at a rate $C_t=C_0e^{-kt}$, where C_t is the drug concentration at time t and k is the terminal elimination rate. This assumption is questionable for ACTs as their absorption and subsequent conversion to its active metabolite dihydroartemisinin (DHA) occur over a time period of 1-2 hours, roughly equivalent to their half-life (Figure A1). To address this assumption we track the time course of artemisinin absorption and conversion as illustrated in Figure 1 i.e. absorption across the gut (component

A) into the serum (component *B*) at rate *x*, its elimination from the body at rate *y* or its conversion to the active metabolite (DHA) (component *C*) at rate *z* and the subsequent elimination of DHA from the body at rate *k*.

The drug-dependent killing function, *f(C)*, was described using the standard Michaelis-Menten equation

$$f(C) = V \bullet \left(\frac{C^n}{C^n + IC_{50}{}^n} \right) \qquad [1]$$

where *C* is the drug concentration (mg/l) which decays over time, *V* is the maximal drug-killing rate (per day), *IC50* is the concentration at which 50% of the maximal killing rate occurs (mg/l) and *n* is the slope of the dose response curve. The problem is therefore to find how *C* varies over time following treatment so that it can be incorporated into Equation 1.

We use a standard one-compartmental model (Figure 1) that appears appropriate for constituents of current ACTs (Appendix, part 2), to track the changes in concentration over time. To avoid confusion, we note that "one compartment" is used in the standard PK sense i.e. only one body compartment (in this case, serum) is investigated besides the gut. The change in drug concentration occurring for each component over time (allowing for complications caused by the presence of the drug/metabolite from previous dosages) can be described by three differential equations

$$\frac{dA}{dt} = -Ax \qquad [2]$$

$$\frac{dB}{dt} = Ax - By - Bz \qquad [3]$$

$$\frac{dC}{dt} = Bz - Ck \qquad [4]$$

To find the amount of converted and unconverted drug in the serum at time *t*, Equations 3 and 4 were integrated using laplace transformations (209) (Appendix, part 1). Integrating Equation 3 gives

$$B(t) = \frac{x(D + A`)}{(x - (y + z))}\left(e^{-(y+z)t} - e^{-xt}\right) + B`e^{-(y+z)t} \qquad [5]$$

where *B(t)* is the amount (mg) of unconverted drug in the serum at time *t, A`* is the amount (mg) of drug in the gut at the immediate end of the previous time step i.e. at *t*=0 (*A`*=0 if this is the first dose of a multi-dose regimen), *D* is the drug dosage (mg) given and *B`* is the amount (mg) of unconverted drug in the serum at the immediate end of the previous time period i.e. at *t*=0 (*B'*=0 if it is the first dose). Inclusion of any drug left over from the previous day (denoted *A`*, *B`* and *C`*) is essential when including repeat dosages.

Integrating Equation 4 (Appendix, part 1) gives

$$C(t) = \left(zx(D + A`)\left[\frac{e^{-kt}}{(y + z - k)(x - k)} + \frac{e^{-qt}}{(k - (y + z))(x - (y + z))} + \frac{e^{-xt}}{(k - x)(y + z - x)}\right] + \frac{zB`}{(y + z - k)}\left(e^{-kt} - e^{-(y+z)t}\right) + C`e^{-kt}\right)\frac{M_C}{M_B} \qquad [6]$$

where *C(t)* is the amount of converted drug present in the serum, *k* is the elimination rate of the converted drug, *C`* is the amount (mg) of converted drug in the serum at the immediate end of the previous time step (*C`*=0 for the first dose) and *M* represents the molecular weight of both the unconverted drug (M_B) and converted drug (M_C). We are tracking drugs in mg so the ratio of the molecular weights of species *B* and *C*, M_B and M_C respectively, are required to account for the changes in molecular weight that occur during conversion.

The drug-dependent killing described in Equation 1 required the amount of drug to be converted to a concentration (mg/l). This was found by dividing the amount of drug by the volume of distribution (l) which is the weight of the patient *W*, multiplied by the volume of distribution *Vd* per kg. The value of *Vd* differs between the drugs so Vd_B and Vd_c represent volumes of distribution for drug forms B and C respectively.

The concentration of component *B* at time *t*, $C_B(t)$, is therefore

$$C_B(t) = \frac{B(t)}{W \bullet Vd_B} \qquad [7]$$

and the concentration of component *C* at time *t*, $C_C(t)$ is

$$C_c(t) = \frac{C(t)}{W \bullet Vd_C} \qquad [8]$$

The use of laplace transformations in PK is relatively well established (209) so it would be straightforward to extend the calculations for increasing numbers of compartments, drug forms and conversion elimination routes.

2.2. Pharmacodynamics – parasite killing by multiple drugs

The PK/PD modelling now allows for artemisinin absorption and conversion (described above), so the ability to track more than two drug concentrations simultaneously and convert them into a drug-killing rate is crucial. This feature is absent from previous pharmacological models of malaria, which track only a single drug (73) although we previously extended the methodology to track up to two drugs (364). Existing pharmacological models typically use a standard differential equation (73) to find a mathematical description for the rate of change in total parasite growth and death rates

$$\frac{dP}{dt} = P\left(a - f(I) - f(C)\right) \qquad [9]$$

where *P* is the number of parasites in the infection, *t* is time after treatment (days), *a* is the parasite growth rate (per day), *f(C)* represents the drug-dependent rate of parasite killing

which depends on the drug concentration C, and $f(I)$ the killing resulting from the hosts background immunity.

As antimalarial drugs are now typically deployed as combination therapies and as each drug may affect parasites in its unconverted and/or converted forms, predicting the changing numbers of parasites requires an expansion of Equation 9

$$\frac{dP}{dt} = P\left(a - f(I) - \sum_{d=1}^{r} f(C_d)\right) \qquad [10]$$

where r is the number of drugs, the drug effect $f(C_d)$ is the effect of each drug, d. Note that we regard each active entity as a distinct "drug". For example artemether-lumefantrine (AR-LF) includes three drug forms lumefantrine (LF), artemether (AR) (unconverted) and its active metabolite DHA (dihydroartemisinin). Note that Equation 10 assumes drugs kill independently; this is discussed further below

Integrating Equation 10 allows us to predict the number of parasites at any time, t, after treatment with any number of drugs. This was done by first integrating Equation 9 using the separation-of-variables technique

$$\frac{1}{P}dP = \left[a - f(I) - f(C)\right]dt \qquad [11]$$

Integrating both sides of Equation 11 gives

$$\int_0^t \frac{1}{P}dP = \int_0^t \left[a - f(I) - f(C)\right]dt$$

so

$$\ln\left[P_t\right] - \ln\left[P_0\right] = \int_0^t a\,dt - \int_0^t f(I)dt - \int_0^t f(C)dt = at - a0 - f(I)t - f(I)0 - \int_0^t f(C)dt$$

Taking the exponential of both sides (and noting that *a* times *0 =0*) gives

$$\frac{P_t}{P_0} = e^{(a-f(I))t} - \frac{1}{e^{\int_0^t f(C)dt}}$$

so

$$P_t = P_0 \bullet e^{(a-f(I))t} \bullet \frac{1}{e^{\int f(C_d)\bullet dt}} = P_0 e^{(a-f(I))t} e^{-\int_0^t f(C)dt}$$

[12]

The problem is now to integrate *f(C)*. Assuming there are *r* separate drugs/metabolites with antimalarial activity. In this case, *f(C)* becomes

$$f(C) = \sum_{d=1}^{r} f(C_d)$$

[13]

So for each drug/metabolite *d* we need to calculate its concentration over time C_d using the compartment model Equations (7 and 8) and the substitute C_d into the killing rate equation

$$f(C_d) = \frac{V_d \bullet {C_d}^n}{{C_d}^n + {IC_{50}}^n}$$

[14]

Note in Equation 14, V_d is the maximum drug killing *V* for drug *d*, not to be confused with the volume of distribution *Vd*.

Substituting Equation 13 into 12 gives

$$P_t = \frac{P_0 e^{(a-f(I))t}}{\prod_{d=1}^{r} e^{\int_0^t f(C_d)dt}}$$

[15]

or, equivalently,

$$P_t = P_0 e^{(a-f(I))t} \prod_{d=1}^{r} e^{-\int f(C_d)}$$

[16]

Note that C_d may be a complicated expression (including Equations 7 and 8) and so $\int f(C_d)$ has to be integrated numerically. As before (364), if the predicted parasite number (P_t) falls below 1 we assume the infection has been cleared and the patient cured, immunity is currently ignored (see Winter & Hastings (364) for further discussion).

2.3. Modelling drug killing when two or more drugs are present

These computational extensions to the mechanistic PK/PD modelling allow for the presence of two or more drug forms simultaneously present in the human host, and active against the infection. It therefore becomes necessary to consider and specify how these drug forms interact in their effect against the parasites. There appears to be four main computational choices.

Independent modes of action. This is the mode of action explicitly developed above and summarised in Equation 16. Most drug combinations are designed to contain drugs with independent modes of action, so this is a common scenario and would be revealed by drugs having additive action in pharmacodynamic studies (64).

Non-independent action. The total drug action may be greater than, or less than, that expected from the sum of the two drugs independently. This is commonly referred to as ‘synergy’ or ‘anatogonism’ but see Chou (64) for a fuller discussion of the dangers inherent in using these terms. It is difficult to even define these terms (64), still less quantify them, so an empirical approach based on data obtained from isobolograms (109) would have to be used to convert drug concentrations into killing.

Identical modes of action. This seems plausible if there are different, but structurally similar, forms of same drug; artemisinins are a good example in this context. One computational possibility is simply to use the sum of their concentrations in Equation 1 i.e.

$$f\left(C_x + C_y\right) = V \bullet \left(\frac{\left(C_x + C_y\right)^n}{\left(C_x + C_y\right)^n + IC_{50}{}^n} \right) \qquad [17]$$

Where x and y are the two forms. Problems arise if *V* or IC50 differ between the two forms. The maximal killing rate may plausibly be the same for each form but it is entirely plausible that structural differences between the forms alter binding of the drugs and hence their IC50 values. It is difficult to compute the joint killing under these circumstances because it is difficult to envisage how to weight the differing IC50 values.

Dominant form killing. This is a computational compromise. The amount of killing of each related drug form over a time period is calculated and the higher killing rate used in the calculations. This is particularly useful for rapidly eliminated drugs that are essentially either present at full effect or absent (see, for example, Figure A2). This is the approach we shall use for artemisinins in the analyses described below. So, for example, when modelling the artemisinins, the drug killing for both forms (i.e. the parent drug and the active metabolite) were calculated during each time step and the drug form with the higher parasite killing is used to update parasite numbers at the end of the time step.

2.4. Modelling artemisinin combination therapies

Pharmacological 'mechanism-based' modelling (73) has been used previously to investigate key features of antimalarial drug treatment either as monotherapies (16, 144, 149, 302) or with recent emphasis on the current generation of ACTs (364). We have previously touched upon the potential consequences of increasing artemisinin resistance using standard pharmacokinetic-pharmacodynamic (PK/PD) modelling techniques (364) however, as mentioned in the paper, the model relied heavily on two main assumptions built in to the existing methodology. First, that all drugs are instantaneously absorbed and, if appropriate,

converted to their active metabolites. Whilst this may be reasonable for drugs with a long half-life it is not practical for drugs like the artemisinins where absorption and conversion times are almost equal to their short half-lives. The second assumption, that no more than two drugs could be present simultaneously, was reasonable when modelling the ACTs if both drugs were instantaneously absorbed and converted. However, conversion of the artemisinins requires that the artemisinins be modelled as two separate component drugs i.e. the parent drug and the DHA metabolite together with the partner drug and so modelling the ACTs requires a minimum of three drugs be tracked simultaneously. Here we have addressed the methodological challenges of incorporating the absorption and conversion phases of drugs into PK/PD modelling while simultaneously tracking the concentration of more than two drugs, a feature absent in previous pharmacological models (16, 144, 149).

The PK/PD model parameters required to simulate treatment are given in Table A1 and described in the Appendix, part 2. The PK extensions for the artemisinins required additional parameters describing the drug absorption rate across the gut, the conversion rate to DHA and the elimination of DHA from the body (Figure 1). These parameters and their associated distributions can be found in Table A1 with details of model calibration and validation included in the Appendix (part 2). Variation in model parameters was previously (364) added assuming a coefficient of variation of 30% in all parameters. In reality, some parameters are much more variable (225) while others maybe less so. We now incorporate more appropriate levels of variation into the PK/PD parameters using drug specific distributions thus making results more compelling for specific ACTs. To validate the model's predictive ability, the maximum serum concentration (Cmax) and time to achieve Cmax (Tmax) were compared to field data (Appendix, part 2).

The methodology described above now allows for the action of both the unconverted and converted forms of the artemisinins. However, given that they have similar modes of action their effect on parasite numbers is unlikely to be additive (as is assumed in Equation 11). As such, the drug effect, $f(C)$, for each of the artemisinin forms was calculated each time-step but only the dominant form (i.e. parent drug or active metabolite) with the greater drug killing effect was used to compute the number of parasites in the next time step. Activity, and hence killing, of artemisinins and the partner drug were assumed to be independent.

A major change was made to the artemisinin maximal drug kill rate (V). Previous estimates of the V (360, 364, 399) have been based upon the assumption that drug killing is maximal immediately after treatment and remains so for 48 hours after treatment. This is quantified by the parasite reduction ratio (PRR); a ratio of the number of parasites at time of treatment scaled by their number 48 hours after treatment. So, assuming the decline in parasitaemia is first order, the parasite count (P_t) at any given time (t) is given by

$$P_t = P_0 e^{-Vt} \qquad [12]$$

where P_0 is the number of parasites present at the start of treatment.

This appears to be reasonable for drugs given at relatively high doses with a long half-life because the maximal killing will extend over the 48 hours after treatment. However, it is unrealistic for the artemisinins whose short half-lives mean parasites are typically only exposed to high concentrations of artemisinins during the first 6-8 hours following treatment (Figures S1 and S2). The steady decline in parasite numbers after this period presumably reflects dead or dying parasites being cleared by host mechanisms. PK/PD modelling of drug effect assumes deaths only occur in the presence of the drug (i.e. 6-8 hours post-treatment) hence the need for this increased kill rate. So, given PRR = P_0/P_t (360) (where P_t is usually assumed to be 48 hours), the relationship between PRR and parasite killing rate V is

$$V = -\frac{1}{t}\ln\left(\frac{1}{PRR}\right) \qquad [13]$$

When t is assumed to be 48 hours then the maximal drug kill rate (V) is 4.6 (360, 364). However, if we assume artemisinin maximal drug killing occurs only during 6 hours with a PRR of 1000 (White (360) gives a range of 10^3 to 10^5 for the artemisinins) then V is 27.6. Note, if the maximal drug killing is assumed to occur over 8 hours and the PRR is assumed to be 10,000 (within the range reported in White (360)) V again equals 27.6. consequently our artemisinin maximum killing rate is approximately 7-fold higher than in previous simulations.

Two treatment combinations were investigated, artesunate-mefloquine (AS-MQ) and AR-LF, both are highly effective ACTs currently used to treat malaria. Variation in how humans metabolise the drug and parasite drug sensitivity was added to the model parameters (Table A1) using parameter specific estimates of co-efficient of variation, CV. The technical details regarding parameter variability are included in the Appendix, part 2.

The extended pharmacokinetic-pharmacodynamic (PK/PD) model can then be implemented to address a critical feature of current ACT deployment: how is the observed increase in artemisinin tolerance likely to affect the long-term effectiveness of ACTs? The crucial operational question is whether there is likely to be a sudden catastrophic decrease in ACT effectiveness, a gradual decline or, a best case scenario, a margin of safety such that we can have relatively large increases in artemisinin tolerance/resistance before ACT failures start to increase?

The partner drugs, LF and MQ, are currently largely effective monotherapies (if administered correctly) so increasing artemisinin resistance would, by definition, have little or no impact on therapeutic outcome. To avoid this trivial case, we investigated how increasing levels of artemisinin resistance impacted treatment failure rates if resistance to the partner drug was already present or spreading. When modelling MQ treatments the MQ IC50 values were either 1-, 2-, 5-, 10-, 15-, 20- or 25-fold greater than the current default value (TableA1) and when modelling LF treatments LF IC50 values were either 1-, 2-, 5-, 10-, 20-, 25- or 50-fold greater than the current default value (Table A1). Resistance to artemisinins was investigated in two ways. First by increasing the IC50 of the AS, AR or DHA (the active metabolite) independently and then by assuming the IC50s of the parent species and DHA were completely correlated i.e. the IC50s were increased simultaneously by the same amount. This was necessary because it is not clear whether parasites will evolve resistance independently to the artemisinin entities or whether there will be substantial cross-resistance to different entities (see later discussion) The IC50 range of both artemisinin forms included one value 10-fold smaller than the mean and values 1-, 20-, 40-, 80- or 100-fold greater than the mean.

Details of implementation are in the Supplementary Information, part 3. For each of the 10,000 patients simulated the model recorded whether an infection (with one clone) was cleared and, if so, the parasite clearance time (PCT; defined as the time taken for an infection to fall below the limit of microscopic detection, which was assumed to be 10^8). This was

done first for the partner drugs without the artemisinin component, i.e. as monotherapies, to give a baseline failure rate. Then, by comparing the results of the monotherapy with those of the ACTs we were able to quantify the ability of the artemisinin component to reduce failure rates and PCTs.

3. Results

The artemisinin drug concentration profiles of the model are consistent with those measured in the field (Figure A1). Analysis of both ACTs showed that adding an artemisinin to a partner drug reduced failure rates below that of the monotherapy regardless of the initial levels of partner drug resistance (Figure 2), except for the trivial case when partner drugs were fully effective as monotherapies. For AS-MQ, the exact proportion of failures prevented by the artemisinin component was dependent on the initial level of resistance to the partner drug. Regardless of whether the IC50s of the artemisinins were correlated, adding an artemisinin at its default IC50 value to a partner drug reduced failure rates by between 70 and 90%. This is a relative reduction, for example, a 50% reduction is equivalent to fall in failure rates from 40% to 20% or from 12% to 6% (Figure 2, panels A, C and E). The observation that adding AS to a standard monotherapy (chloroquine, amodiaquine, sulfadoxine-pyrimethamine and MQ) reduced the absolute risk of failing treatment but did not result in a fully effective ACT was in line with results seen in the field (1). The results also show that the addition of AR to LF monotherapies reduced failure rates to zero when modelling the mean parameter values (Figure 2, panels B, D and F).

Figure 2 shows the failure rates of the ACTs when the IC50s of the two artemisinin drug forms were either varied independently (Figure 2, panels A to D) or varied simultaneously (Figure 2, panels E and F). When the IC50s of the artemisinin drug forms were varied independently increasing the IC50 of either had very little effect in the failure rates (Figure 2, panels A, B, C and D). This was particularly clear for AR-LF treatments where increasing either AR or DHA IC50 caused no measurable increase in drug failure rates (Figure 2, panels B and D). This occurs because resistance to one form is compensated by continued sensitivity to the other form because both forms are potentially capable of high rates of parasite

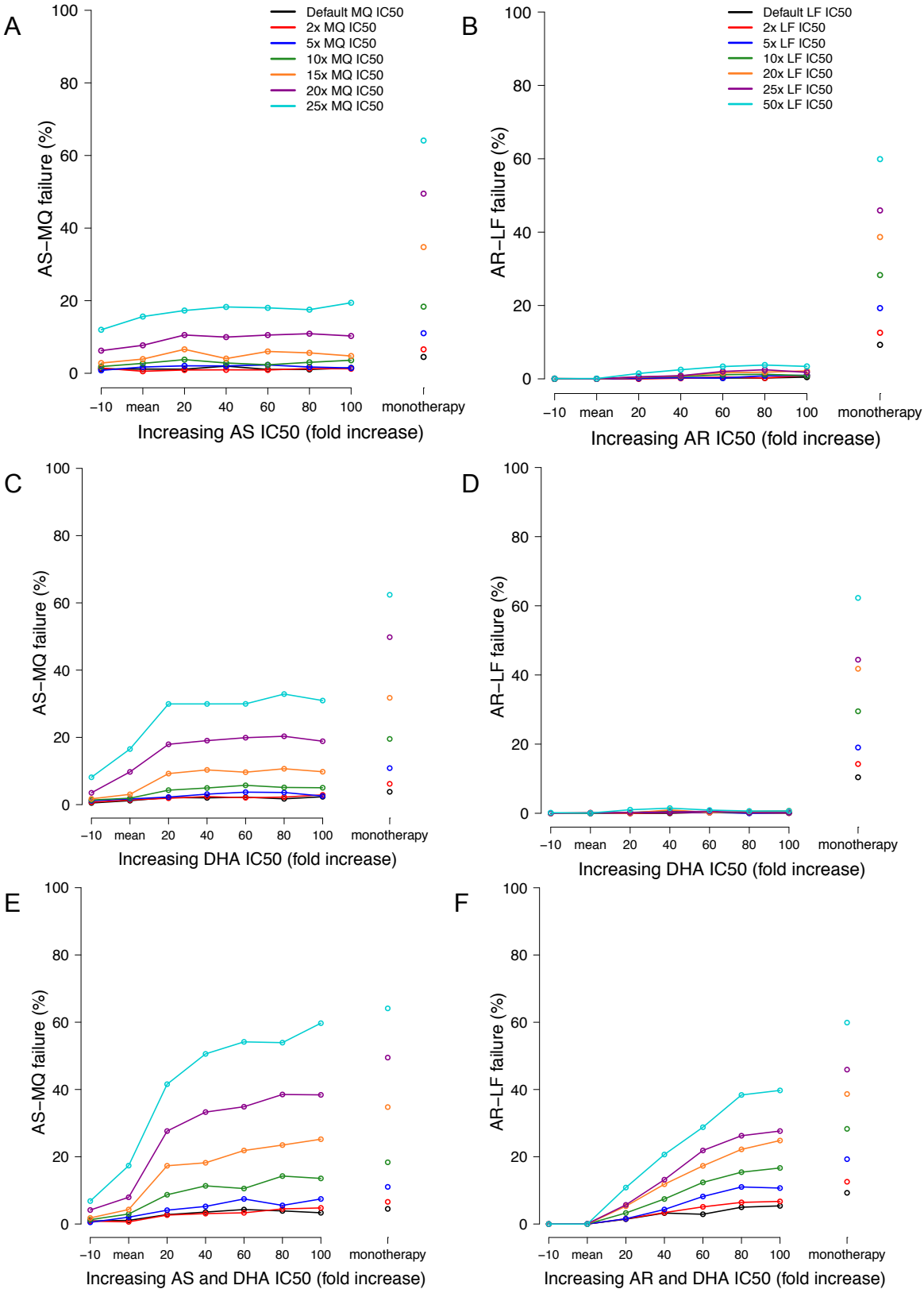

Figure 2. Change in failure rates associated with either increasing AS/AR IC50 (top), increasing DHA IC50 (middle) or simulating increasing both AS/AR and DHA IC50 (bottom). Left-hand column includes AS-MQ treatment and the right-hand column AR-LF treatment. Note that failure rates for monotherapies are shown as columns to the immediate right of the x-axis.

(Figure A2). Increasing AS IC50 alone also had little effect on the AS-MQ failure rates (Figure 2, panel A), again highlighting the importance of its active metabolite on parasite survival. When DHA IC50 was increased by 20-fold in AS-MQ treatment (Figure 2, panel C), treatment failures increased by 25 to 65% (relative increase) depending on the level of resistance to the partner drug. This is the only time increasing either the artemisinin drug forms alone affected treatment outcome and further DHA IC50 increases (above 20-fold) had little further effect on treatment outcome (Figure 2, panel C). Failure rates to AS-MQ assuming the artemisinin drug forms were uncorrelated (Figure 2, panels A and C) remained lower than those seen when assuming they were correlated (Figure 2, panel E) thus implying both artemisinin drug forms are still playing an active role in parasite killing. Further DHA IC50 increases above 20-fold had no discernable effect on treatment outcome and failure rates remained lower than those seen when the IC50's were correlated thus implying that while not as potent as AR and DHA it still plays an active role in parasite killing. For both ACTs, increases in failure rate as a result of increasing artemisinin resistance were much larger if the IC50s of the artemisinin drug forms were simultaneously increased. Rapid loss of protection was most noticeable for AS-MQ with small IC50 increases (20 and 40-fold), well within the range of natural variation (225), increasing failure rates by 65-70% (Figure 2, panel E). Loss of protection was more gradual following AR-LF treatments (Figure 2, panel F) but both ACTs showed failure approaching those of the of the monotherapies as artemisinin IC50s increased to 100-fold greater than the mean.

The PCT appears to be determined predominantly by the level of resistance to the artemisinin component with the initial level of partner drug resistance being relatively unimportant (Figure 3). This was particularly evident following AR-LF treatment where increasing the IC50 of LF had no discernable effect on PCT (Figure 3, panels B and D) while increasing MQ resistance only caused the PCT to vary by up to one day (Figure 3, panels A and C). When the IC50s of the two artemisinin species were increased simultaneously, the addition of artemisinin to the monotherapy reduced PCTs by approximately 2 to 3 days for both ACTs. As seen with the treatment failures (Figure 2), increasing the IC50 of AS/AR or DHA independently had little/no effect on PCT (Figure 3, panels A to D) and PCT did not approach that of the monotherapy because the other artemisinin species retained its effectiveness. When the IC50s were increased simultaneously both artemisinin species lost their effectiveness (Figure 3, panels E and F) while the PCT increased almost linearly with

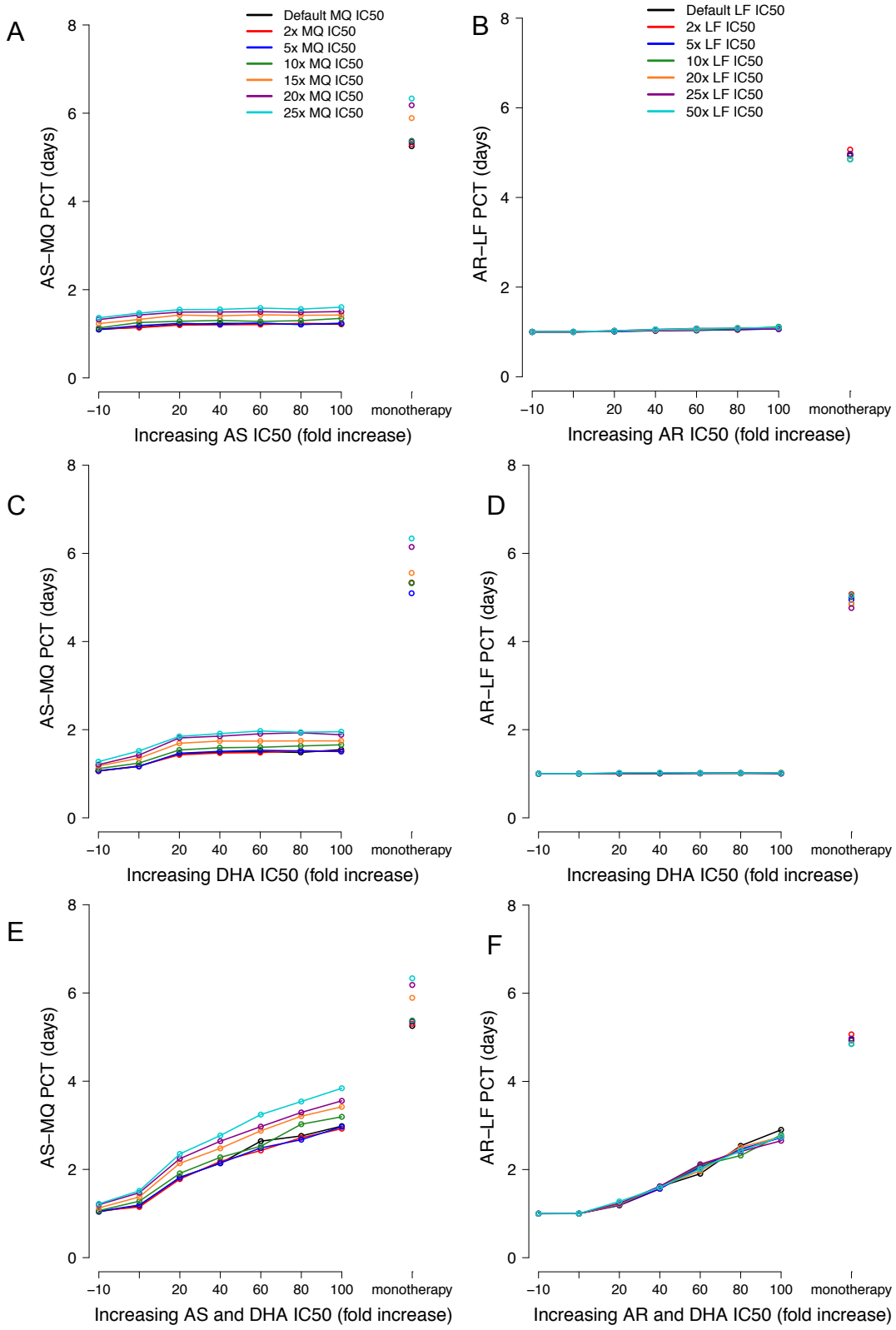

Figure 3. Change in parasite clearance times (PCT) associated with either increasing AS/AR IC50 (top), increasing DHA IC50 (middle) or simultaneously increasing both AS/AR and DHA IC50 (bottom). Left-hand column includes AS-MQ treatment and the right-hand column AR-LF treatment. Note that PCTs for monotherapies are shown as columns to the immediate right of the x-axis.

increasing artemisinin resistance and approached the PCTs seen with monotherapies (Figure 3, panels E and F).

4. Discussion

The extended PK/PD mechanism based modelling was easily applied to ACTs and produced results and predictions consistent with field data on failure rates (1) and increasing PCT associated with resistance. The main operational concern surrounding the evolution of artemisinin resistance is that it will lead to clinical failure in patients treated with ACTs (374). Obviously, if the partner drug is effective as a monotherapy, then the presence or absence of artemisinin resistance has no clinical effect. Problems arise as resistance spreads to the partner drugs, a process slowed by the addition of an artemisinin (126). The results clearly show that adding AS to a failing drug (MQ) reduced the treatment failure rates by up to 90% (relative reduction) but did not result in a fully effective ACT (Figure 2, panel E). This observations is in line with the findings of the International Artemisinin Study Group who performed a meta-analysis of individual patients from 16 randomised trials (n=5948) studying the effect of adding AS to either CQ, AQ, SP or MQ (1). While the total population failure rates were reduced by 42-65% when averaged across all drug regimens, the addition of AS to MQ monotherapy reduced failure rates by approximately 90-95% (1). The results for AR-LF show that the addition of AR with default IC50 values was sufficient to save a failing LF monotherapy by reducing failure rates to <1% for all levels of partner drug resistance regardless of whether the IC50s of the AR and DHA are increased simultaneously or independently (Figure 2, panels B, D and F). However, this observation was much more difficult to validate than those of AS-MQ as there is almost no published data on the *in vivo* efficacy of LF monotherapy and so it is impossible to quantify the proportion of failures averted specifically by the addition of AR. We also note that for both ACTs, only when the IC50s were correlated did increasing the IC50 eventually lead to failure rates approximately equal to those of the monotherapy therefore removing any benefit afforded to the partner drug by the artemisinin. These occurred after 50-100 fold increases in artemisinin IC50 which is large, but around the same magnitude as the natural variation observed in field

isolates (225). The key question is whether the IC50s are correlated; field data suggest they are (Appendix, part 2).

Increasing PCTs are currently being observed in the field (7, 241, 242, 316, 374); Dondorp *et al*. (85) for example, show that parasites resistant or tolerant to artemisinins take 3 or 4 days to clear parasites as compared with less than 2 days for artemisinin sensitive parasites; this pattern was also apparent in the results presented here (Figure 3). The simulated results showed the initial level of resistance to the partner drug had very little effect on the PCT and whilst this may seem strange it can be explained relatively easily. While the partner drug is undeniably important when determining the treatment outcome (i.e. success or failure), the PCT is determined almost solely by the short-lived but fast-acting artemisinin component, which causes a rapid decline in parasite numbers but is not present long enough to completely clear the parasite load (364). As with dug failure rates, PCT only approached those of the monotherapies when the IC50s were increased simultaneously again consistent with field data that the IC50s are correlated (Appendix, part 2). For both ACTs, PCT began to increase after relatively small increases in artemisinin IC50 of 20- to 40-fold (within the range of natural variation (225)).

It is important to realise that cross-resistance and mode of drug action are related, but distinct entities. Drugs with identical modes of action may show complete cross-resistance if mutations occur at their site of action which prevents both/all forms of the drug from binding therefore blocking their activity. Alternately, resistance may emerge through mutations that alter the drugs' ability to reach or accumulate at their site of action. Malaria is often characterised by the latter where mutations in membrane transporters, notably mdr and crt, are implicated in resistance to a range of antimalarial drugs (91). These transporters depend more on the chemical scaffold (charge and structure) of the drug than its active site so it is not *a priori* certain that cross-resistance will inevitable occur between a parent drug and its active metabolite. A lack of cross resistance would be hugely beneficial as it means parasites would have to evolve resistance to both forms of the drug but, unfortunately, our simulations suggest a model of complete cross resistance provides the best fit to the malaria observations.

Increasing tolerance / resistance to artemisinins was modelled using the standard assumption that it will arise through increased IC50 values. Artemisinin resistance may be atypical in this respect as it appears to manifest through increased clearance rate of parasites following

treatment with unchanged IC50, possible due to the drug(s) having activity against a more restricted range of stages in the malaria cell cycle (see below). The mechanistic approach assumes instantaneous killing of parasites irrespective of their stage, so deceased activity against some stages would be manifested as decreased drug maximal killing rate (V in Equation 1) in the methodology; interesting this parameter was found to be a far more potent determinant of resistance than the IC50 (364). It would be possible to re-run the above simulations altering V rather than IC50 but we chose to use the more conventional approach in the first instance as we consider this primarily a computational paper; we shall explore this approach in future studies applying the methodology more specifically to malaria.

Malaria differs from many other pathogens in having a distinct 48-hour intracellular cycle that essentially consists of invasion of red blood cells (RBC), digestion of host haemoglobin, parasite multiplication within the RBC, cell rupture and re-invasion of new RBCs. Drugs consequently have different stage specificity profiles depending on what metabolic processes are occurring in each stage (for example, many drugs target haemoglobin digestion so are primarily active against parasites in this stage of their cycle). Our analyses ignored these drug stage-specificities. It would however be easy to re-compute the dynamics using one hour time steps and using a 48hour array to move parasites through the 48-hour development cycle as done previously (147, 287, 398). We chose not to do so for two main reasons. Firstly, stage specificity requires that PD parameters be specified for each stage and that the initial distribution of parasite stages in the infection be specified. Secondly, and more importantly in our opinion, is that the PK/PD computations assume instantaneous killing of parasites depending on current drug concentration whereas, in reality, there is a delay in killing. The delayed killing can be incorporated into the methodology by postulating a hypothetical 'metabolite' whose production or elimination is disrupted by the drug, and that parasite death occurs as a function of metabolite level; the time taken for metabolite levels to reach 'lethal' levels introduces a time-lag into the killing (3, 254). This is an elegant way of incorporating a delay but it requires further parameterisation of the metabolite's production and elimination, specification of a killing rate as a function of metabolite level, and calibration against field data. Patel and colleagues (254) estimated the delay in artemisinin killing as around 5 hours. A recent study attempted to simulate ACT dynamics using a stage structured approach and concluded that it did not match well field data (398); we are unsurprised because the short-term dynamics will be critically dependent on stage-specific PD parameterisation and no time lag was built into the model. Hence, our approach was to ignore short-term dynamics and run

the enhanced PK/PD methodology, ignoring stage specify and delayed drug action (363); the objective was to simulate the fate of the infection over the longer term rather than the dynamics immediately post-treatment. Consistency of our results with field and clinical observations suggest this is a robust approach but it is important to recognise the alternative modelling approaches can be designed, and that our enhanced PK/PD methodology can easily form the basis for an improved stage-specific model run in 1-hour time steps.

The rationale behind this paper is that combining good quality field and clinical data into a sophisticated PK/PD model should allow a thorough investigation of ACT effectiveness in the context of increasing artemisinin tolerance/resistance. It therefore provides a methodological framework for clinical pharmacologists to interpret their results. However the predictive power of mathematical modelling is governed by the crucial step of model calibration and the availability of comprehensive, good quality PK/PD data in the literature is surprisingly scarce (Supporting Information, part 2). This has the potential to limit the usefulness of models as predictive tools. Given the amount of effort and resources required to conduct PK/PD studies and that their explicit aim is usually to improve human therapy, it seems appropriate to consider how best to report such studies for maximum impact. We therefore make three specific suggestions that authors may consider to maximise their studies' chance of influencing policy choice. Firstly, all available population PK/PD data, including those required purely for intermediate calculations should be reported. For example, terminal elimination rates are invariably reported but parameters required in their calculation, for example volumes of distributions (often confounded with bioavailability) are often omitted (321). We are uncomfortable with the rationale underlying the common assertion that DHA is the main active species during artemisinin treatment (see above and Figure A2); we would therefore recommend that PK parameters for parent species such as artesunate and artemether also be measured and reported. Secondly, the nature and extent of natural variation in the parameters are vitally important and can result in some patients developing low drug concentrations possibly leading to therapeutic failures or high concentrations potentially leading to toxicity. The distributions (normal, log-normal, etc) with their associated coefficients of variations (CV) are therefore almost equally important as their mean values. For example, many authors cite CV estimates larger than the mean, which obviously indicates a non-normal distribution: such data are much more useful if accompanied by their distributions (herein we were forced to assume they were log-normal). Finally, there are wide variations in reported mean values between studies; these are

generally ascribed to sampling different populations or age groups but a more critical appraisal in terms of any impact of different methods of analysis would also be helpful. An excellent example is that of Tan *et al*. (326) who, after describing the population PK of AS and DHA in healthy patients, compare their results with those of other AS and DHA PK studies and provide a detailed discussion explaining how and why the results may differ.

Despite the caveats mentioned above, our results and implications are clear. The kill rate of both artemisinin forms appears to be important in determining treatment outcome and their IC50's are likely to be correlated. AS-MQ is more sensitive to increases in artemisinin drug resistance than AR-LF with the number of failures increasing quickly with relatively small increases in AS and DHA IC50s. Both ACTs show increasing PCT associated with increasing artemisinin IC50, an observation already seen in the field (52, 86, 87, 241, 365). Our results suggest this is indicative of a rapid loss of protection provided by the artemisinins against the partner drug(s). If, or when, resistance against the partner drug starts to increase, most plausibly driven by mismatched half-lives (132, 133, 352), then a rapid reduction in ACT clinical effectiveness is likely to occur. We conclude that policies designed to isolate and minimise the spread of artemisinin resistance are to be greatly encouraged (374).

Appendix

1. Pharmacokinetics – incorporating the absorption, conversion and elimination of drugs

The artemisinin model outlined in Figure 1 was described using equations 2 to 4 in the main text. These three differential equations were used to describe the change in the amount of drug in the gut (equation 2) and the amount of unconverted and converted drug in the serum (equations 3 and 4 respectively). Using Laplace transforms and the convention (209) of overhead bars to indicate transformed variables, we transform the equations as follows. Equation 2, describing the amount of drug in the gut, becomes

$$s\overline{A} - A(0) = x\overline{A}$$

or

$$\overline{A} = \frac{A(0)}{(s+x)}$$

where A(0) is the amount of drug present at time zero in the gut which equals the dosage administered (D) plus any drug present from previous treatments ($A`$) giving

$$\overline{A} = \frac{A`+D}{(s+x)} \qquad [A1.1]$$

Equation A1.1 can be solved by substituting $p=A`+D$

$$\overline{A} = \frac{p}{(s+x)}$$

back transforming into the time domain and re-substituting gives

$$A(t) = (A` + D)e^{-xt}$$

[A1.2]

Note, if no treatments are present (i.e. if $A`=0$), equation A1.2 becomes

$$A(t) = De^{-xt}$$

[A1.3]

Equation 3, describing the amount of unconverted drug in the serum, becomes

$$s\overline{B} - B(0) = x\overline{A} - (y+z)\overline{B}$$

or

$$\overline{B} = \frac{x\overline{A} + B(0)}{(s+y+z)} = \frac{x\overline{A}}{(s+y+z)} + \frac{B(0)}{(s+y+z)}$$

the drug is not given intravenously so $B(0)=B`$, the drug present from previous treatments. Substituting $\overline{A}$ from equation 1a.1 gives

$$\overline{B} = \frac{x(D+A`)}{(s+y+z)(s+x)} + \frac{B`}{(s+y+z)}$$

[A1.4]

Equation A1.4 can now be solved by substituting $p=x(D+A`)$ and $q=(y+z)$ to give

$$\overline{B} = \frac{p}{(s+q)(s+x)} + \frac{B`}{(s+q)}$$

back transforming into the time domain and re-substituting gives

$$B(t) = \frac{x(D+A`)}{(x-(y+z))}\left(e^{-(y+z)t} - e^{-xt}\right) + B`e^{-(y+z)t}$$

[A1.5]

Note, if no previous treatments are present (i.e. if $A`=0$ and $B`=0$), $B(t)$ becomes

$$B(t) = \frac{xD}{(x-(y+z))}\left(e^{-(y+z)t} - e^{-xt}\right)$$

[A1.6]

Equation 4, describing the amount of converted drug in the serum, becomes

$$s\overline{C} - C(0) = z\overline{B} - k\overline{C}$$

or

$$\overline{C} = \frac{z\overline{B} + C(0)}{(s+k)} = \frac{z}{(s+k)}\overline{B} + \frac{C(0)}{(s+k)}$$

where $C(0)=C`$, the amount of drug present from previous treatments. Note, the fraction was split at this point to help with the transformations later. Substituting $\overline{B}$ from equation A1.6 gives

$$\overline{C} = \frac{z}{(s+k)}\left(\frac{x(D+A`)}{(s+y+z)(s+x)} + \frac{B`}{(s+y+z)}\right) + \frac{C`}{(s+k)}$$

or

$$\overline{C} = \frac{zx(D+A`)}{(s+k)(s+y+z)(s+x)} + \frac{zB`}{(s+k)(s+y+z)} + \frac{C`}{(s+k)}$$

[A1.7]

Equation A1.7 can now be solved by substituting $p=zx(D+A`)$, $q=(y+z)$ and $r=zB`$

$$\overline{C} = \frac{p}{(s+k)(s+q)(s+x)} + \frac{r}{(s+k)(s+q)} + \frac{C`}{(s+k)}$$

Back transforming into the time domain and re-substituting gives

$$C(t) = zx(D + A`)\left[\frac{e^{-kt}}{(y+z-k)(x-k)} + \frac{e^{-qt}}{(k-(y+z))(x-(y+z))} + \frac{e^{-xt}}{(k-x)(y+z-x)}\right] + \frac{zB`}{(y+z-k)}\left(e^{-kt} - e^{-(y+z)t}\right) + C`e^{-kt}$$

[A1.8]

Tracking the amount of drug in mg requires that the changes in the molecular weight be accounted for, this was done using the ratio of the molecular weights (see main text for more information).

Note, if drug from previous treatments are absent because it is the first dose of the regimen (i.e. if *A`=0, B`=0* and *C`=0*), *C(t)* becomes

$$C(t) = zxD\left[\frac{e^{-kt}}{(y+z-k)(x-k)} + \frac{e^{-qt}}{(k-(y+z))(x-(y+z))} + \frac{e^{-xt}}{(k-x)(y+z-x)}\right]$$

[A1.9]

2. Model calibration for analysis of ACTs

This extended model required additional model parameters to describe the absorption rate across the gut, the conversion rate to DHA and elimination of DHA following AS and AR treatments (Figure 1). All data were taken from published clinical studies, where analysis had been carried out in laboratories conforming to good laboratory practice (140, 236) i.e. patient blood samples were immediately centrifuged after sampling and the separated plasma stored at between -20 (140) and -50ºC (236).

Newton *et al*. (236) determined the pharmacokinetic parameters of AS absorption and conversion in three adult patients in western Thailand. They used open one- and two-compartment models, fitted to plasma concentration-time data to derive standard PK parameters. Curve-fitting was performed with WinNonlin and compartment models

Table A1. Mean antimalarial drug parameters for artesunate-mefloquine and artemether-lumefantrine combination therapies. The amount of variation (i.e. CV) is given in square brackets

	Artesunate-Mefloquine			Artemether-Lumefantrine		
	Artesunate	DHA	Mefloquine	Artemether	DHA	Lumefantrine
Volume of distribution (Vd)	7·1[236] [94[224]]	1·49[236] [48[211]]	20·8[359] [38[165, 302]]	5·21[140] [82[4]]	3·7[140] [48[211]]	21[68] [263[97, 329]]
Absorption rate constant (x)	252[236] [112[326]]	-	-	23·98[140] [68[4, 345]]	-	-
Conversion rate (z)	30·96[236] [36·2[326]]	-	-	11·97[140] [65[4, 345]]	-	-
Elimination rate constant (k)	-	25·4[236] [23[57, 83, 237, 326]]	0·053[350] [63[165]]	-	44·15[140] [23[57, 83, 237, 326]]	0·16[110, 212, 350] [5[83]]
Concentration producing half the desired effect (IC50)	0·0016[2, 18] [86[211]]	0·009[211] [117[211]]	0·027[44] [78[211]]	0·0023[a] [79[264]]	0·009[211] [117[211]]	0·032[44, 321] [102[211]]
First order rate constant of parasite killing (V)	27·6	27.6	3·45[359]	27·6	27·6	3·45[359]
Slope Factor (n)	4[321]	4[321]	5[321]	4[b]	4[321]	4[321]

[a] Unpublished data from Liverpool School of Tropical Medicine
[b] Assumed to be like artesunate

chosen using the Akaike Information Criterion (AIC). Hietala *et al*. (140) determined the pharmacokinetics of AR absorption and conversion using data from 50 paediatric patients in central Tanzania. They found the distribution of AR was best described using a two-compartment model with first-order absorption whilst DHA concentrations were best described by a covariate-free one compartment model. The population PK/PD parameters were then determined using NONMEN version VI. Although Hietala *et al*. (140) determined that a two-compartment model provided the best fit to data this was reliant on the assumption that the absorption rate constant was fixed to 1/hour.

Both studies provide estimates of the volume of distribution and elimination rate for the converted form of the drugs (DHA). The DHA estimates differed and so, for consistency, we chose to use the Newton *et al*. (236) estimates when modelling AS and the Hietala *et al*. (140) estimates when modelling AR (see part 4, assumptions, for further discussion). Finally,

neither study showed significant routes of elimination of AS/AR from the body and so is was assumed that the drugs were fully converted to DHA (i.e. y=0).

The simulated drug concentration-time profiles of both the artemisinins using the default parameters in Table A1 are given in Figure A1 and the corresponding kill curves in Figure A2. To validate the models predictive ability the maximum serum concentration (Cmax) and time to achieve Cmax (Tmax) were compared to field data. The PK profile of AS absorption and conversion to DHA was simulated using PK parameters from Newton *et al*. (236). Figure A1.A shows both the Cmax and Tmax of AS (420ng/ml and 0·5hrs) within the range presented by Newton *et al*. (236) (AS: 62-510ng/ml and 0·25-0·5hrs) and while the Cmax of DHA (600ng/ml) is slightly lower the range presented in Newton *et al*. (236) (817-2853ng/ml). The Cmax range for DHA is so large (see also Byakika-Kibwika *et al*.(49)) that we are confident the models are consistent with clinical data. The PK profile of AR absorption and conversion to DHA was simulated using PK parameters from Hietala *et al*. (140). However, this study does not provide estimates of the corresponding Cmax and Tmax parameters and so the resulting PK profile was validated against the results of van Agtmael *et al*. (345). We note that van Agtmael *et al*. (345) presents a variety of Cmax and Tmax values for both AR and DHA. For example, the drug concentration-time profiles of AR and DHA (after both AR monotherapy and AR-LF combination therapy) in Figures 1-3 of van Agtmael *et al*. (345) all clearly show the Cmax of AR to be higher than DHA (although exact Cmax values vary). However, somewhat confusingly, Tables 1 and 2 (of van Agtmael *et al*. (345)) show that, following AR monotherapy, the Cmax of DHA measured higher than that of AR. Whilst this observation directly contradicts the PK profiles plotted in their figures it is not discussed within the paper. For the purposes of validating the simulated PK profile, we compared the ratio of AR:DHA concentrations to those a typical patient (Figure 3, van Agtmael *et al*. (345)). As in the paper, DHA Cmax (57ng/ml) was found to be approximately one third that of AR (163ng/ml). Figure A1.B also shows the simulated Tmax of AR (1·5-2 hours) and DHA (2-2·5 hours) are approximately equal to those reported in the study (345)

Various studies assert that the rapid conversion of artemisinin derivatives to DHA means most of the antimalarial activity is derived from the DHA component, particularly following AS treatments (see for example (159, 286, 303, 320, 361)). As a recent high profile example, Saralamba *et al*. (286) state “the parasiticidal effect of artesunate was not incorporated here because the total drug exposure of artesunate was <10% of that of DHA in these patients

A.

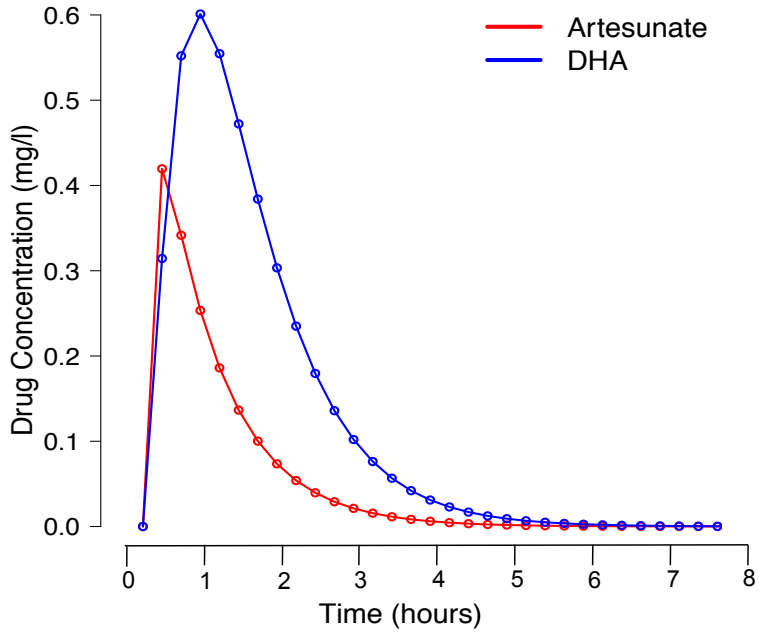

B.

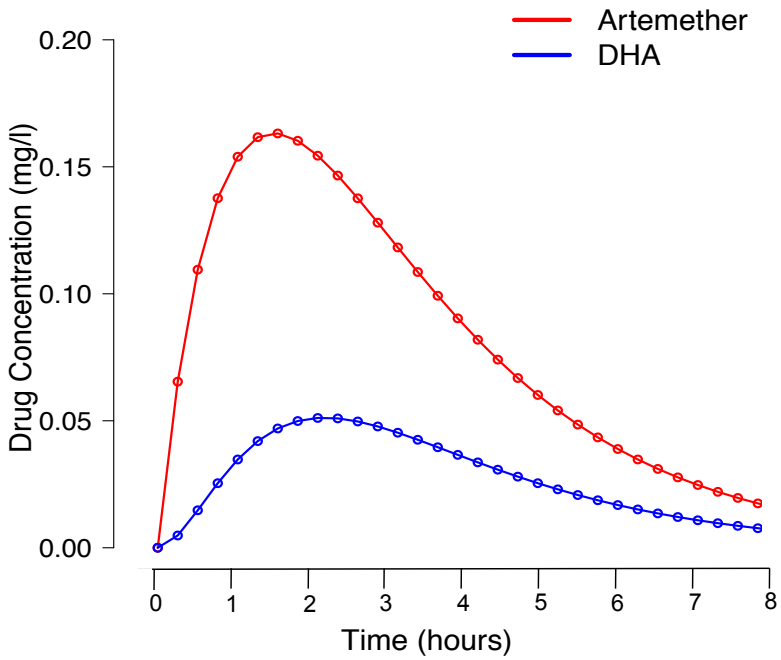

Figure A1. The simulated PK profiles of the artemisinin forms given as the parent drug and subsequently converted to DHA. Given as (A) artesunate or (B) artemether; generated using the model shown in Figure 1 mathematical derivation described herein and using the parameters of Table A1. The timescale and concentrations match well with those observed *in vivo* (see, for example, (49, 236, 345)). Note that DHA is the major component when dosing with artesunate, but the minor component when dosing with artemether.

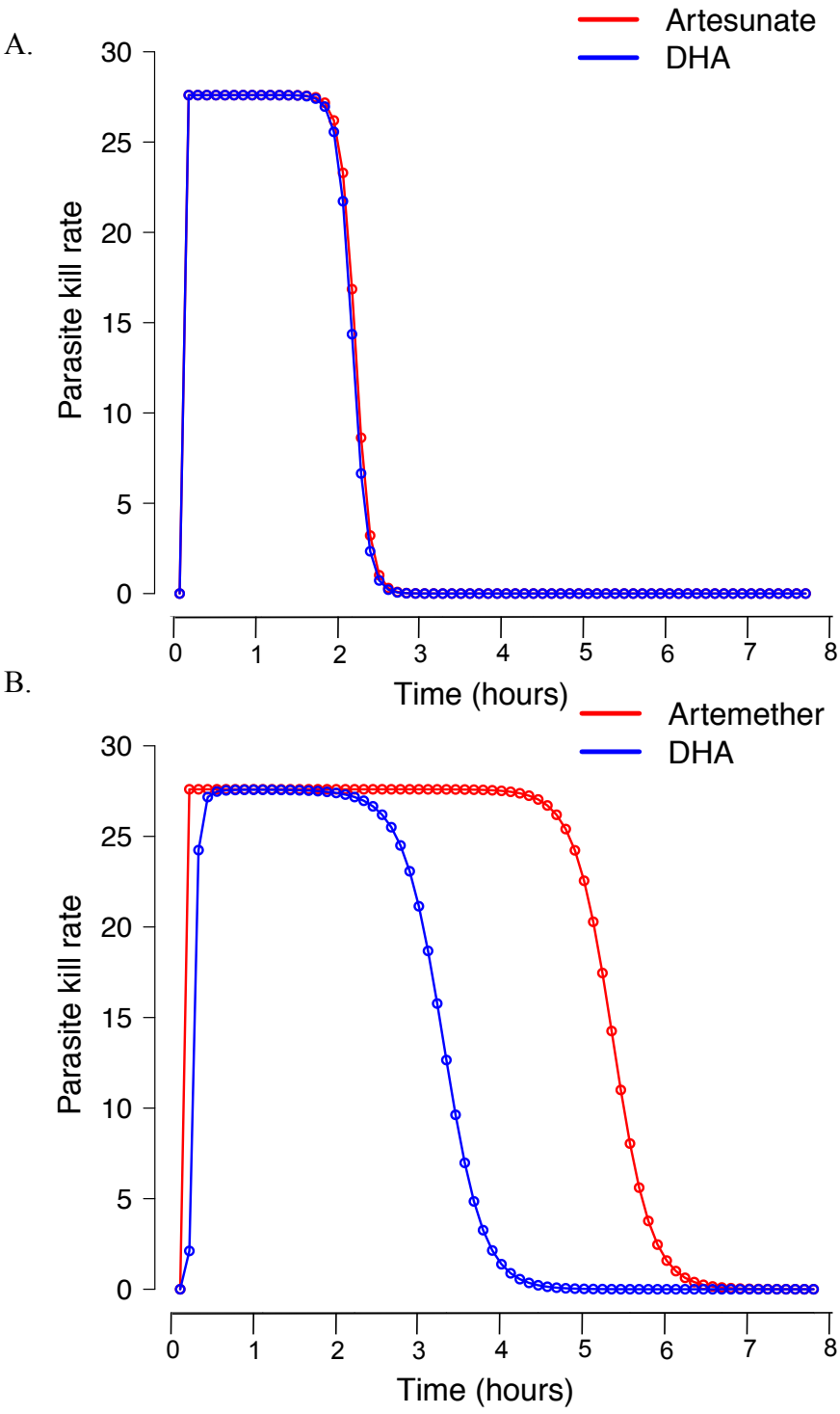

Figure A2. The simulated parasite kill curves of the parent artemisinin drug forms (artesunate and artemether) and their active metabolite DHA. Treatment with (A) artesunate and (B) artemether. Curves generated using the mathematical derivation described herein and using the parameters of Table A1.

(86)". Dondorp *et al*. (86) also report DHA accounted for >90% of the artemisinin species but concentration is not directly related to killing rate (Figure A2). Antimalarial drug dosages are massive compared to IC50 levels so both entities are usually working at near-saturated killing rates. Multiplying concentration profiles in Figure A1 by their Michaelis-Menten killing (Equation 1) gives similar kill rates for both species. This is illustrated in Figure A2 where the drug kill curves for both AS/DHA and AR/DHA suggest the parent drug and the active metabolite (DHA) are both likely to contribute to the parasite killing and supported by the simulated results when the IC50's are varied independently (see main text). While it maybe reasonable to assume that DHA is usually the dominant species it is not inevitable that this will always be the case (86). The huge amount of variation characteristic of human PK parameters (for example, see the CV estimates in Table A1) means it is inevitable that some people will slowly convert AS/AR to DHA, and rapidly eliminate the latter. Thus it is entirely plausible that AS and AR will have significant impacts in many patients and we would urge pharmacologists to measure and report their concentrations in order to understand the clinical impact.

A key operational question is whether mutations encode resistance to all artemisinins independently or whether there is any cross-resistance. Answering this question will provide crucial insights into how resistance to artemisinins is likely to spread. For example, if the IC50's of the artemisinin forms (primarily AS, AR or DHA) are completely correlated then parasites will evolve resistance in the same way that they would to any other single drug. However if the IC50s are uncorrelated, resistance would need to be acquired to both components independently, in much the same way as it would to two drugs in combination. The latter would result in a much slower spread of resistance that the former. This can be tested if field isolates or laboratory strains are simultaneously assayed for drug sensitivity to a range of artemisinins. Unfortunately such data are rare, however the results presented here, alongside the results in a recent paper by Delves *et al*. (77), have allowed us to determine the likely correlation between artemisinin IC50s. Specifically, the simulations indicate that both components of the artemisinin are active (Figure A2) while the simulated ACT failure rates and PCT only became consistent with field data when the IC50s of the artemisinins were increased simultaneously. Delves *et al*. (77) describe the half maximal inhibitory concentrations (IC50s) of 39 different antimalarials measured in 7 different *P.falciparum* strains. We found the IC50 of all the artemisinin derivatives to be positively correlated (Table A2). This correlation was particularly strong (0.831; $p<0.005$) for AS and DHA, a drug and

Table A2. Data describing the half-maximal inhibitory concentration (IC50) of 5 different antimalarials measured in 7 different *P.falciparum* strains by Delves *et al.*(77), was used to determine whether the IC50s of the artemisinins are correlated.

		Artemether	Artemisinin	Artemisone	DHA
Artemisinin	Pearson Correlation (Sig. 2-tailed)	0·893** p = 0.007	1		
Artemisone	Pearson Correlation (Sig. 2-tailed)	0·439	0·347	1	
DHA	Pearson Correlation (Sig. 2-tailed)	0·537	0·506	0·703	1
Artesunate	Pearson Correlation (Sig. 2-tailed)	0·717	0·802* p = 0·03	0·762* p = 0·047	0·831* p = 0·02

active metabolite routinely used as a first line treatment of malaria. We do note that a sample size of seven is small and standard deviation of each IC50 value within each isolate was often large, presumably a result of the variation in assay sensitivity. Both these factors are likely to reduce the power to detect correlations between the drugs. Despite this lack of power, all correlations were positive and 4/10 were statistically significant. Given these results and those of the simulation, it would indicate a likely correlation between the IC50 of the artemisinin components and that both the parent drug and active metabolite are responsible for the parasite killing (Figure A2) and we can conclude that the two components will be subject to joint selection pressure.

Variation was added to model parameters using parameter-specific estimates of CV.
For consistency and where possible, parameter-specific estimates of variability were taken from the same source as the default value (Table A1). Unfortunately some papers reported only the range of values measured so it was not possible to calculate a CV. In these cases, the estimates of variability were taken from other available studies (Table A1). For completeness we also include the changing failure rates seen if CV is assumed to be constant, in this case 30% (Figure A3) as in our previous study (364). It is gratifying to note that the impact of

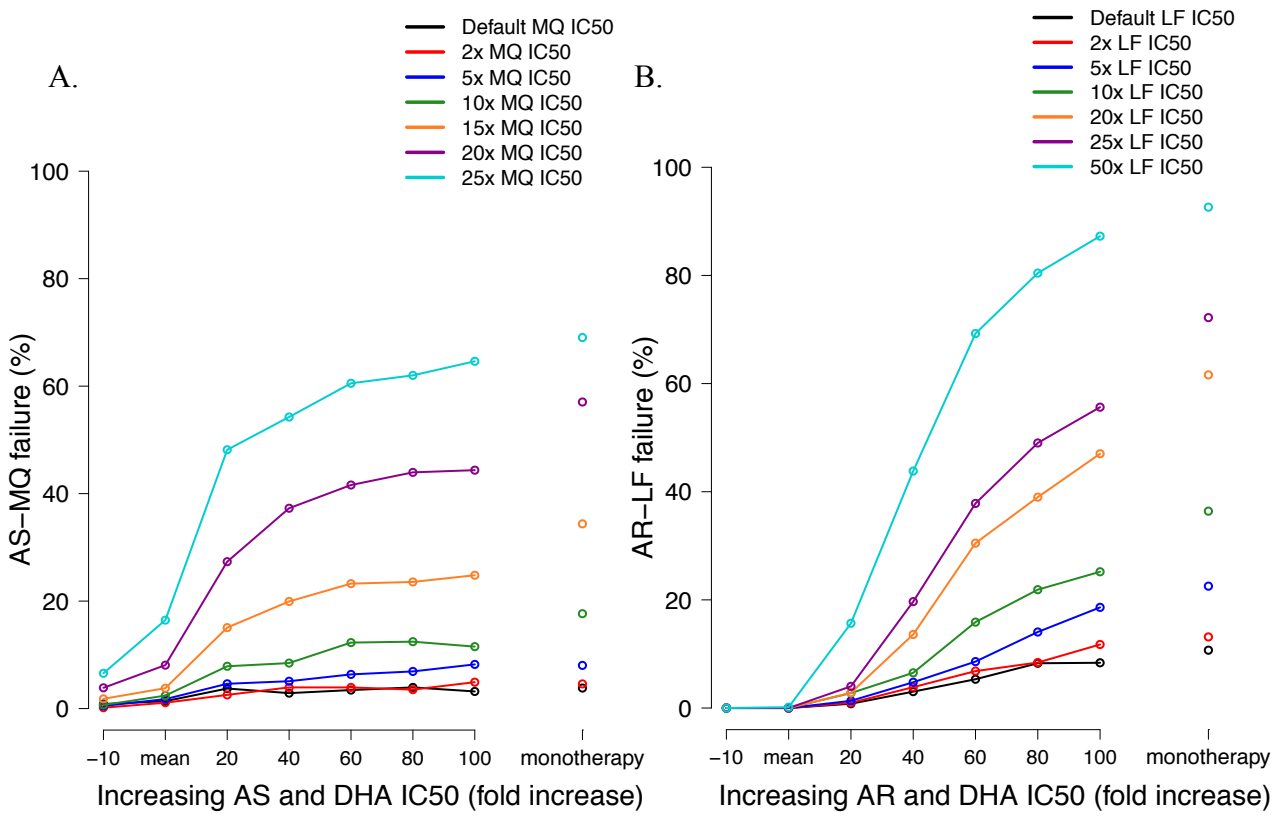

Figure A3. Change in failure rates associated with increasing AS/AR and DHA IC50 when the coefficient of variation in all parameters is always 30% (A) AS-MQ treatment and (B) AR-LF treatment.

increasing levels of resistance is robust to how the CV was assigned (compare Figure A3 with Figure 2, panels E and F in the main text).

The CVs were used to determine the distribution of parameters but were often so large that a significant proportion of negative results (which are biologically impossible and hence unusable) would have occurred if we had assumed a normal distribution. We therefore assumed those parameters with a CV of <50% to be normally distributed whilst those with a CV >50% were log-normally distributed.

For log-normally distributed parameters, the logarithmic mean, μ, was found using

$$\mu = \log\left(\frac{m^2}{\sqrt{v + m^2}}\right) \qquad [3.1]$$

where m was the arithmetic mean value, which in this case was equivalent to the default value (Table A1) and v was the variance. Here, the variance was equal to the arithmetic mean multiplied by the CV, squared.

The standard deviation, σ, of the log-normally distributed parameter is

$$\sigma = \sqrt{\log\left(\frac{v}{m^2 + 1}\right)} \qquad [3.2]$$

The parameter value obtained from the log normal distribution was then back converted for use in the model by finding the exponential of the randomly generated number.

Regardless of the parameter distribution all random numbers generated must be positive. Each time a number was generated the program checked for values less than 0 and, if necessary, generated another random number in the same way until a positive value was chosen. Random parameter values were generated using these distributions to simulate the PK properties of individual patients and PD profiles of their infections.

The mechanistic PK/PD model presented here has met the methodological challenges involved in incorporating the absorption and conversion phases of the artemisinins whilst also tracking the concentration of more than two drugs. However, the new model structure required one further assumption, that all artemisinin species could be adequately described with a one-compartment model structure (i.e. only one compartment besides the gut is investigated, in this case the serum). There is currently considerable uncertainty in the literature as to which structural PK model provides the best fit to data for the artemisinin derivatives. Simpson *et al*. (303) note that many studies of the artemisinin derivatives have

either been unable to fit satisfactory PK models (166, 212, 220, 301), fit only a one-compartment model (96, 139, 301) or required some PK parameters to be fixed (96, 220, 301). Given the confusion, we continue to assume a one-compartment model for all artemisinin species is satisfactory but the methodology could be easily extended to two-compartment models although this would require estimating and including additional PK parameters. It was also assumed that both artemisinin species have the same mode of action and so only the 'dominant' form with the higher kill rate was used. While this assumption is reasonable, the new methods (allowing more the action of more than two drugs simultaneously) mean it can easily be relaxed.

The extent of drug absorption and bioavailability can cause significant variability in the outcome of drug treatments. This is particularly true in the case of lumefantrine where the oral bioavailability is highly dependent on food intake and often poor in cases of acute malaria (97). When running simulations, we assumed all patients had uncomplicated malaria and followed dosing regimens precisely thus allowing us to ignore any potential complications arising from bioavailability and absorption.

The effect of combination therapies on parasite numbers were modelled assuming that partner and artemisinin act independently and that drug effect is additive, i.e. no synergy or antagonism. This was a reasonable assumption in previous simulations (364) where the ACTs were modelled assuming the partner drug and only one active component for the artemisinins (i.e. instant absorption and if necessary converted) acted upon the parasites. The new methodologies described herein explicitly allow for the action of both artemisinin components (i.e. the parent drug and active metabolite) but to assume that this effect is independent and thus additive seems unrealistic given their similar modes of action. As such we chose to use only the dominant drug form (parent or metabolite) with the higher kill rate to influence the parasites over each time step. However, given the methodological extensions allowing for the action of more than two drugs simultaneously, this assumption can easily be relaxed. For completeness, the results of simulations allowing for independent action of the two artemisinin components has been included (Figure A4 and A5). We also note that this assumption that drug action is additive cannot be extended for combinations such as sulfadoxine-pyrimethamine and atovaquone-proguanil which may show synergy. Unfortunately, quantifying and even defining "synergy" or "antagonism" seems to be a topic of much debate; Chou (64) discusses the "controversy and confusion" surrounding drug

combinations whilst Greco *et al*. (115) list no less than 13 different methods of determining synergy. With no consensus method available to define drug synergy mathematically, the best method of inclusion is likely to be the empirical approach taken for SP by Gatton *et al*. (109).

When looking for the addition parameters required to describe artemisinin absorption and conversion it became apparent that the estimates of DHA volume of distribution and elimination rate differed depending on whether the metabolite was measured following treatment with AS or AR (140, 236). It is not clear whether this response is a real biological phenomenon, for example AS and AR may differentially induce DHA elimination processes, or whether it reflects normal inter-study variability. Using two different estimates of DHA PK was obviously not ideal but with no way to choose between the estimates and for consistency with the other studies (140, 236), it seemed reasonable to use both. The need for consistency was also the reason estimates of the volume of distribution for AS and AR differed from those previously published in Winter & Hastings (364).

While we do use multiple dosing regimens there was assumed to be no change in PK parameters due to auto-induction enzymes nor change due to improved clinical status after treatment has started. Running the model in shorter time steps would of course allow for these factors to be easily incorporated but were omitted here in the interests of simplicity.

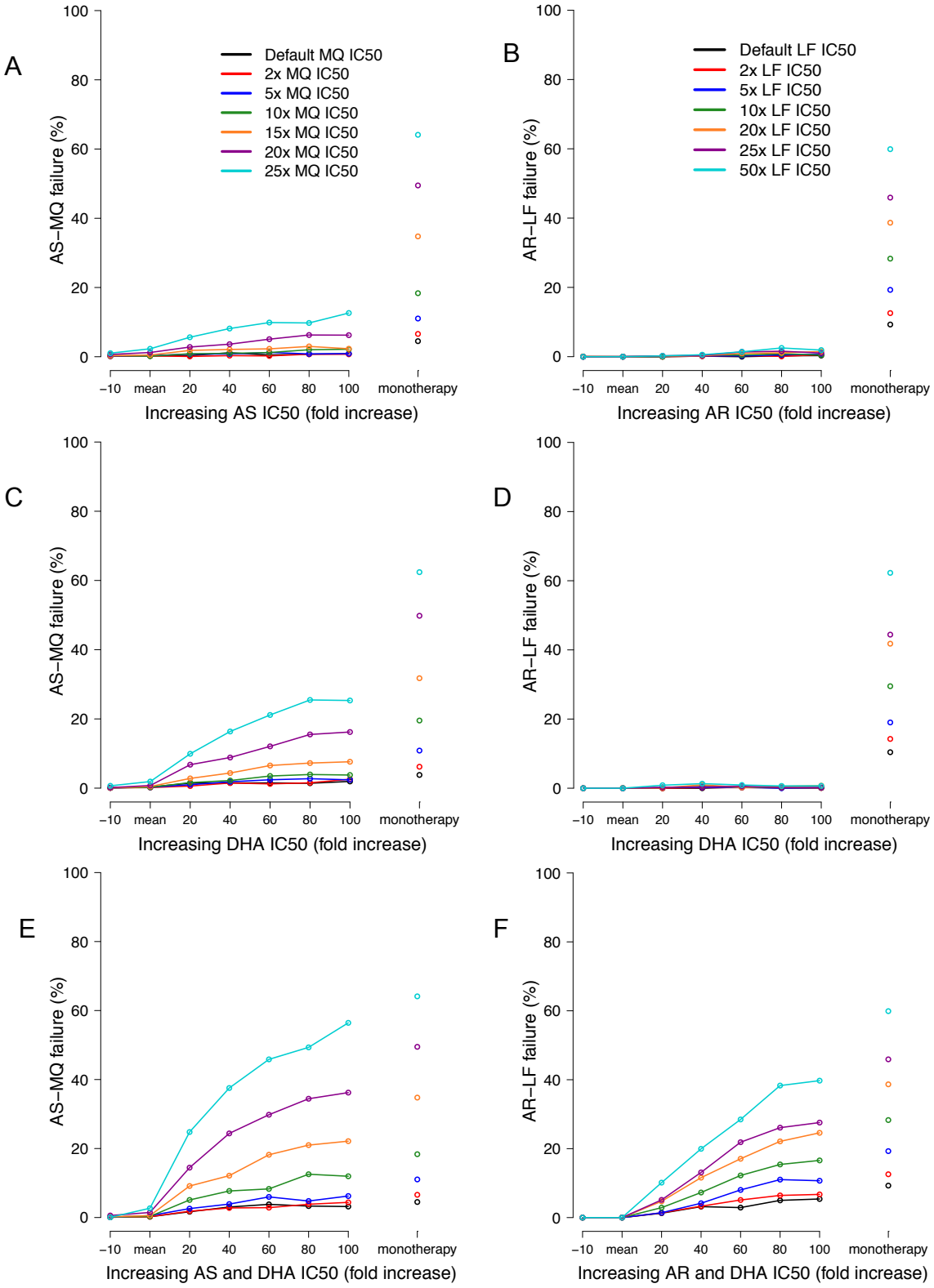

Figure A4. Change in failure rates associated with either increasing AS/AR IC50 (top), increasing DHA IC50 (middle) or increasing AS/AR and DHA IC50 (bottom) (A) AS-MQ treatment and (B) AR-LF treatment assuming independent action of the artemisinin components. Note that failure rates for monotherapies are shown as columns to the immediate right of the x-axis.

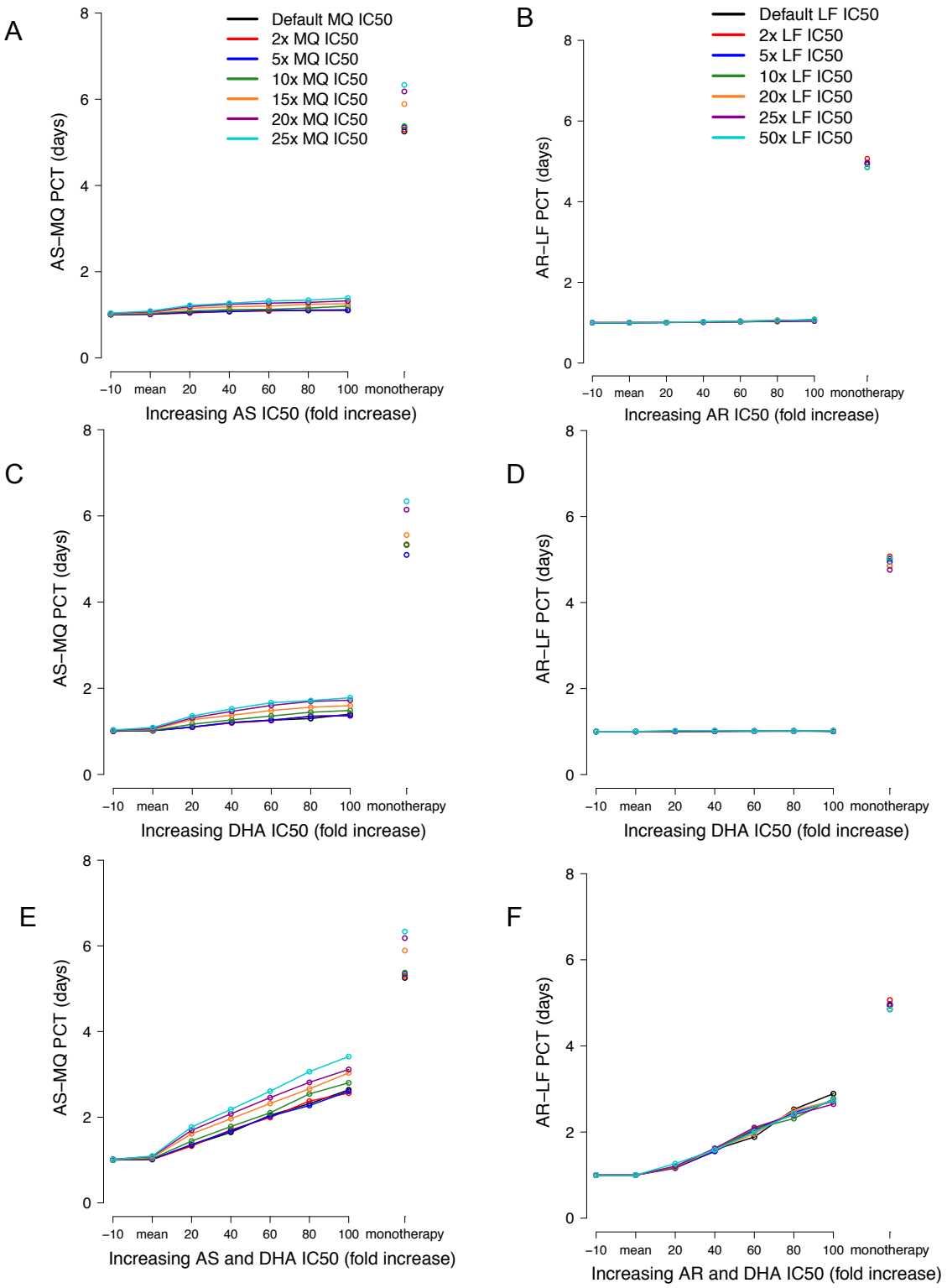

Figure A5. Change in parasite clearance times (PCT) associated with either increasing AS/AR IC50 (top), increasing DHA IC50 (middle) or increasing AS/AR and DHA IC50 (bottom) (A) AS-MQ treatment and (B) AR-LF treatment assuming independent action of the artemisinin components. Note that PCTs for monotherapies are shown as columns to the immediate right of the x-axis.

3. Implementation

This model was implemented in R (version 2.9.2) (270) although earlier versions were run in Maple (version 13). Both packages gave the same result but the results presented here were generated in R. Substituting equations 7 and, where appropriate, 8 for each drug into equation 11 enabled us to track parasite numbers and while the resulting equation was complicated, it was solved numerically using R (using the "integrate" command in the "stats" package). The model ran in half-day time steps for the first seven days to allow for multiple dosing and one-day time steps thereafter to speed up simulations. We chose to use numerical integration of half/single day time steps as it is more explicit allowing us to give dosages twice per day and, if required, change PK parameters over the course of treatment to reflect changes in the auto-induction of enzymes (as in quinine (335)). However we do note that it is possible to find the treatment outcome algebraically after the final dose (144).

The dosing regimens investigated were AS-MQ (4mg/kg/day AS with 8.3mg/kg/day MQ for three days) or AR-LF (1.7mg/kg AR with 12mg/kg LF given twice daily for three days) (380). The PK/PD parameter estimates are given in Table A1 and unless otherwise specified (Supporting Information, part 2), were previously validated in Winter & Hastings (364).

Chapter 4

Simulating Clinical Trial Data as a Resource for Optimising Analysis Methods

1. Introduction

Increasing tolerance to the newest class of antimalarials, the artemisinins (150, 260, 285), means there is an urgent need for new drugs to combat malaria. Traditional mechanisms for drug development have typically provided few drugs to treat diseases in the developing world. The discovery and bringing to market of new drugs is lengthy and complicated, taking an average of ten to fifteen years and costing between $800 million and $1 billion (82). Clinical trials are a major part of this development, typically lasting between 6-7 years and conducted in 3 phases each with an increasing number of patients.

Phase 1 (in healthy volunteers) and phase 2 trials (in patients) are used primarily to determine how new drugs work in humans, to test drug safety (pharmacokinetics, PK), predict a dosage range and in phase 2 focus on proof-of-concept and assessment of drug efficacy. Phase 3 trials look at drug effectiveness in large groups of patients in several locations. Drugs used to treat malaria typically have long half-lives (the obvious exception being the artemisinins) and phase 3 trials must allow for a minimum of 28 days but as much as 63 days (322, 368) follow-up to adequately characterise antimalarial drug effectiveness. Conducting large antimalarial phase 3 drug trials with extended patient follow-up in developing countries is logistically challenging, particularly as local infrastructure is often poor and drop out rates are often high. Trials typically enrol a few hundred up to a few thousand patients (216), and it

is the size and comparatively long duration of phase 3 trials that means they are one of the most expensive, time consuming and difficult trials to design and run.

The logistical challenges posed by clinical trials are further complicated by the variety of analysis methods available and by patients deemed to have infections with mixed genotypes at follow-up appointments. Mixed genotype infections are defined as those with more than one clone present at the time of follow-up, these maybe clone/s present in the original infection and/or clone/s acquired from new infections (Figure 1). They occur because patients enrolled within the studies are almost always at risk of reinfection during the follow-up period and so analysis of clinical trials must include a method of classification for mixed infections. Methods of analysis for clinical trials typically include either intention-to-treat (ITT), per-protocol (PP) or time-to-event (or survival) analyses (158). ITT analysis involves comparing treatment groups that include all patients originally allocated for randomisation while PP analysis compares treatment groups including only those patients who completed the treatment originally allocated (296). Survival analysis provides a tool for analysing the time-to-event data commonly collected within a clinical trial (304). In 2003, WHO attempted to standardise these methods and established a protocol for the design and analysis of malaria trials (368). They determined that trials should be analysed using survival analysis and provide a method for classifying infections with mixed genotypes. Despite the guidelines, analytical analysis and classification methods still vary (67) and it is impossible to investigate the performance of these methods using field data where the true results (in the absence of analysis bias) are unknown.

Figure 1 shows the change in drug concentration and parasite number over time, within a patient whose original infection contains multiple clones and who acquires multiple new infections. The salient features we note on Figure 1 include

1. Infections at time of treatment have between 10^{10} and 10^{12} parasites, the detection limit is 10^{8} and once below this limit we can no longer tell what happens to the parasites (red/green lines indicate parasites are either cleared (green) or recrudesce later (red)). Where MOI is high, several clones maybe preset at the time of treatment (red and green lines) and at any point following treatment new infections a likely to occur (grey and orange lines). A patient's infection may therefore have a mixture of clones including those persisting from the time of treatment and those acquired from new infections.

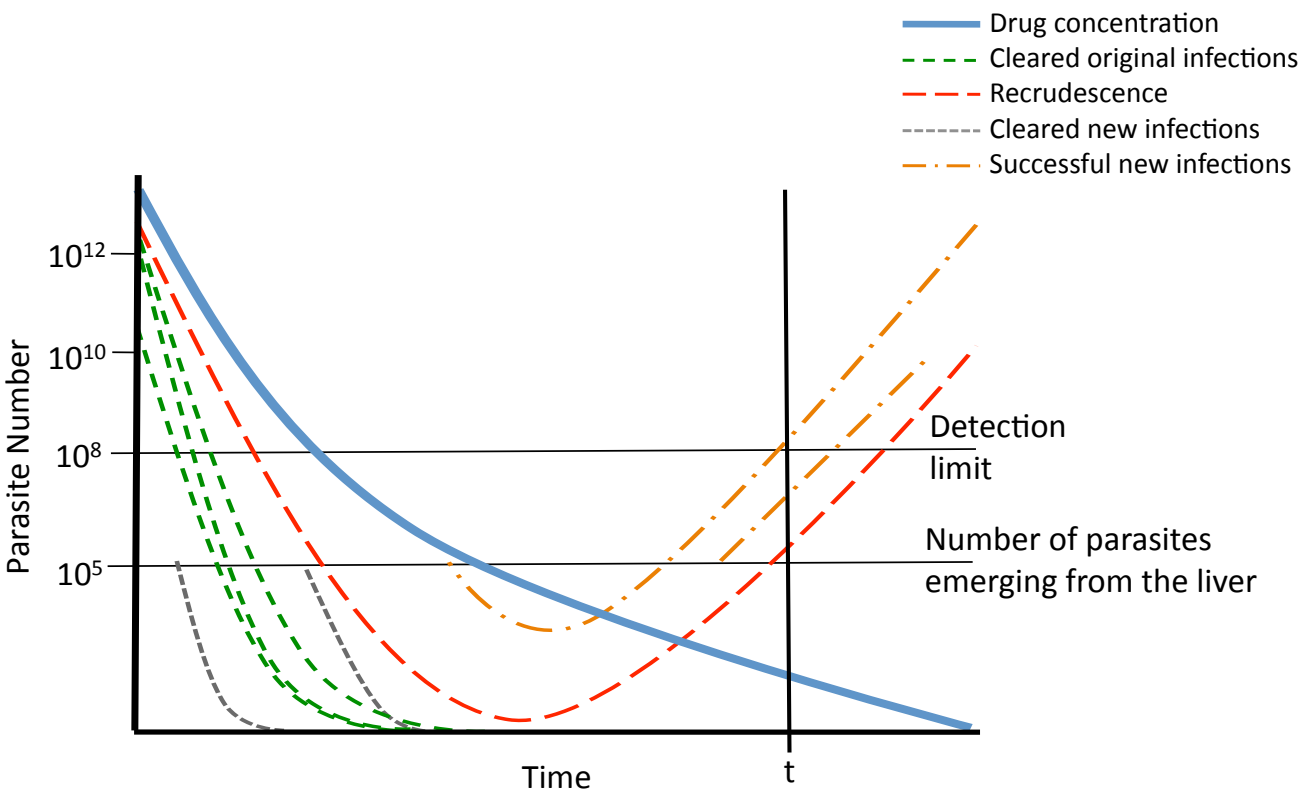

Figure 1. The changing drug concentration (blue) and parasite number over time, within a patient. Those parasites clones present at the time of treatment can either be cleared by the drug (green) or recrudesce later (red). New infections can also either be cleared by the existing drug (grey) or become established within the patient (orange).

2. However the relative numbers of each clone means some maybe missed from the analysis (for example, the grey lines represent clones with continually low numbers).
3. Some drugs have a long half-life and so failures can occur more than 50 days after treatment (red line) hence the long period of follow-up and high drop out rates
4. New infections occur at a relatively high rate, approximately 6 to 16 per person per year in areas of high transmission. Current drugs do not affect the liver stages and so new infections emerge with approximately 10^5 parasites, these will then either be cleared (gray lines) or cause new infections (orange lines).
5. At time '*t*' there are several clones present, genotyping will give a 'mixed' result i.e. the sample will contain a mixture of alleles, some which were present at the time of treatment and some which were not.

Generating simulated datasets, where we know the 'true' answers, seemed to provide an ideal opportunity to assess the different methods of analysis. We will generate simulated data designed to address the following questions/issues that typically arise during the analysis of trial data

A. Dealing with data of patients who don't attend all follow-up appointments
B. Calculating drug effectiveness on a per parasite clone basis
C. The best use of genetic markers to distinguish new infections from reinfections
D. The extent to which genotyping resolution/sensitivity affects results

A. Patient drop out data

High patient drop out rates frequently cause recrudescent infections to be missed. The phase 3 of clinical trials typically include between 100 and 500 individuals and for treatments to be deemed successful patients must attend all appointments for the trial duration. The WHO currently recommend a follow-up duration of 28 days for all antimalarials and extend this to 42 days for treatments containing either MQ or piperaquine (PQ) (380). Treatment failures can occur at any time during follow-up at which point patients are no longer required to attend further appointments. Consequently treatment successes require longer follow-up periods than treatment failures. Patients can be lost from trials for a number of reasons, for example they may be withdrawn by their doctor, they may withdraw consent, travel outside the catchment area or in some cases they may die. In almost all clinical trials some patients are lost to follow-up (a systematic review of loss to follow-up in randomised controlled studies was conducted by Akl *et al.* (2)) and the data from these patients is often removed before result analysis (PP vs ITT analysis) (368). This may bias results as the extended follow-up period required to define a treatment as "successful" means patients drop-outs are more likely to occur in this group. Our first aim was to generate computer-generated data to determine whether there is a better way to deal with the data lost to patient dropouts.

B. Failure rate per clone

Molecular studies have demonstrated that a patient with malaria can be simultaneously infected with multiple, genetically distinct *Plasmodium falciparum* clones (117, 259, 308). The number of 'clones' present in the patient at a specific time point is called the multiplicity of infection (MOI) and can be found using hyper-variable genetic 'markers' such as *msp-1*, *msp-2* and *glurp* (386). Following antimalarial treatment, outcome is currently measured as success or failure per human but an association between MOI and both clinical episodes and treatment failure (12, 181) has been demonstrated although not conclusively established. In this case, the higher the transmission the more likely the patient will be infected with multiple clones. If true, this implies a cure is always easier to achieve in areas of low transmission where only a single clone has to be cleared by treatment compared to high transmission areas where success may require up to six clones to be cleared simultaneously. If this is the case it is not feasible to compare the drug success rates of different studies with different levels of transmission. To address this problem and allow for comparison between studies, we would like to calculate treatment outcome on a per-clone as well as per-human basis.

C. New versus recrudescent infections

Malaria transmission intensity is usually expressed in terms of the entomological inoculation rate (EIR) and this can typically vary from <1 to >1000 infective bites per person per annum (31). Where EIR are high locally, treated patients often develop a new infection during the course of follow-up. In some areas of Africa with very high transmission more than 50% of patients develop recurrent parasitaemia within 28 days of treatment (46). This suggests as many as 50% of the reported treatment failures may be re-infections (rather than true treatment failures), to deal with this we need to accurately differentiate re-infections from recrudescence.

In principal, re-infections can be distinguished from drug failures by their molecular signature alleles at highly variable 'marker' genes. For example, if alleles A, B, C were detected at the time of treatment and the patient develops malaria four weeks later, this infection will be classed as a drug failure only if alleles A, B and/or C are present. Note that

each marker has many alleles and so comparisons must in fact determine whether the same alleles (rather than the simply markers) are present before or after treatment. Genotyping is the current method recommended by the World Health Organisation (386) to distinguish a new infection from a recrudescent infection with the majority using up to three markers, typically *msp-1*, *msp-2* and *glurp*. These are highly genetically diverse markers (see for example (230)) that are believed to have no influence on treatment outcome, but do allow us to compare pre- and post-treatment parasite clones. Whilst genotyping provides a measure of the genetic diversity of an infection, genotyping techniques have not been standardised. The results are open to interpretation (308) and the differing methods used across laboratories (99) have a varied ability to measure diversity (67), this can have potentially large effects on estimates of treatment efficacy. In an effort to improve this measure of diversity a combination of markers is often used, two parasite clones may have the same allele at one marker but different alleles at another (315).

A recent paper by Juliano *et al*. (162) highlights the main sources of error associated with parasite strain genotyping (a.k.a. PCR-correction) (i) sequestered parasites are absent from the peripheral blood at time of sampling, (ii) parasites present as a minor variant and missed by less sensitive genotyping methods (iii) parasites missed due to over amplification of the more abundant DNA sequences, a particular problem when using nested PCR (iv) the effect of antimalarials on the abundance and composition of the host parasite population is unknown, (v) the chance of reinfections with new parasites with the same genotype (162). Phase III trials are now shifting to non-inferiority trials comparing drug regimens with high cure rates rather than superiority trials that are usually conducted in areas where the recommended treatment is failing (37). Drugs compared in non-inferiority trials are expected to perform equally well and so even minor misclassification of newly acquired or recrudescent infections can have a significant impact on the estimated risk of treatment failure and hence the decisions of policy makers regarding optimal drug therapy. The accuracy of genotyping via PCR-correction has understandably attracted considerable attention (67, 107, 308, 322). For example, Juliano *et al.* (161) show 5 out of 6 (83%) patients from clinical trails in Thailand and Cambodia were incorrectly classified as being reinfected when using standard PCR (polymerase chain reaction) protocol. When using the more sensitive heteroduplex tracking assays (HTA) and direct DNA sequencing they found these infections to be recrudescences (161). This misclassification leads to overestimates of drug efficacy and may delay switches in first-line antimalarial policy.

Distinguishing a new infection from a re-infection is further hampered by the risk that pre- and post-treatment samples will have matching alleles by chance. While this chance is relatively low in areas with a low EIR (116), the risk increases with increasing MOI and/or with increasing transmission intensity. An over-estimation of the true risk of treatment failure is likely to occur when transmission is high as a large proportion of drug failures are likely to be new infections misclassified as a recrudescence (116). An antimalarial efficacy study carried out in Uganda (53) found the chance of two random infections having identical alleles by chance was 5% for *msp-1* (45 unique alleles detected), 2% for *msp-2 (*57 alleles) and 7% for *glurp* (28 alleles). Genotyping is currently carried out without consideration for the increased likelihood that genotypes may match by chance when MOI and/or transmission intensity are high (67, 116). A recrudescence is simply defined by the detection of at least one identical marker allele in both the pre- and post-treatment samples (315, 386). The extent to which transmission intensity may affect genotyping classification and thus the accuracy of results from clinical trials has not been studied (116). We would like to know how genotyping techniques, sensitivity and resolution affect estimates of antimalarial efficacy.

D. Genotyping sensitivity

During genotyping analysis, it is difficult to detect 'minor' alleles if they are present in less than 10-20% the frequency of the most common allele, this often leads to misclassification of drug success rates (129). This can be a particular problem if MOI is high, Färnert *et al*. (100) for example showed the composition of infecting clones in Tanzanian children changed daily over 14-days. Sama *et al.* (284) used mathematical models to analyse the infection dynamics of heavily parasitized patients in northern Ghana and estimated that on average only 47% (42-51, 95% CI) of the parasite clones present were detected in a finger-prick sample. The effect of genotyping sensitivity was subsequently looked at in the field by Koepfli *et al.* (175), their study in Papua New Guinea (PNG) included sampling children on fourteen consecutive days to find the proportion of clones typically missed in a single bleed, in this case 18-31%.

2. Liverpool School of Tropical Medicine's (LSTM) role in the project

This work was done in collaboration with Alice Parry (masters and PhD student) at the department of Mathematics and Statistics, Lancaster University and her supervisor (Dr Thomas Jaki). The strategy was to identify key questions about analysis of field data (outlined above) and simulate datasets at LSTM designed to address these questions. The simulated results were generated using a modified version of the model described by Winter & Hastings (364), with appropriate modifications as described below. The resulting simulation data was forwarded to Parry for statistical analysis.

3. Methods

3.1. General Methods

The methods used to generate the results presented here are an extension of those published in Winter & Hastings (364). We chose to investigate three antimalarial drug treatments, two were current first-line artemisinin combination therapies (ACTs) artemether-lumefantrine (AR+LF) and artesunate-mefloquine (AS+MQ). The third treatment was chloroquine (CQ) monotherapy, which although no longer officially deployed in the formal health sector, was included here for historical comparison. The dosing regimens of the drugs investigated and the PK/PD parameters used are included in Table 1. Natural variation was incorporated into the model PK/PD parameters by simply assuming that each parameter was normally distributed, with a co-efficient of variation of 30% (364). It is important to note that when assigning parameters within the model the fates (survival/death) of the different clones in each human were non-independent, as they share the same host environment. For example, background levels of immunity and rates of drug metabolism vary substantially between humans, if a human has a low level of immunity or rapidly metabolised a drug then all the clones present during treatment shared this (relatively benign) human environment. Consequently, pharmacokinetic parameters were considered to be a human attribute, unique to each human but common to all clones within a human.

Although we allowed for environmental similarities, we assumed no genetic relatedness between clones within a human and so the pharmacodynamic properties (IC50, maximum parasite kill rates and slope factor), the parasite growth rate and initial numbers present were assigned to each clone independently.

To address the questions outlined above, the model of Winter & Hastings (364) required the following three modifications

i. The presence of more than one clone at the start of treatment

The number of clones present at the start of treatment was assigned to each patient using data collected by Nsanzabana (244, 245) and used in Hastings *et al.* (129). The data was collected from an area of high transmission in Tanzania where MOI typically ranged from one to eight (Figure 2). The probability of a patient being assigned a specific MOI was defined by on this frequency distribution of MOI measured. The initial number of parasites present at the start of treatment for each clone was chosen from a uniform distribution between 10^{10} and 10^{12}.

ii. The acquisition of new infections during the course of treatment

The model was adapted to allow patients to acquire new infections during the course of follow-up. The number of new infections was assigned to each patient at the beginning of the simulation and simulated using the average number of reinfections occurring per patient per year. In this case we used reinfection data from Northern Ghana (284) where maximum likelihood estimates suggested on average any individual would acquire 16 new infections per year. This data is consistent was data on effective ACTs. For example, Bukirwa *et al.* (46) report more than 50% of patients developed recurrent parasitaemia within a month of treatment (51% of patients following AR-LF treatment and 66% of patients after AS-AQ

Table 1. Standard adult dosages recommended by WHO (2006) and mean antimalarial drug parameters for artemether, artesunate, chloroquine, lumefantrine and mefloquine [a]

Variable	Default value				
	Artemether	Artesunate	Chloroquine	Lumefantrine	Mefloquine
Dose (mg/kg)	1.6mg/kg twice daily for 3 days	4mg/kg once daily for 3 days	10mg/kg once on days 1 and 2, 5mg/kg once on day 3	19.2mg/kg twice daily for 3 days	25mg/kg once
Volume of distribution (*Vd*)	17.4[110]	2.75[301]	300[359, 397]	21[68]	20.8[359]
Elimination rate constant (*k*)	3.96 [b]	16.6 [212, 321]	0.023[359]	0.16[110, 212, 350]	0.053[350]
Conc. required to produce half the desired effect (IC_{50})	0.0023 [b]	0.001[44, 211]	0.036 [0.02 [211, 225]]	0.032[44, 321]	0.55 [0.027 [44]]
Maximal parasite-killing rate constant (*V*)	4[355]	4.6[355]	3.45[355]	3.45[355]	3.45[355]
Slope factor (*n*)	4 [c]	4[321]	1.6 [b]	4[321]	5[321]

[a] The two values in square brackets indicate those that were later used in Winter & Hastings

[b] unpublished data from LSTM

[c] assumed to be like AS

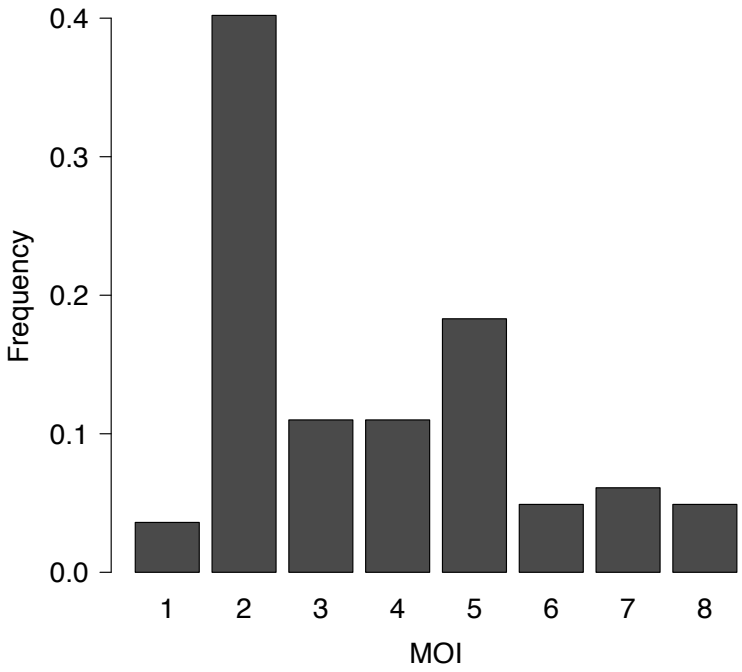

Figure 2. The probability of a patient being assigned a specific MOI was dependent on the frequency distribution of MOI measured in the field. The data plotted here was collected by Nsanzabana (245) in an area of high transmission in Tanzania (1993-1994).

treatment). If we assume reinfections can occur at any time in the month following treatment we can predict each patient will acquire approximately 6 new infections each year. However, we know patients were taking effective ACTs with long half lives so we can crudely assume no new infections became established for the first two weeks. Following treatment (due to their long half-life), 50% of patients get new infections in a 2-week period and so are likely to receive an average of 12 new infections each year. Areas with lower transmission would obviously have lower reinfection rates. For example, reinfection rates have recently been measured in an area of moderate transmission in PNG and show children (treated with AR-LF (189)) acquired approximately 6 new infections per child per year (226)

The probability of a new infection occurring during the designated follow-up period was found by dividing the number of re-infections per year, by the number of days in a year and then multiplying by the number of days in the patient follow-up period. For

example, if simulated patients were followed for 63 days after treatment (the typical length of an antimalarial clinical trial) and were assumed to have 16 new infections per year, they will have an average of 2.8 (16/365 * 63 = 2.8) new infections during the follow-up period. Variation was added by choosing the exact number of new infections randomly from a poisson distribution..

In cases where patients were re-infected during follow-up we assumed parasites first became susceptible to drug treatment on emergence from the liver. Initial parasite number was therefore based on the emergence of 10^5 merozoites whilst random sampling determined the specific day parasites emerged.

iii. Tracking of individual clones using molecular markers.

We simulated the commonly used markers *msp-1, msp-2* and *glurp* alongside the microsatellites *TA109*, *TA1*, and *ARA2*. At the beginning of each simulation, each clone present at the start of treatment or later appearing in a new infection was assigned a specific allele for each of the markers.

The allele frequency data for *msp-1* and *msp-2* were taken from a study in Papua New Guinea by Schöpflin *et al.* (294) with raw data kindly provided by Ingrid Felger (Figure 3). Polymerase chain reaction (PCR) is a simple enzymatic technique used for the amplification of DNA fragments and allows for the detection of nucleic acid polymorphisms. Schöpflin *et al.* (294) use nested PCR (nPCR), a more sensitive and specific form of PCR, to identify the genetic variation (i.e. different alleles) in the markers. Porter *et al.* (263) note that the insensitivity of nPCR to small changes in the number of base pairs (bp) means variants differing by less than 20bp are routinely considered to be the same allele. The raw data contained details of allele length (bp), class and codes however for simplicity in the model the 24 *msp-1* and 35 *msp-2* alleles were arbitrarily numbered and any potential misclassification of alleles as a result of base pair repeats was ignored. The frequency with which alleles were measured in the field was used to determine the probability of a clone containing that

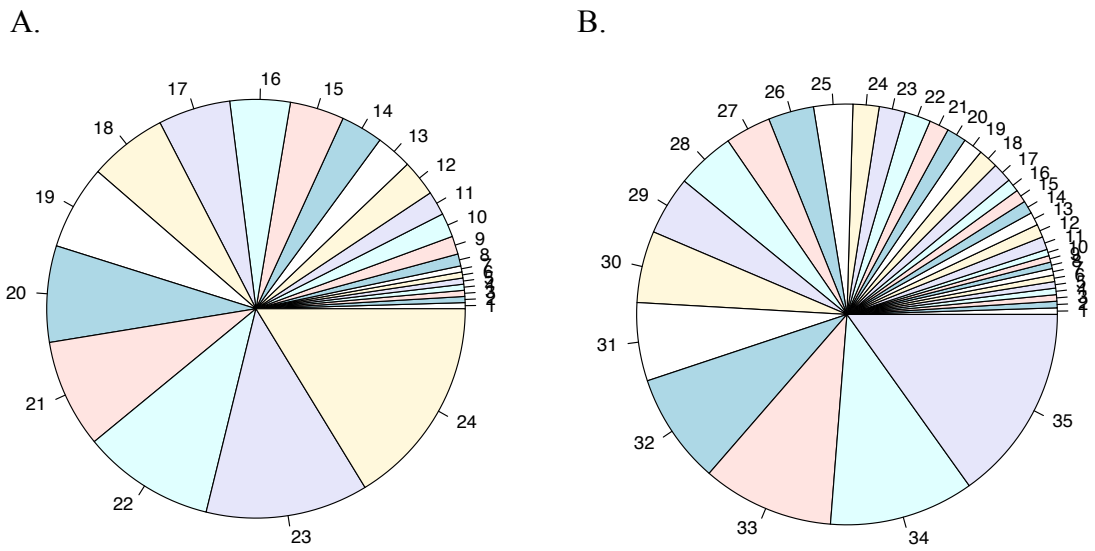

Figure 3. The allele frequency distribution of (A) *msp-1* and (B) *msp-2* markers, the data were taken from a study in Papua New Guinea with moderately high transmission by Schöpflin *et al.* (294).

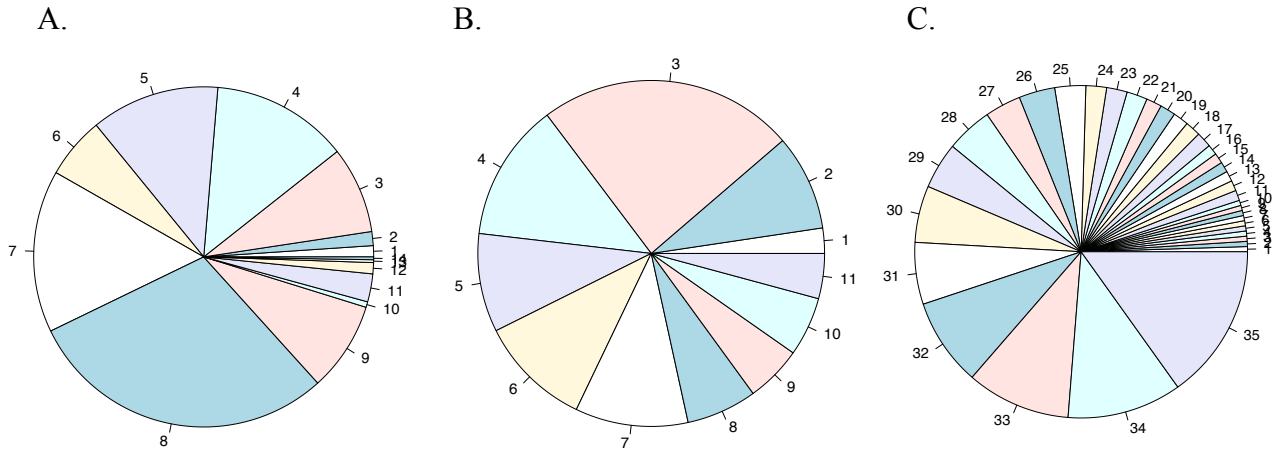

Figure 4. The allele frequency distribution of the microsatellite markers (A) *TA109*, (B) *TA1* and (C) *ARA2* in an area of moderately high transmission in Malawi (between 2002 and 2003), as described in Mzilohowa *et al.* (231).

allele in the simulation. The microsatellite markers *TA109* (14 alleles), *TA1* (11 alleles), and *ARA2* (12 alleles), were originally described by Anderson *et al.* (339) however the distributions used here came from a more recent dataset collected in Malawi and described by Mzilahowa *et al.* (231) (Figure 4). Again each allele was arbitrarily numbered and the probability of a clone containing a given allele corresponded with the frequency that allele was seen in the field. The frequency distribution of *glurp* alleles was not found in time to be included in the simulations, see discussion.

Note - although no information regarding allele size, class or code was passed to Parry, the information can of course be provided if necessary.

3.2. Simulation Details

A population of 10,000 individuals was simulated for each of the three treatment regimens. Each patient in the simulation had a malaria infection which could include multiple clones and were at risk of acquiring new infections during the period of follow-up. These details along with the timing of new infections (if any), patient PK and parasite PD parameters were all assigned to the patient at the beginning of the simulation. The model tracked drug concentration and parasite number for 100-days following the first treatment dose. While clinical trials typically run for up to 63 days (368), the 100-days of follow-up allowed us to determine the degree to which a trials follow-up period censors data. Simulations ran in half-day time steps for the first seven days allowing multiple drug dosages to be administered but to speed up simulations all subsequent days were modelled in one-day time steps.

To answer such a diverse range of questions a large amount of data about both the patient and the parasites was recorded and subsequently passed to Parry for analysis. For each human this included the specific PK parameters, their initial MOI, the number of new infections that occurred and the day new infections emerged from the liver. For each parasite clone present at any point during the follow-up period the initial parasitaemia, the growth rate, the specific PD parameters, the associated

genotype and the exact number of parasites present on each day of the follow-up period was recorded. This data could then be used to determine the day each original clone in the infection first becomes undetectable in the blood (i.e. parasite numbers < 10^8), the day a clone is cleared from the body (i.e. parasite numbers < 1) if treatment is successful and the day recrudescence occurs (i.e. parasite numbers >10^8) if treatment fails (Figure 1).

To address each of the questions outlined above we suggest the following strategies.

A. Patient drop out data

All the necessary patient information required to address this question is included in the data set. The results can be easily manipulated to examine the methods of dealing with data lost to follow-up. For example by omitting data from the simulated results it is possible to produce results that mimic patients who fail to attend all follow-up appointments.

B. Failure rate per clone

The simulated data set includes information about the exact fate of each clone, each day after treatment. This can be used alongside the MOI of the patient's initial infection to determine a failure rate per clone.

C. New versus recrudescent infections

The simulations provide data about every clone present in both the original host infection and any new infections, with this information it is easy to determine the true cause of treatment failure. Field conditions (i.e. non-detectability of clones present at low frequencies (see D)) can be recreated by omitting data, analysis of the complete

and edited results will then show how closely field studies estimate the reasons behind treatment failure.

D. Genotyping Sensitivity

All clones present within the body were assigned a specific genotype and the alleles present each day recorded. The relative numbers of each clone can be used to determine the strength of the genotyping signal. For example, if clone A has 10^{10} parasites and clone B has 10^{6} then it is unlikely clone B will ever be detected. From this we can then examine the effects of genotyping sensitivity.

4. Discussion

This work was done under strict time constraints early in the project; it was assumed that as the methodology and parameter calibration developed new simulated data would be provided. The main methodology employed here was described and validated in Winter & Hastings (364) however at the time of running simulations model calibration was incomplete (see below). Consequently, drug parasite clearance times and failure rates do not match those presented in Winter & Hastings (364).

The widespread resistance of parasites to CQ and MQ made it difficult to find recent papers with reliable IC50 estimates for fully sensitive parasites. The IC50 values presented here for CQ and MQ (Table 1) are therefore higher than those that have since been validated in the paper. For CQ the difference is small (0.032 to 0.002) and it's effect on the results negligible, the failure rates are still reliably within the range given in field estimates at 97% successful. The estimated MQ IC50 of 0.55 used here is significantly higher than the 0.027 used in Winter & Hastings (364), as a consequence the treatment failure rates for AS-MQ (86%) mimic those of a grossly failing regimen. The AR-LF data was typical of a drug just beginning to fail (87% success) and can be used alongside the very successful (CQ) and very unsuccessful

(AS-MQ) regimens to analyse drugs with varying degrees of resistance. Time constraints also prevented the inclusion of the *glurp* marker allele distribution however this can easily be added at a later date. Descriptions of the *glurp* allele frequencies have been collected by Cattamanchi *et al*. (53) in Uganda and more recently by Mwingira *et al*. (230) in Burkina Faso, São Tomé, Malawi, Tanzania and Uganda.

Variation was incorporated into the model by assuming all model parameters were normally distributed with a co-efficient of variation of 30%. Whilst this was initially required to allow the relative importance of parameter values to be assessed it was not the most realistic scenario. We know some parameters, such as IC50 are much more variable (Mu *et al*. (225) report a range of greater than 100-fold) whilst others maybe much less variable. Work is on going to find more sophisticated descriptions of model parameters.

As is necessary with all models, assumptions were made during this models construction. The assumptions were as follows.

i. Drugs were instantly and fully absorbed and converted (if necessary) to their active metabolite. Whilst absorption lag-time maybe negligible for drugs with a long half-life (in this case CQ, LF and MQ) it becomes more important for the artemisinins with half-lives as short as 40 minutes.
ii. The number of new infections is allocated independently of initial MOI, this ignores potential issues of spatial heterogeneity. Intuitively, those patients with a higher MOI are more at risk of acquiring new infections and hence more likely to become re-infected during patient follow-up.
iii. Patients complied fully with the designated treatment regimen.
iv. Assume there is no genetic relatedness between the clones, infections within a host can include multiple genetically distinct parasite clones
v. There was no sequestration of malaria-infected erythrocytes. This is usually characteristic of infections with *P.falciparum*, Koepfli *et al*. (175) reported parasites can be sequestered in the internal organs for up to 20 hours of the 48 hour lifecycle. Naturally if parasites are sequestered in the organs they will not be

present in the peripheral blood thus increasing the risk of missing clones when genotyping in a single blood sample.

The model presented here was developed using the methodology described in Winter & Hastings (364). Parry chose to focus her analysis on just one of the issues that typically arise during analysis of clinical trial data (see A-D of the introduction) i.e. determining the effectiveness of drugs on a per clone basis. The model described herein produced plausible datasets and the results are now published (see Appendix (158)). This methodology has since been extended to mathematically incorporate the absorption, conversion and distribution phases of the drugs (168) as described in Chapter 2 of this thesis. This updated methodology will be used to generate new datasets and, while unlikely to make qualitative differences to Parry's results, will produce results that are biologically more realistic. Parry decided against using results generated using these new methods while developing the methods described in Jaki *et al.* (158) but will use them in her future work. Parry now aims to develop a methodology that allows drug effectiveness to be analysed by its ability to cure patients, and it's ability to prevent re-infections, beginning with analyses with two binary endpoints (i.e. treatment cure/failure and the presence/absence of new infections on day 28). I have now generated the new datasets for two treatment combinations (AS-MQ and AR-LF) consisting of the requested 2,500,000 individuals. The sample size was calculated by Parry to allow statistical analysis of 10,000 clinical trials including up 250 people per trial. The technical challenges associated with generating samples of this size required that I run the models remotely on servers for high performance computing available within LSTM. However it should be noted that with the model extensions outlined in the chapter, the model is still capable of addressing all the questions outlined above and so this work also forms the basis for a grant application to further develop methods of analysing antimalarial drug clinical trials (see Chapter 7 for more information).

Appendix

Co-authorship paper

Research Article

Statistics in Medicine

Received 27 February 2012, Accepted 22 November 2012 Published online in Wiley Online Library

(wileyonlinelibrary.com) DOI: 10.1002/sim.5706

Analysing malaria drug trials on a per-individual or per-clone basis: a comparison of methods

Thomas Jaki,[a] Alice Parry,[a*†] Katherine Winter[b] and Ian Hastings[b]

There are a variety of methods used to estimate the effectiveness of antimalarial drugs in clinical trials, invariably on a per-person basis. A person, however, may have more than one malaria infection present at the time of treatment. We evaluate currently used methods for analysing malaria trials on a per-individual basis and introduce a novel method to estimate the cure rate on a per-infection (clone) basis. We used simulated and real data to highlight the differences of the various methods. We give special attention to classifying outcomes as cured, recrudescent (infections that never fully cleared) or ambiguous on the basis of genetic markers at three loci. To estimate cure rates on a per-clone basis, we used the genetic information within an individual before treatment to determine the number of clones present. We used the genetic information obtained at the time of treatment failure to classify clones as recrudescence or new infections. On the per-individual level, we find that the most accurate methods of classification label an individual as newly infected if all alleles are different at the beginning and at the time of failure and as a recrudescence if all or some alleles were the same. The most appropriate analysis method is survival analysis or alternatively for complete data/per-protocol analysis a proportion estimate that treats new infections as successes. We show that the analysis of drug effectiveness on a per-clone basis estimates the cure rate accurately and allows more detailed evaluation of the performance of the treatment.

Keywords: clone; cure rate; malaria; per-clone; per individual

1. Introduction

Malaria treatments need to be monitored on a regular basis to ensure that the therapies used are still effective. The current standard for these trials, and trials of new treatments, is randomised controlled trials. Superiority trials were the standard design used when first-line drugs were failing, but artemisinin-based combination therapies (ACTs) are all currently effective, so interest is moving to non-inferiority trials to confirm effectiveness [1, 2]. Taking a blood sample and estimating the number of parasites by the proportion of parasitised red blood cells prior to treatment detect whether a subject is infected and subsequently treated. Converting the proportion of parasitised red blood cells to an absolute number of parasites aids pharmacological analysis. A typical symptomatic infection has between 10^{10} and 10^{12} parasites, and only parasite counts greater than 10^{8} are detectable by microscopy. The undetectable parasite counts together with the possibility of multiple genetically distinct infections (clones) present at one time make antimalarial drug trials in resource-poor environments particularly challenging. Figure 1 shows the possible clone dynamics and outcomes within one patient.

We can seen from the figure that the time points at which the effectiveness of a treatment is assessed is highly important as infections appear to have cleared while the parasite is still present, although in undetectable numbers. The consequence is that current trials evaluate parasite counts regularly up to

[a]*Medical and Pharmaceutical Research Unit, Department of Mathematics and Statistics, Lancaster University, Lancaster, U.K.*
[b]*Liverpool School of Tropical Medicine, Pembroke Place, Liverpool L5 3QA, U.K.*
**Correspondence to: Alice Parry, Medical and Pharmaceutical Research Unit, Department of Mathematics and Statistics, Lancaster University, Lancaster, U.K.*
†*E-mail: a.parry1@lancaster.ac.uk*

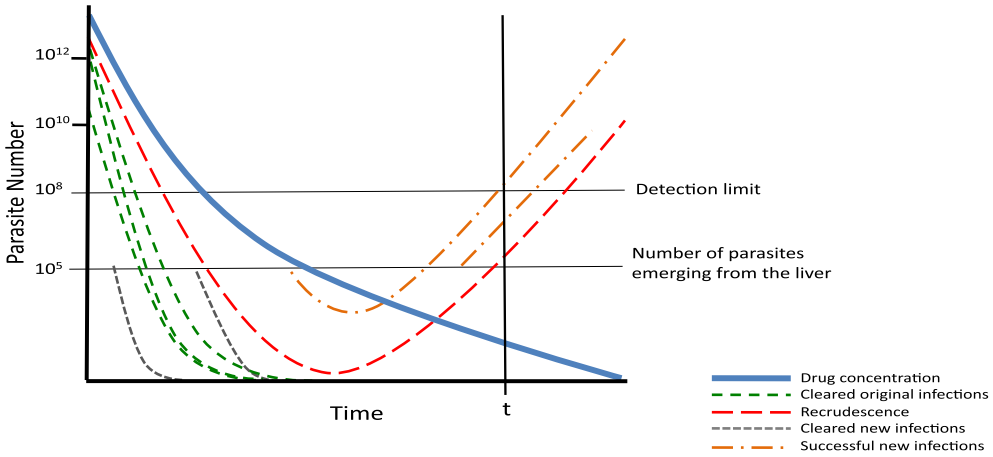

Figure 1. The changing drug concentration (thick solid line) and parasite number over time, within a patient. Those parasite clones present at the time of treatment can either be cleared by the drug (dashed) or recrudesce later (long dash). New infections can also either be cleared (small dash) by the existing drug or become established within the patient (dot-dash).

day 63 with evaluations on days 3, 7, 10, 14, 21, 28, 35, 42, 49, 56 and 63. We consider a treatment effective if the patient is clear of the parasite at all time points after day 3 as the parasite may be detectable up to day 3 because of the time required to clear a large number of parasites. This intense follow-up schedule is responsible for only 100–200 patients having complete observations out of the 300–500 patients typically recruited.

An infected person being still liable to be bitten and re-infected with a genetically distinct clone further complicates the assessment of the effectiveness of malaria treatments. Field data suggest that people acquire up to 16 new infections per year [3]. Consequently, there may be as many as 10 genetically distinct clones present in an individual at the time of treatment in areas of high transmission [4]. In principle, we can distinguish new infections from an infection that has never been fully cleared (recrudescent) by their molecular signatures or markers, which are genotyped using polymerase chain reaction (PCR), although in practice some uncertainty remains. Often, three markers are used with the two most frequently used markers, Merozoite surface protein 1 (*msp-1*) and Merozoite surface protein 2 (*msp-2*). A correct classification of infections is crucial to assessing if a treatment has successfully cleared an existing infection in the presence of parasites.

The World Health Organisation (WHO) have established a trial protocol for the design and analysis of malaria trials, stating that trials should be analysed using survival methods and providing a method for the classification of mixed genotypes [5]. Mixed genotypes occur when a treated individual contains at least two clones at a follow-up time point: one is a new infection, and one was present at the start of treatment and has never been fully cleared (recrudescent). Despite the report being released in 2003, there are still various classification and analytic methods used in practice [6, 7].

Methods of classifying infections that can be found in the literature largely differ in whether mixed infections are classified as new infections or recrudescences. For example, Dorsey *et al.* [8] used the proportion of new alleles in the mixed infections and assigned an outcome according to whether the proportion is greater than a half. The handling of early treatment failures (ETF), where the individual fails treatment on days 1–3, also varies. After day 4, the infection may be a new infection appearing, but before, it is more likely to be a highly robust initial infection. Verret *et al.* [9] treated ETF as recrudescences, whereas others treated them along with other infections. Table I shows different approaches to classification that have been found in the literature.

Even when the classification has been made, there still remain differences in the method of analysis (Table II). The variety of methods includes intention-to-treat (ITT), per-protocol (PP), and time-to-event analyses. The methods of analysis also involve choosing between a simple proportion estimate of the number of individuals cured and survival analysis. Furthermore, new infections may be regarded as either of the following:

(i) Drug failures because an infection is still present at the end of treatment
(ii) Successes as none of the original infections was detected before the time of failure (ToF)

Table I. Range of classification methods used to differentiate infections.

Method		Classification	Examples
I	All alleles are different pre-treatment and post-treatment Mixed infections All alleles are the same pre-treatment and post-treatment	New Recrudescence	[10]
II	All alleles are different pre-treatment and post-treatment Mixed infections ETF All alleles are the same pre-treatment and post-treatment	New Recrudescence	[11]
III	All alleles are different pre-treatment and post-treatment Mixed infections ETF All alleles are the same pre-treatment and post-treatment	New Recrudescence	[11]
IV	All alleles are different pre-treatment and post-treatment Mixed infections (less than 50% of alleles are different) Mixed infections (more than 50% of alleles are the same) All alleles are the same pre-treatment and post-treatment	New Recrudescence	[12]
V	All alleles are different pre-treatment and post-treatment Mixed infections All alleles are the same pre-treatment and post-treatment	New Removed Recrudescence	[10]

ETF, early treatment failure.

There are also differences in adjusting for the probability of matching alleles purely by chance. The consequence is that despite the WHO recommendation, no real standard of analysing malaria trials exists.

Analysing malaria trial data from the individual patient outcome allows insights into the effectiveness of a treatment only on the patient level. For a comparison of the effectiveness across locations, for example, such analyses are insufficient as it is simpler to clear a patient with only one clone, the likely situation in low-transmission areas, than if 10 clones are present as can be observed in high-transmission areas. Figure 2 depicts the proportion of subjects completely free of malaria at 28 days dependent on the number of clones present at time of treatment of a real data example, which is discussed in more detail later. The overall trend suggests that as the number of clones present at the start increases, the proportion of individuals completely cured reduces. Note that a trend test is non-significant, however, which may be due to patients being only followed until day 28 so that it is expected that some of the clones will still recrudesce later. Little research that focuses on the clones within an individual and how this affects the treatment outcome has been undertaken. Reasons for this may include the complexity of such evaluations and the shift in focus of the analysis. In the most extreme case, one can find that a treatment cures a high percentage of clones, yet hardly any patients are infection free after treatment because of high multiplicity of infection (MOI) and a high frequency of a particularly resistant clone in the population. A complication of the per-clone analysis is that PCR genotyping only provides information on certain markers of the parasite genome. Hence, the same alleles could be found at a given locus purely by chance despite originating from genetically different infections. Research by Brockman *et al*. [13] suggests that it is often impossible to assign multilocus genotypes to individual clones that can be tracked throughout the course of follow-up. This implies that it is not currently possible to detect which alleles belong to which clones. Instead, we only know an estimate of how many clones are present and a multiclonal genotype for the individual. A direct consequence of this is that the failure time of each clone is unknown, ruling out the use of survival analysis on a per-clone basis, the recommended analysis on an individual level by the WHO.

Per-clone and per-person analyses are not mutually exclusive, and we should not view them as competitors but rather as complementary approaches. Per-person analysis is important for clinicians and patients, whereas per-clone analysis is important for surveillance because areas of differing MOI could be compared at an equal level. It could be argued that per clone would be a better analysis as you gain more information if a person with MOI $= 13$ is completely cleared than you do if a person with MOI $= 1$ is cleared. It also allows a more explicit analysis of the 'mixed' genotypes such as those in Table IV, which will be discussed in more detail later. Importantly, the fate of the clones within an

Table II. Different methods used to analyse malaria trials.

	Method of analysis
Unadjusted	
A	ITT simple estimate (number cleared/total) using all patients enrolled in the study
B	PP simple estimate (number cleared/total) using only those that clear (ACPR) and recurrent patients
C	mITT Kaplan–Meier product limit formula—all patients enrolled in the study. Censoring for patients with interrupted follow-up. Recurrent patients classed as failures
D	Proportion of cure at day 14, where cure is being clear of infection at day 14
E	Proportion of cure at day 28, where cure is being clear of infection at day 28
Adjusted—genotyping	
A1	Exclusion criteria: none New infections: treated as successes Unsuccessful genotyping: treated as failure
A2	Exclusion criteria: none New infections: treated as failures Unsuccessful genotyping: treated as failure
B1	Exclusion criteria: all except those that clear (ACPR) or recrudesce New infections: excluded Unsuccessful genotyping: excluded
B2	Exclusion criteria: problems with follow-up and genotyping New infections: treated as successes
B3	Exclusion criteria: problems with follow-up and genotyping New infections: treated as failures
C1	Exclusion criteria: unsuccessful genotyping New infections: censored along with those with interrupted follow-up
Accounting for probability of randomly matching alleles of distinct clones	
A1a–C1a	Repeat methods A1–C1, taking into account the probability of matching by chance (p.match)

ACPR, adequate clinical and parasitological response; ITT, intention to treat; mITT, modified intention to treat; PP, per protocol.

'Unadjusted' means that the genetic marker information was unavailable (or not used) to distinguish new infections from recrudescences. 'Adjusted' uses the marker information as summarised in Table I. We classify patients for whom genotyping was performed but whose results were inconclusive or unavailable as unsuccessfully genotyped.

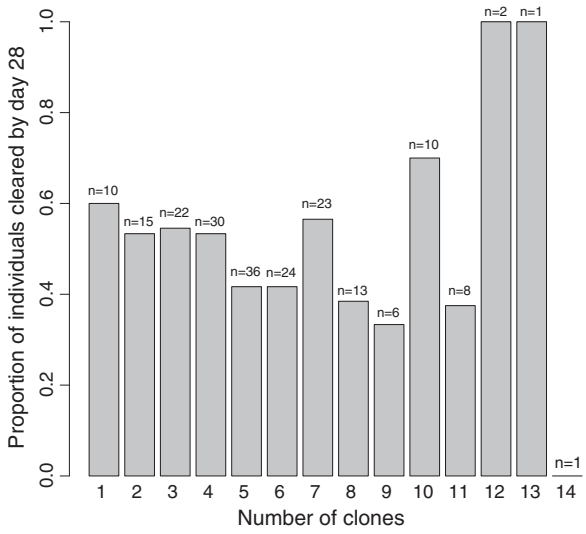

Figure 2. Proportion of individuals completely clear of malaria 28 days after treatment by the number of clones present at time of treatment in a real trial dataset.

infected person is not independent as people vary in their drug metabolism rates, so clones share the same pharmacological environment.

There are several further complications associated with estimating and tracking the clones. It is, for example, only possible to detect parasites that are present in the blood in large enough numbers ($>10^8$), which leads to uncertainty about what alleles/clones are present at the time of treatment because some may be below the limit of detection (Figure 1). The number of detected parasites, however, does not remain constant but fluctuates daily. When we try to detect clones, it is difficult to detect a clone if it is present in relatively small numbers compared with a more numerically dominant clone. If clones are present in numbers less than 10–30% of the numerically dominant allele, then they will not be detected. Sama *et al*. [3] found that only 47% of the clones present in the host were detected when a blood sample was taken because of the oscillating number in the blood. This means that an infection may appear to be cleared when it was actually just not detectable at follow-up. Assessing a subject on two or more consecutive days would allow for an increase in the detection rate but obviously reduce the number of complete observations even further.

Because of the complexity of the data, we have made assumptions in the investigations to follow. In practice, there will be clones that are undetectable on the day the sample was taken and also some that were masked by a numerically dominant allele as described earlier. We have not addressed this issue in our evaluations as all methods will be equally affected by this, implying that the relative comparisons are still valid. Consider, for example, a clone that is not detected on the initial day. Detecting this clone at any later time point will always result in this clone being classed as a new infection, independent of the method of analysis used. Similarly, a clone that was previously detected but masked at a later time point will be viewed as a cleared clone. We have therefore assumed perfect detection for this work as long as clones are present in numbers greater than 10^8. In addition, we have assumed complete data throughout and consequently removed incomplete observations due to incomplete genotyping or loss to follow-up in the real dataset used. This assumption will again have no impact on the relative comparisons of methods that estimate a proportion cured. When working with simulated data, we only use information that would be available from field data in our comparison. For example, it is possible to track individual clones in the simulated data and 'distinguish' between clones with the same alleles at the measured markers. For our evaluations, however, we only note that the allele was detected, but not in how many clones. Once parasites are detected (defined as present in numbers greater than 10^8) at a follow-up day, the patient receives further treatment (for ethical reasons) and is then removed from follow-up. The evaluations presented here therefore follow patients to their ToF or day 63, whichever is sooner.

In summary, the evaluation of malaria treatments contains four main challenges:

(i) Classification of infections detected during follow-up
(ii) Analysis method
(iii) Per-clone versus per-individual analysis
(iv) Ambiguous genetic data

In this work, we will approach these challenges in two parts. In the first, we will conduct a thorough evaluation of methods used to classify and analyse malaria trial data on a per-individual basis. Collins *et al*. and Verret *et al*., for example, have undertaken similar investigations [6, 9]. In contrast to previous work, which was exclusively based on real trial data, we will focus attention on simulated data where the truth is known about all clones. This enables an informed comparison of the different methods rather than just highlighting differences. We also used a real trial dataset as a complement to the simulated data. The second part of this work develops a novel methodology to analyse malaria trial data on a per-clone level. We again evaluate the performance of the estimation scheme on both simulated and real trial data.

2. Data

We have used two different data sources in this work. The first set of data is simulated following the methods described in [14], with extensions to allow for multiple clones, new infections and molecular genotyping. It aims to replicate the course of infections in patients over a 100-day period following treatment. We generated data using infection and re-infection rates similar to those found in Tanzania, a high-transmission area, and validated them against field data [14]. See Appendix A for further information regarding data generation.

We simulate four datasets, each of 10 000 individuals, according to the dynamics of the three different treatments: artemether–lumefantrine (AL), artesunate–mefloquine (AS_MQ) and chloroquine (CQ). As a comparison of methods is difficult in datasets with no treatment failures, we adjusted the half maximal inhibitory concentration (IC50) parameters (Appendix A) so that the four treatments had very different cure rates. We have simulated the first two datasets according to the pharmacokinetics (PK)/pharmacodynamics (PD) characteristics of AL with cure rates of approximately 90% (AL90) and 80% (AL80), whereas the datasets based on CQ and AS_ MQ have cure rates of approximately 50% and 10%, respectively. It is important to highlight that we are not suggesting that, for example, the cure rate of AS_MQ is really 10%. Instead, PK/PD characteristics in the simulations matched those of AS_MQ, but we increased the IC50 parameter to obtain high failure rates. We focus on a subset of 500 subjects (the size of a standard trial) from the AL datasets, whereas we will use the other data for verification and confirmation purposes. The simulated variables were the number of clones at time of treatment, genetic information from the three markers, initial parasite number and parasite numbers from days 1 to 100 for each clone (both recrudescences and new infections). The genetic information simulated the allele frequencies observed from field data at three genetic markers: *msp-1*, *msp-2* and *TA109*. We will use arbitrary numbers rather than the allele names for simplicity of use.

Table III shows a summary of cure rates on per-individual and per-clone bases for one simulated dataset of 500 individuals. It shows the detectable cure (DC) rate, that is, the proportion of individuals/clones whose initial infections have cleared. We give the DC for different times after treatment as well as on the ToF, which will be used as the main parameter for reference. We define ToF as the first visit time after day 3 when any parasites (new or recrudescences) are present in numbers of $> 10^8$. This definition is consistent with practice as a patient would be censored on ToF and treated, irrespective of it being a new or a recrudesced infection. For completeness, the table also provides the proportion of individuals/clones cured when both new infections and recrudescences are viewed as failures. We compute the true cure (TC) rate under the assumption of detectability of all infections irrespective of their actual count. The entries for mean DC and mean TC correspond to the mean cure rates across 20

Table III. Per-individual and per-clone cure rates of the four simulated datasets.

		Per individual				Per clone			
	Day	AL90	AL80	CQ	AS_MQ	AL90	AL80	CQ	AS_MQ
DC rate	14	0.938	0.862	0.494	0.093	0.964	0.917	0.686	0.193
	28	0.926	0.866	0.636	0.166	0.957	0.921	0.779	0.305
	42	0.918	0.842	0.648	0.176	0.953	0.905	0.779	0.314
	63	0.916	0.798	0.604	0.156	0.950	0.880	0.744	0.276
	100	0.908	0.774	0.540	0.114	0.944	0.870	0.700	0.203
	ToF	0.926	0.818	0.616	0.164	0.963	0.891	0.623	0.194
Mean DC	ToF	0.935	0.800	0.619	0.169	0.972	0.894	0.636	0.200
Cure rate when recrudescences and new infections are classed as failures	14	0.886	0.602	0.460	0.078	0.961	0.913	0.680	0.189
	28	0.876	0.604	0.570	0.146	0.948	0.907	0.753	0.278
	42	0.872	0.598	0.584	0.162	0.938	0.865	0.729	0.260
	63	0.870	0.584	0.558	0.148	0.902	0.732	0.641	0.195
	100	0.864	0.562	0.506	0.108	0.720	0.535	0.495	0.108
	ToF	0.876	0.584	0.558	0.148	0.948	0.817	0.612	0.193
Mean	ToF	0.883	0.592	0.568	0.156	0.958	0.832	0.626	0.199
TC rate	14	0.716	0.302	0.016	0.006	0.859	0.601	0.128	0.018
	28	0.880	0.765	0.318	0.022	0.931	0.847	0.569	0.054
	42	0.898	0.766	0.448	0.036	0.940	0.868	0.657	0.090
	63	0.908	0.770	0.494	0.046	0.944	0.870	0.682	0.115
	100	0.908	0.770	0.498	0.048	0.945	0.870	0.684	0.121
Mean	63	0.905	0.759	0.492	0.049	0.954	0.871	0.687	0.125

We calculated estimates using one dataset of 500 individuals, except the mean values (e.g. 'mean DC'), which are the average over 20 datasets of size 500.
DC, detectable cure; TC, true cure; ToF, time of failure.

datasets of size 500. Day 14 cure rates are lower than later assessments as clones that do eventually clear still have parasites present in small numbers in the early stages of the trial. As expected, the TC rates are slightly lower than the DC rates because of the undetected clones at the assessment time point, although the difference is relatively small at the end of the study. The mean number of clones detected in an individual at the time of treatment is the same for all three datasets (3.48) for ease of comparisons between the treatments. In the simulated dataset, we assume follow-up days 3, 7, 10, 14, 21, 28, 35, 42, 49, 56 and 63 and assume that patients are not seen at any other time.

The second set of data comes from a trial in Tororo, Uganda, a high-transmission area. The dataset contains 419 individuals divided between the two treatments amodiaquine + artesunate and AL. Our focus will be on the 199 individuals, which were randomised to the AL treatment and were successfully genotyped. The markers used were *msp-1*, *msp-2* and *TA40*, and the average number of clones detected in an individual at the start of treatment is 4.43, which is slightly higher than in the simulated datasets (3.48). Bukirwa *et al*. and Greenhouse *et al*. give further details about the trial [15, 16].

3. Methods

3.1. The genetic information available

Table IV provides an example of the genetic information obtained from the genotyping of a specific individual before and after treatment, that is, on ToF. Note that the alleles presented in one row do not necessarily correspond to a multilocus 'clonal' genotype because assigning alleles to clones is not possible. In the example, we have two alleles 10 and 24 at *msp-1* and 25 and 35 at *msp-2*, but we cannot tell if multilocus genotypes are 10/25 with 24/35 or 10/35 with 24/25. So that we can estimate the number of clones present, it is natural to use the number of distinct alleles detected so that one would estimate two clones present initially; the number of clones present at the ToF is less clear. Marker *msp-1* suggests that five clones are present, whereas *msp-2* and *TA109* only show four different alleles. This discrepancy is, of course, due to two clones sharing, by chance, the same allele at *msp-2* and *TA109*, and consequently, the number of clones present at the ToF should be estimated as five. As a result, more markers will allow for a more accurate estimation of the number of clones [13]. Note that new infections may accumulate after treatment, which is why there are a greater number of clones after treatment in the example given in Table IV.

At the ToF, up to five different alleles are present at a given marker, indicating that there are probably five infections present. Upon close examination, we can see that all alleles present at treatment are also detected at ToF, suggesting that both initial clones survived. This gives some indication that the original infections have not been cleared as the genetic information is the same. To make an informed decision about that, we will need to carefully investigate the specific alleles observed using the 'rules' summarised in Table I. Even once a classification has been found, there is the possibility that the alleles at treatment and at ToF are new infections due to the possibility of the alleles matching by chance. By comparing the alleles detected before treatment and at the ToF and taking into account the probability that they may match by chance, we can assign the clones as a recrudescence or a new infection (Table I).

Table IV. Example of an individual's genotyping results.

msp-1	*msp-2*	*TA109*
Before treatment		
10	25	5
24	35	7
At ToF		
10	13	4
20	23	5
21	25	7
23	35	12
24		

We provide alleles (represented by numbers) present at each marker before treatment and at the ToF.
ToF, time of failure.

3.2. *Classifying the data: interpreting the genotypes*

The interpretation of genotype results for an individual subject has not yet been standardised. Collins *et al*. [6] published a systematic review of such studies, which found that 'all trials considered an outcome recrudescence if all alleles from both samples (pre and post-treatment) matched and a new infection if no alleles matched'. The differences in classifying infections occur when dealing with the 'mixed' results where some but not all alleles are the same at the beginning and at the end of the study (Table I). Following the recommendation by the WHO [17], the majority of trials classified a 'mixed' result as a recrudescence as there were some alleles that were the same, although this is conservative because of the problem of alleles matching by chance. Some studies defined all mixed results as new infections, and some classified the sample as a recrudescence if more than half of the alleles matched; otherwise, they recorded it as a new infection.

The methods described earlier have all been used to classify individuals rather than the clones. It is, however, possible to combine these methods to interpret results on a per-clone basis. Specifically, we can make the following deductions:

- If all alleles are different at the time of treatment and at the ToF
  - all the original clones have cleared or at least are undetectable
  - all the clones detected at ToF are new infections
- If all alleles are the same at the time of treatment and at the ToF, then all detected clones are clones that failed treatment. Note, however, that there is the possibility that the observed alleles might just match by chance, although this probability is small.
- If an individual contains some alleles that are the same at the time of treatment and at the ToF and some that are different, a definitive decision on the fate (cure/fail) for a given clone present at the time of treatment is not possible. In this case, the smallest proportion of matching alleles found across all markers is used to estimate the proportion of recrudescences at the ToF. See Table V for examples of this.

As the proportion of recrudescences has not been used before to classify mixed infections on a per-clone basis, Table V gives a few examples. We denote the proportion of matching alleles before treatment and at the ToF for each marker as elements in the vector a. The example again uses three markers so that the length of the vector is 3, but extensions to more markers are straightforward. In summary, the number of original infections that survived treatment is given as the value of the smallest element of a times the number of clones at ToF. For example, if the vector a contains at least one 0, then none of the alleles identified at the start and at the end of the study is identical for at least one marker. In this case, all the clones found at the end of the study will be classified as new infections. Examples of this are I–III in Table V. Similarly, if a contains all 1s, then all clones are recrudescences. Example IV has a third of alleles the same for all markers. Because there are three possible clones, this suggests that one clone is a recrudescence and the other two are new infections. For example V, one can see that at least one-fifth is the same for all alleles, so one clone will be classified as a recrudescence. Note that we have assumed that when a proportion is the same across markers, such as $a = (0.3, 0.3, 0.3)$, this proportion comes from the same clone. This assumption will lead to a slight underestimation of the cure rate as too many infections will be classed as recrudescences. Conversely, the probability that the original and recrudescent clones share the same alleles by chance will increase the average values in a and hence underestimate the number of recrudescences. Further, notice that this approach does not require whole

Table V. Examples of various proportions of alleles matching pre-treatment and at time of failure for each of the three markers.

	a			Estimated number	
Sample	*msp-1*	*msp-2*	*TA109*	of clones	Classification
I	0	0	0	2	0 recrudescences and 2 new infections
II	0	0	0.25	4	0 recrudescences and 4 new infections
III	0	0.28	0.28	7	0 recrudescences and 7 new infections
IV	0.33	0.33	0.33	3	1 recrudescences and 2 new infections
V	0.2	0.4	0.4	5	1 recrudescences and 4 new infections
VI	0.25	0.4	0.4	5	1.25 recrudescences and 3.75 new infections

The estimated number of clones at time of failure and the corresponding classification are also given.

infections to be classified but instead allows for probabilistic assignments. Suppose, for example, that for two of the markers, five alleles are detected at the end of the study whereas only four alleles are found for one marker (example VI). This might be because different clones have the same allele by chance or because one allele is present in too few numbers to be detected. If we now have one out of four matching on the one marker and two out of five for the others, we can classify one-fourth of the five clones (1.25 clones) present at the end of the study as recrudescences and the other three-fourths (3.75 clones) as new infections for the purposes of estimating an overall per-clone cure rate. In example VI, if there were seven clones present at the start and five at the ToF, using a would suggest that 5.75 clones had been cleared, 1.25 had recrudesced and 3.75 were new infections.

3.3. Per-individual analysis

When we analyse the data on a per-individual basis, the method of classification and the method of analysis need to be considered. Table I describes the different methods of classifying patient outcome (cured and not cured). A full account of methods for analysis is given in Table II. We will only use data without any dropout in which case PP and ITT will be identical so that we will pay no further attention to the issue of PP or ITT analysis. Despite this, there remains a large number of combinations of classification and analysis methods, making it impossible to evaluate all combinations. We have therefore chosen a selection of the key methods in the comparisons presented. More specifically, we will use methods B, C, B1, B2, B3 and C1 and methods B1a to C1a given in Table II in our comparisons.

The biggest difference between the methods of analysis is whether a proportion cured is used as the trial outcome or time-to-event analysis, both providing slightly different interpretations of the results. For the time-to-event analysis, the event of interest is taken as the ToF, that is, time to the infection becoming detectable ($>10^8$). One of the main drivers of differences in the results is the interpretation of new infections in the analysis. The methods range from classifying them as a treatment failure or success, censoring them or removing them from the analysis completely, which obviously will have a profound impact on the results. A further point to consider, which to date is often overlooked, is accounting for the probability of a random match of alleles. An individual that has the same alleles before and after treatment is classified as a recrudescence. There is, however, a possibility that a new infection bears the same alleles as those present in the recrudescent clones. In this case, the clone would in fact be a new infection but would be misclassified as recrudescent. We will use the method of Greenhouse *et al.* [16] to account for this by calculating the probability of a random match and then reweighting the number of recrudescences accordingly. More specifically, we can make the following corrections:

(1) Let f_i denote the proportion of times allele i is contained in the population of q alleles detected at marker M, where $i = 1, \ldots, q^{(M)}$.
(2) For individual j, $N_{j,\text{post}}$ denotes the number of alleles present at the ToF. Generate all $\binom{C=q^{(M)}}{N_{j,\text{post}}}$ combinations of alleles. For each combination c, calculate the corresponding probabilities p_c, by $p_c = \prod_{i=1}^{N_{j,\text{post}}} f_i$.
(3) Let $\mathbf{A}_{j,\text{pre}}$ be the vector of alleles present prior to treatment for individual j. If we look through all combinations C, a match has occurred if at least one allele from $\mathbf{A}_{j,\text{pre}}$ is present in combination $c = 1, \ldots, C$. We calculate the probability of a match for each marker M by the sum of the combination probabilities that match divided by the sum of all combination probabilities,

$$p_{\text{match}}^{(M)} = \frac{\sum_{c=1}^{C} p_c I\left(\text{any } \mathbf{A}_{j,\text{pre}} = c\right)}{\sum_{c=1}^{C} p_c} \tag{1}$$

where $I(\cdot) = 1$ if the condition in parenthesis is true and 0 otherwise.
(4) The product is taken over the markers to obtain an overall estimate of p_{match} for each individual, and $\bar{p}_{\text{match}}$ denotes the average across all individuals. The reweighted number of recrudescent infections is then given by

$$n_{\text{recru}} = \frac{n_{\text{obs. recru}} - \bar{p}_{\text{match}} \cdot n_{\text{total}}}{1 - \bar{p}_{\text{match}}} \tag{2}$$

where $n_{\text{obs. recru}}$ is the number of initially classified recrudescent infections and n_{total} is the number of subjects with parasites at the end of the study.

3.4. *Per-clone analysis*

When we estimate the efficacy of a treatment on a per-clone basis, the problem of randomly matching alleles also occurs. Denote the ith allele in subject j, present at time k for marker M, by $A^{(M)}_{i,j,k}$, where k is pre-treatment or post-treatment. There are n subjects in the study, and denote the number of alleles at time k in subject j as $N_{j,k}$. If $A^{(M)}_{i,j,\text{pre}} = A^{(M)}_{i,j,\text{post}}$, the clone is likely a recrudescence, whereas otherwise, the clone is probably a new infection. To correct for the probability of a random match, we assume that the occurrence of an allele is independent of the subject (i.e. each subject is equally susceptible to each clone), and consequently $P(A^{(M)}_{i,j,\text{pre}} = a^{(M)}|\text{new infection}) = P(A^{(M)}_{i,j,\text{post}} = a^{(M)}|\text{new infection}) = P(A^{(M)} = a^{(M)}|\text{new infection})$, where $a^{(M)}$ is an available allele from the distribution of alleles for marker M. We then estimate the probability of an allele being seen given it is a new infection using Equation (3). This equation sums over all alleles in all individuals, selecting those that match the allele a.

$$P(A^{(M)} = a^{(M)}|\text{new infection}) = \frac{\sum_{k=\{\text{pre, post}\}} \sum_{j=1}^{n} \sum_{i=1}^{N_{j,k}} I\left(A^{(M)}_{i,j,k} = a^{(M)}\right)}{\sum_{k=\{\text{pre, post}\}} \sum_{j=1}^{n} N_{j,k}} \tag{3}$$

Using the definition of conditional probability, we find that

$$P(A^{(M)} = a^{(M)}|\text{new infection}) = \frac{P(A^{(M)} = a^{(M)} \;\&\; \text{new infection})}{P(\text{new infection})} \tag{4}$$

We can easily find an estimate for the probability of a new infection, $P(\text{new infection})$, from the data once an initial classification of the alleles (i.e. not accounting for the probability of a random match) has been made. Finally, to obtain an estimate for the probability of a random match, $P(A^{(M)} = a^{(M)}\ \&\ \text{new infection})$, we can then use $P(A^{(M)} = a^{(M)}|\text{new infection}) * P(\text{new infection})$. Because these probabilities are calculated for each marker, we use the product of the probabilities as an overall estimate of matching by chance. It is clear that an infection with a high probability of randomly matching the alleles is more likely to be a new infection.

The adjusted cure rate is then estimated as

$$ACR = \frac{1}{n}\sum_{j=1}^{n} \frac{1}{N_{j,\text{pre}}} \sum_{i=1}^{N_{j,\text{pre}}} P\left(A^{(M)} = a^{(M)}_{i,j,k} \;\&\; \text{new infection}\right) \tag{5}$$

A few things should be pointed out for this method. Firstly, using the initial classification to estimate the probability of a new infection introduces bias into the results. This is because the number of new infections is calculated from the initial classification of infections before any reweighting has occurred. Using the probability of a match increases the probability of a new infection as they would initially be incorrectly classified as a recrudescence. A simple way to eliminate this bias is by iteratively reweighting. Specifically, we repeated the whole method, including the reweighting using the probability of a random match, using the previous value for the probability of a new infection until the probability of a new infection converged. Usually, it takes 5–10 iterations for convergence. We then use the estimate after the last iteration to obtain the probability of a random match and subsequently the average cure rate. In our investigations, we found, however, little, if any improvement, suggesting that the probability of a new infection is not highly influential for the adjusted cure rate. In contrast, the frequency of the alleles proved to be more important.

The second point for consideration concerns the combination of the probabilities across the markers. Greenhouse *et al*. [16] used the product of the probabilities based on the assumption of independence of markers. Under this assumption, the product of the individual estimates provides an unbiased estimator for the probability of a random match. In contrast, if there was perfect correlation between the markers, then one would only need to consider one marker. Although it is often argued that linkage equilibrium holds for the markers typically used, the actual relationship may still be somewhere in between the two extremes. To gain some insight into the behaviour of the estimator based on the independence assumption and the assumption of perfect correlation, we include a comparison of the estimators based on taking the product and the average and just using *msp-2* to estimate the probability of a random match.

We also included the average as it considered the standard method of combining several results to obtain an overall value. Additionally, we investigate the benefit from including more markers by increasing the number of markers from 1 to 3.

4. Results

4.1. Per individual

In the following, we will present our comparison of methods for analysing malaria trials on a per-individual basis. Figure 3 provides the estimated cure rates across 20 distinct simulated datasets of size 500 for patients using AL90 and AL80. Note that we have undertaken the same evaluations for the other two treatments, but because they are qualitatively the same, we have omitted them for brevity. We have applied the five different classification methods as described in Table I and four of the analysis methods (Table II) and summarised the results for each combination in box plots. Specifically, the methods of analysis used are B1, B2, B3 and C1, which we subsequently refer to as 'new=exc', 'new=succ', 'new=fail' and 'Surv (new=cens)', respectively. As a baseline for the performance of the analysis methods, we have applied each method to the datasets, assuming perfect classification. In Table III, horizontal lines denote the DC rate at ToF and the TC rate. The different classification methods appear to only have a small impact on the results except that classification II gives slightly higher results. When we look at the impact of the classification of new infections, however, it becomes apparent that for some methods, the results are closer to the baseline than others. Treating new infections as successes or censoring them provides similar results, but treating them as failures drastically reduces the estimated cure rate. In particular, it is clear that results for censoring new infections or treating them as successes give estimates closest to the truth, relative to alternative methods, for all classification methods.

When we look at the impact of classification on the results more closely, it is notable that the cure rate, when a new infection is treated as a failure, is constant for classification methods I–IV. This is because the estimated cure rate does not depend on the mixed outcomes but only the total number of mixed outcomes. For the same reasons, classification V yields a higher cure rate in this case as all mixed infections have been removed. Overall, it is difficult to choose between classification methods as the results are so similar. There is little difference between methods I and III except for the treatment of ETF, which in our datasets does not seem to play a major role. The ordering of the methods is the same regardless of the classification method. Method II produces the highest cure rate as the methods result in a greater number of new infections rather than recrudescences. As method IV uses the proportion of a half to decide the individual outcome, it is reasonable to explain that this is why the result is between methods I and II.

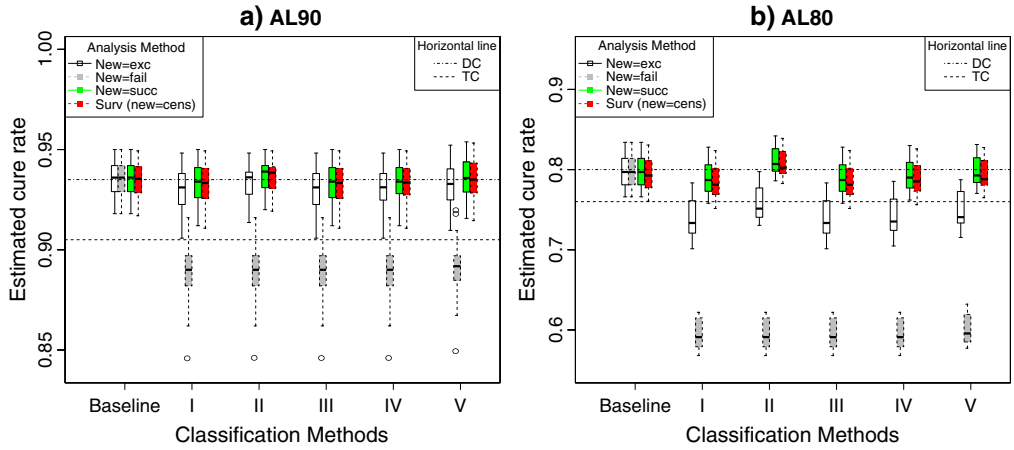

Figure 3. Per-individual results: summary of estimation results for (a) AL90 and (b) AL80 based on 20 datasets of size 500 using various methods for analysis and classification . *New=exc*: new infections excluded; *new=fail*: new infections treated as failures; *new=succ*: new infections treated as successes; *Surv (new=cens)*: new infections are censored. TC = true cure rate; DC = detectable cure rate. Baseline values assume perfect classification but use different definitions of success in the analysis.

Figure 4 illustrates the same methods for analysis and classification on a single dataset of size 500 for all four different treatments. In addition to the raw estimators, they also include the estimators reweighted for the probability of a random match [16]. All four plots show similar patterns although less pronounced in the AS_MQ results. Correcting for the probability of a match either leaves the cure rate unchanged or increases it. The method does not correct by a constant amount across the datasets, however. We can see that the correction is greater for the AL results than for the AS_MQ dataset, where little impact is seen. In general, it therefore seems that correcting for the probability of a random match does generally improve estimation, although for low cure rates, its impact is negligible.

Applying the different methods of analysis and classification to the dataset from Tororo, Uganda (Figure 5), shows similar patterns as seen before, but this time more pronounced. Because the true values are no longer known, we have used the values obtained in [16] as a reference: 0.79 before and 0.87 after the correction. Methods I and III once more have similar results, whereas method II has the highest cure rates. Treating new infections as failures is constant regardless of classification method; censoring and classing new infections as successes are similar, whereas excluding new infections is in between. The correction for random matching depends on the number of new infections, resulting in a large impact of the correction for method II. Because of very low numbers (3 out of 199) of initially classified recrudescent infections in method II, using the Greenhouse correction results in values greater than 1. This is because the correction aims to reduce the number of infections that have been incorrectly classified as a recrudescence when they are actually new infections. With only three recrudescent infections, the correction suggests that the true number of recrudescent infections should be −13.76, which is of course not possible.

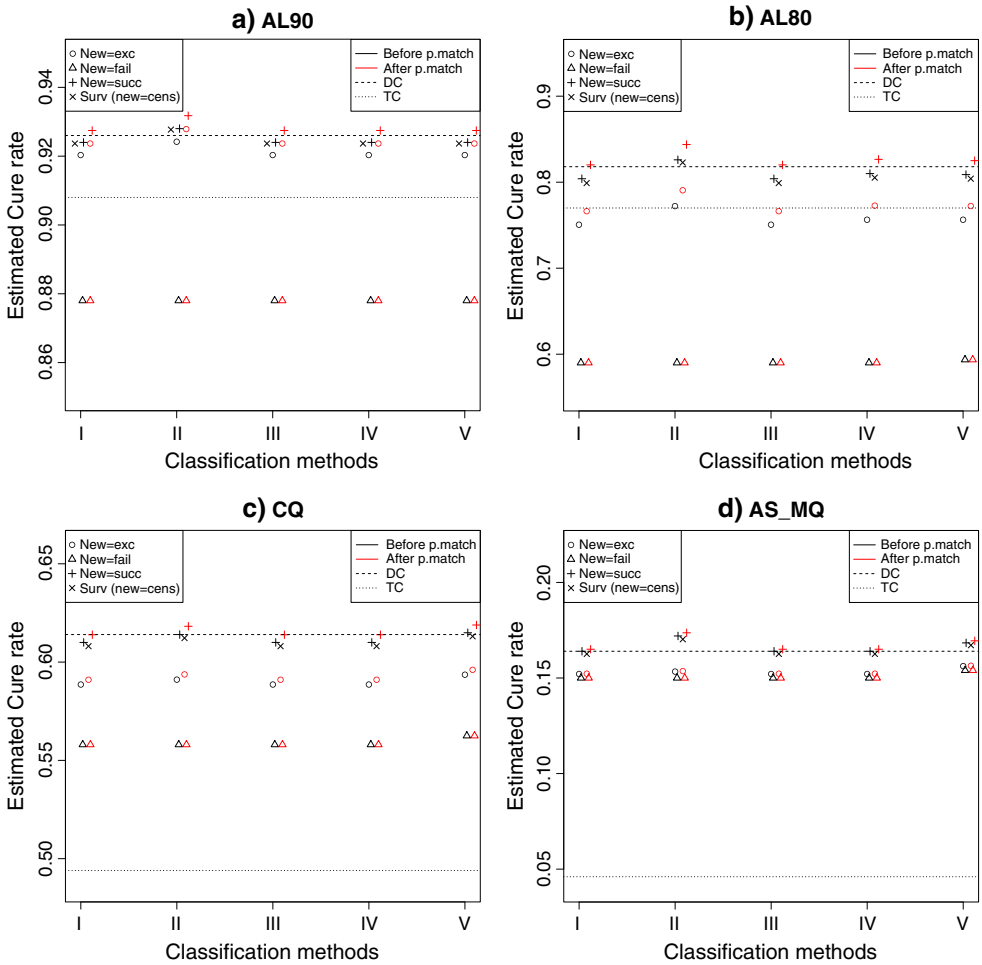

Figure 4. Per-individual results: results for one dataset of four different treatments including the impact of correcting for random matches. Note that no correction for random matching is used in the survival analysis and that in some cases, such as 'new=failure', correcting for random matching results in exactly the same cure rates as without. TC = true cure rate; DC = detectable cure rate.

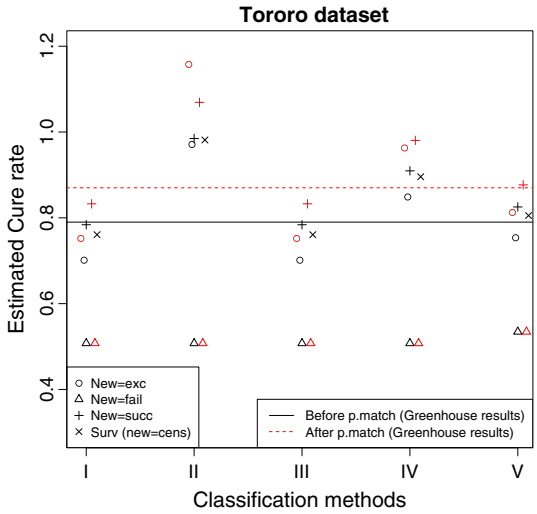

Figure 5. Per-individual results: comparisons of analysis and classification methods on dataset from Tororo, Uganda.

4.2. Per clone

We now focus on investigating the performance of the method of estimating cure rate on a per-clone basis and evaluate the impact of reweighting to account for random matching. Figure 6 shows the results from the per-clone analysis for the 20 different datasets of size 500 using AL90 and AL80. We give box plots for estimation without reweighting for random matching alleles and reweighted estimation results using the single markers and then a combination of all three by means of a product or average. The initial classification (before reweighting) is a slight overestimate of the DC rate although this difference is very small. Looking at the DC rate on the day of failure (Table III) averaged over the 20 datasets (0.972, 0.894) and the average across the 20 estimated cure rates in the AL datasets (0.974, 0.895) gives a difference of only 0.002 and 0.001. This suggests that the estimation on a per-clone basis is highly accurate even before random matching of alleles is accounted for. As a consequence, the various methods used to reweight the estimate do not improve the estimate as seen in the per-individual analysis, suggesting that the correction is not necessary. Investigating the impact of correcting for random matching on data with lower cure rates based on the average across 20 datasets of size 500 (Figure 7) once again shows that hardly any improvement can be seen by correcting for random matching in the per-clone analysis. Note also that although it appears in the graph that the cure rate for CQ is overestimated, the estimate is only

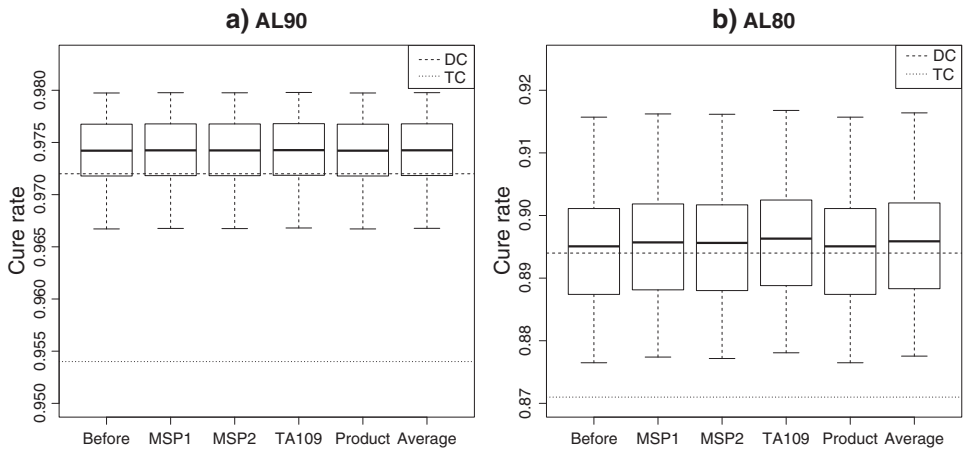

Figure 6. Per-clone results: summary of estimation results for (a) AL90 and (b) AL80 based on 20 datasets of size 500 with and without reweighting for random matching. TC = true cure rate, DC = detectable cure rate. *Before* = before reweighting, *msp-1/msp-1/TA109* = using one marker to correct for random matching, *Product/Average* = using the product/average of the three markers to correct for random matching.

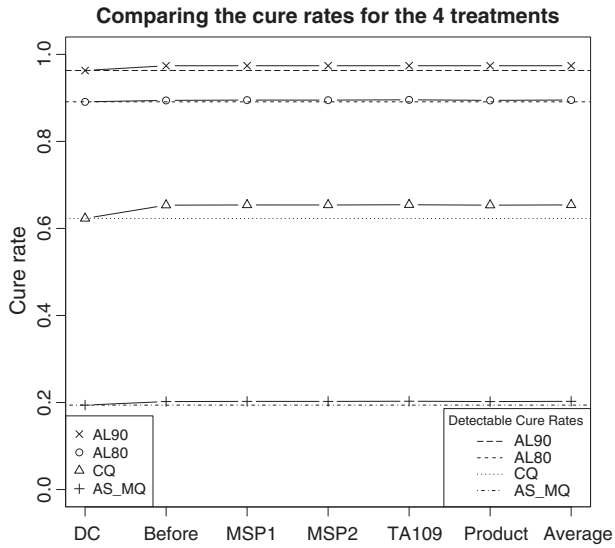

Figure 7. Per-clone results: evaluation of different analysis methods for four different treatments. Reweighting is based on product of marker-specific reweighting, and results are averaged across 20 independent datasets. AL = artemether–lumefantrine; AS_MQ = artesunate–mefloquine; CQ = chloroquine.

Table VI. Table of the cure rates for the per-clone analysis applied to a real dataset from Tororo, Uganda.

	Before reweighting	*msp-1*	*msp-2*	*TA40*	Product	Average
Cure rate	0.7784	0.7779	0.7777	0.7777	0.7776	0.7778

slightly higher than the detectable value ($\approx$1%) and that the detectable value is contained in the box plots of the individual estimates of the 20 datasets.

Finally, we investigate the results of analysing the real dataset in Table VI. We estimate the cure rates in the same way as for the simulated data. As before, the impact of reweighting is very small, suggesting that this correction is not required in the per-clone analysis.

5. Discussion

The first aim of this study was to compare existing methods employed in the analysis of malaria clinical trials using simulated data where the true and DC rates are known. The methods differ mainly in the classification of mixed infections and in the way new infections are incorporated into the analysis. We find that the method of classifying mixed infections had little impact on the results and that the most appropriate method for classifying new infections was as successes or censoring. We initially felt that the approach to classify new infections as successes was based on wishful thinking, and hence, the performance of this approach was a big surprise to us. Considering a re-infection rate of 12 per year, for example, would imply that on average 1 month after treatment, a new infection would emerge. If the treatment failed to clear the initial infection, the recrudescence would therefore have a substantial head start over the new infection so that it seems plausible that treatment failure would have been recognised before a new infection becomes apparent. Essentially, a new infection would therefore indicate that no recrudescence has occurred, giving some justification for classing new infections as a success. The estimates obtained improve slightly when correcting for random matching. In our second aim, we introduce the per-clone method of analysis and evaluate the estimators produced. We find that a per-clone analysis does estimate the cure rate adequately. In contrast to the per-individual analysis, correcting for randomly matching alleles does not yield any notable improvement.

In practice, most cure rates will be greater than 90%, and consequently, the performance of the method for such cure rates is of most practical importance, which is why the AL90 dataset was included. In our investigations, we did, however, evaluate the methodology across a wide range of cure rates and found that for both the per-individual and per-clone analyses, the performance of the methods did not differ

depending on the underlying cure rates. Throughout our investigations, we have made a few simplifying assumptions, however. We assume perfect detection of clones, which is not the case in reality because PCR technology only usually detects the numerically dominant clones and any genetic signals less than around 30% of the major signal are usually ignored as 'noise' [18]. Similarly, the sequestration of certain stages of the blood means around 50% of clones present at the time of treatment do not contribute a genetic signal and so are not detected. We ignore this effect here as the relative merits of the methods will remain. For an evaluation of how close the estimates are to the TC rates, however, further evaluations will be necessary.

In our work, we have recreated and examined data from high-transmission areas because they are the most methodologically challenging. Low-transmission areas are simpler because MOI at treatment is low, so genetic matching due to chance is much reduced, and the rate of acquisition of new infection is much slower. This makes the data far less ambiguous than in high-transmission areas. In addition, the added value of the per-clone analysis is greater if more than one infection is present in a patient as otherwise the result will be identical to the per-individual estimate. We have also made the unrealistic assumption that we have complete data. We believe that the presence of missing data results in a clearer distinction between treating new infections as successes, which inherently assumes complete data, and survival analysis where incomplete data still contribute to the estimation. In light of the added information, we therefore agree with the recommendation by the WHO that survival methods ought to be the method of choice unless a per-protocol analysis is of interest in which case only complete data would be considered. A final limitation to the work presented here lies in the focus on point estimates although standard errors and confidence intervals are of equal importance. The number of different approaches investigated prevented a thorough treatment of these in this manuscript. To obtain standard errors for any of the methods discussed, we can, however, use bootstrap confidence intervals [19].

A challenge encountered in this work was defining the 'TC rate' on an individual basis. If an individual carries several infections, some of which have cleared, some that have returned and some that are new, it is unclear how to define the clinical outcome of such a subject. For this study, we classified mixed infections as recrudescences. The reason for this choice was that at least one recrudescent clone must be present in the individual in this case, and therefore, the treatment has failed to clear the infection present at the start of the study. This is the usual definition of a drug failure.

Analysing infections on a per-clone basis poses an entire different set of challenges. It is, for example, not always clear how many clones an individual is carrying at the time of treatment or ToF because of multiple clones having the same allele at the measured markers. We have treated the number of clones at the time of treatment/ToF as a fixed known value despite only being able to estimate it. It is in fact a random quantity. Additionally, we assumed that alleles present initially and at ToF correspond to the same clone if such a match is present on all markers. If these assumptions do not hold, the cure rate would be higher as fewer clones would be classed as recrudescences.

Our main conclusions are as follows:

(a) Survival methods should be used for estimating drug effectiveness on a per-individual basis.
(b) Classification of mixed infections is not highly influential to the overall performance.
(c) The introduced per-clone estimator is accurate and yields additional insight in the performance of the treatment.

And the final recommendations based on this work are therefore to do the following:

(a) Use survival methods when possible
(b) Report the per-clone failure rate in addition to the per-individual failure rate
(c) Use three markers for genotyping. More markers will improve the results further, although the improvement is only small.

Appendix A. Data generation

The methods used to generate the datasets presented here are an extension of those published in [14]. We chose to investigate three antimalarial drug treatments, two are current first-line ACTs: AL and AS_MQ. The third treatment was CQ monotherapy, which although no longer officially deployed in the formal health sector was included here for historical comparison. Winter and Hastings validated the dosing regimens of the drugs investigated and the PK/PD parameters used [14].

It is important to note that when parameters within the model are assigned, the fates (survival/death) of the separate clones in each human are non-independent, as they share the same host environment.

For example, background levels of immunity and rates of drug metabolism vary substantially between humans; if a human has a low level of immunity or rapidly metabolised a drug, then all the clones present during treatment shared this (relatively benign) human environment. Consequently, we considered PK parameters to be a human attribute, unique to each human but common to all clones within a human. Although we allowed for environmental similarities, we assumed no genetic relatedness between clones within a human, and so we assigned the PD properties (IC50, maximum parasite kill rates and slope factor), the parasite growth rate and the initial numbers present to each clone independently.

The model discussed in [14] required the following three modifications.

(i) *The presence of more than one clone at the start of treatment*

Molecular studies have demonstrated that a patient with malaria can be simultaneously infected with multiple, genetically distinct clones of *Plasmodium falciparum* [11]. The number of 'clones' present in the patient is called the MOI and can be found using hypervariable genetic 'markers' such as *msp-1* and *msp-2*. Following antimalarial treatment, outcome is currently measured as success or failure per human, but an association between MOI and both clinical episodes and treatment failure has been demonstrated [20, 21] although not conclusively established. If true, this implies that a cure is always easier to achieve in areas of low transmission where only a single clone has to be cleared by treatment compared with high-transmission areas where success may require numerous clones to be cleared simultaneously. If this is the case, it is not feasible to compare the drug success rates of different studies with different levels of transmission. To address this problem and allow for comparison between studies, we would like to calculate treatment outcome on a per-clone as well as per-human basis.

We assigned the number of clones present at the start of treatment to each patient using data collected by Nsanzabana [22]. We collected the data from an area of high transmission in Tanzania where the MOI typically ranged from 1 to 8 (Figure A.1). The probability of a patient being assigned a specific MOI was dependent on this frequency distribution of MOI measured. We chose the initial number of parasites present at the start of treatment for each clone from a uniform distribution between 10^{10} and 10^{12}.

(ii) *The acquisition of new infections during the course of treatment*

We adapted the model to allow patients to acquire new infections during the course of follow-up. We assign the number of new infections to each patient at the beginning of the simulation and found it using the average number of re-infections occurring per patient per year. In this case, we used re-infection data from Northern Ghana [3] where maximum likelihood estimates suggested that on average any individual would acquire 16 new infections per year. We could crudely obtain other estimates using data on effective ACTs. For example, Burkirwa *et al.* [15] reported that more than 50% of patients developed recurrent parasitaemia within a month of treatment. If we

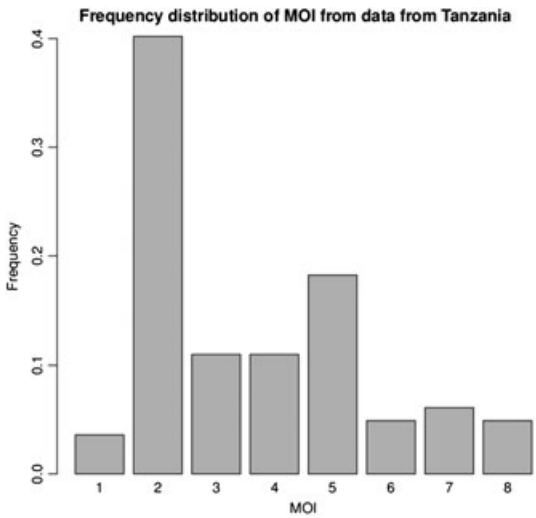

Figure A.1. The probability of a patient being assigned a specific multiplicity of infection (MOI) was dependent on the frequency distribution of MOI measured in the field. Nsanzabana [22] collected the data plotted here.

assume that re-infections can occur at any time in the month following treatment, we can predict that each patient will acquire approximately six new infections each year. However, if we know patients were taking effective ACTs with long half-lives, we can crudely assume that no new infections became established for the first 2 weeks. Following treatment (because of their long half-life), 50% of patients have new infections in a 2-week period and so are more likely to receive an average of 12 new infections each year. We found the probability of a new infection occurring during the designated follow-up period by dividing the number of re-infections per year by the number of days in a year and then multiplying by the number of days in the patient follow-up period. We added variation by randomly choosing the exact number of new infections from a Poisson distribution.

In cases where patients were re-infected during follow-up, we assumed that parasites first became susceptible to drug treatment on emergence from the liver. Initial parasite number was therefore based on the emergence of 10^5 merozoites, whereas random sampling determined the specific day parasites emerged.

(iii) *Tracking of individual clones using molecular markers*

In principle, we can distinguish re-infections from drug failures by their molecular signatures or 'markers'. Genotyping is the current method recommended by the WHO [17] to distinguish a new infection from a recrudescent infection, with the majority using up to three markers. We chose to incorporate the commonly used markers *msp-1* and *msp-2* alongside the microsatellite *TA109*. At the beginning of each simulation, we assigned each clone present at the start of treatment or later appearing in a new infection a specific allele for each of the markers.

We took the allele frequency data for *msp-1* and *msp-2* from a study in Papua New Guinea [23] with raw data provided by Ingrid Felger (Figure A.2). Porter *et al*. [25] noted that the insensitivity of nested PCR to small changes in the number of base pairs means variants differing by less than 20 bp are routinely considered to be the same allele. The raw data contained details of allele length (bp), class and codes; however, for simplicity in the model, we arbitrarily numbered the 24 *msp-1* and 35 *msp-2* alleles and ignored any potential misclassification of alleles as a result of base pair repeats. We used the frequency with which alleles were measured in the field to determine the probability of a clone containing that allele in the simulation. Anderson *et al*. originally described the microsatellite marker *TA109* (14 alleles) [26]; however, the distributions used here came from a more recent dataset collected in Malawi [24]. Again, each allele was arbitrarily numbered, and the probability of a clone containing a given allele corresponded with the frequency with which that allele was seen in the field.

A.1. Simulation details

We simulated a population of 10 000 individuals for each of the three treatment regimens. Each patient in the simulation had a malaria infection in which the original host infection could include multiple clones and were at risk of acquiring new infections during the period of follow-up. We assigned these details along with the timing of new infections (if any), patient PK and parasite PD parameters to the patient at the beginning of the simulation. The model tracked drug concentration and parasite number for 100 days

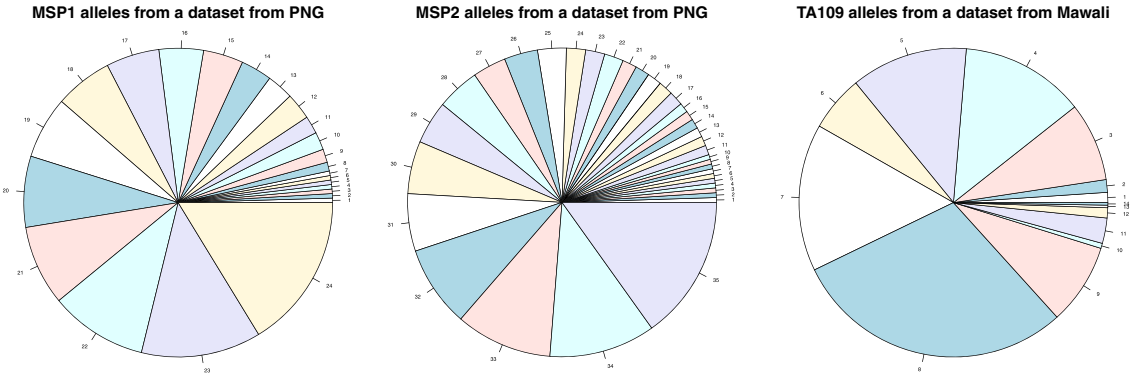

Figure A.2. The allele frequency distribution of *msp-1* and *msp-2* markers, the data were taken from a study in Papua New Guinea [23] and a study of the microsatellite marker *TA109* in Malawi [24].

following the first treatment dose. It ran in half-day time steps for the first 7 days, allowing multiple drug dosages to be administered, but to speed up simulations, we modelled all subsequent days in 1-day time steps.

We recorded a large amount of data about both the patient and the parasites. For each human, this included the specific PK parameters, their initial MOI, the number of new infections that occurred and the day new infections emerged from the liver. For each parasite clone present at any point during the follow-up period, we recorded the initial parasitaemia, the growth rate, the specific PD parameters, the associated genotype and the exact number of parasites present on each day of the follow-up period. We could then use these data to determine the day each original clone in the infection first becomes undetectable in the blood (i.e. $<10^8$), the day a clone is cleared from the body if treatment is successful and the day recrudescence occurs (becomes patent, i.e. $>10^8$) if treatment fails (Figure 1).

A.2. Justifications

The widespread resistance of parasites to CQ and MQ made it difficult to find recent papers with reliable IC50 estimates for fully sensitive parasites. The IC50 values presented for CQ and MQ are therefore higher than those that have since been validated in [14]. However, there is no point analysing simulated results in which everyone is cured, and so the IC50 values used allow us to analyse drugs with varying degrees of resistance. Descriptions of the allele frequencies have been collected in Uganda [27] and more recently in Burkina Faso, So Tom, Malawi, Tanzania and Uganda [28]. We incorporated variation into the model by assuming that all model parameters were normally distributed with a coefficient of variation of 30%.

As is necessary with all models, we made assumptions during this model's construction. The assumptions were as follows:

(i) Drugs were instantly absorbed and converted (if necessary) to their active metabolite. Although absorption lag time may be negligible for drugs with a long half-life (in this case CQ, lumefantrine and MQ), it becomes more important for the artemisinins with half-lives as short as 40 min.
(ii) We allocated the number of new infections independently of initial MOI; this ignores potential issues of spatial heterogeneity. Intuitively, those patients with a higher MOI are more at risk of acquiring new infections and hence more likely to become re-infected during patient follow-up.
(iii) Patients complied fully with the designated treatment regimen.
(iv) There is no genetic relatedness between the clones; infections within a host consist of multiple genetically distinct parasite clones.
(v) There was no sequestration of malaria-infected erythrocytes. This is a usual characteristic of infections with *P. falciparum*. Koepfli *et al*. [29] reported that parasites can be sequestered in the internal organs for up to 20 h of the 48-h life cycle. Naturally, if parasites are sequestered in the organs, they will not be present in the peripheral blood, thus increasing the risk of missing clones when genotyping in a single blood sample.

Acknowledgements

The authors are grateful to Prof. Bryan Greenhouse for granting us access to his dataset. Dr Jaki's contribution to this report is his independent research arising from his Career Development Fellowship (NIHR-CDF-2010-03-32) supported by the National Institute for Health Research. The views expressed in this publication are those of the authors and not necessarily those of the NHS, the National Institute for Health Research or the Department of Health. Dr Hastings and Ms Winter's contributions were supported by the Bill and Melinda Gates Foundation (grant 37999.01), the Swiss Tropical and Public Health Institute and the Liverpool School of Tropical Medicine.

References

1. Stepniewska K, White NJ. Some considerations in the design and interpretation of antimalarial drug trials in uncomplicated falciparum malaria. *Malaria Journal* 2006; **5**(127).
2. Borrmann S, Peto T, Snow RW, Gutteridge W, White NJ. Revisiting the design of phase III clinical trials of antimalarial drugs for uncomplicated *Plasmodium falciparum* malaria. *PLoS Medicine* 2008; **5**(11):1546–1552.
3. Sama W, Owusu-Agyei S, Felger I, Vounatsou P, Smith T. An immigration-death model to estimate the duration of malaria infection when detectability of the parasite is imperfect. *Statistics in Medicine* 2005; **24**(21):3269–3288.
4. Vafa M, Troye-Blomberg M, Anchang J, Garcia A, Migot-Nabias F. Multiplicity of *Plasmodium falciparum* infection in asymptomatic children in senegal: relation to transmission, age and erythrocyte variants. *Malaria Journal* 2009; **7**(17).

5. World Health Organization. *Assessment and Monitoring of Antimalarial Drug Efficacy for the Treatment of Uncomplicated Falciparum Malaria*, World Health Organization, 2003. Available from: http://whqlibdoc.who.int/hq/2003/WHO_HTM_RBM_2003.50.pdf [accessed on 06/09/2010].
6. Collins WJ, Greenhouse B, Rosenthal PJ, Dorsey G. The use of genotyping in antimalaria clinical trials: a systematic review of published studies from 1995–2005. *Malaria Journal* 2006; **5**(122).
7. Price RN, Dorsey G, Ashley EA, Barnes KI, Baird JK, d'Alessandro U, Guerin PJ, Laufer MK, Naidoo I, Nosten F, Olliaro P, Plowe CV, Ringwald P, Sibley CH, Stepniewska K, White NJ. World antimalarial resistance network I: clinical efficacy of antimalarial drugs. *Malaria Journal* 2007; **6**(119).
8. Dorsey G, Njama D, Kamya MR, Cattamanchi A, Kyabayinze D, Staedke SG, Gasasira A, Rosenthal PJ. Sulfadoxine/pyrimethamine alone or with amodiaquine or artesunate for treatment of uncomplicated malaria: a longitudinal randomised trial. *Lancet* 2002; **360**:2031–2038.
9. Verret W, Dorsey G, Nosten F, Price R. The effect of varying analytical methods on estimates of anti-malarial clinical efficacy. *Malaria Journal* 2009; **8**(77).
10. Guthmann JP, Pinoges L, Checchi F, Cousens S, Balkan S, Van Herp M, Legros D, Olliaro P. Methodological issues in the assessment of antimalarial drug treatment: analysis of 13 studies in eight African countries from 2001 to 2004. *Antimicrobial Agents and Chemotherapy* 2006; **50**(11):3734–3739.
11. Slater M, Kiggundu M, Dokomajilar C, Kamya MR, Bakyaita N, Talisuna A, Rosenthal PJ, Dorsey G. Distinguishing recrudescences from new infections in antimalarial clinical trials: major impact of interpretation of genotyping results on estimates of drug efficacy. *American Journal of Tropical Medicine and Hygiene* 2005; **73**(2):256–262.
12. Staedke SG, Mpimbaza A, Kamya MR, Nzarubara BK, Dorsey G, Rosenthal PJ. Combination treatments for uncomplicated falciparum malaria in Kampala, Uganda: randomised clinical trial. *Lancet* 2004; **364**(9449):1950–1957.
13. Brockman A, Paul RE, Anderson TJ, Hackford I, Phaiphun L, Looareesuwan S, Nosten F, Day KP. Application of genetic markers to the identification of recrudescent *Plasmodium falciparum* infections on the northwestern border of Thailand. *American Journal of Tropical Medicine and Hygiene* 1999; **60**(1):14–21.
14. Winter K, Hastings IM. Development, evaluation, and application of an in silico model for antimalarial drug treatment and failure. *Antimicrobial Agents and Chemotherapy* 2011; **55**(7):3380–3392.
15. Bukirwa H, Yeka A, Kamya MR, Talisuna A, Banek K, Bakyaita N, Rwakimari JB, Rosenthal PJ, Wabwire-Mangen F, Dorsey G, Staedke SG. Artemisinin combination therapies for treatment of uncomplicated malaria in Uganda. *PLoS Clinical Trials* 2006; **1**(1).
16. Greenhouse B, Dokomajilar C, Hubbard A, Rosenthal PJ, Dorsey G. Impact of transmission intensity on the accuracy of genotyping to distinguish recrudescence from new infection in antimalarial clinical trials. *Antimicrobial Agents and Chemotherapy* 2007; **51**(9):3096–3103.
17. World Health Organization. *Methods and Techniques for Clinical Trials on Antimalarial Drug Efficacy: Genotyping to Identify Parasite Populations*, World Health Organization, 2007. Available from: http://whqlibdoc.who.int/publications/2008/9789241596305_eng.pdf [Accessed on 06/09/2010].
18. Hastings IM, Nsanzabana C, Smith TA. A comparison of methods to detect and quantify the markers of antimalarial drug resistance. *American Journal of Tropical Medicine and Hygiene* 2010; **83**(3):489–495.
19. Efron B, Tibshirani RJ. *An Introduction to the Bootstrap*. Chapman and Hall: London, 1993.
20. Arnot DE. The influence of the genetic complexity of *Plasmodium falciparum* infections on the epidemiology of malaria. *Transactions of the Royal Society of Tropical Medicine and Hygiene* 2002; **96**:131–136.
21. Kyabayinze DJ, Karamagi C, Kiggundu M, Kamya MR, Wabwire-Mangen F, Kironde F, Talisuna A. Multiplicity of *Plasmodium falciparum* infection predicts antimalarial treatment outcome in Ugandan children. *African Health Sciences* 2008; **8**:200–205.
22. Nsanzabana C. Dynamics of malaria parasite resistance markers in two areas of different transmission intensity. *PhD Thesis*, University of Neuchatal, Switzerland, 2008.
23. Schoepflin S, Valsangiacomo F, Lin E, Kiniboro B, Mueller I, Felger I. Comparison of *Plasmodium falciparum* allelic frequency distribution in different endemic settings by high-resolution genotyping. *Malaria Journal* 2009; **8**:250.
24. Mzilahowa T, McCall PJ, Hastings IM. "Sexual" population structure and genetics of the malaria agent *P. falciparum*. *PLoS One* 2007; **2**:e613.
25. Porter KA, Burch CL, Poole C, Juliano JJ, Cole SR, Meshnick SR. Uncertain outcomes: adjusting for misclassification in antimalarial efficacy studies. *Epidemiology and Infection* 2010; **139**:544–551.
26. Anderson TJC, Su X, Bockarie M, Lagog M, Day KP. Twelve microsatellite markers for characterization of *Plasmodium falciparum* from finger-prick blood samples. *Parasitology* 1999; **119**:113–125.
27. Cattamanchi A, Kyabayinze D, Hubbard A, Rosenthal PJ, Dorsey G. Distinguishing recrudescence from reinfection in a longitudinal antimalarial drug efficacy study: comparison of results based on genotyping of msp-1, msp-2, and glurp. *The American Journal of Tropical Medicine and Hygiene* 2003; **68**:133–139.
28. Mwingira F, Nkwengulila G, Schoepflin S, Sumari D, Beck HP, Snounou G, Felger I, Olliaro P, Mugittu K. *Plasmodium falciparum msp1, msp2* and *glurp* allele frequency and diversity in sub-Saharan Africa. *Malaria Journal* 2011; **10**:79.
29. Koepfli C, Schoepflin S, Bretscher M, Lin E, Kiniboro B, Zimmerman PA, Siba P, Smith TA, Mueller I, Felger I. How much remains undetected? Probability of molecular detection of human plasmodia in the field. *PLoS One* 2011; **6**:e19010.

Chapter 5

OpenMalaria

1. Introduction

1.1. Project Background

There are many effective interventions now available for malaria control. These typically include those targeting the vector population for example, insecticide-treated nets (ITNs) and indoor residual spraying (IRS), or those targeting the host population either through prevention of an infection (i.e. intermittent preventive treatment in pregnancy (IPTp) in infants (IPTi) or children (IPTc)) or through diagnosis and effective treatment of an established infection. However, both the parasite and vector have proven adept at acquiring and rapidly spreading resistance to the currently available antimalarial drugs (see for example (378)) and insecticides (232). Considering the complexities of the malaria parasite lifecycle and the resource poor setting in which malaria occurs, it is easy to see why current control efforts are struggling to meet the ambitious goal of global eradication (118). An invaluable tool in a comprehensive malaria control program would undoubtedly be a safe, effective malaria vaccine however research towards this end has been challenging. Development has been hindered by the extensive antigenic variation present within the parasites (291), the complexity of the parasite life-cycle and our limited understanding of how the parasites interact with the human immune system (183). Despite the challenges, research into a malaria vaccine is progressing with a number of vaccine candidates currently in phase I and II of clinical trials (reviewed in (71)) and RTS,S, the most clinically advanced vaccine, in phase III trials (347).

While the last decade has seen significant progress towards a safe and effective malaria vaccine, testing potential vaccines in the field is a very costly process usually taking several years. Clinical trials must determine the effectiveness of the vaccine in various risk populations and if successful, the vaccine must be integrated into the existing public health system (272). With a number of vaccine candidates available, determining how best to prioritise the development of different programs, the best methods of vaccine deployment and the cost-effectiveness of deployment strategies was a particular concern. When looking at other infectious diseases, this decision-making process has previously benefitted from the use of mathematical models. In 2003, the Swiss Tropical and Public Health Institute (Swiss TPH, then Swiss Tropical Institute) began developing micro-simulation models of the clinical epidemiology of malaria with funding from The Bill & Melinda Gates Foundation (BMGF) and support from the both PATH Malaria Vaccine Initiative (MVI) and GlaxoSmithKline. Their aim was to provide mathematical models of malaria epidemiology capable of exploring the potential of the vaccine candidate RTS,S with emphasis on vaccine supply, demand, benefits and cost; details of this model were published in a supplement to the American Journal of Tropical Medicine and Hygiene (204, 275, 276, 309, 310, 313).

The Swiss TPH model has now been incorporated in to a Malaria Vaccine Model (MVM) by MVI (256). The MVM connects the outputs generated by Swiss TPH models with a demand forecast model to provide a comprehensive picture of new vaccines' potential in terms of demand, public health and finance. The demand module estimates the vaccine dosage schedule over a defined period based on United Nations population data, UN Children's fund (UNICEF) and WHO vaccine coverage rates and the required vaccine uptake entered by the user (255). The public health module predicts the impact of vaccine deployment using epidemiological models developed at Swiss TPH. The models determine the number of cases, deaths and disability-adjusted life years (DALYs) averted (based on disease burden data from WHO and the Malaria Atlas Program (MAP)) to quantify the impact of specific vaccine deployment scenarios. Finally, the financial module calculates the investment needed to achieve the desired public health impact (255).

Through development of the MVM it became evident that the individual stochastic malaria models could be extended to investigate a wider range of potential vaccines, vector control methods and intermittent preventative treatment in infants (IPTi) (311). Consequently, the original project was extended in 2006 (again with financial support from BMGF) to allow simulations of malaria at either a village or district level. Subsequent extensions (2008 and 2012) allowed for the inclusion of malaria mosquito vector dynamics and including improved simulations of diagnosis, drug action, host-seeking behaviour, the contribution of the informal sector and of the implications of both IPT and transmission-reducing interventions (311). The core software "OpenMalaria" is an open source program written in C++ currently under development by teams from the Swiss TPH, Liverpool School of Tropical Medicine (LSTM) and the Network Dynamics and Simulation Science Laboratory at Virginia Bioinformatics institute.

OpenMalaria is constructed in a modular way with several distinct components designed to capture the relevant aspects of malaria epidemiology. The details of the original models were previously published in a supplement to the American Journal of Tropical Medicine and Hygiene with an overview of the mathematical description included in the first paper (313) and an overview of the model implementation is detailed here in appendix 1.The model currently contains components representing infection of humans, blood stage parasite densities, infectiousness of humans to mosquitoes, incidence of morbidity and mortality (312). It is capable of simulating the dynamics of malaria parasitaemia throughout an infection, the transmission dynamics of the mosquito vector (59, 61), the dynamics of host immunity, the processes leading to illness and death within a patient and predicting the epidemiological impact of interventions (including vaccines (257, 314, 331), IPT (277, 278) and vector control (60)), cost-effectiveness analyses (203).

1.2. LSTM's role in the project

LSTMs remit was to incorporate antimalarial drug resistance in to OpenMalaria. A strategic decision was made to do this using pharmacological-based models describing the effect of drug treatment on parasite burden. My role, which constitutes

the contents on this thesis, was to implement this strategy. Due to the size and complexity of the OpenMalaria program, the basic methodologies were first investigated using a stand-alone model written in R (270) (described in Chapters 2 and 3). The stand-alone model used pharmacokinetic-pharmacodynamic (PK/PD) models to calculate the rate of change in parasite density in a single patient over time following treatment. The changing density was dependent on initial parasitaemia, the parasite multiplication rate, the proportion of parasites killed by antimalarial drugs and the proportion cleared by host immunity. After establishing the methodology, we had to develop a strategy to incorporate the mathematics developed to describe the antimalarial drug effects in the stand-alone model into OpenMalaria. In OpenMalaria, existing within-host models track the parasite density, parasite multiplication rate, and effects of host immunity while a case management models make all decisions regarding treatment choice, timings and dosages (discussed in more detail below).

In this chapter I focus on how the drug treatment model was developed and implemented, including how it interacts with other model elements (Figure 1). A brief overview of how this model fits into to the broader context of OpenMalaria and how the larger program is run can be found in Appendix 1. To successfully integrate the drug effect methodology required the code be converted from the R programming language to C++ and re-written to allow interactions with existing models, specifically the within-host and clinical management models (Figure 1). A short summary of modelling within the C++ programming environment can be found in Appendix 2.

The main methodologies utilised to describe antimalarial drug treatment were developed using stand-alone models (described in Chapters 2 and 3) and adapting these methods to run within the framework of OpenMalaria was challenging. OpenMalaria is a large program with multiple collaborators writing and committing code. As such, it was impossible for me to implement the drug treatment models into such a complex program without considerable help from two computer programmers (Tiago Antao (previously based at LSTM) and Diggory Hardy (previous based at the Swiss TPH)) and some decisions regarding the running of the drug treatment models were the result of group discussions. I will now discuss who implemented each

section of the code for the drug treatment models and outline the group decisions made throughout its development before continuing with the model methodology.

Prior to beginning my PhD, Tiago Antao worked on the OpenMalaria program and wrote the code for three of the classes in the *PkPd* namespace (*LSTMPkPdModel*, *LSTMdrug* and *LSTMDrugType*). He designed them to accept details about the drug treatment regimen (via the *medicate* command, see later) from the clinical management module and to return the output of the drug treatment models (later termed the "drug factor") to the within-host modules. These classes did not include any of the methods required to model drug action and calculate the drug factor, both of which are the focus of this chapter.

It was decided by myself, Ian Hastings, Melissa Penny (responsible for the within-host models), Valerie Crowell (responsible for the clinical management models) and Diggory Hardy that the drug treatment model would calculate and return a single "drug factor" to the within-host models each day. This was done primarily so the models output would fit with the one-day time steps required by the clinical management models (see section 2.2.1). The "drug factor" was therefore required to represent the action of all drugs present in the body at the start of the time step and any new dosages given though out the time step (see methods below)

The methodology to describe antimalarial drug effect was developed, calibrated and validated using our stand-alone PK/PD model (364) developed in R (270). These methods were developed with a view to ultimately incorporating them in to OpenMalaria and so I re-wrote the relevant methods describing drug action in to the C++ programming language used by OpenMalaria. I incorporated these methods into the three classes (*LSTMPkPdModel*, *LSTMdrug* and *LSTMDrugType*) within the *PkPd* namespace; this required a comprehensive understanding of the class system previously implemented by Antao (described below). Diggory Hardy then checked the general running of the drug treatment model for syntax errors or bugs in the code. While I was with Hardy for this initial trouble-shooting phase he decided that it would be quicker for him to perform the checks and me to clarify any problems he encountered (rather than him explaining how to perform the relevant checks within OpenMalaria). Note that this "policing" check is required to ensure I/we did not

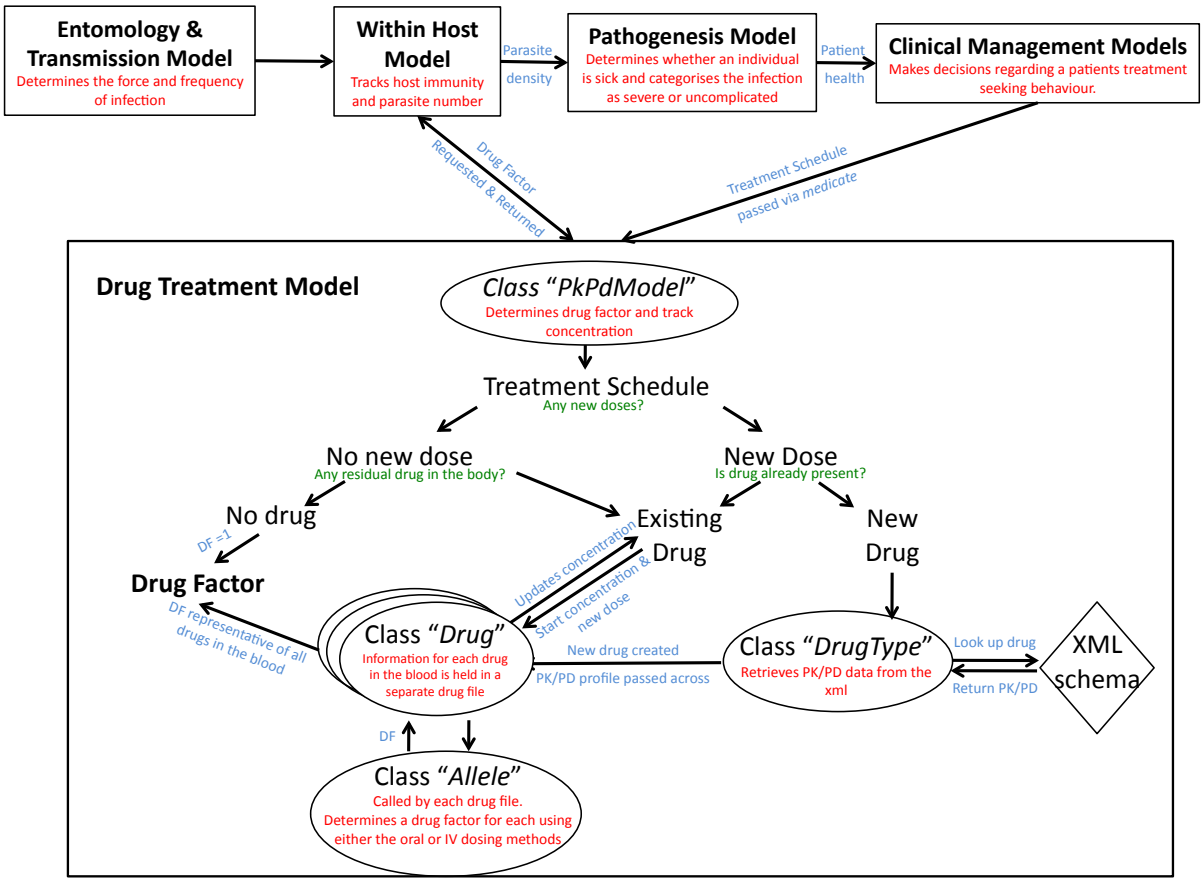

Figure 1. The population simulated within OpenMalaria is defined by a number of models (outlined in Appendix 1.3); an overview of the interactions between these models and the drug treatment model is shown above. The drug treatment model consists of four classes contained within the PKPD namespace; *PkPdModel*, *Drug*, *DrugType* and *DrugAllele*. At the beginning of each time step the treatment schedule is passed to the *PkPdModel* class via *medicate*. What follows is a series of decisions (shown in the flow chart above) that determine the drug factor (DF) for each time step based upon the contents of the *medicate* command. This drug factor is then returned to the within-host models.

Shape key: The square boxes surround models while the ovals represent the classes within a model and the diamond indicates input files.

Colour key: Red indicates the function of a particular model or class, blue described the information exchanged between two components and the green details the options being assessed within the model.

inadvertently introduce bugs or ambiguities that would affect the whole program. We later improved the methodology of the PK/PD model to allow for artemisinin absorption and conversion (described in Chapter 3) and subsequently included these methods with OpenMalaria. I converted the new methods to C++, updated the methods used within the drug treatment model and Hardy again helped check the running of the new code. The resulting drug treatment model was able to successfully reproduce the drug concentration profiles and parasite kill rates generated within by our stand-alone model.

The methodology required to model the action of intravenous (IV) drugs was developed at the request of Crowell to allow investigation into treatment outcomes for patients with severe malaria. Modelling drug action via continuous IV infusion required an additional duration parameter to represent the duration of the infusion. As the clinical management model is responsible for all decisions regarding drug treatment (passed to the drug treatment model via the *medicate* command), it was logical to extend the *medicate* command to include the duration parameter. While I was responsible for developing the IV dosing methodology, Hardy wrote the code for the new methods in OpenMalaria; as the main computer programmer working on the project at the time he was deemed better equipped to safely deal with the technical aspects of the coding changes. To implement the model I therefore explained the model changes required to use the new dosing methods (i.e. which equations tracked the drug concentration over time, how they would change if a drug is given via IV and the need for the additional duration parameter) and Hardy implemented the changes. Given there were now two methods available for the calculation of drug effect (depending on the required method of drug administration), we needed to include a means for the model to determine which methods were required. Through discussions with Hardy we decided the most efficient way to do this would be to use the duration parameter essentially as a switch. So, if the duration parameter is zero or missing, we assume oral drug administration and the model uses the oral dosing methods. However, if the duration parameter is present and greater than zero, we assume the drug is given via IV and the IV dosing methods are used.

As mentioned above, we eventually aim to use the drug treatment model to investigate drug resistance. This will require parasite PD parameters to represent

increasingly drug resistant parasites rather than the fully sensitive values we use now. After communicating this to Hardy he/we decided to set up a new class *LSTMDrugAllele* which will eventually be used to pick parasite PD parameters based upon the alleles present within an infection and determine the drug factor for each clone. The current status of this class is described below.

2. Methods

2.1. Basic Model

The primary role of the drug treatment model was to quantify the parasiticidal effect of all antimalarials present within a human over a one-day time step. For the purposes of OpenMalaria, this drug-dependent killing was described using a single value termed the 'drug factor', which is the proportion of parasites that will survive the day. It therefore takes a value always between zero and one; a value of zero indicates parasites were fully cleared by the drug while a value 1 indicated there was no drug effect.

The drug factor (*f(C)*) was calculated using the standard Michaelis-Menten equation.

$$f(C) = V \bullet \left(\frac{C^n}{C^n + IC_{50}{}^n} \right) \qquad [1]$$

where *C* is the drug concentration (mg/l) which decays over time, *V* is the maximal drug-killing rate (per day), *IC50* is the concentration at which 50% of the maximal drug killing occurs (mg/l) and *n* is the slope of the dose response curve.

Defining the change in *C* over time depends on the method of drug administration and the assumptions we make about the drugs absorption and conversion. The validated PK/PD model of Winter & Hastings (364) describes how *C* varies if we assume

instantaneous absorption and conversion (included here in Chapter 2, equation 3), this methodology was later extended in Kay-Winter & Hastings (168) to allow for artemisinin absorption and its subsequent conversion to its active metabolite DHA (included here in Chapter 3, equations 5-8).

While oral dosing is often the cheapest, most convenient and safest method of administration it is not always an option. For example, the patient may be unable to swallow the tablet or the drug may need to be administered very quickly. One of the fastest methods of administration is intravenous (IV) infusion as it allows the drug to be administered directly into the blood stream and also has the advantage of providing more control over the level of drug in the blood. There are currently two drugs recommended by WHO for IV administration: artesunate (AS) and quinine (QN), with a preference for AS in both adults and children where possible (380). For the purposes of modelling, the duration of IV AS is so short (usually a single injection lasting a few seconds) that we can assume instantaneous absorption and use the methods described above following oral administration to describe the change in *C*. However, rapid administration of quinine is unsafe (380). It must be administered as a slow, rate-controlled infusion and so calculating the change in *C* over time *t* must account simultaneously for the instant absorption of QN into the blood and the gradual elimination of QN from the body. This process was described using a differential equation

$$\frac{dC}{dt} = R - kC \qquad [2]$$

where *R* is the rate of infusion (mg/kg/day), found by dividing the dose (mg) by the patients weight (kg) and multiplied by the IV duration (days), and *k* is the elimination rate. Equation 2 was integrated using laplace transformations (appendix 3) to find the concentration at time *t*

$$C = \frac{R}{k \bullet Vd}\left(1 - e^{-kt}\right) + C_0 \bullet e^{-kt} \qquad [3]$$

where *Vd* is the volume of distribution.

After the infusion ends, the concentration declines in the normal manner

$$C_t = C_0 e^{-kt} \quad [4]$$

where C_0 is the concentration when the infusion end.

2.2. Model implementation and architecture

This chapter focuses on the development of a drug treatment model to quantify the effects of the antimalarial drugs on parasites in patients. To do this, the model must exchange information with both the clinical management models and the within-host models in each time step and so here I present a brief overview of these interactions (show visually in Figure 1) and go on to describe the architecture and implementation or the drug treatment model.

2.2.1. Clinical management models

The clinical management models determine whether, when and how a sickness is treated (assuming the pathogenesis model has first determined the patient has a malaria infection and has classified it as either uncomplicated or severe although presumptive treatment of non-malaria fevers can occur). There are currently two different clinical models implemented in OpenMalaria, one running in 5-day time steps and the other in 1-day time steps, each utilising different methods to predict the clinical and parasitological outcomes. In the 5-day model, outcomes are determined immediately within the clinical model and patients have a simple cure/fail response to treatment. In the more recent 1-day model, the effect of treatment on parasite density is calculated daily using the full PK/PD modelling techniques. In this case, the clinical model must work together with the models for drug action, severe outcomes and within-host dynamics and requires an event-scheduler model. The event-scheduler includes both a clinical outcomes element to schedule of sickness events (fever start/end, recovery/death outcomes) and a case-management model. The case-management model contains decision trees to determine the treatment-seeking behaviour and health-system outcomes of each individual with treatment schedules

split according to infection type i.e. uncomplicated or severe. The treatment scheduler passes a description of the chosen drug regimen to our drug models using a command called *medicate*.

2.2.2. Within-host models

The within-host models track the parasite densities within the human hosts and are designed to cover the liver/pre-patent stage of an infection, the asexual blood stage (merozoites), the sexual blood stage (gametocyte) (275) and acquired natural immunity (204). Natural immunity in this model is acquired only after considerable exposure to parasites during an infection (310) mainly acting by controlling parasite densities (204). To update the parasite density at the end of each time step the within-host models require a drug factor from the drug treatment model to quantify the parasiticidal effect of all drugs present. Given their direct effect on parasite densities the drug treatment model can be considered part of the within host models but it is important to note that they are contained within the *PkPd* namespace (and not the *WithinHost* namespace and class).

2.2.3. Drug treatment model

We developed a drug treatment model to run within OpenMalaria capable of interacting with the clinical management and within-host models described above, and the XML schema file (containing the models input parameters, described in Appendix 1). Briefly, the model receives all details surrounding drug treatments (i.e. which drug/s are given, the route of administration, the dosages and timings) from the clinical management models via the *medicate* command, retrieves the drug PK (*Vd* and *k*) and parasite PD (IC50, *V* and *n*) information from an XML schema file and passes a drug factor to the within-host models. General details regarding the set-up and running of OpenMalaria, the structure of XML schema files and a brief description of the models interacting the drug treatment model are contained within appendix 1 while the structure of programs written in C++ and their associated terminology are outlined in appendix 2. The code describing the drug treatment

model is contained within the *PkPd* namespace and split across four classes; *LSTMPkPdModel*, *LSTMdrug*, *LSTMDrugType* and *LSTMDrugAllele*.

The *LSTMPkPdModel class* is the pharmacokinetic and pharmacodynamic interface used by each human's within-host model. The within-host model calls the *LSTMPkPdModel class* each time step to obtain a drug factor and thus calculate infection densities in the next time step. The drug factor must take into account the action of all drugs present in the body at the start of the time step and any new dosages given though out the time step. The implementation required to calculate the drug-specific drug factors was built into the *LSTMdrug class* (see below). The *LSTMPkPdModel* base *class* collates all drug factors calculated by the separate *instances* of the *LSTMdrug class* to find the combined drug factor of all the drugs acting within a human in that specific time step; it is this combined drug factor that is then returned to the within-host models.

The *LSTMdrug class* is a derived *class* (appendix 2) of the *LSTMPkPdModel* class, included to reflect the need to model several drugs. Each drug present within a simulated human is represented by a separate *instance* (appendix 2) of the *LSTMdrug class*. If treatments include a new drug then a new *instance* is created and if an existing drug is eliminated from the body than the relevant *instance* is removed. Each *instance* of this *class* accesses the drugs PK and PD information from the XML (extensible mark-up language) input file (appendix1) via the *LSTMDrugType class* (explained below) and determines the drug factor for each drug over the course of a single time step.

All decisions regarding a patients treatment are made within the case management models and details of new dosages to be administered are passed to the *LSTMdrug class* of the drug treatment models via the *medicate* function. This is done at the end of each time step to allow treatments to be administered at the immediate start of the next time step. *Medicate* is made up of four elements including a drug type (available codes are specified in the drug library, see details of the *LSTMDrugType class* below), the hour of drug administration to allow multiple dosages within each day, the dosage to be given and the treatment duration. If the duration parameter is zero or missing then the drug is assumed to be administered orally and the dosage is therefore in mg

of active ingredient. If a non-zero value is given, the dose is administered via continuous IV infusion. In this case the duration parameter represents the duration of the infusion (in hours) and the specified dosage is given in mg of active ingredient per kg weight of the patient.

The drug factor may need to be calculated more than once within a single time step to reflect for example, the effect of any drug concentrations carried forward from the previous time step and any new dosages administered throughout the current time step. Implementation of the drug factor calculations was contained within the *LSTMDrugAllele class* (a *class* derived from the *LSTMdrug* base *class*). Each drug factor is therefore calculated within the *LSTMDrugAllele class* and returned to the *LSTMdrug instance* where they are combined into a single drug factor representing the combined effect of the existing and new drug dosages, of a single drug, over one time step. This single drug factor is then returned to the *LSTMPkPdModel* class to be combined with those of other *LSMTdrug instances*. At the end of a time step, the drug concentration is updated and the day's dosages cleared. *Instances* are then passed from one time step to the next until the drug concentration is deemed negligible at which point the class instance is removed and no longer associated with that human.

The *LSTMDrugType* class is a derived *class* of *LSTMdrug* and as mentioned above, provides each *instance* of *LSTMdrug* with the PK/PD parameters require to track drug concentration and determine the drug factor. I included a library of the PK/PD parameters for all currently calibrated drugs into OpenMalaria's XML input file. Each time a new *instance* of *LSTMdrug* is created, the *LSTMDrugType class* is called. It begins by using the drug abbreviation defined by *medicate* to check whether the drug exists within the XML library and whether it is already present within the human. If the drug exists in the library and is not already present in another *LSTMdrug instance* it accesses the relevant pharmacological data directly from the XML.

3. Discussion

The goal of OpenMalaria is to provide a mathematical model of malaria epidemiology with which the scientific community can investigate the effects of various intervention strategies including malaria vaccines, vector control strategies and antimalarial drug treatment. The model is capable of analysing different deployment scenarios and their associated costs alongside their effect on patient morbidity and mortality. The work within this chapter describes the development and implementation of the drug treatment models designed to allow OpenMalaria to explicitly model antimalarial drug effectiveness.

The calibration and validation of the drug treatment model described here was carried out using the stand-alone R model described in Chapters 2 and 3 (168, 364) and the model outputs have been shown to provide a good fit to field data. It is important to note however that the PK/PD parameters used within OpenMalaria currently do not allow for heterogeneity and assume all parasites are fully sensitive to the antimalarial drugs. While this is an acceptable assumption when developing the models it does not reflect real-life field conditions. In reality, parasites sensitivity ranges from completely sensitive to fully resistance. To address this, the model will be developed to allow for a choice of parasite PD parameters based upon the alleles present within an infection. The specific alleles present will be assigned randomly according to their initial frequency within the population. While it was not possible to implement this methodology within the time constraints of the thesis, the current drug treatment model provides valuable insight into the effectiveness of antimalarial treatment regimens.

It was decided early in the development of OpenMalaria that all individuals within the simulation should follow the same age-weight growth curve. To incorporate our drug treatment module into the confines of OpenMalaria we were forced to adopt this assumption however, in reality, the weight of individuals of the same age varies largely both within and between countries (344). This lack of age/weight distribution within the model limits the potential questions we can ask. For example, variation in age/weight is most pronounced in children so investigating drug effectiveness in

children must allow for the natural differences in age/weight observed in the field. Recent work by van Buuren *et al*. (344) and Hayes (136) has focussed on optimising age-based dosing regimens for antimalarials. They began by prioritising the development of growth reference curves rarely available in resource poor settings and pooled the limited data available to provide centile curves of weight-by-age at both country and regional levels (136, 344). I discussed the inclusion of variable age/weight distributions into OpenMalaria with some of the programming project members however it was ultimately decided that the benefits of adding age/weight distributions to the model were out-weighed by disadvantages of adding another level of complexity to the model and hence the increase in model run time.

Despite the limitations imposed by working within the existing OpenMalaria program, the model described herein has been successfully implemented. The results have been compared with that of the validated stand-alone models described in Chapters 2 and 3 and provide a good match to field data. However, while the drug treatment model is capable of predicting drug effectiveness against fully sensitive parasites, the clinical management and within-host models are still under development. The results presented within this thesis were therefore generated using our stand-alone model. Our comparatively simple stand-alone models allowed us much more flexibility when developing the model methodology and investigating the implications of increasing drug resistance.

Appendix 1.

OpenMalaria

Specific details of the set-up and running of OpenMalaria

1.1. **Running OpenMalaria**

Simulations run using OpenMalaria require a number of steps and always begin with an initial set-up and warm-up period to create the human and, if necessary, mosquito populations. This ensures the modeller has a stable population (i.e. run to equilibrium) available on which their intervention of interest can be applied. Each of the simulated malaria infections within each individual have distinct parasite densities which vary by time step while the level of malaria transmission can be assumed to vary seasonally (312). All details of the intervention period are calculated sequentially with the state at time *t* dependent on the state immediately before time *t*; for a typical simulated population of humans the models run in either 1-day or 5-day time steps. The results of each updated time step is determined by multiple model components acting together to describe new infections, parasites densities, acquired immunity, uncomplicated and severe malaria episodes, direct and indirect mortality, infectiousness to mosquitoes, and case management (312); an overview of this process is described in Figure A1.

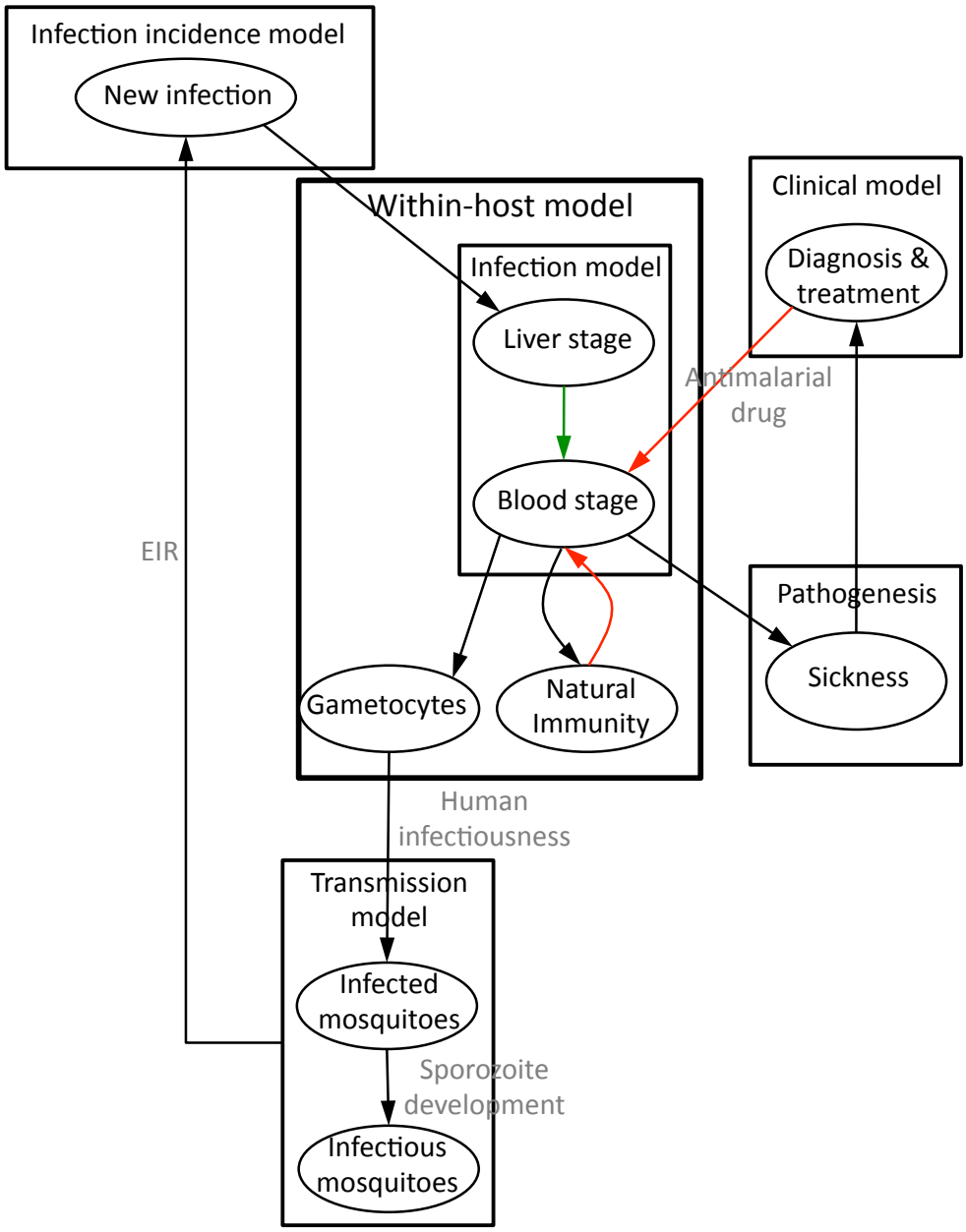

Figure A1. Recreated using the figure currently available on the OpenMalaria wiki (http://code.google.com/p/openmalaria/wiki/ModelsOverview). It provides an overview of malaria infection cycle assumed by the model.

Colour key: green arrows represent an increase in parasite number while red arrows represent a decrease.

Shape key: oval nodes are processes affecting something, and boxes surround models.

1.2. Model software and fitting

The individual-based stochastic simulations performed using OpenMalaria are computationally intensive and so, in an effort to improve performance and flexibility, they

were written in the C++ programming language (see appendix 2 for an overview of programming with C++). There are currently two main ways of running predictive simulations

1. The model can be run as a stand-alone program on the user's computer however population size is important and larger populations increase computational time and RAM (Random-access memory; a form of computer data storage) usage. Generally, populations of 100,000 individuals for the 5-day time-step model or 10,000 individuals for the one-day time-step model should require roughly two hours of computation (http://code.google.com/p/openmalaria/). Running the program on an individual computer can be done in one of two ways, either by installing openmalariaTools (recommended) or by building the executables from the source (requiring a significant amount of knowledge about computer programming). The openmalariaTools is a GUI (Graphic User Interface) created to allow easy interaction with OpenMalaria, the user simply chooses the required options in the GUI rather than inputting different commands in a terminal.
2. Running more complex, time-consuming, power-intensive simulations, for example model fitting, sensitivity analysis and exploration of multiple intervention strategies all require a huge amount of computational power. In this case the models can be run using the Berkeley Open Infrastructure for Network Computing (BOINC) (http://boinc.berkeley.edu/), an open-source software for volunteer computing. BOINC takes applications (like OpenMalaria) that have large computational requirements and divides the work across multiple volunteer computers. Members of the public usually provide the volunteer computing power by downloading the BOINC software to their computer, which runs when their computers are not being used. Specific information about how OpenMalaria uses the volunteer computing power can be found on www.malariacontrol.net

Each simulation performed using OpenMalaria requires an input file from the user to define their desired scenario. A scenario details the user's population of choice for example the population age structure, the level of transmission and the health system attributes, and the user's choice of intervention strategy/strategies. OpenMalaria requires this input file be written in Extensible Mark-up Language (XML), a typical XML scenario file includes the following elements

- Scenario element to encloses everything within the file. It is used to indicate the start and end of the input parameters included to tell the program when to begin and end reading data in from the XML.
- Demography element to describe the population size and age structure. The standard age-structure data comes from Ifakara, Tanzania with the population size determined by the user (population size has a major impact of the run time and amount of noise (or variation) resulting from model stochasticity)
- Monitoring element detailing the output type required. This can either be continuous reporting of single values or survey data that may be irregular and usually sub-divided by age group.
- Intervention element describing the type and timing of the interventions to be deployed.
- Health system element of which there are currently two possible models available (see below for more detail).
- Entomology element including a description of the transmission model. There are two transmission models available, independent of the length of a time step. The first is a simple model, termed "non vector" and allows for a response to human infectiousness and uses a forced infection rate from mosquitoes. The second model is a more detailed model of vector transmission allowing the modelling of vector stage interventions.
- Pharmacology element describing all the PK and PD parameters required in the 1-day time step model to determine drug effectiveness. This will be developed in the future to include initial levels of resistance and the corresponding parameters
- Model element which groups together the remaining data required by the model
    i. Clinical data includes only a *healthSystemMemory* attribute which determines if/when a sickness bout occurs

ii. Parameter data describes a list of parameters that were fitted, for example the pathogenesis model requires a severe malaria threshold while the within host models require parameters describing immunity decay.
iii. Model attributes include the number of days in a time-step, the number to seed the random-number generator and the number of time steps by which blood-stage infection is delayed after biting.

Model outputs are written to text files and typically contain predictions of age- and time-specific epidemiological qualities (infection prevalence and density, multiplicity of infection, incidence and severity of morbidity and levels of intervention coverage) (312) but this can be tailored to the users needs.

The parameters used within the OpenMalaria (with the exception of those used by the drug treatment models) were estimated by fitting to a set of 61 database covering ten different epidemiological scenarios (for full details see text S1 and table 1 in (311)). The parameters required for the drug treatment models were calibrated and validated independently of OpenMalaria using the stand-alone R model described in Chapters 2 and 3 before incorporation in the XML scenario files.

1.3. Model Components

The simulated human populations within OpenMalaria are defined by a number of models including the demography model, transmission models, within-host models, pathogenesis models and it necessary, the clinical management models.

Demography Model

The demography model is responsible for maintaining the core features of the human population structure. For example, humans may be out-migrated to maintain the age structure whilst newborns are added to maintain the population size. Humans may also be removed from the model as a result of indirect deaths (i.e. those not caused by malaria), malaria deaths or if/when they reach the maximum age of the model.

Transmission Model

The transmission models regulate the inter-human transmission of malaria; the infectiousness of humans at the end of each time-step translates into a risk of exposure to infectious mosquitoes in the next time-step. The number of *P.falciparum* inoculations (per person per year, denoted by the EIR: Entomological Inoculation Rate) is calculated each time-step and new infections initiated.

Within-host Model

The within-host models are responsible for calculating and updating the parasite density of each infection, each time-step, allowing for the effect of host immunity and drug therapies.

Pathogenesis Model

The pathogenesis models use the parasite density to determine whether an individual is sick and if so, whether the infection is classified as uncomplicated or severe (276, 313) . After classification of the infection, the clinical management models determine the treatment seeking behaviour of the patient.

Appendix 2.

Object Orientated Programming (OOP)

To fully understand the architecture of the OpenMalaria program it is crucial to have at least a basic understanding of the object orientated programming (OOP) and the technical jargon that accompanies it. In this appendix I provide a brief overview of OOP in C++ and its associated terminology.

2.1. Object orientated programming

Object orientated programming (OOP) is a conceptual approach to designing computer programs. Simple, non-OOP programs tend be a long to-do list of commands. As programs increase in complexity, programmers tend to group together smaller sections of code that carry a specific task into *functions*. However, the data contained within these programs tends to be 'global' i.e. accessible to all parts of the program. As the programs grow further in size and complexity, allowing any function to modify any piece of data tends to lend to bugs in the code. In contrast, the object orientated approach encourages the programmer to place data where it is not directly accessible by the rest of the program and instead to use specially written functions which act as intermediaries for retrieving or modifying data. These intermediaries are the *objects* and therefore the eponyms in OOP. Each *object* contains data with a set of methods for accessing and managing it. In essence an OOP is a collection of these interacting *objects* and although each *object* is an independent entity they are capable of receiving messages, processing data and sending messages to each other. These features become especially useful when more than one programmer is contributing code (i.e. a collection of commands) to a project.

2.2. Classes and instances

Classes in C++ are collections of variables and *functions* used to represent an *object*, essentially like a buildings blueprints. The purpose of a *class* is to make the program more modular (a process termed "encapsulation") and each *class* contains the data to describe an *object* and the code (or *functions*) to access and modify the data. An *instance* in OOP is an occurrence (or a copy) of an *object*, and *instances* of the same *class* share the same common features but with a different set of specific attributes. For example, if we consider a *class* 'Drug' which describes all the common features of a drug such as its pharmacokinetic (PK) parameters and dosage schedule, and includes the methods (i.e. *functions*) required to calculate its concentration in the body and subsequent effect (Figure A2). For the purposes of the program, each 'Drug' *class* is essentially the same in so far as they all contain the drug PK parameters, a dosage schedule and a defined list of functions. The different *instances* of the *class* have different attributes. In this example, the two *instances* shown in Figure A2 represent two different drug types (artesunate and mefloquine) and while they have the same set of data and functions, the specific attributes (or values) of the data differ in each *instance* e.g. differing pharmacological parameters and dosing schedules.

The modular structure provided by *classes* allows for the concept of information hiding and encapsulation. The premise being that all data within the program does not need to be 'global' (globally available data is accessible to all parts of the program simultaneously). Each *class* comes with one or more access specifiers whose primary purpose is to separate the *class* interface (the code that allows the class to interact with the aspects of the program) from the *class* implementation (the code describing the *object*). These access specifiers control the level of access other program elements have to data contained within the *class* and how classes inherit such constraints. Access specifier typically include one of three levels of restriction

i. Public restriction allows any part of the program, including those outside the *class*, to access all the code within the *class*
ii. Protected restriction allows the *class* itself and any derived *classes* (see 2.3. Inheritance) to access and inherit the data while essentially hiding it from all other *classes*.

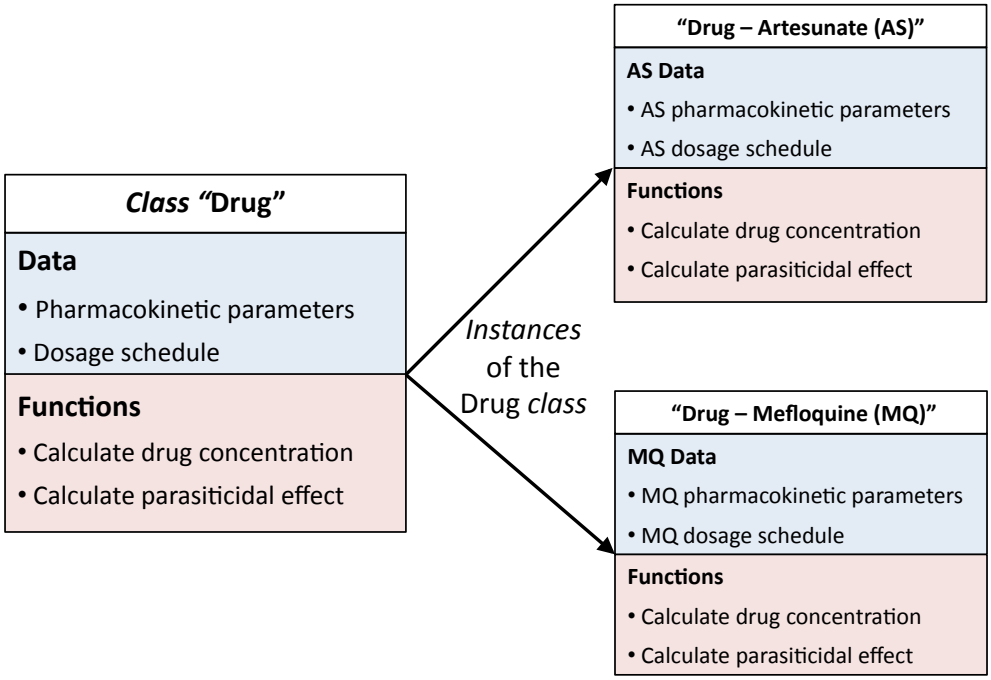

Figure A2. A *class* is used to describe the form of an *object* and contains the data representation and methods (*functions*) for maintaining the data in one package. The box on the left of the figure represents a *class* "Drug" and includes the data required to describe a drug and the methods to manipulate the data, in this case to calculate the drug concentration and parasiticidal effect. In OOP, an *instance* is essentially a copy of an *object*. The two *instances* shown here on the right represent the two *instances* of the same *class* "Drug". They share the same common features (i.e. the same data and methods) but have different attributes.

iii. Private restriction makes the code accessible to only the *class* in which it is contained; this is the highest level of data hiding.

An additional feature of the C++ language is the ability to declare a *function* as a "friend" of a *class*. Such 'friend' *functions* may access the *class* code deemed as private or protected. This approach is typically used if a *function* needs to access private data in *objects* from two different *classes*. However it should be used with caution, too many external functions declared as friends of a *class* with protect or private data reduces the advantages gained by encapsulating the separate *classes* in the object-orientated approach.

The final requirement of a *class* is that it contains two functions termed the constructor and destructor. These are special *functions* responsible for creating and disposing of *function variables* belonging to the *class*. The constructor is used to initialise the *variables* while the destructor essentially cleans up after the *class* and frees any memory allocated within the *class*. Both the access specifiers of both the constructor and destructor *functions* must be public to allow the *class* data to be created (if private, the constructor cannot be called when the object is created and so *function* variables cannot be created) .

2.3. Inheritance

In addition to the design of stand-alone classes (described above), C++ allows for a more advanced design based on the concept of *inheritance* between classes. *Inheritance* is an important feature in OOP in which *classes* can be organised into a hierarchical structure. It allows the programmer to create *classes* that are derived from other *classes*, known as the base classes, so that they automatically include all the *variables* and *functions* of the base classes. This means, when creating a new *class*, the programmer can reuse the data and functions from within the base *class* thereby reducing implementation time. C*lasses* can also be derived from more than one class, inheriting the data and functions from multiple base classes.

The example depicted in Figure A2 described a *class* 'Drug' with two *instances* representing two new drug types. If we extend this example and consider that drugs can either be administered orally or via IV infusion. The *inheritance* feature in C++ allows for the creation of two derived *classes* of the base 'Drug' *class* (Figure A3). Both derived *classes* contain the common properties of the base *class* such as the *class* attributes and common functions but they allow existing functions to be edited and/or new functions to be created within a specific the derived class (Figure A3). In this example, the derived classes are modified to represent the different methods of drug administration (Figure A3). As before, different instances of the same derived class can be created and share the same common data and methods but with their own unique attributes.

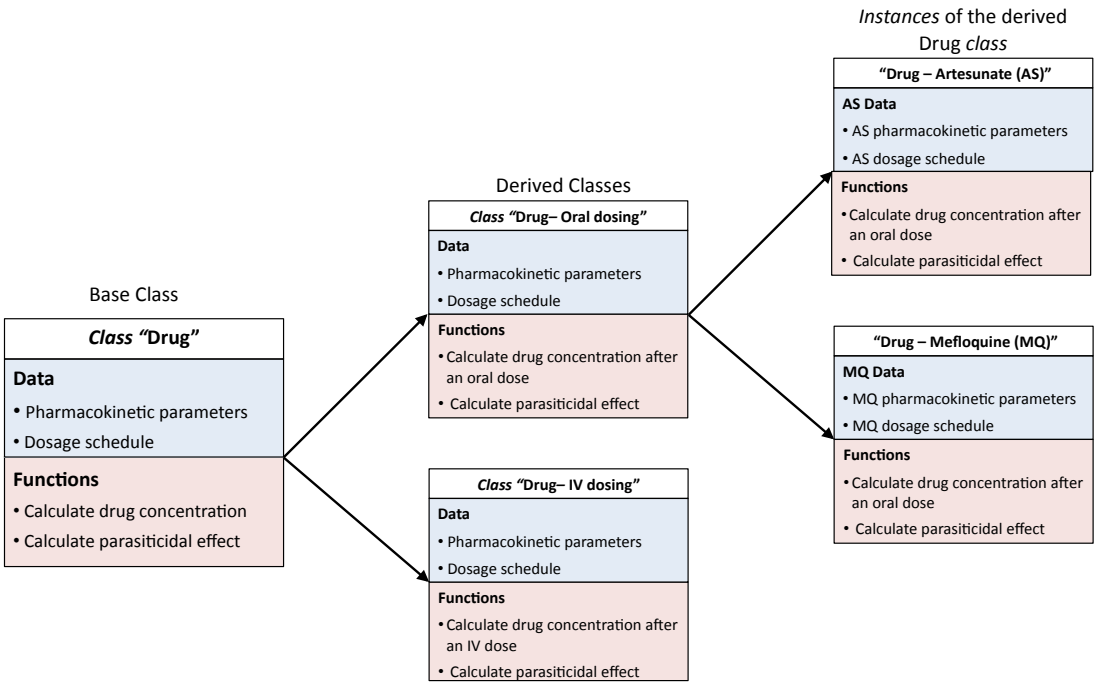

Figure A3. The base 'Drug' class show in the left box describes an *objects* data and the methods required to manipulate the data. Using the inheritance feature in C++, it is possible to create two derived *classes*. The derived *classes* inherit the common features (i.e. data and functions) of the base *class* and allow us to modify these features as required. Here, the methods in the derived classes (centre boxes) have been modified to reflect the different routes of drug administration. Different *instances* of these derived *classes* contain all the features of the derived *class* but have different attributes; in this case, the attributes are those applicable to AS and MQ.

2.4. Namespaces

In C++ namespaces allow entities like *classes*, *objects* and *functions* to be grouped under one name thus dividing the global scope of the program into 'sub-scopes' each with their own name. This feature is designed to simplify the writing of programs that combine pre-existing code from several contributors (like OpenMalaria). When multiple users contribute to a single computer program there is an increased risk that two classes/functions/variables will inadvertently have the same name, this causes a

particular problem for the program as it is unable to distinguish between the defined versions. Namespaces essentially allow the contributor to package their code into a unit called a namespace. All *classes*/*functions*/*variables* can then be referred to with respect to their namespace by using the namespace as a prefix, for example *namespace* :: *function*.

Appendix 3.

IV drug administration

For drugs administrated from IV infusion, the change in concentration *C* over time can be described as

$$\frac{dC}{dt} = R - kC$$

[A3.1]

where *R* is the rate of infusion (mg/kg/day), found by dividing the dose (mg) by the patients weight (kg) and multiplied by the IV duration (days), and *k* is the elimination rate. Equation 2 was integrated using laplace transformations to find the concentration at time *t*

To find the concentration *C* at time *t*, equation A3.1 was integrated using laplace transformations and the convention (209) of overhead bars to indicate transformed variables

$$s\overline{C} - C(0) = \frac{R}{s} - k\overline{C}$$

[A3.2]

where *C(0)* is dependent on the drug concentration in the blood at the immediate end of the previous time step *C'* augmented by any new doses *D* (mg/kg), so

$$C_0 = C' + \left(\frac{D}{Vd \bullet W}\right)$$

[A3.3]

Equation A3.2 rearranges to give

$$\overline{C}(s+k) = \frac{R}{s} + C_0$$

$$\overline{C} = \frac{R}{s(s+k)} + \frac{C_0}{(s+k)}$$

Back transforming into the time domain gives

$$C = \frac{R}{k}\left(1 - e^{-kt}\right) + C_0 \bullet e^{-kt} \qquad [A3.4]$$

Using equation A3.4 gives the amount (mg) of drug in the body at time *t*. To determine how the drug affects parasite density this amount was converted into a concentration by dividing the amount in the body (mg) by the volume of distribution (l/kg)

$$C = \frac{R}{k \bullet Vd}\left(1 - e^{-kt}\right) + C_0 \bullet e^{-kt} \qquad [A3.5]$$

Note the body weight multiplier in R cancels the weight factor in the denominator.

The effect of the intravenously administered drug is found by substituting Equation A3.5 into the Michaelis-Menten killing equation described in Equation 1

$$\int f(C)dt = V\int \frac{\left(\frac{R}{k}\left(1 - e^{-kt}\right) + C_0 \bullet e^{-kt}\right)^n}{\left(\frac{R}{k}\left(1 - e^{-kt}\right) + C_0 \bullet e^{-kt}\right)^n + K^n} dt \qquad [A3.6]$$

It is not possible to find the integral of this equation so it is solved numerically in C++ between the defined limits of 0 and *t*.

Chapter 6

Estimating the windows of selection for antimalarial drugs.

ABSTRACT

One force driving drug resistance through a population is resistant parasites' ability to survive "residual" drug levels persisting from previous treatment. High levels of drug use and long drug half-lives mean a high proportion (up to 80%) of the population may have residual drug levels selecting for resistance. Field studies can quantify the second force by estimating a window of selection (WoS), defined as the time difference between the earliest detection of increasingly resistant clones. We investigate whether these field data accurately estimate the true window of selection using standard pharmacokinetic-pharmacodynamic models. The simulated results were consistent with field data and effective ACTs were able to clear sensitive (and mildly resistant) infections when treated directly. Clinical estimates of WoS routinely overestimated the 'true' WoS following both AR-and AS-MQ treatments. The 'true' WoS were much lower than anticipated with a 50-fold IC50 increase resulting in a 2 or 5 day WoS for AR-LF and 4 or 11 days for AS-MQ (10^{th} and 25^{th} centile respectively). In this case, clinically estimated WoS were shown to be poor predictors of the 'true' WoS and urge authors to use the methodology within to evaluate the accuracy of clinical WoS for other drugs/regimens.

1. Introduction

Artemisinin combination therapies (ACT) are now widely deployed, very effective, first-line treatments for uncomplicated *Plasmodium falciparum* malaria in most endemic countries (380). The artemisinin component is extremely fast acting and highly potent but rapidly eliminated so they are always co-administered with a second partner drug with a longer half-life. The long half-lives of the partner drugs are clinically beneficial, providing prophylaxis after treatment (305, 307), but the rapid elimination of artemisinin means the partner drugs persist as a monotherapy for extended periods of time after treatment thereby selecting for resistant parasites. Tolerances to increasing concentrations of long half-life drugs (in this case the 'partner' drugs) may gradually evolve in parasite populations to the point where full therapeutic failure of ACTs may occur. Field studies have observed this increasing tolerance for SP (132, 133, 352), LF (305) and MQ (267) whose half-lives are approximately 4 days for sulfadoxine (109), 8 days for pyrimethamine (109), 4-5 days for LF (96) and 2-3 weeks for MQ (355). Aduik *et al.* (1) have also shown that the addition of an artemisinin to a failing drug with a long half-life does not fully restore drug effectiveness. This ability of the long-lasting 'partner' drug to evolve resistance is arguably the Achilles heel of ACTs.

The genetic process whereby parasites evolve increasing tolerance to the partner drug is usually quantified as a window of selection (WoS). As a specific example, Watkins and Mosobo (352) noted parasites with the *dhfr*108 mutation could be observed in patients 15 days after treatment with SP (sulfadoxine-pyrimethamine) , whereas wild-type infections were only observed after 50 days; thus implying a WoS of 35 days. Similarly Sisowath *et al*. (305) estimated a WoS of 15 days associated with the *pfmdr1* D1246Y mutation after lumefantrine treatment. Routine genotyping in clinical trials means such data are readily available and there is increased interest in using these data to estimate WoS (130, 133, 305, 352). In endemic areas people often take antimalarial drugs presumptively on a regular basis to treat any type of fever. This is likely to result in lengthy selection windows for most drugs for example, if 5 courses of SP are taken per year then there will be 5x35=175 days per person in which

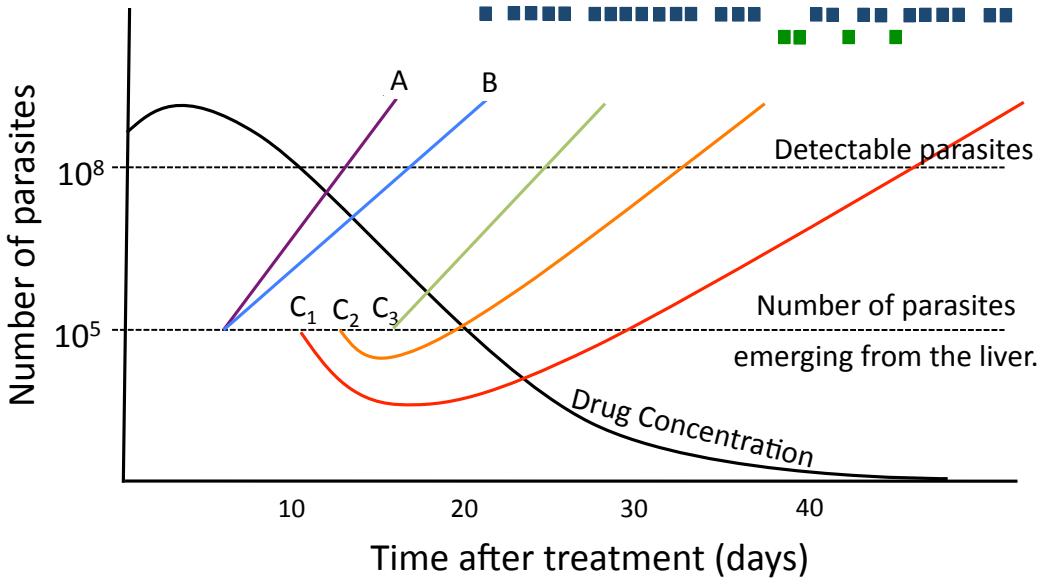

Figure 1. Potential problems that may arise when using patency to estimate the 'clinical' windows of selection (WoS). Field studies typically measure the WoS by comparing the times different genotypes become detectable in patients. The data at the top of the figure are field data from Sisowath *et al.* (305), showing that resistant parasites bearing the *pfmdr1* D1246Y mutation (top row; blue squares) become detectable in patients approximately 20 days after treatment and about 15 days earlier than sensitive parasites (bottom row; green squares). We are interested in whether these 'clinical' WoS are good representations of the 'true' WoS.

For each new infection we assumed 10^5 parasites emerged from the liver and became detectable when there were 10^8 parasites (horizontal dashed lines), the black line shows the decrease in drug concentration over time (for illustration we assume a single dose regimen). Lines A and B show two clones that emerge on the same day but grow at different rates as a result of differing IC50s, become patent several days apart. Here, field estimates based on the day parasites become detectable would quantify a window of selection of around 5 days when in fact there is none. Lines C_1-C_3 illustrate how the earliest emerging parasites may not necessarily correspond to the first patent infection. C_1 is the earliest successfully emerging clone but residual drug levels cause an initial drop in parasite numbers and so C_2, which emergences slightly later, is able to become patent sooner. Similarly, by the time C_3 emergences from the liver, drug levels have fallen sufficiently that it no longer effects the newly emerged clone and so C_3 is able to emerge before both C_1 and C_2. The 'clinical' WoS is actually wrong: the true order of survival is C_1, C_2, C_3 but the clinical order is C_3, C_2, C_1. This effect is not genotype-specific but it introduces an element of chance that may reduce the correlation between 'true' and 'clinical' WoS.

persisting drug concentrations are selecting for the dhfr108 mutation. This implies that selection for resistance via WoS may be widespread and intense.

These WoS estimates are widely cited and we refer to them as 'clinical' WoS to denote their origin in clinical observations. In fact the 'true' WoS is the period in which infections bearing the mutation can emerge from the liver (we assume the drugs do not kill the parasites while in the liver stage) and survive to produce a patent (i.e. detectable) infection while sensitive parasites are killed by residual drug concentrations (321). Unfortunately, it is impossible to directly observe 'true' WoS because the 10^5 parasites that emerge from the liver are below patency so we are forced to rely on clinical WoS i.e. the time at which they have grown to patency (assumed to be 10^8). However, it is not clear how well the clinical WoS estimates the 'true' WoS and there are several plausible reasons why they may be poor estimators (Figure 1). This paper uses the pharmacokinetic-pharmacodynamic (PK/PD) model described in Winter & Hastings (168, 364) to simulate WoS for increasingly resistant infections with the aim to quantifying how accurately clinical WoS estimate the 'true' window of selection.

2. Method

We used the validated mechanistic PK/PD model of Winter & Hastings (364), with the additional absorption and conversion phases for the artemisinins, and the parameter specific estimates of variation as described in Winter & Hastings (168) (Table A1). The model was applied to two treatment combinations artesunate-mefloquine (AS-MQ) and artemether-lumefantrine (AR-LF), both highly effective ACTs currently used to treat malaria. Using the model, we determined the probability that parasites survived residual drug levels and used this probability to determine whether the clinically observed WoS accurately predicts the 'true' WoS. We focus solely on increasing resistance to the partner drugs and incorporate it into simulations by increasing the IC50 of the partner drug. We do not consider resistance to the artemisinins because they are present in the body for such a short time they are

unlikely to impact estimates of WoS; however we include the artemisinin component in simulations determining the fate of parasites emerging on days 1, 2 and 3.

For each treatment arm we modelled 2500 patients; all patients were treated at day 0 and followed for 365 days. The patients drug pharmacokinetic (PK) parameters were assigned using the means and distributions in Table A1 and each patients infection consisted of one parasite clone with the parasites PD parameters randomly allocated using the means and distributions given in Table A1. We assumed there were no parasites present on the day of treatment (i.e. day 0) but that 10^5 parasites emerged from the liver the day after treatment (i.e. day 1). These parasites encountered residual drug levels persisting from the initial treatment and we investigated the fate of the clone, scored as either survival or death, each day following liver emergence. If the clone survived, the time to patency (i.e. $>10^8$ parasites) was determined by standard PK/PD modelling and recorded. If the clone did not survive, we repeated the above steps assuming that parasites emerged from the liver on day 2, then assuming they emerged on day 3 and so on until we found the earliest day each clone could successfully emerge in the patient (the patient scored as "missing data" if their infection failed to become patent by day 100). This process generated a distribution of earliest possible emergence days for the 2500 human / parasite combinations.

We repeated the process described above to simulate "alleles" encoding increasing drug resistance; each of the 2500 patients retained their PK parameters to ensure consistency across alleles while the parasite PD parameters were re-assigned. We simulated six resistance alleles whose mean IC50 was increased 2, 10, 15, 20, 25 and 50-fold greater than the mean (Table A1); each allele therefore generated a distribution of 2500 earliest emergence days occurring over the simulated one year period. In reality, patients in clinical trials are rarely (if ever) followed for more than the recommended 63 days for drugs with a long half-life (368). To reflect this we also looked at the effect of reducing the duration of the patient follow-up to that more typical of a clinical trial and include the results of the censored population (i.e. only patients with infections present before day 63).

The question then arises as to how to translate these distributions into WoS. It would be inappropriate to define the start of the WoS as the lowest possible emergence day

in the distribution, because this will depend on chance and on sample size. We therefore defined the day the WoS opened for any allele as the day post treatment on which ≥25% of clones could survive residual drugs (we also used a definition of 10% but this made little difference, see later). The WoS acting between 2 alleles is therefore the time difference between the openings of their respective WoS.

Having established the "true" (i.e. according to our simulations) WoS, it is necessary to investigate how well field data generated by clinical trials recovers them. We simulate 2500 patients, all treated on day 0 and followed up for 100 days, with PK parameters drawn from Table A1. We assume that on average any individual would acquire 16 new infections per year based on data from Northern Ghana (284). For each individual, the specific number of new infections was chosen from a Poisson distribution with this mean value, 16. To maintain the population size, if an individual had no new infections (i.e. if a value of zero was chosen) another number was selected in the same way. The day on which each of the new infections emerged from the liver was randomly sampled from the follow-up period. Each newly emerging infection had PD values chosen from Table A1. In humans with more than one new emergence, each emergence was genetically distinct (i.e. had different PD values). The fate of each emergence in a human was determined as before (survival/death and, if survival, time to patency). The simulated patient was then categorized as having "no re-infection" (if no patent infection appeared before day 100 of follow-up) or "re-infected" with a time of first patency. This generates a distribution of times to first patency analogous to the data of Sisowath *et al*. (305) shown on Figure 1. We repeat this process for each of the six resistance alleles; the 2500 humans had their PD parameters reassigned for each allele with increasing IC50 values. Once again, the problem arises as to how to define when the WoS opens for each allele in the simulated field data. Most observers "eyeball" the data (e.g. the Sisowath *et al*. (305) data on Figure 1) and compare the earliest patency days; as noted above this is unsatisfactory because it depends on chance and the sample size of each allele (determined by its frequency). For consistency, we chose to compare field estimates of WoS by assuming they opened at the 25th centile of the distribution of earliest patency days (again checking the results are consistent with a definition using a 10% centile). As before the WoS between different allele is the time difference between their WoS opening.

The probability of surviving direct ACT treatment was also recorded to provide a baseline probability of successful treatment, against which the survival probabilities of later emerging parasites could be compared. This allowed us to determine whether the WoS can be estimated when observed drug failure rates are high. We assumed that between 10^{10} and 10^{12} parasites (chosen from a uniform distribution) from a single clone were present at the time of treatment, simulated the outcome (i.e. survival/death) and determined the probability of each IC50 "genotype" surviving direct treatment.

3. Results

The choice of model parameters were previously validated in Winter & Hastings (168, 364) and the results generated herein are again highly consistent with field data. Fully effective ACTs were able to clear infections with either fully sensitive or mildly resistant parasites when treated directly (Figure 2). All clones emerging on day 2 were highly unlikely to survive treatment with either AR-LF (Figure 2A) or AS-MQ (Figure 2B). When LF resistance was low (i.e. equal to or two-fold greater than the default value) it typically took 20-25 days before 50% of new infections could successfully emerge from the liver (Figure 2A); Sisowath *et al.* (305, 307) found reinfections with LF-sensitive parasites occurring 24 to 30 days after treatment. The probability of successful reinfection (with LF sensitive parasites) then increased rapidly to approximately 90% by day 40. For LF-resistant infections in which the IC50 was between 10 and 50-fold greater than the mean, the chance of parasites successfully emerging from the liver increased rapidly from less than 5% on day 2 to more than 90% on day 40. Following treatments with AS-MQ (Figure 2B), new infections with sensitive and mildly resistant (i.e. IC50 just 2-fold greater than the mean) parasites remained low (<30%) for the first 15-20 days after treatment. The probability of these emerging clones resulting in successful new infections increased to 60-70% 40 days post-treatment. As resistance to MQ increased, parasites were able to cause new infections earlier. Between 20 and 50% of new infections with resistant parasites (i.e. IC50s 20-fold greater than the mean) were able to survive 5 days after

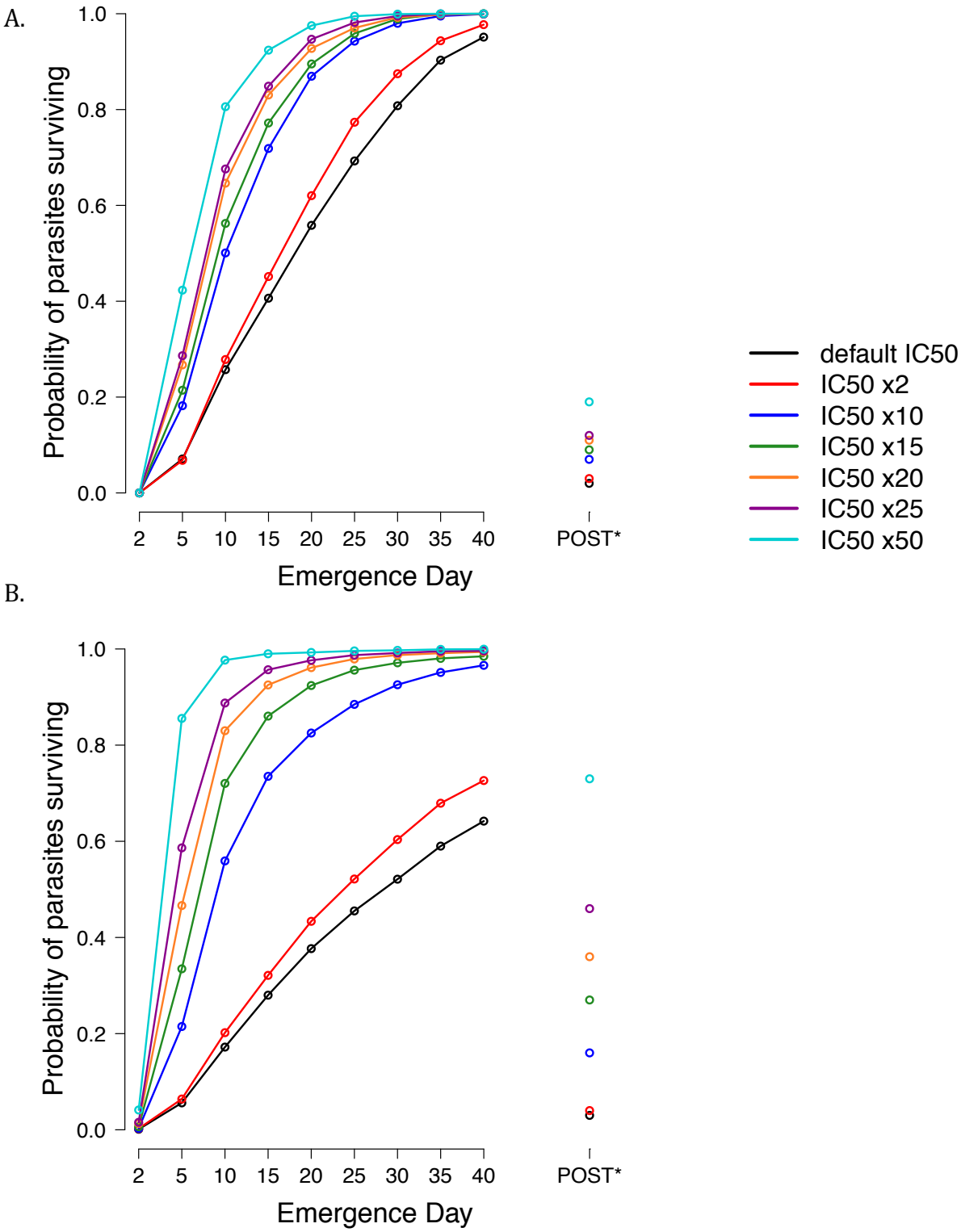

Figure 2. The probability of drug resistant parasites emerging from the liver and surviving to cause a patent new infection 2, 5, 10, 15, 20, 25, 30, 35 or 40 days after treatment with (a) artemether-lumefantrine or (b) artesunate-mefloquine. Note the probability of surviving treatment (POST) with monotherapies are shown to immediate right of the x-axis.

* POST – Probability of surviving therapy

treatment, this increased to more than 90% survival on day 30. The simulated results show AS-MQ was able to prevent new infections by sensitive and mildly resistant parasites for longer than AR-LF. This implies MQ has the longer post-treatment prophylactic period and we note Sagara *et al.* (283) reported reinfections in Peru occur less frequently in their follow-up period of 28 days following AS-MQ treatment than AR-LF.

The probabilities that each genotype survived direct treatment with either ACT are given in Figure 2 and Table A1. Most infections treated with AR-LF had less than a 0.15 probability of surviving direct treatment, only when the IC50 was increased 50-fold did the probability of survival increase to 0.19. In contrast, treatment of infections with AS-MQ in which the IC50 is more than 2-fold greater than the mean had >0.15 probability of surviving direct treatment. This increased to as much as 0.46 and 0.73 for infections with IC50 values 25 and 50-fold greater than the mean.

While the probability of surviving treatments differs between the two ACTs, both show the largest increase in survival occurring between days 2 and 5. This is likely to be due to the presence of the artemisinin component on day 2 and its absence by day 5 (by convention, treatment starts on day 0 so artemisinins are present on days 0, 1 and 2). Somewhat counter intuitively, the probability of surviving direct treatment was always greater than the probability of parasites surviving emergence on day 2. The most likely explanation is that the established infections treated on day 1 are present in much greater numbers (10^{10}-10^{12}) than the newly emerging parasites in day 2 (10^{5}).

To accurately estimate the WoS, the time difference between detection of different "genotypes" (observed in the field when they become patent i.e. $>10^{8}$ parasites) must be approximately equal to the time difference between the earliest emergences of different genotypes from the liver (Figure 2, Table A1). The key research question is therefore to determine whether the clinical WoS reliably estimates the 'true' WoS. This appears to be true for clones treated with AR-LF; estimated WoS were accurate to within 1-4 days (Table 1), indicating that the observed patency was a good predictor of true WoS. Clinical estimates of WoS following AS-MQ treatment were much less accurate. The true WoS was consistently overestimated by as much as 19 days (Table 1). While these results were determined using the 25th centile cut-off

Table 1. Simulations of 2500 patients (followed for one year after treatment) infected with increasingly drug resistant parasites and treated with either (A) AR-LF or (B) AS-MQ [a]

AR-LF

IC50	10th centile True WoS		10th centile Clinical WoS	25th centile True WoS		25th centile Clinical WoS
default to 2-fold	0		4	0		3
2-fold to 10-fold	1	[1 vs 13]	7	4	[4 vs 13]	8
10-fold to 15-fold	0		2	0		2
15-fold to 20-fold	1		1	1		1
20-fold to 25-fold	0	[1 vs 4]	1	0	[1 vs 5]	1
25-fold to 50-fold	0		2	0		3

AS-MQ

IC50	10th centile True WoS		10th centile Clinical WoS	25th centile True WoS		25th centile Clinical WoS
default to 2-fold	0		8	2		11
2-fold to 10-fold	3	[3 vs 33]	19	6	[9 vs 43]	25
10-fold to 15-fold	0		6	1		7
15-fold to 20-fold	0		3	1		5
20-fold to 25-fold	1	[1 vs 10]	2	0	[2 vs 14]	2
25-fold to 50-fold	0		5	1		7

[a] The square brackets indicate the cumulative differences in WoS (i.e. default to 15-fold and 15- to 50-fold)

described in the methods and 16 new infections per year, the results were consistent when using the 10th centile cut-off (Table A2) and/or the number of new infections per year was reduced to 8 (results not presented). It is important to note however that these errors are cumulative and if we consider larger increases in IC50 the ability of clinical trials to estimate the 'true' WoS is reduced for both regimens. The 25th centile results for AR-LF show the 'true' WoS is over estimated by 9 days when the IC50 is increased from the default value by 15-fold and by 4 days when the IC50 is increased from 15-fold to 50-fold greater than the mean (Table 2). The poor predictive ability of clinical 'WoS' are particularly evident following AS-MQ treatment (25th centile) where the 'true' WoS is overestimated by 33 days (15-fold IC50 increase) and 12 days (15 to 50-fold increase).

Table 2. Simulations of 2500 patients (followed for 63 days after treatment) infected with increasingly drug resistant parasites and treated with either (A) AR-LF or (B) AS-MQ [a]

AR-LF

	10th centile			25th centile		
IC50	True WoS		Clinical WoS	True WoS		Clinical WoS
default to 2-fold	0		3	0		2
2-fold to 10-fold	1	[1 vs 13]	8	4	[4 vs 12]	8
10-fold to 15-fold	0		2	0		2
15-fold to 20-fold	1		1	1		2
20-fold to 25-fold	0	[1 vs 5]	1	0	[1 vs 6]	1
25-fold to 50-fold	0		3	0		3

AS-MQ

	10th centile			25th centile		
IC50	True WoS		Clinical WoS	True WoS		Clinical WoS
default to 2-fold	0		-1	1		2
2-fold to 10-fold	2	[2 vs 9]	7	5	[7 vs 12]	7
10-fold to 15-fold	0		3	1		3
15-fold to 20-fold	0		2	1		3
20-fold to 25-fold	1	[1 vs 8]	2	0	[2 vs 10]	2
25-fold to 50-fold	0		4	1		5

[a] The square brackets indicate the cumulative differences in WoS (i.e. default to 15-fold and 15- to 50-fold)

Censoring the results to reflect follow-up periods typical of a clinical trial had mixed results (Table 2 and Figure A2). Following AR-LF treatment, all individuals had a successfully emerging infection prior to day 63 and so the 'true' WoS remained unchanged by the reduced follow-up period (Figures S1 and S2). In contrast, approximately half of the earliest patent infections (with fully sensitive parasites) occurred after the 63-day follow-up period (Figure A2) and so the censored estimates following AR-LF treatment saw the clinically estimated window opening earlier (at both the 25th and 10th centile cut-offs). Despite the earlier opening of the clinical WoS the relative time the windows were open was almost identical (clinically estimated WoS were always within one day of the uncensored results). AS-MQ treatment has

been shown to result in fewer new infections than AR-LF (e.g. (283)) and our results show that only a fifth of the simulated infections (in fully sensitive parasites) occur before the 63-day cut-off of clinical trials. The reduced follow-up period has an even greater effect on estimates of the earliest patent infections, less than 300 of the 2500 patients simulated had a patent infection (with fully sensitive parasites) within the 63-day follow-up period. This reduced follow-up period resulted in estimates of the earliest patent infection almost half that seen when patients were followed for a year (Figures S1 and S2). So, rather than comparing the $10^{th}/25^{th}$ centile values as intended when following patients for a full year, we are actually comparing much lower centiles. When uncensored, the clinical WoS for AS-MQ overestimated the true window by approximately 10-fold (10^{th} centile) and 3- to 6-fold (25^{th} centile). When the results were censored this overestimation was reduced to 3 to 8-fold and 2 to 5-fold (10^{th} and 25^{th} centile respectively).

4. Discussion

The aim of this paper was to discover how accurately genotyping data obtained during antimalarial drug clinical trials are able to estimate windows of selection. The results show that estimating WoS from the clinically observed patency of different genotypes is a poor surrogate for the 'true' WoS, particularly when IC50 increases are large. The results in Table A2 show the earliest emergence day of parasites from the liver occur up to four weeks earlier than the emergence of the fastest patent infections seen in the field (clones C1 versus C3 in Figure 1) while the day the earliest parasites become patent occurred up to two weeks later than the fastest patent infections. This is likely to be a result of the delay in growth rate caused by residual drug levels in the earliest emerging infections, they typically required up to two weeks longer than the later (and hence faster) emerging clones to reach patency (i.e. $>10^8$). We do note that when simulating field data (to determine the 'clinical' WoS) we ignore heterogeneity in the biting rate and hence (presumably) liver emergence rate.

There is currently interest in the improved diagnostics of malaria treatment, both through technical assistance for improved microscopy, and through provision of rapid

diagnostic tests (RDTs). The primary purpose of these interventions is to ensure treatment is restricted to confirmed malaria case so that treatment is appropriate to the condition, to reduce use of expensive ACTs and ensure patient treated for the true underlying condition if it is not malaria. As further justification, reducing overall drug use will reduce selection for resistance. For example, if a drug had a WoS of 15 days and a patient was given 6 treatments throughout the year, there would be 90 days or approximately 25% of the year in which the resistant parasites were preferentially selected for. A decrease in overall drug use will lead to a decrease in this selection pressure which can only be quantified by true WoS hence the importance of verifying whether clinical WoS accurately reflect the true WoS.

Three processes drive drug resistance: the ability to survive treatment, the WoS and intra-host dynamics (126). The ability of a mutation to survive treatment can already be quantified by clinical trials. The role of WoS required confirmation that the true WoS for a mutation is closely quantified by the clinically observed WoS, as has been investigated here. Quantifying intra-host dynamics is less easy although some progress has been made in mouse models (351) and through inference from clinical data (125). Thus, we can be reasonably confident that we can accurately quantify 2 of the 3 forces driving resistance. The results presented here provide compelling evidence that clinically observed WoS do not adequately estimate the 'true' WoS for AR-LF or AS-MQ treatments. It should therefore be noted that this is only applicable to the two drug regimens investigated. We would urge authors to use the methodology contained within this and previous papers (168, 364) to determine the accuracy of the clinical WoS for other drugs and/or drug regimens.

The clinically estimated WoS appear to be poor predictors of true WoS particularly when looking at the cumulative results (given in square brackets, Table 1). The true WoS is much lower than most people would expect *a priori*. For example, the WoS following a default to 50-fold IC50 increase was 2 or 5 days for AR-LF (10^{th} and 25^{th} centile respectively) or 4 or 11 days for AS-MQ. Censoring the results to simulate the duration of a clinical trial (i.e. 63 days of follow-up) improved the predictive ability of AS-MQ (although it had little effect of AR-LF which tended to emerge before the 63-day cut off). Despite this improvement, the 'true' WoS was still overestimated by 2- to 8-fold thus confirming the poor predicative ability of the clinical WoS.

Appendix

We use this Appendix to include data that support and expand some of the interpretations and conclusions drawn in the main text, but whose inclusion would detract from the main argument

Table A1. Dosages and mean antimalarial drug parameters for artesunate, artemether, DHA, lumefantrine and mefloquine with the corresponding coefficient of variation estimates given in square brackets

	Artesunate-Mefloquine			Artemether-Lumefantrine		
	Artesunate	DHA	Mefloquine	Artemether	DHA	Lumefantrine
Dosage Regimen	4mg/kg/day artesunate with 8.3mg/kg/day mefloquine for three days [380]			1.7mg/kg artemether with 12mg/kg lumefantrine twice daily for three days [380]		
Volume of distribution (Vd)	7.1[236] [94[224]]	1.49[236] [48[210]]	20.8[359] [38[165, 302]]	5.21[140] [82[4]]	3.7[140] [48[210]]	21[68] [263([16, 40)]]
Absorption rate constant (x)	252[236] [112[326]]	-	-	23.98[140] [68[4, 345]]	-	-
Conversion rate (z)	30.96[236] [36.2[326]]	-	-	11.97[140] [65[4, 345]]	-	-
Elimination rate constant (k)	-	25.4[236] [23[57, 83, 237, 326]]	0.053[350] [63[165]]	-	44.15[140] [23[57, 83, 237, 326]]	0.16[110, 212, 350] [5[83]]
Concentration producing half the desired effect (IC50)	0.0016[4, 109] [86[210]]	0.009[210] [117[210]]	0.027[44] [78[210]]	0.0023[a] [79[264)]]	0.009[210] [117[210]]	0.032[44, 321] [102[210]]
First order rate constant of parasite killing (V)	27.6[364]	27.6[364]	3.45[359]	27.6[364]	27.6[364]	3.45[359]
Slope Factor (n)	4[321]	4[321]	5[321]	4[b]	4[321]	4[321]

[a] Unpublished data from Liverpool School of Tropical Medicine

[b] Assumed to be like AS

Table A2. Simulations of 10,000 patients infected with increasingly drug resistant parasites and treated with either (A) artemether-lumefantrine or (B) artesunate-mefloquine. The probability of surviving therapy (POST*) was calculated to provide a baseline probability of treatment failure assuming between 10^{10} and 10^{12} parasites were present on the day of treatment. The earliest parasite emergence was defined as the first day an IC50 "genotype" had more than a 25% chance of survival. The earliest emergence (and the day it subsequently became patent) did not necessarily result in the fastest patent infection (i.e. Figure 1 shows C_3 becomes patent before C1) and so the day the fastest genotype became patent (and the day it would have emerged from the liver) was also recorded.

(A) Artemether-lumefantrine

IC50	POST*	Earliest emergence	Patency of earliest emergence	Fastest emergence	Patency of fastest emergence
Mean	0.02	10	40	30	50
x2	0.03	10	37	27	46
x10	0.07	6	28	18	36
x15	0.09	6	25	17	35
x20	0.11	5	24	16	33
x25	0.12	5	23	15	31
x50	0.19	5	21	12	28

(B) Artesunate-mefloquine

IC50	POST*	Earliest emergence	Patency of earliest emergence	Fastest emergence	Patency of fastest emergence
Mean	0.03	14	61	49	81
x2	0.04	12	53	40	70
x10	0.16	6	33	22	45
x15	0.27	5	27	17	38
x20	0.36	4	25	14	33
x25	0.46	4	24	13	31
x50	0.73	3	21	9	24

[a] All units are in days after treatment, except POST* which is a probability.

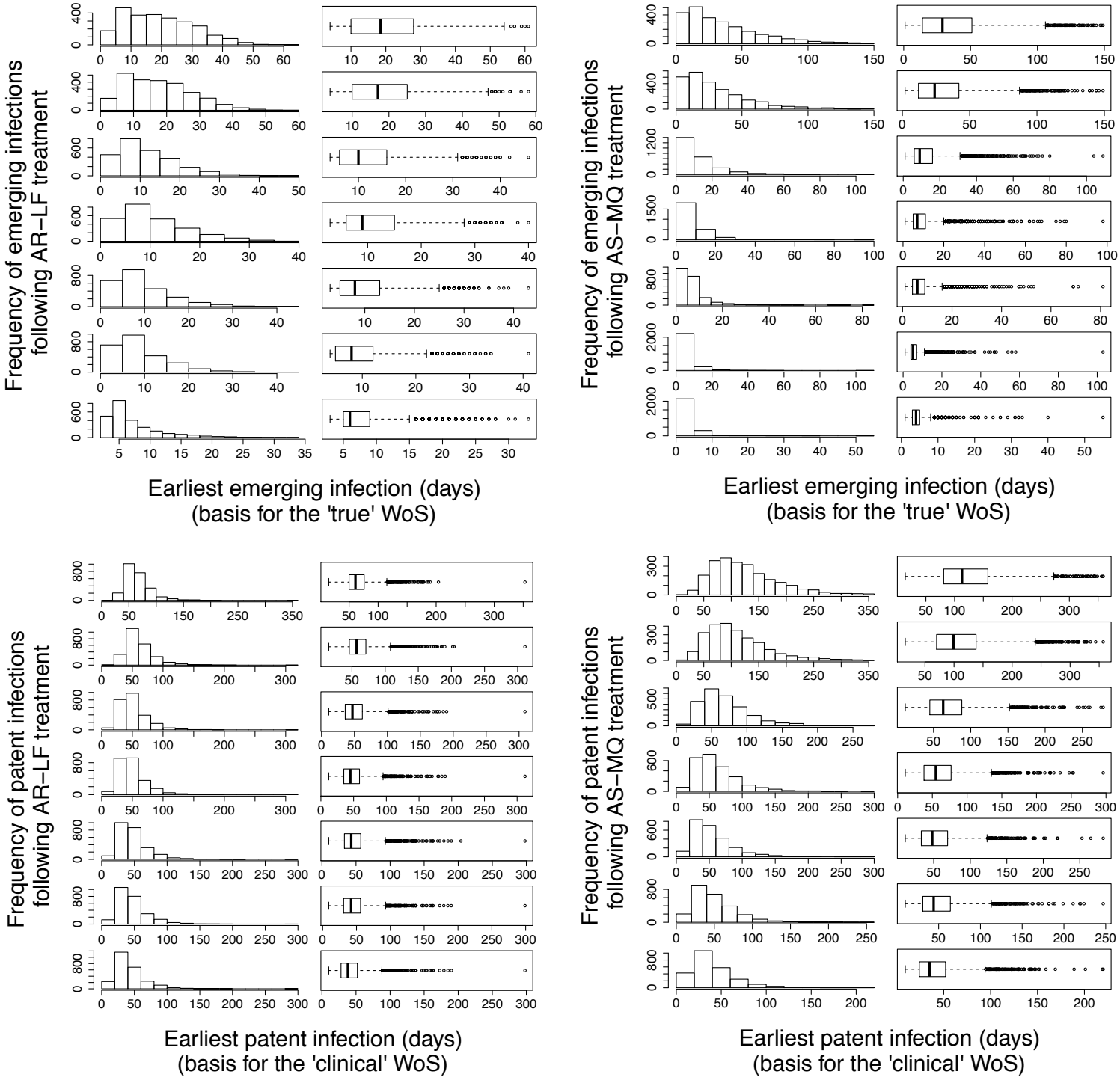

Figure A1. Estimates of the 'true WoS was determined from the distribution of earliest emerging infections (top row). The 'clinical' WoS was estimated using the distribution of the earliest patent infections (bottom row). The true and clinical WoS was estimated for two drug regimens, AR-LF (left column) and AS-MQ (right column), with patients infected with increasing resistant parasites (top graphs show the mean IC50 increasing to x2, x10, x15, x20, x25 and x50 greater than the mean in the bottom graph) and followed for one year after treatment.

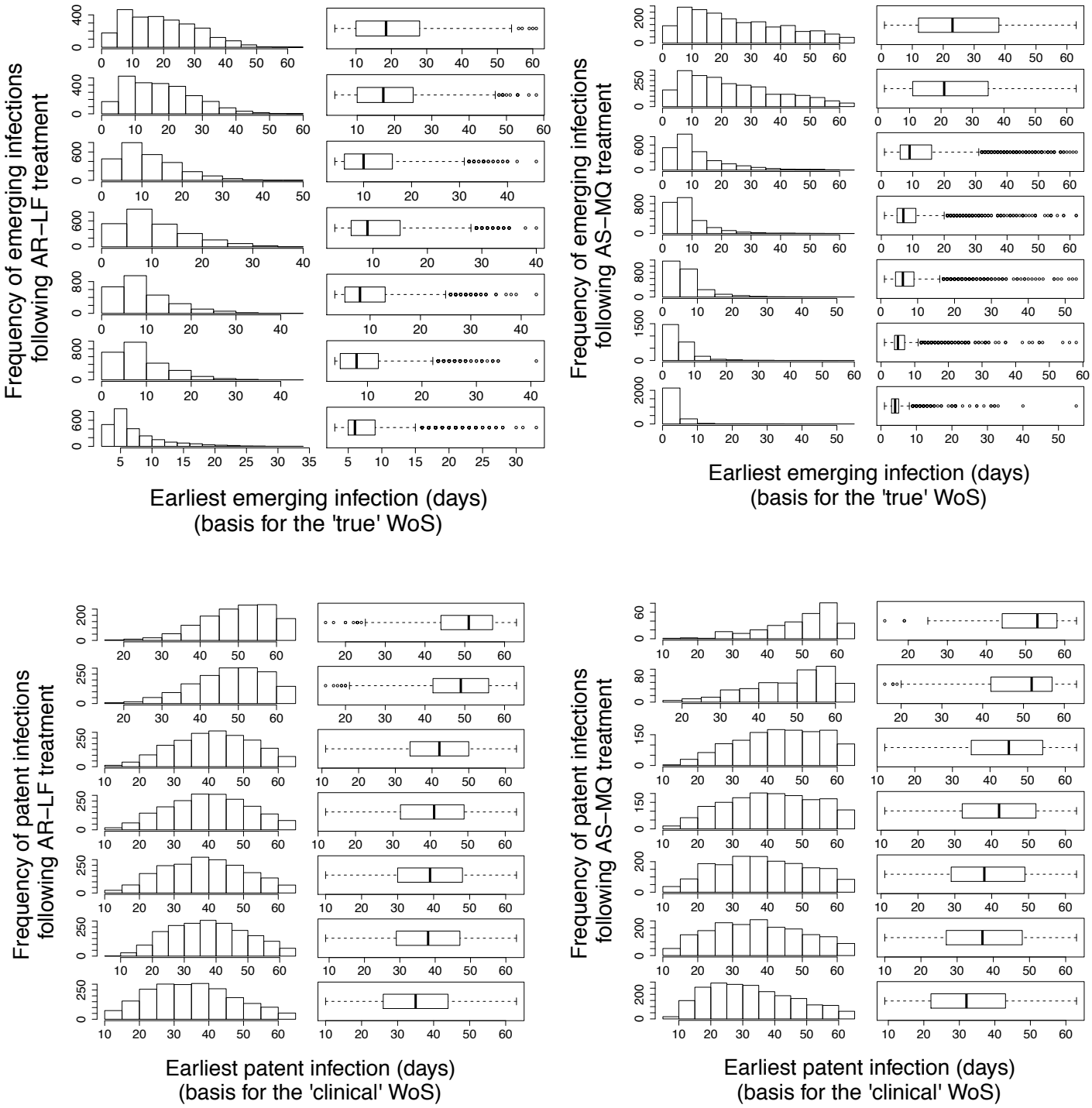

Figure A2. Estimates of the 'true WoS was determined from the distribution of earliest emerging infections (top row). The 'clinical' WoS was estimated using the distribution of the earliest patent infections (bottom row). The true and clinical WoS was estimated for two drug regimens, AR-LF (left column) and AS-MQ (right column), with patients infected with increasing resistant parasites (top graphs show the mean IC50 increasing to x2, x10, x15, x20, x25 and x50 greater than the mean in the bottom graph) and followed for 63 days (the length of a typical clinical trial).

Chapter 7

Discussion

Mathematical models, in this case of antimalarial drug therapy, have the potential to provide valuable insights into questions that cannot be easily answered in the field either because they are too expensive, unethical or too complex (i.e. they would require many trials to disentangle the effects). However, the current choice of pharmacological models for antimalarial drug treatment is limited in large part to those investigating monotherapies. Given that WHO now recommends drug combinations, preferably artemisinin combination therapies (ACTs), be used to treat uncomplicated malaria (379), the future value of such models is limited. The purpose of this thesis was to develop the methodology of pharmacological models so their results are more compelling for the new generation of ACTs and use them to investigate the effectiveness of antimalarial drug treatment.

The previous thesis chapters describing the development of the basic PK/PD model (Chapter 2), the extensions to the model (Chapters 3 and 4) and the simulations of field data aimed at optimising clinical trial analysis (Chapters 4 and 6) were all written with the intention to submit the work for publication. As such, each chapter includes a lengthy discussion of our major findings, their significance and the models strengths / limitations (including the model assumptions). This discussion chapter will therefore focus first on a recent paper discussing the development of antimalarial PK/PD models and go on to summarise the extent to which this thesis meets its original aims.

1. Recent Publications

To ensure a thorough analysis of the antimalarial PK-PD models currently available, I now discuss a recent PK-PD model described by Zaloumis *et al*. (399) with reference to our own model and the recent murine malaria model described in Patel *et al.* (254). Both models (254, 399) were published after developing the model described herein (Chapters 2 and 3; (168, 364)) and so are not discussed in earlier chapters.

Zaloumis *et al*. (399) focus on how the distribution of parasite age changes post-treatment as a consequence of the concentration of the antimalarial drug. They track the number of parasites in each developmental stage hourly and compare the simulated distribution of parasites with those in patients. They use the model to attempt to assess the utility of PK/PD models for determining treatment outcome in patients. While we (364) focus on how robust drug regimens are to small changes in parasite sensitivity and, how vulnerable regimens are to the evolution of drug resistance.

There are a number of methodological differences between our PK/PD model and that of Zaloumis *et al*. (399). Primarily, their model allows for the stage-specificity of drug action by incorporating the age distribution of the parasite population (as describe in the discrete-time model of Saralamba *et al.* (285) and originally outlined by Hoshen *et al.* (143, 145)). This addition requires their model to run in hourly time steps as opposed to the half- and full-day time steps used in Winter & Hastings (364). Both papers model three first-line treatments for malaria (AR-LF, AS-MQ and DHA-PQ) but the choice of PK/PD parameters and their associated distributions differ between the two models. Given the large amount of variation in PK/PD data reported by field studies this is not surprising but should be considered when comparing model outputs (see later).

Our model generated results consistent with field data and we used the model to identify the most important factors effecting treatment outcome. Zaloumis *et al*. (399) primarily fitted their model to clinical data for the first 3-5 days following treatment but found their results were a poor fit to the data. They went on to compare different

AS-MQ and DHA-PQ dosing regimens with increasing EC50 (drug concentrations *in vivo* that correspond to 50% parasite killing) values, but conclude that their model did not provide the results expected from clinical efficacy studies. Both papers (364, 399) examine the models sensitivity to changes in parameter values, specifically the IC50, the slope factor (i.e. the slope of the concentration effect curve) and the parasite kill rate constant (Vmax) of the artemisinin and partner drug in AR-LF, AS-MQ and DHA-PQ combination therapies. Winter & Hastings (364) also consider the effects of initial parasite number, the parasite growth rate, and the volume of distribution and elimination rate of both the artemisinin and partner drug while the analysis of Zaloumis *et al*. (399) includes the parasite multiplication factor (fixed to 10 in our model), the mean age distribution of initial parasite burden, and the standard deviation of the initial parasite burden. The general conclusion of both papers is that the IC50 and Vmax of the partner drug (with the exception of PQ Vmax, see below) are particularly important determinants of treatment outcome while the IC50 and Vmax of the artemisinin drug have only a marginal effect on the treatment outcome. Both papers also agree that the slope factor of either the artemisinin or the partner drug had no association with treatment outcome for any of the ACTs modelled. The models differ in their opinion of the importance of PQ Vmax on treatment outcome. The parameter analysis described in Winter & Hastings (364) ranks PQ Vmax as the most important parameter (of all PK/PD model parameters) when determining DHA-PQ treatment outcome while Zaloumis *et al*. (399) found it to be only weakly associated with the proportion of patients cured.

The conflicting opinions of the two papers, particularly in terms of the models predictive ability, is likely to be the result of a number of factors. As mentioned above, the choice of model parameters and their associated distributions differ significantly and would inevitably result in different conclusions even if the same model were used. However, the primary reason for the difference of opinion is likely to be due to the length of the modelling time steps. Zaloumis *et al*. (399) use one-hour time steps to look at the hourly change in parasites of different ages. In contrast, we examine treatment outcome using half- and full-day time steps; our model was developed with the intention to eventually incorporate the methodology into OpenMalaria and so the one-day time steps used therein largely influenced our choice

A recent paper by Patel *et al.* (254) describes a mechanism-based growth model for *P.berghei* in murine malaria, reflecting the four erythrocytic stages (rings, early trophozoites, late trophozoites and schizont) of the parasite life-cycle, and incorporates the parasite killing effect of DHA. Their resulting model highlights the statistical superiority of a delayed effects model (rather than immediate drug killing) when describing DHA PK/PD. The superiority of this delayed effects model maybe the result of a lag time in drug action following administration of an artemisinin. Previous studies have noted an initial increase in parasite number following the first dose of an artemisinin (112, 300), although the reasons for this are not entirely clear. Gordi *et al.* (112) hypothesise that an initial increase in parasitaemia may be the result of time lags arising either as drugs distribute to the site of action, as drugs are converted to an active metabolite, and/or as parasites rapidly return from the site of sequestration to circulation. Despite the potential reasons, it is apparent that when modelling drugs with short half-lives (such as the artemisinins) and using hourly time steps, incorporating this lag time is crucial. Patel *et al.* (254) also found the inclusion of a schizont efflux pathway to represent the sequestration of parasites or trapping of parasites in the microvasculature, allowing subsequent return to the circulation significantly improving their final model. The problems encounter by Zaloumis *et al*. (399) hourly time step model are therefore likely to be the result of their assumptions regarding instantaneous drug effect and may have been improved by including a schizont efflux pathway.

2. General discussion

In the introduction to this thesis I outline the historical progression of mathematical models and summarise previous work utilising PK/PD models to investigate antimalarial drug treatment. In the discussion above, I extend this summary to include the recent developments of two pharmacological models. Despite the diverse range of mathematical models available, their potential as a tool for investigating drug action and their ability to predict the probable consequences of evolving drug resistance has yet to be realised. The primary purpose of this thesis was to develop pharmacological models of antimalarial drug treatment with particular consideration for modelling the

newest class of antimalarials, the artemisinins. I will now discuss the extent to which this work meets this aim, its subsequent inclusion in the OpenMalaria project, and its application to optimise clinical trial analysis.

In Chapter 2 we investigate how robust drug regimens are to small changes in parasite drug sensitivity or how vulnerable the regimens are to the evolution of resistance. These questions can only be answered retrospectively in the field and so we developed a pharmacological model of antimalarial drug treatment that was sufficiently compelling to address these questions *in silico*.

PK/PD models are the consensus method of modelling the effects of antimicrobial treatments (73), and track the change in parasite number in the body over time following treatment. We utilised these methods with three key extensions to the basic methodology for malaria. First, antimalarials typically include multiple doses and so the calculation of the drug concentration was adapted to reflect its dependence on the existing concentration of drug in the body augmented by the administration of new dosages. Second, it is now customary to deploy antimalarials as combination therapies to improve therapeutic efficacy and delay the development of drug resistance. As such, we extend the basic methodology to allow for the action of two drugs acting simultaneously on the parasite burden assuming they act independently of each other in the combination. Finally, we briefly incorporate acquired immunity using the data of Pongtavornpinyo *et al.* (262) to simulate clinical trials as a proof of principal.

The simulated cure rates, parasite clearance times and periods of chemoprophylaxis (i.e. the time until new infections are noted) for various antimalarial therapies were shown to closely match field observations. The model was first used to examine the relative importance of model parameters. We concluded the maximal parasite kill rate (V) of the partner drug consistently had the largest effect on treatment closely followed by the parasite growth rate (a) for most treatments. The analyses also show the slope factor of the concentration-effect curve (n) (for either drug in the combination) to be relatively unimportant to the ultimate outcome of treatment. As mentioned above, Zaloumis *et al*. (399) have since shown with their model that the value of V was equally important and n equally unimportant in the ultimate success or failure of a specific treatment regimen. The only unexpected result of our simulations

was the small apparent effect of the initial parasite number on treatment outcome. The implications behind the relative importance of model parameters and the possible reasons for this unexpected result are discussed within Chapter 2.

When the model was applied to "clinical trial" simulations we found good consistency with most features considered in clinical trials but show the predictive ability of day 7 serum levels was surprisingly poor. It is thought that low day 7 concentrations are associated with an increased risk of treatment failure and it has been suggested that measurement of day 7 serum levels becomes a routine part of clinical trials (362). This proposal has been widely accepted and promoted by several influential bodies including reference laboratories, WWARN and the WHO (23, 193, 385). While our analyses show that low drug levels on day 7 are associated with increased odds of failing treatment the predicative ability of serum levels, assessed as sensitivity, specificity and area under the ROC curve, was generally poor. This led us to recommend that clinical trials report the results of a ROC analysis alongside the typical odds ratio of treatment failure associated with low day 7 serum levels.

The model was finally used to investigate the implications of the increasing tolerance and possible resistance to artemisinins recently observed in the field (32, 241, 260, 282, 285, 384). The key question was whether there was likely to be a gradual decline in the protectiveness afforded to the partner drug or, whether we should expect a worst-case scenario in which there is a rapid decline in the protective effect. We concluded that the latter scenario was most likely and as such, support the assertions that measures are urgently need to prevent the evolution and spread of artemisinin resistance (50, 87, 377).

The work within Chapter 2 illustrates the value mathematical models provide when capable of generating results consistent with field data. While we do not suggest they will ever replace the vital knowledge gained from clinical trials, they do allow us to make predictions about the potential impact of different scenarios (in this case the consequences of increasing tolerance and possible resistance to artemisinins) and offer invaluable insights into areas that cannot be addressed either ethically or financially in the field. While the results of this modelling approach were a success, we do note it relied upon a number of necessary assumptions. These assumptions

were all biologically justifiable and included at the time to minimise the complexity of both the model methodology and calibration.

Treatment choice for uncomplicated malaria has recently shifted towards the use of combination therapies including two or more drugs, preferably the ACTs (380). However, the methodologies used in PK/PD models typically rely on the assumption that only one drug is used in treatment (three notable exceptions that model two drugs include (148, 364, 399)), that the drug is immediately available in its active form at the site of action and that the parent drug is not further converted to active metabolites. Given that antimalarial therapy now typically includes a short acting artemisinin drug, which is converted to a second active metabolite, and a longer lasting partner drug, these assumptions will potentially limit the future application of PK/PD models. In Chapter 3, we address these assumptions and develop the methodology in a number of specific directions allowing for (i) the time lags and the drug concentration profiles of drugs absorbed across the gut wall and, if necessary, converted to another active form (ii) multiple drugs within a treatment combination (iii) differing modes of action of drugs in combination (iv) modelling drugs converted to an active metabolite with similar modes of action. This refined and substantially extended model produced results consistent with field data and was subsequently used to investigate the public health implications of increasing drug tolerance and resistance for two first-line ACTs. Our results predict that as artemisinin resistance spreads there is likely to be a rapid decline in ACT effectiveness thus emphasising the importance of containing artemisinin resistance before it results in widespread drug failure.

Good quality, comprehensive PK/PD data in the literature is surprisingly scarce and so correctly calibrating the models has proven to be one of the most time-consuming and subjective steps in the modelling process. We note in Chapter 3 that previously published estimates of the artemisinin maximal parasite kill rates are likely to have underestimated the true value. Parasite killing by a drug is usually assumed to occur throughout the parasites 48-hour life cycle and while this seems reasonable for drugs with a long half-life it unlikely to be true for the artemisinins. Their short half-lives mean they are only present in the body and hence available to act upon parasites, for approximately 6-8 hours post-treatment. Allowing for this shortened period of activity

led us to estimate artemisinin kill rates approximately seven-fold higher than previously assumed. We found the generally poor reporting of PK/PD data severely limits it value for subsequent re-application and has the potential to reduce the predictive power of mathematical models. We end Chapter 3 by making three specific recommendations to improve this situation thus maximising the potential of costly clinical trials.

Our aim in Chapter 4 was to simulate clinical trial data as a resource for optimising clinical trial analysis. In 2003 WHO attempted to standardise protocol for the design and analysis of malaria clinical trials (368) however, in practice the analytical analysis and classification methods employed still vary (67). We identified four key questions/issues arising during analysis of field data (i) dealing with the data of patients who don't attend all follow-up appointments (ii) calculating drug effectiveness on a per clone basis (iii) the best use of genetic markers to distinguish new infections from reinfections (iv) the extent to which genotyping resolution/sensitivity affects results. It is impossible to investigate these issues in the field where the true results (in the absence of analytic bias) are unknown. Instead mathematical models capable of reproducing realistic clinical trial data provide ideal opportunities to assess the different methods of analysis given the true results are known. We simulated the clinical trial data using a modified version of the model described in Chapter 2 (364). Briefly, these modifications allow for the presence of multiple clones in the initial infection, the acquisition of new infections during follow up and molecular genotyping of infections. This work was done in collaboration with Alice Parry (masters and PhD student) from Lancaster University; she performed all the model analyses and made the decision to focus on only one of the research questions outlined above. The resulting paper by Jaki *et al.* (158) uses our simulated data to evaluate the capability of the different analysis methods used in malaria clinical trials and introduces the novel concept of evaluating drug effectiveness on a per clone basis. The paper concludes that of the currently available analysis methods, survival analysis provides the best estimation of drug effectiveness. The newly developed method to determine treatment effectiveness on a per clone basis is accurate and provides additional insights into treatment performance.

This thesis was funded by the BMGF as part of the Swiss TPH OpenMalaria project with the remit to develop a drug treatment model capable of investigating drug resistance. The project background, its current status and my contributions to the project are outlined in Chapter 5. Given the size and complexity of the OpenMalaria program, the drug treatment model was largely developed through the stand-alone models described in Chapter 2 and 3. These stand-alone models ran much faster and provided us with much more flexibility than would have been possible within OpenMalaria.

After establishing the methodology, we successfully incorporated the mathematics describing the antimalarial drug effects into the existing structure of OpenMalaria. It should be noted that to work within the boundaries of OpenMalaria addition model assumptions (not present in chapters 2 and 3) were required. These included a lack of heterogeneity in PK/PD parameters and hence the assumption that all parasites were fully sensitive to the antimalarial drugs. We recognise that while acceptable for the purposes of the models this does not reflect the situation in the field. To address this, variability in the PD parameters based upon the alleles present within an infection should be included however the time constraints of the thesis have prevented us from implementing this. It was also decided that there would be no variation in the weight of individuals of the same age within the model. This lack of age/weight distribution has the potential to limit the questions we can ask of the simulated data. For example, if all children follow the same growth curve we cannot adequately investigate the dosing bands of age-based dosing regimens. I discussed the possible inclusion of variable age/weight distributions using the region specific growth centile curves described in van Buuren *et al.* (344) with the modelling group. However it was ultimately decided by more senior members of the project that this added an unnecessary level of complexity to an already complex model. Despite the constraints imposed within OpenMalaria, the drug treatment model now has the potential to answer key questions about the effectiveness of antimalarial drug therapies.

Windows of selection (WoS) are important drivers of drug resistance and in Chapter 6 we aimed to discover how accurately field trials estimate the 'true' WoS. Drug resistance spreads through a population because (i) parasites can survive direct treatment and/or (ii) survive "residual" drug levels persisting from previous treatment.

This force of resistance can be quantified in field studies by estimating a window of selection (WoS) and is typically estimated by comparing how soon after treatment different genotypes become detectable. WoS estimates are widely cited and we refer to them as 'clinical' WoS to denote their origin in clinical observations. In fact the 'true' WoS is based upon the earliest emergence of different genotypes from the liver. Unfortunately, it is impossible to observe this emergence because parasites (assuming 10^5 emerge) are below the microscopic limit of detection (assumed to be 10^8) and so we are forced to rely on 'clinical' WoS i.e. the time at which they have grown to patency. To determine how accurately field observations estimate the 'true' WoS we applied the validated mechanistic pharmacokinetic-pharmacodynamic model describe in Chapters 2 and 3 to simulate the WoS for increasingly resistant infections.

The results showed that the estimates of WoS taken from clinical trials were a poor predictor of the 'true' WoS. The 'true' WoS was routinely over estimated by up to 12 or 9 days (15-fold IC50 increase, 10^{th} and 25^{th} centile respectively) following AR-LF treatment and up to 30 or 34 days following AS-MQ (15-fold IC50 increase, 10^{th} and 25^{th} centile respectively). Censoring the results to reflect the reduced follow-up period typical of clinical trials (i.e. 63 days) improved the predictive ability of the later emerging AS-MQ but had little effect on AR-LF. We also note the 'true' WoS were much shorter than would be expect *a priori*; 2 or 5 days for AR-LF and 4 or 11 days for AS-MQ (50-fold IC50 increase; 10^{th} and 25^{th} centile respectively). We conclude that previous studies, based on clinically obtained WoS, are likely to have greatly over-estimated the 'true' WoS and hence the impact of long drug half-lives in driving resistance.

3. Limitations

Any modelling approach has limitations; here I focus on three previously unmentioned limitations that appear to be most relevant.

3.1. Protein binding

Protein binding generally refers to the binding of a drug to proteins in the blood plasma. The level of protein binding is dependent on a drugs affinity for the plasma proteins and has the potential to influence drug efficacy. Only the unbound fraction of drug is responsible for its pharmacological effect and so the less bound a drug is, the larger its effect will be. When developing our models we used estimates of IC50 assuming they accounted for the level of protein binding. However some models, such as that of Zaloumis *et al*. (399) described above, use IC50 estimates measured *in vitro* (uncorrected for binding) and calculate the free (i.e. unbound) drug by multiplying by the unbound fraction in the *in vitro* testing media.

3.2. Modelling time steps

We developed the models described herein with the specific intention of incorporating the relevant drug killing methodologies into OpenMalaria. To aid this process we chose to develop our model using the one-day time steps required by the OpenMalaria. While these one day time steps were a logical choice for our model, it would be straightforward enough to either lengthen or shorten the time step length as necessary (for example, we use half-day time steps in the first seven days to allow 12 hourly dosing).

7.3. Impact of drugs on transmission

This work focuses on the ability of antimalarial drugs to cure the disease but we recognise that they also have the potential to affect transmission and understanding this affect would allow us to maximise the impact of available resources. To effectively reduce transmission antimalarials must target the sexual stage gametocytes within an infection but it is the asexual parasite stages that are responsible for the symptomatic disease, so antimalarials are primarily active against the latter forms. Antimalarial drugs with a gametocytocidal effect are limited to CQ (partial activity against immature gametocytes (41)), the artemisinins (highly active against immature gametocytes (63, 268, 327)), the ACTs (associated with lower rates of gametocyte

carriage (40, 251, 317)), methylene blue (broad activity against both mature and immature gametocytes (70)) and primaquine (effective against mature gametocytes (42, 63, 268, 298)). A comprehensive review of the epidemiology and infectivity of *P.falciparum* and *P.vivax* gametocytes, including a detailed summary of the current status of antimalarials with gametocytocidal effects is provided by Bousema & Drakeley (41). Some antimalarials, such as pyrimethamine and proguanil, are also able to affect transmission by killing developing ookinetes in the mosquito midgut when transferred to the mosquito during a blood meal (48). This activity is termed sporontocidal and while the drugs do not directly kill gametocytes their ultimate effects on transmission are analogous to the gametocytocidal drugs (48).

The announcement of the malaria elimination agenda (337) has renewed interest in antimalarials targeting gametocyte carriage, particularly primaquine. The WHO currently recommends the addition of a single dose of primaquine to treatment regimens for *P.falciparum* malaria in areas where transmission is low and where artemisinin resistance is a threat (380). The rationale being that its gametocytocidal activity has the potential to reduce the transmission (see for example, (41, 392)). However, these recommendations come with a caveat that states "when the risk for G6PD (glucose-6-phosphate dehydrogenase) deficiency is considered low or testing for deficiency is available". Unfortunately these safety concerns have limited the use of primaquine as a transmission blocker in Africa given the high frequency of the G6PD deficiency polymorphism in the population. The lack of evidence regarding primaquines ability to block transmission and whether it is ultimately safe for use in Africa, lead to a meeting of group experts March, 2012 (95). The primary outcome of the meeting was a suggested series of phase 1, 2, 3 and 4 studies designed to measure primaquines PK and PD and test the drugs efficacy both *ex vivo* and *in vivo*, particularly in high risk groups (95). This risk/benefit trade-off could be further informed by modelling the impact of drug use on transmission.

Modelling the gametocytocidal effect of antimalarials to investigate their affect on transmission was outside the remit of this thesis and while not a simple task we do note its inclusion in our model is entirely plausible. It would require us develop the model to (i) track the gametocyte population within an infection (rather than just the total number of parasites) (ii) to mathematically quantify a drugs gametocytocidal

activity (iii) to transform the number of gametocytes in the patient to a measure of host infectivity to mosquitoes. Modelling the stage-specific action of antimalarials is well documented (143, 145, 254, 285, 399) and would be straight forward to include in our current PK/PD model; we have avoided it thus far in the interest of simplicity. Possibly the most complex step involves determining a patient's infectivity to mosquitoes from the number of gametocytes in their infection. This has been done indirectly by Ross *et al.* (275) to specifically model host infectivity within OpenMalaria. The process of gametocytogenesis is poorly understood and to avoid incorporating it directly Ross *et al.* (275) estimate host infectivity using patient's asexual parasite density. When fitted to data from malaria patients they were able to reliably reproduce gametocyte densities in modelled patients and explain observed patterns of infectiousness in human hosts.

4. Future directions

The work conducted in this thesis has successfully developed the methodology of PK/PD models and highlighted just a few of the ways they can be utilised. I will now discuss how the modelling approach described herein has/will form the basis for further work.

Through out this thesis we have repeated called attention to the ability of PK/PD models to answer questions that are simply unethical to address in the field. Typical examples include the effects of poor patient compliance (e.g. delayed, reduced or missing doses) or administration of doses above or below recommended therapeutic dose ranges, particular in the most vulnerable groups such as infants and children. This concept formed the basis of a recent Medical Research Council (MRC) grant titled "Pharmacological modelling in decision support of antimalarial drug dosing regimens" (principal investigator Dr Ian Hastings and co-applicant Dr Dianne (Anja) Terlouw). One of the grants primary aims is to develop a model of antimalarial drug treatment that can be applied to optimise drug deployment strategies. It will focus specifically on the development of robust, effective drug dosing regimens based on age-, height- and weight-bands for programmatic use in children. van Buuren *et al.*

(344) recently developed regional weight-for-age reference curves using data from target populations in malaria endemic regions of Africa, Asia and Latin America and used them to predict optimal age-based dosing regimens for the ACTs (unpublished). This work will test those predictions by combining these weight-for-age distributions with our extended PK/PD model (168). To date, Eva Maria Stähli-Hodel (LSTM) has combined the models and used the simulated data to investigate extreme but plausible treatment scenarios (mainly of compliance) that would be ethically impossible to measure in the field (318) (Appendix).

In Chapter 4 we identified key questions / issues arising during clinical trials analysis and simulated clinical trial data using our modified PK/PD model to address them. This work was done in collaboration with statisticians from Lancaster University, they performed the statistical analysis of the simulated results and chose to focus was on one of four key issues identified (158). The results of our simulations now provide the basis for a further MRC grant application currently under review, titled "Improving the design and analysis of drug efficacy/effectiveness studies in malaria and in selected neglected tropical diseases (NTDs)" (principal investigator Ian Hastings (LSTM) with co-applicants Thomas Jaki (Lancaster University) and Russell Stothard (LSTM)) (decision due in July). The grant proposes to use data generated by our extended PK/PD model (described in Chapter 3) to improve analysis of malaria drug trials. I will update the model methodology described in Chapter 4 to allow for the absorption and conversion of the artemisinins (as described in Chapter 3) when treating patients with ACTs and simulate treatment outcome for large samples of patients (i.e. >10,000 patients). These data would initially be used to address the issue of clones undetected during molecular analysis, specifically (i) quantifying the bias and loss in accuracy in methods of analysis when clones are undetected (ii) developing efficient designs relating to data collection (iii) developing improved methodologies for analysis that accounts for the non-detecting of clones. The grant would then go on to use the simulated data to optimise the design and analysis of drug effectiveness studies and eventually extend these modelling techniques to drug studies in other tropical parasitic infections.

5. Concluding remarks

In this thesis I describe the development of a pharmacological model of antimalarial drug treatment. The methodology focuses specifically on two previously neglected areas, modelling combination therapies that include two or more drugs and modelling the newest class of antimalarials, the artemisinins. There is widespread concern about the increasing tolerance and possible resistance to the artemisinins currently observed in the field. We apply our model to investigate the potential implications of this and make verifiable predictions about the expected effect on treatment outcome if this trend continues. We further demonstrate the importance of mathematical models by simulating 'field data' with which we assess the best methods of measuring the period of chemoprophylaxis (i.e. time until new infection), determine the value of 'window of selection' estimates and optimise analysis of clinical trials.

The work draws attention to the distinct lack of comprehensive, good-quality PK/PD datasets in the literature. This, more than any of our model assumptions, has the greatest potential to limit the future applications of the model. We recognise that clinical trials require a huge investment of both time and money and so it seems prudent to maximise their potential to inform future work. We make suggestions to improve this situation and identify the key PK/PD data that can, and should, be measured and reported in future field studies. Despite the difficulties described above, our results and conclusions are clear. We have shown the detailed pharmacological models developed here can produce results consistent with field data. With them we can quantitatively predict the future effectiveness of antimalarial drug treatments focussing specifically on the likely impact of evolving drug resistance. Finally, we demonstrate how models can be used to investigate techniques currently used in the field.

Great progress has been made over the past century in the modelling of malaria and it is clear that to achieve the ambitious goal of malaria eradication the usefulness of mathematical models should not be overlooked. This is a sentiment shared by the recent malaria eradication research agenda (malERA) (336) and the roll back malaria program (384). To fully integrate mathematical models into future policy decisions

and research agendas will require substantial collaboration between the models end users (i.e. the health policy decision makers, program implementers, funding bodies and other researchers) and those developing and implementing the models.

Appendix

Co-authorship poster

MALARIA JOURNAL

POSTER PRESENTATION Open Access

An *in silico* drug treatment model to assess the robustness of regional age-based dosing regimens for artemisinin-based combination therapies

Eva Maria Staehli Hodel*, Katherine Kay, Daniel Hayes, Anja Terlouw, Ian Hastings

From Challenges in malaria research
Basel, Switzerland. 10-12 October 2012

The standard drug development process for antimalarials and other drugs uses weight-based dosing (mg/kg) to predict blood concentrations of the drug, and hence their effect. Consequently, the current World Health Organization *Guidelines for the treatment of malaria* [1] provide target doses and therapeutic dose ranges in mg/ kg/day. However, in resource-poor settings, age-based dosing is often employed instead of weight-based dosing because of the scarcity of correctly functioning weighing scales outside of clinical settings. Due to the wide variation in weight by age this approach inevitably results in over- and underdosing of a proportion of the population.

We have recently developed a modelling method to create statistically robust global and regional malaria-specific weight-for-age references representative of the malaria-endemic countries [2] and employed it to predict optimized age-based regimens for artemisinin-based combination therapies (ACTs) for case management of uncomplicated malaria (unpublished). The presented work now assesses the robustness of these age-based regimens using an *in silico* model of antimalarial drug treatment to predict treatment outcome based on individual infection parameters such as parasite numbers, variation in patient pharmacokinetics, and parasite variation in their drug sensitivity [3]. This extended pharmacokinetic/pharmakodynamic model for ACTs allowed us to investigate extreme treatment scenarios in a large number of patients over long follow-up periods that for ethical reasons could not be applied in clinical trials: typical examples include poor adherence (e.g. delayed, reduced or missed doses) or administration of doses above or below recommended therapeutic dose ranges and particularly in most vulnerable individuals such as infants and young children. Pharmacological modelling of antimalarial treatment cannot replace the gold standard of clinical trials, but the model outputs can identify patient groups that are at higher risk of treatment failure due to underdosing or adverse events due to over-dosing.

We acknowledge the Medical Research Council for funding of this work.

Published: 15 October 2012

References

1. World Health Organization: **Guidelines for the treatment of malaria.** Geneva;, 2 2010.
2. van Buuren S, Hayes DJ, Stasinopoulos DM, Rigby RA, ter Kuile FO, Terlouw DJ: **Estimating regional centile curves from mixed data sources and countries.** *Statistics in Medicine* 2009, **28**:2891-2911.
3. Winter K, Hastings IM: **Development, evaluation and application of an *in silico* model for antimalarial drug treatment and failure.** *Antimicrob Agents Chemother* 2011, **55**:3380-3392.

doi:10.1186/1475-2875-11-S1-P91
Cite this article as: Staehli Hodel *et al.*: An *in silico* drug treatment model to assess the robustness of regional age-based dosing regimens for artemisinin-based combination therapies. *Malaria Journal* 2012 **11**(Suppl 1):P91.

Liverpool School of Tropical Medicine, Liverpool, L3 5QA, UK

References

1. **Adjuik, M., A. Babiker, P. Garner, P. Olliaro, W. Taylor, and N. White.** 2004. Artesunate combinations for treatment of malaria: meta-analysis. Lancet **363:**9-17.
2. **Akl, E. A., M. Briel, J. J. You, F. Lamontagne, A. Gangji, T. Cukierman-Yaffe, M. Alshurafa, X. Sun, K. A. Nerenberg, B. C. Johnston, C. Vera, E. J. Mills, D. Bassler, A. Salazar, N. Bhatnagar, J. W. Busse, Z. Khalid, S. D. Walter, D. J. Cook, H. J. Schünemann, D. G. Altman, and G. H. Guyatt.** 2009. LOST to follow-up Information in Trials (LOST-IT): a protocol on the potential impact. Trials **10:**40.
3. **Al-Sallami, H. S., V. V. Pavan Kumar, C. B. Landersdorfer, J. B. Bulitta, and S. B. Duffull.** 2009. The time course of drug effects. Pharm Stat **8:**176-185.
4. **Ali, S., M. H. Najmi, J. Tarning, and N. Lindegardh.** 2010. Pharmacokinetics of artemether and dihydroartemisinin in healthy Pakistani male volunteers treated with artemether-lumefantrine. Malar J **9:**275.
5. **Alonso, P. L., G. Brown, M. Arevalo-Herrera, F. Binka, C. Chitnis, F. Collins, O. K. Doumbo, B. Greenwood, B. F. Hall, M. M. Levine, K. Mendis, R. D. Newman, C. V. Plowe, M. H. Rodríguez, R. Sinden, L. Slutsker, and M. Tanner.** 2011. A research agenda to underpin malaria eradication. PLoS Med **8:**e1000406.
6. **Anderson, R. M., R. M. May, and S. Gupta.** 1989. Non-linear phenomena in host-parasite interactions. Parasitology **99:**S59-S79.
7. **Anderson, Tim J. C., S. Nair, S. Nkhoma, Jeff T. Williams, M. Imwong, P. Yi, D. Socheat, D. Das, K. Chotivanich, Nicholas P. J. Day, Nicholas J. White, and Arjen M. Dondorp.** 2010. High Heritability of Malaria Parasite Clearance Rate Indicates a Genetic Basis for Artemisinin Resistance in Western Cambodia. J Infect Dis **201:**1326-1330.
8. **Anderson, T. J. C., S. Nair, H. Qin, S. Singlam, A. Brockman, L. Paiphun, and F. Nosten.** 2005. Are transporter genes other than the chloroquine resistance locus (*pfcrt*) and multidrug resistance gene (*pfmdr*) associated with antimalarial drug resistance? Antimicrob Agents Chemother **49:**2180-2188.

9. **Aneke, S. J.** 2002. Mathematical modelling of drug resistant malaria parasites and vector populations. Math Meth Appl Sci **25:**335-346.
10. **Antao, T., and I. M. Hastings.** 2010. Environmental, pharmacological and genetic influences on the spread of drug-resistant malaria. Proc R Soc B **278:**1705-1712.
11. **Antia, R., M. Nowak, and R. Anderson.** 1996. Antigenic variation and the within-host dynamics of parasites. Proc Natl Acad Sci USA **93:**985-989.
12. **Arnot, D. E.** 2002. The influence of the genetic complexity of Plasmodium falciparum infections on the epidemiology of malaria. Transactions of the Royal Society of Tropical Medicine and Hygiene **96:**131-136.
13. **Aron, J. L.** 1988. Mathematical modelling of immunity to malaria. . Math Biosci **90:**385-396.
14. **Aron, J. L., and R. M. May.** 1982. The population dynamics of malaria. In: Anderson RM, ed. The population dynamics of infectious disease: theory and applications. Chapman & Hall, London.
15. **Attaran, A.** 2004. Rescuing malaria treatment, or not? Lancet **364:**1922-1923.
16. **Austin, D., N. White, and R. Anderson.** 1998. The dynamics of drug action on the within-host population growth of infectious agents: melding pharmacokinetics with pathogen population dynamics. J Theor Biol **194:**313-339.
17. **Bacaer, N., and C. Sokhna.** 2005. A reaction-diffusion system modeling the spread of resistance to an antimalarial drug. Math Biosci Eng **2:**227-238.
18. **Bailey, N. T. J.** 1982. The biomathematics of malaria. Charles Griffin, London.
19. **Baird, J. K.** 2005. Effectiveness of antimalarial drugs. N Engl J Med **352:**1565-1577.
20. **Baird, J. K.** 2007. Neglect of *Plasmodium vivax* malaria. Trends Parasitol **23:**533-539.
21. **Baird, J. K.** 2008. Real-world therapies and the problem of Vivax malaria. N Engl J Med **359:**2601-2603.
22. **Barnes, K., W. Watkins, and N. White.** 2008. Antimalarial dosing regimens and drug resistance. Trends in Parasitology **24:**127-134.
23. **Barnes, K. I., N. Lindegardh, O. Ogundahunsi, P. Olliaro, C. V. Plowe, M. Randrianarivelojosia, G. O. Gbotosho, W. M. Watkins, C. H. Sibley,**

and N. J. White. 2007. World Antimalarial Resistance Network (WARN) IV: Clinical pharmacology. Malar J **6:**122.

24. **Barnes, K. I., and N. J. White.** 2005. Population biology and antimalarial resistance: The transmission of antimalarial drug resistance in *Plasmodium falciparum*. Acta Tropica **94:**230-240.
25. **Basco, L. K.** 2009. Field application of *in vitro* assays for the sensitivity of human malaria parasites to antimalarial drugs. World Health Organisation, Geneva**:**1-202.
26. **Basco, L. K., P. E. d. Pécoulas, C. M. Wilson, J. L. Bras, and A. Mazabraud.** 1995. Point mutations in the dihydrofolate reductase-thymidylate synthase gene and pyrimethamine and cycloguanil resistance in *Plasmodium falciparum*. Mol Biochem Parasitol **69:**135-138.
27. **Basco, L. K., and P. Ringwald.** 2003. *In vitro* activities of piperaquine and other 4-Aminoquinolines against clinical isolates of *Plasmodium falciparum* in Cameroon. Antimicrob Agents Chemother **47:**1391-1394.
28. **Basco, L. K., and P. Ringwald.** 2000. Molecular epidemiology of malaria in Yaounde, Cameroon. VI. Sequence variations in the *Plasmodium falciparum* dihydrofolate reductase-thymidylate synthase gene and *in vitro* resistance to pyrimethamine and cycloguanil. Am J Trop Med Hyg **62:**271-276.
29. **Basco, L. K., R. Tahar, and P. Ringwald.** 1998. Molecular basis of *in vivo* resistance to sulfadoxine-pyrimethamine in African adult patients infected with *Plasmodium falciparum* malaria parasites. Antimicrob Agents Chemother **42:**1811-1814.
30. **Baudon, D., G. Martet, B. Pascal, J. Bernard, A. Keundjian, and R. Laroche.** 1999. Efficacy of daily antimalarial chemoprophylaxis in tropical Africa using either doxycycline or chloroquine-proguanil; a study conducted in 1996 in the French Army. Trans R Soc Trop Med Hyg **93:**302-303.
31. **Beier, J. C., G. F. Killeen, and J. I. Githure.** 1999. Short report: entomologic inoculation rates and Plasmodium falciparum malaria prevalence in Africa. Am J Trop Med Hyg **61:**109-113.
32. **Berry, A., A. Senescau, J. Lelièvre, F. Benoit-Vical, R. Fabre, B. Marchou, and J. F. Magnaval.** 2006. Prevalence of *Plasmodium falciparum* cytochrome *b* gene mutations in isolates imported from Africa, and

implications for atovaquone resistance. Trans R Soc Trop Med Hyg **100:**986-988.

33. **Björkman, A., and P. A. Phillips-Howard.** 1990. The epidemiology of drug-resistant malaria. Trans R Soc Trop Med Hyg **84:**177-180.
34. **Bloland, P. B.** 2001. Drug resistance in malaria. World Health Organisation, Geneva**:**1-32.
35. **Bloland, P. B., and M. Ettling.** 1999. Making malaria-treatment policy in the face of drug resistance. Ann Trop Med Parasitol **93:**5-23.
36. **Boëte, C., and J. C. Koella.** 2002. A theoretical approach to predicting the success of genetic manipulation of malaria mosquitoes in malaria control. Malar J **1**.
37. **Borrmann, S., T. Peto, R. W. Snow, W. Gutteridge, and N. J. White.** 2008. Revisiting the design of phase III clinical trials of antimalarial drugs for uncomplicated *Plasmodium falciparum* malaria. PLoS Med **5:**e227.
38. **Borrmann, S., P. Sasi, L. Mwai, M. Bashraheil, A. Abdallah, S. Muriithi, H. Frühauf, B. Schaub, J. Pfeil, J. Peshu, W. Hanpithakpong, A. Rippert, E. Juma, B. Tsofa, M. Mosobo, B. Lowe, F. Osier, G. Fegan, N. Lindegårdh, A. Nzila, N. Peshu, M. Mackinnon, and K. Marsh.** 2011. Declining Responsiveness of Plasmodium falciparum Infections to Artemisinin-Based Combination Treatments on the Kenyan Coast. PLoS One **6:**e26005.
39. **Bosman, A.** 2010. Threat of oral artemisinin-based monotherapies, Artemisinin Conference, Antananarivo, Madagascar.
40. **Bousema, J. T., P. Schneider, L. C. Gouagna, C. J. Drakeley, A. Tostmann, R. Houben, J. I. Githure, R. Ord, C. J. Sutherland, S. A. Omar, and R. W. Sauerwein.** 2006. Moderate effect of artemisinin-based combination therapy on transmission of *Plasmodium falciparum*. J Infect Dis **193:**1151-1159.
41. **Bousema, T., and C. Drakeley.** 2011. Epidemiology and infectivity of *Plasmodium falciparum* and *Plasmodium vivax* gametocytes in relation to malaria control and elimination. Clin Microbiol Rev **24:**377-410.
42. **Bousema, T., L. Okell, S. Shekalaghe, J. T. Griffin, S. Omar, P. Sawa, C. Sutherland, R. Sauerwein, A. C. Ghani, and C. Drakeley.** 2010. Revisiting the circulation time of *Plasmodium falciparum* gametocytes: molecular

detection methods to estimate the duration of gametocyte carriage and the effect of gametocytocidal drugs. Malar J **9:**136.

43. **Brasseur, P., J. Kouamouo, R. S. Moyou, and P. Druilhe.** 1992. Mefloquine resistant malaria in Cameroon and correlation with resistance to quinine. Mem Inst Oswaldo Cruz **87:**271-273.

44. **Brockman, A., R. N. Price, M. Van Vugt, D. G. Heppner, D. Walsh, P. Sookto, T. Wimonwattrawatee, S. Looareesuwan, N. J. White, and F. Nosten.** 2000. *Plasmodium falciparum* antimalarial drug susceptibility on the north-western border of Thailand during five years of extensive use of artesunate-mefloquine. Trans R Soc Trop Med Hyg **94:**537-544.

45. **Bruce-Chwatt, L. J., R. H. Black, C. J. Canfield, D. F. Clyde, W. Peters, and W. H. Wernsdorfer.** 1986. Chemotherapy of malaria. Revised 2nd edition. World Health Organisation**:**1-26.

46. **Bukirwa, H., A. Yeka, M. R. Kamya, A. Talisuna, K. Banek, N. Bakyaita, J. B. Rwakimari, P. J. Rosenthal, F. Wabwire-Mangen, G. Dorsey, and S. G. Staedke.** 2006. Artemisinin Combination Therapies for Treatment of Uncomplicated Malaria in Uganda. PLoS Clinical Trials **1:**e7.

47. **Burki, T.** 2009. Artemisinin resistance could endanger fight against malaria. Lancet **9:**213.

48. **Butcher, G. A.** 1997. Antimalarial drugs and the mosquito transmission of Plasmodium. Int J Parasitol **27:**975-987.

49. **Byakika-Kibwika, P., M. Lamorde, V. Okaba-Kayom, H. Mayanja-Kizza, E. Katabira, W. Hanpithakpong, N. Pakker, T. P. C. Dorlo, J. Tarning, N. Lindegardh, P. J. de Vries, D. Back, S. Khoo, and C. Merry.** 2012. Lopinavir/ritonavir significantly influences pharmacokinetic exposure of artemether/lumefantrine in HIV-infected Ugandan adults. J Antimicrob Chemother.

50. **Campbell, C. C.** 2009. Malaria control--addressing challenges to ambitious goals. N Engl J Med **361:**522-523.

51. **Carneiro, I., L. Smith, A. Ross, A. Roca-Feltrer, B. Greenwood, J. A. Schellenberg, T. Smith, and D. Schellenberg.** 2010. Intermittent preventive treatment for malaria in infants: a decision-support tool for sub-Saharan Africa. Bull World Health Organ **88:**807-814.

52. **Carrara, V. I., J. Zwang, E. A. Ashley, R. N. Price, K. Stepniewska, M. Barends, A. Brockman, T. Anderson, R. McGready, L. Phaiphun, S. Proux, M. van Vugt, R. Hutagalung, K. M. Lwin, A. P. Phyo, P. Preechapornkul, M. Imwong, S. Pukrittayakamee, P. Singhasivanon, N. J. White, and F. Nosten.** 2009. Changes in the Treatment Responses to Artesunate-Mefloquine on the Northwestern Border of Thailand during 13 Years of Continuous Deployment. PLoS ONE **4:**e4551.

53. **Cattamanchi, A., D. Kyabayinze, A. Hubbard, P. J. Rosenthal, and G. Dorsey.** 2003. Distinguishing recrudescence from reinfection in a longitudinal antimalarial drug efficacy study: comparison of results based on genotyping of msp-1, msp-2, and glurp. The American Journal of Tropical Medicine and Hygiene **68:**133-139.

54. **Chavchich, M., L. Gerena, J. Peters, N. Chen, Q. Cheng, and D. E. Kyle.** 2010. Role of *pfmdr1* amplification and expression in induction of resistance to artemisinin derivatives in *Plasmodium falciparum*. Antimicrob Agents Chemother **54:**2455-2464.

55. **Checchi, F., P. Piola, C. Fogg, F. Bajunirwe, S. Biraro, F. Grandesso, E. Ruzagira, J. Babigumira, I. Kigozi, J. Kiguli, J. Kyomuhendo, L. Ferradini, W. R. J. Taylor, and J.-P. Guthmann.** 2006. Supervised versus unsupervised antimalarial treatment with six-dose artemether-lumefantrine: pharmacokinetic and dosage-related findings from a clinical trial in Uganda. Malar J **5:**1475-2875.

56. **Chen, L., F. Y. Qu, and Y. C. Zhou.** 1982. Field observations on the antimalarial piperaquine. Chin Med J (Engl) **95:**281-286.

57. **Chinh, N., N. Quang, N. Thanh, B. Dai, J. P. Geue, R. S. Addison, T. Travers, and M. D. Edstein.** 2009. Pharmacokinetics and bioequivalence evaluation of two fixed-dose tablet formulations of dihydroartemisinin and piperaquine in Vietnamese subjects. Antimicrob Agents **53:**828-831.

58. **Chitnis, N., J. M. Cushing, and J. M. Hyman.** 2006. Bifurcation analysis of a mathematical model for malaria transmission. SIAM J Appl Math **67:**24-45.

59. **Chitnis, N., D. Hardy, and T. Smith.** 2012. A Periodically-Forced Mathematical Model for the Seasonal Dynamics of Malaria in Mosquitoes. Bull Math Biol **74:**1098-1124.

60. **Chitnis, N., A. Schapira, T. Smith, and R. Steketee.** 2010. Comparing the effectiveness of malaria vector-control interventions through a mathematical model. Am J Trop Med Hyg **83:**230-240.

61. **Chitnis, N., T. Smith, and R. Steketee.** 2008. A mathematical model for the dynamics of malaria in mosquitoes feeding on a heterogeneous host population. J Biol Dyn **2:**259-285.

62. **Chiyaka, C., W. Garira, and S. Dube.** 2009. Effects of treatment and drug resistance on the transmission dynamics of malaria in endemic areas. Theor Popul Biol **75:**14-29.

63. **Chotivanich, K., J. Sattabongkot, R. Udomsangpetch, S. Looareesuwan, N. P. J. Day, R. E. Coleman, and N. J. White.** 2006. Transmission-blocking activities of quinine, primaquine, and artesunate. Antimicrob Agents Chemother **50:**1927-1930.

64. **Chou, T. C.** 2006. Theoretical Basis, Experimental Design, and Computerized Simulation of Synergism and Antagonism in Drug Combination Studies. Pharmacological Reviews **58:**621-681.

65. **Cissé, B., C. Sokhna, D. Boulanger, J. Milet, E. H. Bâ, K. Richardson, R. Hallett, C. Sutherland, K. Simondon, F. Simondon, N. Alexander, O. Gaye, G. Targett, J. Lines, B. Greenwood, and J.-F. Trape.** 2006. Seasonal intermittent preventive treatment with artesunate and sulfadoxine-pyrimethamine for prevention of malaria in Senegalese children: a randomised, placebo-controlled, double-blind trial. Lancet **367:**659-667.

66. **Clarke, S. E., M. C. H. Jukes, J. K. Njagi, L. Khasakhala, B. Cundill, J. Otido, C. Crudder, B. B. A. Estambale, and S. Brooker.** 2008. Effect of intermittent preventive treatment of malaria on health and education in schoolchildren: a cluster-randomised, double-blind, placebo-controlled trial. Lancet **372:**127-138.

67. **Collins, W. J., B. Greenhouse, P. J. Rosenthal, and G. Dorsey.** 2006. The use of genotyping in antimalarial clinical trials: a systematic review of published studies from 1995-2005. Malaria Journal **5:**122.

68. **Colussi, D., C. Parisot, F. Legay, and G. Lefèvre.** 1999. Binding of artemether and lumefantrine to plasma proteins and erythrocytes. Eur J Pharm Sci **9:**9-16.

69. **Cooper, R. A., C. L. Hartwig, and M. T. Ferdig.** 2005. *Pfcrt* is more than the *Plasmodium falciparum* chloroquine resistance gene: a functional and evolutionary perspective. Acta Trop **94:**170-180.

70. **Coulibaly, B., A. Zoungrana, F. P. Mockenhaupt, R. H. Schirmer, C. Klose, U. Mansmann, P. E. Meissner, and O. Müller.** 2009. Strong gametocytocidal effect of methylene blue-based combination therapy against falciparum malaria: A randomised controlled trial. PLoS One **4:**e5318.

71. **Crompton, P. D., S. K. Pierce, and L. H. Miller.** 2010. Advances and challenges in malaria vaccine development. J Clin Invest **120:**4168-4178.

72. **Curtis, C. F., and L. N. Otoo.** 1986. A simple model of the build-up of resistance to mixtures of anti-malarial drugs. Trans R Soc Trop Med Hyg **80:**889-892.

73. **Czock, D., and F. Keller.** 2007. Mechanism-based pharmacokinetic–pharmacodynamic modeling of antimicrobial drug effects. J Pharmacokinet Pharmacodyn **34:**727-751.

74. **Dahl, E. L., and P. J. Rosenthal.** 2007. Multiple antibiotics exert delayed effects against the *Plasmodium falciparum* apicoplast. Antimicrob Agents Chemother **51:**3485-3490.

75. **Daily, J. P.** 2006. Antimalarial Drug Therapy: The Role of Parasite Biology and Drug Resistance. J Clin Pharmacol **46:**1487-1497.

76. **Danquah, I., B. Coulibaly, P. Meissner, I. Petruschke, O. Müller, and F. P. Mockenhaupt.** 2010. Selection of *pfmdr1* and *pfcrt* alleles in amodiaquine treatment failure in north-western Burkina Faso. Acta Trop **114:**63-66.

77. **Delves, M., D. Plouffe, C. Scheurer, S. Meister, S. Wittlin, E. A. Winzeler, R. E. Sinden, and D. Leroy.** 2012. The Activities of Current Antimalarial Drugs on the Life Cycle Stages of Plasmodium: A Comparative Study with Human and Rodent Parasites. PLoS Med **9:**e1001169.

78. **Depinay, J.-M. O., C. M. Mbogo, G. Killeen, B. Knols, J. Beier, J. Carlson, J. Dushoff, P. Billingsley, H. Mwambi, J. Githure, A. M. Toure, and F. Ellis McKenzie.** 2004. A simulation model of African Anopheles ecology and population dynamics for the analysis of malaria transmission. Malaria Journal **3**.

79. **Dicko, A., I. Sagara, M. S. Sissoko, O. Guindo, A. I. Diallo, M. Kone, O. B. Toure, M. Sacko, and O. K. Doumbo.** 2008. Impact of intermittent

preventive treatment with sulphadoxine-pyrimethamine targeting the transmission season on the incidence of clinical malaria in children in Mali. Malar J **7:**123.

80. **Diebner, H. H., M. Eichner, L. Molineaux, W. E. Collins, G. M. Jeffery, and K. Dietz.** 2000. Modelling the transition of asexual blood stages of *Plasmodium falciparum* to gametocytes. J Theor Biol **202:**113-127.
81. **Dietz, K., L. Molineaux, and A. Thomas.** 1974. A malaria model tested in the African savannah. Bulletin of the World Health Organization **50:**347-357.
82. **DiMasi, J. A., R. W. Hansen, and H. G. Grabowski.** 2003. The price of innovation: new estimates of drug development costs. J Health Econ **22:**151-185.
83. **Djimdé, A., and G. Lefèvre.** 2009. Understanding the pharmacokinetics of Coartem®. Malar J **8:**S4.
84. **Doberstyn, E. B., A. P. Hall, K. Vetvutanapibul, and P. Sonkon.** 1976. Single-dose therapy of Falciparum malaria using pyrimethamine in combination with diformyldapsone or sulfadoxine. Am J Trop Med Hyg **25:**14-19.
85. **Dondorp, A. M., R. M. Fairhurst, L. Slutsker, J. R. Macarthur, J. G. Breman, P. J. Guerin, T. E. Wellems, P. Ringwald, R. D. Newman, and C. V. Plowe.** 2011. The threat of artemisinin-resistant malaria. N Engl J Med **365:**1073-1075.
86. **Dondorp, A. M., F. Nosten, P. Yi, D. Das, A. P. Phyo, J. Tarning, K. M. Lwin, F. Ariey, W. Hanpithakpong, S. J. Lee, P. Ringwald, K. Silamut, M. Imwong, K. Chotivanich, P. Lim, T. Herdman, S. S. An, S. Yeung, P. Singhasivanon, N. P. J. Day, N. Lindegardh, D. Socheat, and N. J. White.** 2009. Artemisinin resistance in *Plasmodium falciparum* malaria. N Engl J Med **361:**455-467.
87. **Dondorp, A. M., S. Yeung, L. White, C. Nguon, N. P. J. Day, D. Socheat, and L. von Seidlein.** 2010. Artemisinin resistance: current status and scenarios for containment. Nat Rev Microbiol **8:**272-280.
88. **Ducharme, J., and R. Farinotti.** 1996. Clinical pharmacokinetics and metabolism of chloroquine. Focus on recent advancements. Clin Pharmacokinet. **31:**257-274.

89. **Dye, C., and B. G. Williams.** 1997. Multigenic drug resistance among inbred malaria parasites. Proc R Soc Lond B **264:**61-67.

90. **Eastman, R. T., N. V. Dharia, E. A. Winzeler, and D. A. Fidock.** 2011. Piperaquine resistance is associated with a copy number variation on chromosome 5 in drug-pressured *Plasmodium falciparum* parasites. Antimicrob Agents Chemother **55:**3908-3916.

91. **Ecker, A., A. M. Lehane, J. Clain, and D. A. Fidock.** 2012. *Pfcrt* and its role in antimalarial drug resistance. Trends Parasitol **28:**504-514.

92. **Eichner, M., H. H. Diebner, L. Molineaux, W. E. Collins, G. M. Jeffery, and K. Dietz.** 2001. Genesis, sequestration and survival of *Plasmodium falciparum* gametocytes: parameter estimates from fitting a model to malaria therapy data. Trans R Soc Trop Med Hyg **95:**497-501.

93. **Ekland, E. H., and D. A. Fidock.** 2007. Advances in understanding the genetic basis of antimalarial drug resistance. Curr Opin Microbiol **10:**363-370.

94. **Enserink, M.** 2010. Malaria's drug miracle in danger. Science **328:**844-846.

95. **Eziefula, A. C., R. Gosling, J. Hwang, M. S. Hsiang, T. Bousema, L. V. Seidlein, C. Drakeley, and o. b. o. t. P. i. A. D. Group.** 2012. Rationale for short course primaquine in Africa to interrupt malaria transmission. Malar J **11:**360.

96. **Ezzet, F., R. Mull, and J. Karbwang.** 1998. Population pharmacokinetics and therapeutic response of CGP 56697 (artemether+ benflumetol) in malaria patients. Br J clin Pharmac **46:**553-561.

97. **Ezzet, F., M. V. Vugt, F. Nosten, S. Looareesuwan, and N. J. White.** 2000. Pharmacokinetics and pharmacodynamics of lumefantrine (benflumetol) in acute falciparum malaria. Antimicrob Agents **44:**697-704.

98. **Fan, B., W. Zhao, X. Ma, Z. Huang, Y. Wen, J. Yang, and Z. Yang.** 1998. *In vitro* sensitivity of *Plasmodium falciparum* to chloroquine, piperaquine, pyronaridine and artesunate in Yuxi prefecture of Yunnan province. Zhongguo Ji Sheng Chong Xue Yu Ji Sheng Chong Bing Za Zhi (Chinese journal of parasitology & parasitic diseases) **16:**460-462.

99. **Färnert, A., A. P. Arez, H. A. Babiker, H. P. Beck, A. Benito, A. Björkman, M. C. Bruce, D. J. Conway, K. P. Day, L. Henning, O. Mercereau-Puijalon, L. C. Ranford-Cartwright, G. S. J M Rubio, D. Walliker, J. Zwetyenga, and V. E. d. Rosario.** 2001. Genotyping of

Plasmodium falciparum infections by PCR: a comparative multicentre study. Trans R Soc Trop Med Hyg **95:**225-232.

100. **Färnert, A., G. Snounou, I. Rooth, and A. Bjorkman.** 1997. Daily dynamics of Plasmodium falciparum subpopulations in asymptomatic children in a holoendemic area. The American Journal of Tropical Medicine and Hygiene **56:**538-547.

101. **Faye, B., J. L. Ndiaye, R. Tine, K. Sylla, A. Gueye, A. C. Lo, and O. Gaye.** 2010. A Randomized Trial of Artesunate Mefloquine versus Artemether Lumefantrine for the Treatment of Uncomplicated Plasmodium falciparum Malaria in Senegalese Children. Am J Trop Med Hyg **82:**140-144.

102. **Fenner, F., D. A. Henderson, I. Arita, Z. Ježek, and I. D. Ladnyi.** 1988. Smallpox and its eradication. WHO, Geneva**:**1-4.

103. **Fidock, D. A., T. Nomura, A. K. Talley, R. A. Cooper, S. M. Dzekunov, M. T. Ferdig, L. M. Ursos, A. B. Sidhu, B. Naudé, K. W. Deitsch, X. Z. Su, J. C. Wootton, P. D. Roepe, and T. E. Wellems.** 2000. Mutations in the *P. falciparum* digestive vacuole transmembrane protein PfCRT and evidence for their role in chloroquine resistance. Mol Cell **6:**861-871.

104. **Fidock, D. A., T. Nomura, and T. E. Wellems.** 1998. Cycloguanil and its parent compound proguanil demonstrate distinct activities against Plasmodium falciparum malaria parasites transformed with human dihydrofolate reductase. Mol Pharmacol **54:**1140-1147.

105. **Filipe, J. A. N., E. M. Riley, C. J. Drakeley, C. J. Sutherland, and A. C. Ghani.** 2007. Determination of the processes driving the acquisition of immunity to malaria using a mathematical transmission model. PLoS Comput Biol **3:**2569-2579.

106. **Foote, S. J., D. Galatis, and A. F. Cowman.** 1990. Amino acids in the dihydrofolate reductase-thymidylate synthase gene of Plasmodium falciparum involved in cycloguanil resistance differ from those involved in pyrimethamine resistance. Proc Natl Acad Sci USA **87:**3014-3017.

107. **Gatton, M. L., and Q. Cheng.** 2008. Can estimates of antimalarial efficacy from field studies be improved? Trends Parasitol **24:**68-73.

108. **Gatton, M. L., and Q. Cheng.** 2004. Modeling the Development of Acquired Clinical Immunity to Plasmodium falciparum Malaria. Infect Immun **72:**6538-6545.

109. **Gatton, M. L., L. B. Martin, and Q. Cheng.** 2004. Evolution of Resistance to Sulfadoxine-Pyrimethamine in Plasmodium falciparum. Antimicrob Agents **48:**2116-2123.

110. **Giao, P., and P. d. Vries.** 2001. Pharmacokinetic interactions of antimalarial agents. Clin Pharmacokinet **40:**343-373.

111. **Goldin, A., and N. Mantel.** 1957. The employment of combinations of drugs in the chemotherapy of neoplasia. Cancer Res **17:**635-654.

112. **Gordi, T., R. Xie, and W. J. Jusko.** 2005. Semi-mechanistic pharmacokinetic/pharmacodynamic modelling of the antimalarial effect of artemisinin. Br J Clin Pharmacol **60:**594-604.

113. **Gosoniu, L., P. Vounatsou, N. Sogoba, and T. Smith.** 2006. Bayesian modelling of geostatistical malaria risk data. Geosat Health **1:**127-139.

114. **Grande, T., A. Bernasconi, A. Erhart, D. Gamboa, M. Casapia, C. Delgado, K. Torres, C. Fanello, A. Llanos-Cuentas, and U. D'Alessandro.** 2007. A randomised controlled trial to assess the efficacy of dihydroartemisinin-piperaquine for the treatment of uncomplicated falciparum malaria in Peru. PLoS ONE **2**.

115. **Greco, W. R., H. S. Park, and Y. M. Rustum.** 1990. Application of a new approach for the quantitation of drug synergism to the combination of cis-diamminedichloroplatinum and 1-beta-D-arabinofuranosylcytosine. Cancer Res **50:**5318-5327.

116. **Greenhouse, B., C. Dokomajilar, A. Hubbard, P. J. Rosenthal, and G. Dorsey.** 2007. Impact of Transmission Intensity on the Accuracy of Genotyping To Distinguish Recrudescence from New Infection in Antimalarial Clinical Trials. Antimicrob Agents **51:**3096-3103.

117. **Greenwood, B.** 2002. The molecular epidemiology of malaria. Trop Med Int Health **7:**1012-1021.

118. **Greenwood, B. M., D. A. Fidock, D. E. Kyle, S. H. I. Kappe, P. L. Alonso, F. H. Collins, and P. E. Duffy.** 2008. Malaria: progress, perils, and prospects for eradication. J Clin Invest **118:**1266-1276.

119. **Gu, W., and R. J. Novak.** 2005. Habitat-based modeling of impacts of mosquito larval interventions on entomological inoculation rates, incidence, and prevalence of malaria. Am J Trop Med Hyg **73:**546-552.

120. **Gupta, S., and K. P. Day.** 1994. A theoretical framework for the immunoepidemiology of *Plasmodium falciparum* malaria. Parasitol Immunol **16:**361-370.

121. **Gupta, S., A. V. Hill, D. Kwiatkowski, A. M. Greenwood, B. M. Greenwood, and K. P. Day.** 1994. Parasite virulence and disease patterns in *Plasmodium falciparum* malaria. Proc Natl Acad Sci USA **91:**3715-3719.

122. **Gupta, S., and A. V. S. Hill.** 1995. Dynamic interactions in malaria: Host heterogeneity meets parasite polymorphism. Proc R Soc Lond B **261:**271-277.

123. **Gupta, S., K. Trenholme, R. M. Anderson, and K. P. Day.** 1994. Antigenic diversity and the transmission dynamics of *Plasmodium falciparum*. Science **263:**961-963.

124. **Harinasuta, T., P. Suntharasamai, and C. Viravan.** 1965. Chloroquine-resistant falciparum malaria in Thailand. Lancet **2:**657-660.

125. **Harrington, W. E., T. K. Mutabingwa, A. Muehlenbachs, B. Sorensen, M. C. Bolla, M. Fried, and P. E. Duffy.** 2009. Competitive facilitation of drug-resistant Plasmodium falciparum malaria parasites in pregnant women who receive preventive treatment. Proceedings of the National Academy of Sciences **106:**9027-9032.

126. **Hastings, I.** 2011. How artemisinin-containing combination therapies slow the spread of antimalarial drug resistance. Trends Parasitol **27:**67-72.

127. **Hastings, I., and M. Donnelly.** 2005. The impact of antimalarial drug resistance mutations on parasite fitness, and its implications for the evolution of resistance. Drug Resist Updat **8:**43-50.

128. **Hastings, I. M.** 1997. A model for the origins and spread of drug-resistant malaria. Parasitology **115:**133-141.

129. **Hastings, I. M., C. Nsanzabana, and T. A. Smith.** 2010. A comparison of methods to detect and quantify the markers of antimalarial drug resistance Am J Trop Med Hyg. **83:**489-495.

130. **Hastings, I. M., and S. A. Ward.** 2005. Coartem (artemether-lumefantrine) in Africa: the beginning of the end? J Infect Dis **192:**1303-1304.

131. **Hastings, I. M., and W. M. Watkins.** 2005. Intensity of malaria transmission and the evolution of drug resistance. Acta Trop **94:**218-229.

132. **Hastings, I. M., and W. M. Watkins.** 2006. Tolerance is the key to understanding antimalarial drug resistance. Trends Parasitol **22:**71-77.

133. **Hastings, I. M., W. M. Watkins, and N. J. White.** 2002. The evolution of drug-resistant malaria: the role of drug elimination half-life. Philos Trans R Soc B: Biol Sci. **357:**505-519.

134. **Hay, S. I., C. A. Guerra, P. W. Gething, A. P. Patil, A. J. Tatem, A. M. Noor, C. W. Kabaria, B. H. Manh, I. R. F. Elyazar, S. Brooker, D. L. Smith, R. A. Moyeed, and R. W. Snow.** 2009. A world malaria map: *Plasmodium falciparum* endemicity in 2007. PLoS Med **6:**e48.

135. **Hay, S. I., E. A. Okiro, P. W. Gething, A. P. Patil, A. J. Tatem, C. A. Guerra, and R. W. Snow.** 2010. Estimating the global clinical burden of *Plasmodium falciparum* malaria in 2007. PLoS Med **7:**e1000290.

136. **Hayes, D. J.** 2011. Developing age-based dosing regimens for antimalarials. University of Liverpool, Liverpool.

137. **Hayward, R., K. J. Saliba, and K. Kirk.** 2005. *pfmdr1* mutations associated with chloroquine resistance incur a fitness cost in *Plasmodium falciparum*. Mol Microbiol **55:**1285-1295.

138. **Hellgren, U., I. Johansson, F. Dias, Ö. Eriksson, J. Stenbeck, and L. Rombo.** 1991. Chloroquine resistant Plasmodium falciparum malaria in Guinea-Bissau. Trans R Soc Trop Med Hyg **85:**1-36.

139. **Hien, T. T., T. M. E. Davis, L. V. Chuong, K. F. Ilett, D. X. T. Sinh, N. H. Phu, C. Agus, G. M. Chiswell, N. J. White, and J. Farrar.** 2004. Comparative Pharmacokinetics of Intramuscular Artesunate and Artemether in Patients with Severe Falciparum Malaria. Antimicrob Agents Chemother **48:**4234-4239.

140. **Hietala, S. F., A. Martensson, B. Ngasala, S. Dahlstrom, N. Lindegardh, A. Annerberg, Z. Premji, A. Färnert, P. Gil, A. Bjorkman, and M. Ashton.** 2010. Population Pharmacokinetics and Pharmacodynamics of Artemether and Lumefantrine during Combination Treatment in Children with Uncomplicated Falciparum Malaria in Tanzania. Antimicrob Agents Chemother **54:**4780-4788.

141. **Hodel, Eva M., B. Genton, B. Zanolari, T. Mercier, S. Duong, H. P. Beck, P. Olliaro, Laurent A. Decosterd, and F. Ariey.** 2010. Residual antimalarial concentrations before treatment in patients with malaria from Cambodia: Indication of drug pressure. J Infect Dis **202:**1088-1094.

142. **Hodel, E. M., A. M. Kabanywanyi, A. Malila, B. Zanolari, T. Mercier, H.-P. Beck, T. Buclin, P. Olliaro, L. A. Decosterd, and B. Genton.** 2009. Residual antimalarials in malaria patients from Tanzania – Implications on drug efficacy assessment and spread of parasite resistance. PLoS One **4:**e8184.

143. **Hoshen, M., K. Na-Bangchang, W. Stein, and H. Ginsburg.** 2000. Mathematical modelling of the chemotherapy of Plasmodium falciparum malaria with artesunate: postulation of 'dormancy', a partial cytostatic effect of the drug, and its implication for treatment regimens. Parasitology **121:**237-246.

144. **Hoshen, M., W. Stein, and H. Ginsburg.** 1998. Modelling the chloroquine chemotherapy of falciparum malaria: the value of spacing a split dose. Parasitology **116:**407-416.

145. **Hoshen, M. B., R. Heinrich, W. D. Stein, and H. Ginsburg.** 2000. Mathematical modelling of the within-host dynamics of *Plasmodium falciparum*. Parasitology **121:**227-235.

146. **Hoshen, M. B., and A. P. Morse.** 2004. A weather-driven model of malaria transmission. Malaria Journal **3**.

147. **Hoshen, M. B., K. Na-Bangchang, W. D. Stein, and H. Ginsburg.** 2000. Mathematical modelling of the chemotherapy of Plasmodium falciparum malaria with artesunate: postulation of 'dormancy', a partial cytostatic effect of the drug, and its implication for treatment regimens. Parasitology **121:**237-246.

148. **Hoshen, M. B., W. D. Stein, and H. Ginsburg.** 2002. Mathematical modelling of malaria chemotherapy: combining artesunate and mefloquine. Parasitology **124:**9-15.

149. **Hoshen, M. B., W. D. Stein, and H. D. Ginsburg.** 2001. Pharmacokinetic-pharmacodynamic modelling of the anti-malarial activity of mefloquine. Parasitology **123:**337-346.

150. **Huang, F., L. Tang, H. Yang, S. Zhou, X. Sun, and H. Liu.** 2012. Therapeutic efficacy of artesunate in the treatment of uncomplicated Plasmodium falciparum malaria and anti-malarial, drug-resistance marker polymorphisms in populations near the China- Myanmar border. Malar J **11:**278.

151. **Hung, T., T. Davis, K. Ilett, H. Karunajeewa, S. Hewitt, M. Denis, C. Lim, and D. Socheat.** 2004. Population pharmacokinetics of piperaquine in adults and children with uncomplicated falciparum or vivax malaria. Br J Clin Pharmacol **57:**253-262.

152. **Huong, N. M., S. Hewitt, T. M. Davis, L. D. Dao, T. Q. Toan, T. B. Kim, N. T. Hanh, V. N. Phuong, D. H. Nhan, and L. D. Cong.** 2001. Resistance of *Plasmodium falciparum* to antimalarial drugs in a highly endemic area of southern Viet Nam: a study *in vivo* and *in vitro*. Trans R Soc Trop Med Hyg **95:**329-329.

153. **Hurwitz, E. S., D. Johnson, and C. C. Campbell.** 1981. Resistance of *Plasmodium falciparum* malaria to sulfadoxine-pyrimethamine ('Fansidar') in a refugee camp in Thailand. Lancet **1:**1068-1070.

154. **Hyde, J.** 2005. Drug-resistant malaria. Trends Parasitol **21:**494-498.

155. **Hyde, J. E.** 1990. The dihydrofolate reductase-thymidylate synthetase gene in the drug resistance of malaria parasites. Pharmac. Ther **48:**45-49.

156. **Hyde, J. E.** 2007. Drug-resistant malaria − an insight. FEBS Journal **274:**4688-4698.

157. **Iyer, J. K., W. K. Milhous, J. F. Cortese, J. G. Kublin, and C. V. Plowe.** 2001. *Plasmodium falciparum* cross-resistance between trimethoprim and pyrimethamine. Lancet **358:**1066-1067.

158. **Jaki, T., A. Parry, K. Winter, and I. Hastings.** 2012. Analysing malaria drug trials on a per-individual or per-clone basis: a comparison of methods. Stat Med**:**doi: 10.1002/sim.5706.

159. **Jamsen, K. M., S. B. Duffull, J. Tarning, N. Lindegardh, N. J. White, and J. A. Simpson.** 2011. Optimal designs for population pharmacokinetic studies of oral artesunate in patients with uncomplicated falciparum malaria. Malar J **10:**181.

160. **Jelinek, T., M. P. Grobusch, and T. Löscher.** 2001. Patterns of *Plasmodium falciparum* drug resistance in nonimmune travellers to Africa. Eur J Clin Microbiol Infect Dis **20:**284-286.

161. **Juliano, Jonathan J., F. Ariey, R. Sem, N. Tangpukdee, S. Krudsood, C. Olson, S. Looareesuwan, William O. Rogers, C. Wongsrichanalai, and Steven R. Meshnick.** 2009. Misclassification of drug failure in *Plasmodium falciparum* clinical trials in Southeast Asia. J Infect Dis **200:**624-628.

162. **Juliano, J. J., N. Gadalla, C. J. Sutherland, and S. R. Meshnick.** 2010. The perils of PCR: can we accurately 'correct' antimalarial trials? Trends Parasitol **26:**119-124.

163. **Kamya, M., A. Yeka, and H. Bukirwa.** 2007. Artemether-lumefantrine versus dihydroartemisinin-piperaquine for treatment of malaria: a randomized trial. PLoS Clin Trials **2:**1-9.

164. **Kamya, M. R., N. N. Bakyaita, A. O. Talisuna, W. M. Were, and S. G. Staedke.** 2002. Increasing antimalarial drug resistance in Uganda and revision of the national drug policy. Trop Med Int Health **7:**1031-1041.

165. **Karbwang, J., K. N. Bangchang, A. Thanavibul, D. J. Back, D. Bunnag, and T. Harinasuta.** 1994. Pharmacokinetics of mefloquine alone or in combination with artesunate. Bulletin of the World Health Organization **72:**83-87.

166. **Karunajeewa, H. A., K. F. Ilett, K. Dufall, A. Kemiki, M. Bockarie, M. P. Alpers, P. H. Barrett, P. Vicini, and T. M. E. Davis.** 2004. Disposition of Artesunate and Dihydroartemisinin after Administration of Artesunate Suppositories in Children from Papua New Guinea with Uncomplicated Malaria. Antimicrob Agents Chemother **48:**2966-2972.

167. **Karunajeewa, H. A., I. Mueller, M. Senn, E. Lin, I. Law, P. S. Gomorrai, O. Oa, S. Griffin, K. Kotab, P. Suano, N. Tarongka, A. Ura, D. Lautu, M. Page-Sharp, R. Wong, S. Salman, P. Siba, K. F. Llett, and T. M. E. Davis.** 2008. A trial of combination antimalarial therapies in children from Papua New Guinea. N Engl J Med **359:**2545-2457.

168. **Kay, K., and I. M. Hastings.** 2013. Predicting the impact of artemisinin resistance on antimalarial drug effectiveness. PLoS Comput Biol **9:**e1003151.

169. **Killeen, G. F., J. Kihonda, E. Lyimo, F. R. Oketch, M. E. Kotas, E. Mathenge, J. A. Schellenberg, C. Lengeler, T. A. Smith, and C. J. Drakeley.** 2006. Quantifying behavioural interactions between humans and mosquitoes: Evaluating the protective efficacy of insecticidal nets against malaria transmission in rural Tanzania. BMC Infect Dis **6**.

170. **Killeen, G. F., and T. A. Smith.** 2007. Exploring the contributions of bed nets, cattle, insecticides and excitorepellency to malaria control: a deterministic model of mosquito host-seeking behaviour and mortality. Trans R Soc Trop Med Hyg **101:**867-880.

171. **Kitchen, S. F.** 1949. Falciparum malaria. In M. F. Boyd (ed). Malariology., p. 966-1045. The W. B. Saunders Co., Philidelphia, Pa.

172. **Kitchen, S. F.** 1941. The infection in the intermediate host: symptomatology, falciparum malaria.⁋ American Association for the Advancement of Science **15:**196-207.

173. **Kleinschmidt, I., M. Bagayoko, G. P. Clarke, M. Craig, and D. L. Sueur.** 2000. A spatial statistical approach to malaria mapping. Int J Epidemiol **29:**355-361.

174. **Koella, J., and R. Antia.** 2003. Epidemiological models for the spread of antimalarial resistance. Malar J **2:**1-11.

175. **Koepfli, C., S. Schoepflin, M. Bretscher, E. Lin, B. Kiniboro, P. A. Zimmerman, P. Siba, T. A. Smith, I. Mueller, and I. Felger.** 2011. How Much Remains Undetected? Probability of Molecular Detection of Human Plasmodia in the Field. PLoS One **6:**e19010.

176. **Kofoed, P., F. Lopez, and P. Johansson.** 2002. Treatment of children with Plasmodium falciparum malaria with chloroquine in Guinea-Bissau. Am J Trop Med Hyg **67:**28-31.

177. **Korsinczky, M., N. Chen, B. Kotecka, A. Saul, K. Rieckmann, and Q. Cheng.** 2000. Mutations in *Plasmodium falciparum* cytochrome *b* that are associated with atovaquone resistance are located at a putative drug-binding site. Antimicrob Agents Chemother **44:**2100-2108.

178. **Krishna, S., and N. White.** 1996. Pharmacokinetics of quinine, chloroquine and amodiaquine: clinical implications. Clin Pharmacokinet **30:**263-299.

179. **Kweku, M., D. Liu, M. Adjuik, F. Binka, M. Seidu, B. Greenwood, and D. Chandramohan.** 2008. Seasonal Intermittent Preventive Treatment for the Prevention of Anaemia and Malaria in Ghanaian Children: A Randomized, Placebo Controlled Trial. PLoS One **3:**e4000.

180. **Kwiatkowski, D., and M. Nowak.** 1991. Periodic and chaotic host-parasite interactios in human malaria. Proc Natl Acad Sci U S A **88:**5111-5113.

181. **Kyabayinze, D. J., C. Karamagi, M. Kiggundu, M. R. Kamya, F. Wabwire-Mangen, F. Kironde, and A. Talisuna.** 2008. Multiplicity of Plasmodium falciparum infection predicts antimalarial treatment outcome in Ugandan Children. Afr Health Sci **8:**200-205.

182. **Kyle, D., and H. K. Webster.** 1996. Post-antibiotic effect of quinine and dihydroartemisinin on Plasmodium falciparum in vitro: implication for a mechanism of recrudescence. Abstract XIV International Congress for Tropical Medicine and Malaria.

183. **Langhorne, J., F. M. Ndungu, A.-M. Sponaas, and K. Marsh.** 2008. Immunity to malaria: more questions than answers. Nat Immunol **9:**725-732.

184. **Laufer, M. K., P. C. Thesing, N. D. Eddington, R. Masonga, F. K. Dzinjalamala, S. K. Takala, T. E. Taylor, and C. V. Plowe.** 2006. Return of chloroquine efficacy in Malawi. N Engl J Med **355:**1959-1966.

185. **Lawpoolsri, S., E. Y. Klein, P. Singhasivanon, S. Yimsamran, N. Thanyavanich, W. Maneeboonyang, L. L. Hungerford, J. H. Maguire, and D. L. Smith.** 2009. Optimally timing primaquine treatment to reduce *Plasmodium falciparum* transmission in low endemicity Thai-Myanmar border populations. Malar J **8**.

186. **Le Menach, A., S. Takala, F. E. McKenzie, A. Perisse, A. Harris, A. Flahault, and D. L. Smith.** 2007. An elaborated feeding cycle model for reductions in vectorial capacity of night-biting mosquitoes by insecticide-treated nets. Malar J **6**.

187. **Leslie, T., A. Mikhail, I. Mayan, M. Anwar, S. Bakhtash, M. Nader, C. Chandler, C. J. M. Whitty, and M. Rowland.** 2012. Overdiagnosis and mistreatment of malaria among febrile patients at primary healthcare level in Afghanistan: observational study. BMJ **345:**e4389-e4389.

188. **Li, J.** 2004. Simple mathematical models for interacting wild and transgenic mosquito populations. Math Biosci **189:**39-59.

189. **Lin, E., B. Kiniboro, L. Gray, S. Dobbie, L. Robinson, A. Laumaea, S. Schöpflin, D. Stanisic, I. Betuela, M. Blood-Zikursh, P. Siba, I. Felger, L. Schofield, P. Zimmerman, and I. Mueller.** 2010. Differential patterns of infection and disease with *P. falciparum* and *P. vivax* in young Papua New Guinean children. PLoS One **5:**e9047.

190. **Liu, D. Q., R. J. Liu, D. X. Ren, D. Q. Gao, C. Y. Zhang, C. P. Qui, X. Z. Cai, C. F. Ling, A. H. Song, and X. Tang.** 1995. Changes in the resistance of *Plasmodium falciparum* to chloroquine in Hainan, China. Bull World Health Organ **73:**483-486.

191. **Lotka, A. J.** 1923. Contributions to the analysis of malaria epidemiology. Am. J. Trop. Med. Hyg. **3 (Suppl.1):**1-121.

192. **Lou, Y., and X.-Q. Zhao.** 2010. A Climate-Based Malaria Transmission Model with Structured Vector Population. SIAM J Appl Math **70:**2023-2044.

193. **Lourens, C., W. M. Watkins, K. I. Barnes, C. H. Sibley, P. J. Guerin, N. J. White, and N. Lindegardh.** 2010. Implementation of a reference standard and proficiency testing programme by the World Wide Antimalarial Resistance Network (WWARN). Malar J **9:**375.

194. **Luxemburger, C., F. Nosten, D. E. Kyle, L. Kiricharoen, T. Chongsuphajaisiddhi, and N. J. White.** 1998. Clinical features cannot predict a diagnosis of malaria or differentiate the infecting species in children living in an area of low transmission. Trans R Soc Trop Med Hyg **92:**45-49.

195. **Macdonald, G.** 1950. The analysis of infection rates in diseases in which superinfection occurs. Trop Dis Bull **47:**907-915.

196. **Macdonald, G.** 1950. The analysis of malaria parasite rates in infants. Trop Dis Bull **47:**915-938.

197. **Macdonald, G.** 1952. The analysis of sporozoite rate. Trop Dis Bull **49:**569-586.

198. **Macdonald, G.** 1968. The dynamics of malaria Bulletin of the World Health Organization **38:**743-755.

199. **Macdonald, G.** 1956. Epidemiological basis of malaria control. Bulletin of the World Health Organization **15:**613-626.

200. **Macdonald, G.** 1955. The measurement of malaria transmission. Proc R Soc Med **48:**295-302.

201. **Macdonald, G., and G. W. Göeckel.** 1964. The malaria parasite rate and interuption of transmission. Bulletin of the World Health Organization **31:**365-377.

202. **Macete, E., P. Aide, J. J. Aponte, S. Sanz, I. Mandomando, M. Espasa, B. Sigauque, C. Dobaño, S. Mabunda, M. DgeDge, P. Alonso, and C. Menendez.** 2006. Intermittent preventive treatment for malaria control administered at the time of routine vaccinations in Mozambican infants: a randomized, placebo-controlled trial. J Infect Dis **194:**276-285.

203. **Maire, N., S. D. Shillcutt, D. G. Walker, F. Tediosi, and T. A. Smith.** 2011. Cost-effectiveness of the introduction of a pre-erythrocytic malaria vaccine

into the expanded program on immunization in Sub-Saharan Africa: Analysis of uncertainties using a stochastic individual-based simulation model of *Plasmodium falciparum* malaria. Value Health **14:**1028-1038.

204. **Maire, N., T. Smith, A. Ross, S. Owusu-Agyei, K. Dietz, and L. Molineaux.** 2006. A model for natural immunity to asexual blood stages of Plasmodium falciparum malaria in endemic areas. Am. J. Trop. Med. Hyg. **75 (Suppl 2):**19-31.

205. **malERA Consultative Group on Vaccines.** 2011. A research agenda for malaria eradication: vaccines. PLoS Med **8:**e1000398.

206. **Mandal, S., R. Sarkar, and S. Sinha.** 2011. Mathematical models of malaria - a review. Malar J **10**.

207. **Maude, R. J., Y. Lubell, D. Socheat, S. Yeung, S. Saralamba, W. Pongtavornpinyo, B. S. Cooper, A. M. Dondorp, N. J. White, and L. J. White.** 2010. The role of mathematical modelling in guiding the science and economics of malaria elimination. Int Health **2:**239-246.

208. **Maude, R. J., C. J. Woodrow, and L. J. White.** 2010. Artemisinin antimalarials: preserving the magic bullet. Drug Dev Res **71:**12-19.

209. **Mayersohn, M., and M. Gibaldi.** 1970. Mathematical methods in pharmacokinetics. Use of the laplace transformation for solving differential equations. Amer. J. Pharm. Ed **34:**608-614.

210. **Mayxay, M., M. Barends, A. Brockman, A. Jaidee, S. Nair, D. Sudimack, T. Pongvongsa, S. Phompida, R. Phetsouvanh, and T. Anderson.** 2007. In vitro antimalarial drug susceptibility and pfcrt mutation among fresh Plasmodium falciparum isolates from the Lao PDR (Laos). Am J Trop Med Hyg **76:**245-250.

211. **Mayxay, M., M. Barends, A. Brockman, A. Jaidee, S. Nair, D. Sudimack, T. Pongvongsa, S. Phompida, R. Phetsouvanh, T. Anderson, N. J. White, and P. N. Newton.** 2007. *In vitro* antimalarial drug susceptibility and *pfcrt* mutation among fresh *Plasmodium falciparum* isolates from the Lao PDR (Laos). Am J Trop Med Hyg **76:**245-250.

212. **Mcgready, R., K. Stepniewska, N. Lindegardh, E. A. Ashley, Y. La, P. Singhasivanon, N. J. White, and F. Nosten.** 2006. The pharmacokinetics of artemether and lumefantrine in pregnant women with uncomplicated falciparum malaria. Eur J Clin Pharmacol **62:**1021-1031.

213. **McKenzie, F. E., and W. H. Bossert.** 1998. The optimal production of gametocytes by *Plasmodium falciparum*. J Theor Biol **193:**419-428.

214. **McKenzie, F. E., G. F. Killeen, J. C. Beier, and W. H. Bossert.** 2001. Seasonality, parasite diversity, and local extinctions in *Plasmodium falciparum* malaria. Ecology **82:**2673-2681.

215. **McKenzie, F. E., and E. M. Samba.** 2004. The role of mathematical modeling in evidence-based malaria control. Am J Trop Med Hyg **71 (Suppl 2):**94-96.

216. **Meadows, M.** 2002. The FDA's durg review process: ensuring drugs are safe and effective. FDA Consum **36:**19-24.

217. **Mendis, K., B. J. Sina, P. Marchesini, and R. Carter.** 2001. The neglected burden of *Plasmodium vivax* malaria. Am J Trop Med Hyg **64 (Suppl. 1-2):**97-106.

218. **Mideo, N., T. Day, and A. F. Read.** 2008. Modelling malaria pathogenesis. Cell Microbiol **10:**1947-1955.

219. **Miller, Louis H., and X. Su.** 2011. Artemisinin: Discovery from the Chinese herbal garden. Cell **146:**855-858.

220. **Mithwani, S., L. Aarons, G. O. Kokwaro, O. Majid, S. Muchohi, G. Edwards, S. Mohamed, K. Marsh, and W. Watkins.** 2003. Population pharmacokinetics of artemether and dihydroartemisinin following single intramuscular dosing of artemether in African children with severe falciparum malaria. Br J Clin Pharmacol **57:**146-152.

221. **Molineaux, L., H. Diebner, M. Eichner, and W. Collins.** 2001. *Plasmodium falciparum* parasitaemia described by a new mathematical model. Parasitology **122:**379-391.

222. **Molyneux, D. H., K. Floyd, G. Barnish, and E. M. Fèvre.** 1999. Transmission control and drug resistance in malaria: a crucial interaction. Parasitol Today **15:**238-240.

223. **Moore, D. V., and J. E. Lanier.** 1961. Observations on two *Plasmodium falciparum* infections with an abnormal response to chloroquine. Am J Trop Med Hyg **10:**5-9.

224. **Morris, C. A., M. A. Onyamboko, E. Capparelli, M. A. Koch, J. Atibu, V. Lokomba, M. Douoguih, J. Hemingway-Foday, D. Wesche, R. W. Ryder, C. Bose, L. Wright, A. K. Tshefu, S. Meshnick, and L. Fleckenstein.** 2011.

Population pharmacokinetics of artesunate and dihydroartemisinin in pregnant and non-pregnant women with malaria. Malar J **10:**114.

225. **Mu, J., R. A. Myers, H. Jiang, S. Liu, S. Ricklefs, M. Waisberg, K. Chotivanich, P. Wilairatana, S. Krudsood, N. J. White, R. Udomsangpetch, L. Cui, M. Ho, F. Ou, H. Li, J. Song, G. Li, X. Wang, S. Seila, S. Sokunthea, D. Socheat, D. E. Sturdevant, S. F. Porcella, R. M. Fairhurst, T. E. Wellems, P. Awadalla, and X.-z. Su.** 2010. *Plasmodium falciparum* genome-wide scans for positive selection, recombination hot spots and resistance to antimalarial drugs. Nat Genet **42:**268-271.

226. **Mueller, I., S. Schoepflin, T. A. Smith, K. L. Benton, M. T. Bretscher, E. Lin, B. Kiniboro, P. A. Zimmerman, T. P. Speed, P. Siba, and I. Felger.** 2012. Force of infection is key to understanding the epidemiology of *Plasmodium falciparum* malaria in Papua New Guinean children. Proc Natl Acad Sci **109:**10030-10035.

227. **Musset, L., O. Bouchaud, S. Matheron, L. Massias, and J. Le Bras.** 2006. Clinical atovaquone-proguanil resistance of *Plasmodium falciparum* associated with cytochrome *b* codon 268 mutations. Microbes Infect **8:**2599-2604.

228. **Mutabingwa, T., A. Nzila, E. Mberu, E. Nduati, P. Winstanley, E. Hills, and W. Watkins.** 2001. Chlorproguanil-dapsone for treatment of drug-resistant falciparum malaria in Tanzania. Lancet **358:**1218-1223.

229. **Mwai, L., E. Ochong, A. Abdirahman, S. M. Kiara, S. Ward, G. Kokwaro, P. Sasi, K. Marsh, S. Borrmann, M. Mackinnon, and A. Nzila.** 2009. Chloroquine resistance before and after its withdrawal in Kenya. Malar J **8:**106.

230. **Mwingira, F., G. Nkwengulila, S. Schoepflin, D. Sumari, H.-P. Beck, G. Snounou, I. Felger, P. Olliaro, and K. Mugittu.** 2011. Plasmodium falciparum msp1, msp2 and glurp allele frequency and diversity in sub-Saharan Africa. Malaria Journal **10:**79.

231. **Mzilahowa, T., P. J. McCall, and I. M. Hastings.** 2007. "Sexual" population structure and genetics of the malaria agent P. falciparum. PLoS ONE **2:**e613.

232. **N'Guessan, R., V. Corbel, M. Akogbéto, and M. Rowland.** 2007. Reduced efficacy of insecticide-treated nets and indoor residual spraying for malaria control in pyrethroid resistance area, Benin. Emerging Infect Dis **13:**199-206.

233. **Nambozi, M., J.-P. Van Geertruyden, S. Hachizovu, M. Chaponda, D. Mukwamataba, M. Mulenga, D. Ubben, and U. D'Alessandro.** 2011. Safety and efficacy of dihydroartemisinin-piperaquine versus artemether-lumefantrine in the treatment of uncomplicated Plasmodium falciparum malaria in Zambian children. Malar J **10:**50.

234. **Nåsell, I.** 1986. On superinfection in malaria. IMA J Math Appl Med Biol **3:**211-227.

235. **National Research Council (U.S.). Committee on Applications of Ecological Theory to Environmental Problems.** 1986. Ecological knowledge and environmental problem-solving: concepts and case studies. National Academies Press.

236. **Newton, P., Y. Suputtamongkol, P. Teja-Isavadharm, S. Pukrittayakamee, V. Navaratnam, I. Bates, and N. White.** 2000. Antimalarial bioavailability and disposition of artesunate in acute falciparum malaria. Antimicrob Agents **44:**972-977.

237. **Nguyen, D. V. H., Q. P. Nguyen, N. D. Nguyen, T. T. T. Le, T. D. Nguyen, D. N. Dinh, T. X. Nguyen, D. Bui, M. Chavchich, and M. D. Edstein.** 2009. Pharmacokinetics and *ex vivo* pharmacodynamic antimalarial activity of dihydroartemisinin-piperaquine in patients with uncomplicated falciparum malaria in Vietnam. Antimicrob Agents **53:**3534-3537.

238. **Nguyen, M. H., T. M. E. Davis, J. Cox-Singh, S. Hewitt, Q. T. Tran, B. K. Tran, T. H. Nguyen, N. P. Vo, H. N. Doan, and D. C. Le.** 2003. Treatment of uncomplicated falciparum malaria in southern Vietnam: can chloroquine or sulfadoxine-pyrimethamine be reintroduced in combination with artesunate? Clin Infect Dis **37:**1461-1466.

239. **Ngwa, G. A.** 2004. Modelling the dynamics of endemic malaria in growing populations. Discrete Continuous Dyn Syst Ser B **4:**1173-1202.

240. **Ngwa, M., and W. S. Shu.** 2000. A mathematical model for endemic malaria with variable human and mosquito populations. Math Comput Model **32:**747-763.

241. **Noedl, H., Y. Se, K. Schaecher, B. L. Smith, D. Socheat, M. M. Fukuda, and A. R. i. C. A. S. Consortium.** 2008. Evidence of artemisinin-resistant malaria in western Cambodia. N Engl J Med **359:**2619-2620.

242. **Noedl, H., Y. Se, S. Sriwichai, K. Schaecher, P. Teja-Isavadharm, B. Smith, W. Rutvisuttinunt, D. Bethell, S. Surasri, Mark M. Fukuda, D. Socheat, and L. Chan Thap.** 2010. Artemisinin resistance in Cambodia: A clinical trial designed to address an emerging problem in southeast Asia. Clin Infect Dis **51:**e82-e89.

243. **Nosten, F., M. Vanvugt, R. Price, C. Luxemburger, K. Thway, A. Brockman, R. McGready, F. Terkuile, S. Looareesuwan, and N. White.** 2000. Effects of artesunate-mefloquine combination on incidence of malaria and mefloquine resistance in western Thailand: a prospective study. The Lancet **356:**297-302.

244. **Nsanzabana, C.** 2008. Dynamics of Malaria Parasite Resistance Markers in Two Areas of Different Transmission Intensity. University of Neuchatal, Switzerland.

245. **Nsanzabana, C.** 2008. Dynamics of malaria parasite resistance markers in two areas of different transmission intensity. University of Neuchatal, Switzerland.

246. **Nwanyanwu, O. C., N. Kumwenda, P. N. Kazembe, S. Jemu, C. Ziba, W. C. Nkhoma, and S. C. Redd.** 1997. Malaria and human immunodeficiency virus infection among male employees of a sugar estate in Malawi. Trans R Soc Trop Med Hyg **91:**567-569.

247. **Nwanyanwu, O. C., C. Ziba, P. Kazembe, L. Chitsulo, J. J. Wirima, N. Kumwenda, and S. C. Redd.** 1996. Efficacy of sulphadoxine/pyrimethamine for *Plasmodium falciparum* malaria in Malawian children under five years of age. Trop Med Int Health **1:**231-235.

248. **Nzila, A., J. Okombo, E. Ohuma, and A. Al-Thukair.** 2012. Update on the in vivo tolerance and in vitro reduced susceptibility to the antimalarial lumefantrine. J Antimicrob Chemother **67:**2309-2315.

249. **Ohrt, C., T. L. Richie, H. Widjaja, G. D. Shanks, J. Fitriadi, D. J. Fryauff, J. Handschin, D. Tang, B. Sandjaja, E. Tjitra, L. Hadiarso, G. Watt, and F. S. Wignall.** 1997. Mefloquine compared with doxycycline for the prophylaxis of malaria in Indonesian soldiers. A randomized, double-blind, placebo-controlled trial. Ann Intern Med **126:**963-972.

250. **Okell, L. C., C. J. Drakeley, T. Bousema, C. J. M. Whitty, and A. C. Ghani.** 2008. Modelling the impact of artemisinin combination therapy and

long-acting treatments on malaria transmission intensity. PLoS Med **5:**1617-1628.

251. **Okell, L. C., C. J. Drakeley, A. C. Ghani, T. Bousema, and C. J. Sutherland.** 2008. Reduction of transmission from malaria patients by artemisinin combination therapies: a pooled analysis of six randomized trials. Malar J **7:**125.

252. **Paget-McNicol, S., M. Gatton, I. Hastings, and A. Saul.** 2002. The Plasmodium falciparum var switching rate, switching mechanism and patterns of parasite recrudescence described by mathematical modelling. Parasitology **124:**225-235.

253. **Painter, H. J., J. M. Morrisey, and A. B. Vaidya.** 2010. Mitochondrial Electron Transport Inhibition and Viability of Intraerythrocytic Plasmodium falciparum. Antimicrob Agents **54:**5281-5287.

254. **Patel, K., K. T. Batty, B. R. Moore, P. L. Gibbons, J. B. Bulitta, and C. M. Kirkpatrick.** 2012. Mechanism-based model of parasite growth and dihydroartemisinin pharmacodynamics in murine malaria. Antimicrob Agents Chemother **(Ahead of print: AAC.01463-12)**.

255. **PATH Malaria Vaccine Initiative (MVI)** 2012, posting date. The malaria vaccine model fact sheet. [Online.]

256. **PATH Malaria Vaccine Initiative (MVI)** 2012, posting date. Mathematical models explore potential impact of future malaria vaccines. [Online.]

257. **Penny, M. A., N. Maire, A. Studer, A. Schapira, and T. A. Smith.** 2008. What Should Vaccine Developers Ask? Simulation of the Effectiveness of Malaria Vaccines. PLoS One **3:**e3193.

258. **Peters, W.** 1987. Resistance in human malaria IV: 4-aminoquinolines and multiple resistance, p. 659-786, vol. 2. Academic Press, London.

259. **Peyerl-Hoffmann, G., A. K. T Jelinek, G. Kabagambe, W. G. Metzger, and F. v. Sonnenburg.** 2001. Genetic diversity of *Plasmodium falciparum* and its relationship to parasite density in an area with different malaria endemicities in West Uganda. Tropical medicine & international health **6:**607-613.

260. **Phyo, A. P., S. Nkhoma, K. Stepniewska, E. A. Ashley, S. Nair, R. Mcgready, C. L. Moo, S. Al-Saai, A. M. Dondorp, K. M. Lwin, P. Singhasivanon, N. P. Day, N. J. White, T. J. Anderson, and F. Nosten.**

2012. Emergence of artemisinin-resistant malaria on the western border of Thailand: a longitudinal study. Lancet.

261. **Pongtavornpinyo, W.** 2006. Mathematical modelling of antimalarial drug resistance. University of Liverpool.

262. **Pongtavornpinyo, W., S. Yeung, I. M. Hastings, A. M. Dondorp, N. P. J. Day, and N. J. White.** 2008. Spread of anti-malarial drug resistance: Mathematical model with implications for ACT drug policies. Malar J **7:**1475-2875.

263. **Porter, K. A., C. L. Burch, C. Poole, J. J. Juliano, S. R. Cole, and S. R. Meshnick.** 2010. Uncertain outcomes: adjusting for misclassification in antimalarial efficacy studies. Epidemiology and Infection **139:**544-551.

264. **Pradines, B., C. Rogier, T. Fusai, A. Tall, J. F. Trape, and J. C. Doury.** 1998. In vitro activity of artemether against African isolates (Senegal) of Plasmodium falciparum in comparison with standard antimalarial drugs. Am. J. Trop. Med. Hyg. **58:**354-357.

265. **Price, R. N., F. Nosten, C. Luxemburger, F. O. t. Kuile, L. Paiphun, T. Chongsuphajaisiddhi, and N. J. White.** 1996. Effects of artemisinin derivatives on malaria transmissibility. Lancet **347:**1654-1658.

266. **Price, R. N., E. Tjitra, C. A. Guerra, S. Yeung, N. J. White, and N. M. Anstey.** 2007. Vivax Malaria: Neglected and Not Benign. Am J Trop Med Hyg **77:**79-87.

267. **Price, R. N., A.-C. Uhlemann, A. Brockman, R. McGready, E. Ashley, L. Phaipun, R. Patel, K. Laing, S. Looareesuwan, N. J. White, F. Nosten, and S. Krishna.** 2004. Mefloquine resistance in *Plasmodium falciparum* and increased *pfmdr1* gene copy number. Lancet **364:**438-447.

268. **Pukrittayakamee, S., K. Chotivanich, A. Chantra, R. Clemens, S. Looareesuwan, and N. J. White.** 2004. Activities of artesunate and primaquine against asexual- and sexual-stageparasites in falciparum malaria. Antimicrob Agents Chemother **48:**1329-1334.

269. **Pussard, E., and F. Verdier.** 1994. Antimalarial 4-aminoquinolines: mode of action and pharmacokinetics. Fundam Clin Pharmacol **8:**1-17.

270. **R.** Development Core Team (2009). R: A Language and Environment for Statistical Computing.

271. **Reed, M. B., K. J. Saliba, S. R. Caruana, K. Kirk, and A. F. Cowman.** 2000. Pgh1 modulates sensitivity and resistance to multiple antimalarials in *Plasmodium falciparum*. Nature **403:**906-909.

272. **Richie, T.** 2007. High road, low road? Choices and challenges on the pathway to a malaria vaccine. Parasitology **133:**S113.

273. **Roepe, P. D.** 2009. Molecular and physiologic basis of quinoline drug resistance in Plasmodium falciparum malaria. Future Microbiol **4:**441-455.

274. **Rosenberg, R., R. A. Wirtz, I. Schneider, and R. Burge.** 1990. An estimation of the number of malaria sporozoites ejected by a feeding mosquito. Trans R Soc Trop Med Hyg **84:**209-212.

275. **Ross, A., G. Killeen, and T. Smith.** 2006. Relationship between host infectivity to mosquitoes and asexual parasite density in *Plasmodium falciparum*. Am J Trop Med Hyg **75 (suppl 2):**32-37.

276. **Ross, A., N. Maire, L. Molineaux, and T. Smith.** 2006. An epidemiologic model of severe morbidity and mortality caused by *Plasmodium falciparum*. Am J Trop Med Hyg **75 (Suppl 2):**63-73.

277. **Ross, A., N. Maire, E. Sicuri, T. Smith, and L. Conteh.** 2011. Determinants of the cost-effectiveness of intermittent preventive treatment for malaria in infants and children. PLoS One **6:**e18391.

278. **Ross, A., M. Penny, N. Maire, A. Studer, I. Carneiro, D. Schellenberg, B. Greenwood, M. Tanner, T. Smith, and S. I. Hay.** 2008. Modelling the epidemiological impact of intermittent preventative treatment against malaria in infants. PLoS One **3:**e2661.

279. **Ross, R.** 1905. The logical basis of the sanitary policy of mosquito reduction. Science **22:**689-699.

280. **Ross, R.** 1911. The prevention of Malaria. 2nd edn. John Murray, London.

281. **Ross, R.** 1908. Report on the prevention of malaria in mauritius. Waterlow and Sons Limited, London.

282. **Sa, J. M., O. Twu, K. Hayton, S. Reyes, M. P. Fay, P. Ringwald, and T. E. Wellems.** 2009. Geographic patterns of *Plasmodium falciparum* drug resistance distinguished by differential responses to amodiaquine and chloroquine. Proc Natl Acad Sci **106:**18883-18889.

283. **Sagara, I., A. Diallo, M. Kone, M. Coulibaly, S. I. Diawara, O. Guindo, H. Maiga, M. B. Niambele, M. Sissoko, A. Dicko, A. Djimde, and O. K.**

Doumbo. 2008. A randomized trial of artesunate-mefloquine versus artemether-lumefantrine for treatment of uncomplicated Plasmodium falciparum malaria in Mali. Am J Trop Med Hyg **79:**655-661.

284. **Sama, W., S. Owusu-Agyei, I. Felger, P. Vounatsou, and T. Smith.** 2005. An immigration–death model to estimate the duration of malaria infection when detectability of the parasite is imperfect. Statistics in Medicine **24:**3269-3288.

285. **Saralamba, S., W. Pan-Ngum, R. J. Maude, S. J. Lee, J. Tarning, N. Lindegardh, K. Chotivanich, F. Nosten, N. P. J. Day, D. Socheat, N. J. White, A. M. Dondorp, and L. J. White.** 2011. Intrahost modeling of artemisinin resistance in *Plasmodium falciparum*. Proc Natl Acad Sci **108:**397-402.

286. **Saralamba, S., W. Pan-Ngum, R. J. Maude, S. J. Lee, J. Tarning, N. Lindegardh, K. Chotivanich, F. Nosten, N. P. J. Day, D. Socheat, N. J. White, A. M. Dondorp, and L. J. White.** 2010. Intrahost modeling of artemisinin resistance in Plasmodium falciparum. Proc Natl Acad Sci **108:**397-402.

287. **Saralamba, S., W. Pan-Ngum, R. J. Maude, S. J. Lee, J. Tarning, N. Lindegårdh, K. Chotivanich, F. Nosten, N. P. J. Day, D. Socheat, N. J. White, A. M. Dondorp, and L. J. White.** 2011. Intrahost modeling of artemisinin resistance in Plasmodium falciparum. Proc. Natl. Acad. Sci. U. S. A. **108:**397-402.

288. **Saul, A.** 2002. Zooprophylaxis or zoopotentiation: the outcome of introducing animals on vector transmission is highly dependent on the mosquito mortality while searching. Malar J **2**.

289. **Saul, A., P. Graves, and B. Kay.** 1990. A Cyclical Feeding Model for Pathogen Transmission and Its Application to Determine Vectorial Capacity from Vector Infection Rates. J Appl Ecol **27:**123-133.

290. **Schellenberg, D., C. Menendez, E. Kahigwa, J. Aponte, J. Vidal, M. Tanner, H. Mshinda, and P. Alonso.** 2001. Intermittent treatment for malaria and anaemia control at time of routine vaccinations in Tanzanian infants: a randomised, placebo-controlled trial. Lancet **357:**1471-1477.

291. **Scherf, A., J. J. Lopez-Rubio, and L. Riviere.** 2008. Antigenic variation in *Plasmodium falciparum*. Annu Rev Microbiol **62:**445-470.

292. **Schneider, P., B. H. K. Chan, S. E. Reece, and A. F. Read.** 2008. Does the drug sensitivity of malaria parasites depend on their virulence? Malar J **7**.

293. **Schoepflin, S., E. Lin, B. Kiniboro, J. T. DaRe, R. K. Mehlotra, P. A. Zimmerman, I. Mueller, and I. Felger.** 2010. Treatment with Coartem (Artemether-Lumefantrine) in Papua New Guinea. Am J Trop Med Hyg **82:**529-534.

294. **Schoepflin, S., F. Valsangiacomo, E. Lin, B. Kiniboro, I. Mueller, and I. Felger.** 2009. Comparison of Plasmodium falciparum allelic frequency distribution in different endemic settings by high-resolution genotyping. Malaria Journal **8:**250.

295. **Schwarte, S., P. Ringwald, K. Mendis, and A. Bosman.** 2010. Regulatory action needed to stop the sale of oral artemisinin-based monotherapy. WHO Drug Information **24:**1-7.

296. **Shah, P. B.** 2011. Intention-to-treat and per-protocol analysis. CMAJ **183:**696.

297. **Shanks, G. D.** 1994. The rise and fall of mefloquine as an antimalarial drug in South East Asia. Mil Med **159:**275-281.

298. **Shekalaghe, S., C. Drakeley, R. Gosling, A. Ndaro, M. van Meegeren, A. Enevold, M. Alifrangis, F. Mosha, R. Sauerwein, and T. Bousema.** 2007. Primaquine clears submicroscopic *Plasmodium falciparum* gametocytes that persist after treatment with sulphadoxine-pyrimethamine and artesunate. PLoS One **2:**e1023.

299. **Shen, L., S. Peterson, A. R. Sedaghat, M. A. McMahon, M. Callender, H. Zhang, Y. Zhou, E. Pitt, K. S. Anderson, E. P. Acosta, and R. F. Siliciano.** 2008. Dose-response curve slope sets class-specific limits on inhibitory potential of anti-HIV drugs. Nat Med **14:**762-766.

300. **Silachamroon, U., W. Phumratanaprapin, S. Krudsood, S. Treeprasertsuk, V. Budsaratid, K. Pornpininworakij, P. Wilairatan, and S. Looareesuwan.** 2001. Frequency of early rising parasitemia in falciparum malaria treated with artemisinin derivatives. Southeast Asian J Trop Med Public Health **32:**50-56.

301. **Simpson, J., T. Agbenyega, K. Barnes, G. Perri, P. Folb, M. Gomes, S. Krishna, S. Krudsood, S. Looareesuwan, S. Mansor, H. McIlleron, R. Miller, M. Molyneux, J. Mwenechanya, V. Navaratnam, F. Nosten, P.**

Olliaro, L. Pang, I. Ribeiro, M. Tembo, M. V. Vugt, S. Ward, K. Weerasuriya, K. Win, and N. White. 2006. Population Pharmacokinetics of artesunate and dihydroartemisinin following intra-rectal dosing of artesunate in malaria patients. Plos Med **3:**2113-2123.

302. **Simpson, J., E. Watkins, R. Price, L. Aarons, D. Kyle, and N. White.** 2000. Mefloquine pharmacokinetic-pharmacodynamic models: implications for dosing and resistance. Antimicrob Agents **44:**3414-3424.
303. **Simpson, J. A., K. M. Jamsen, R. N. Price, N. J. White, N. Lindegardh, J. Tarning, and S. B. Duffull.** 2009. Towards optimal design of anti-malarial pharmacokinetic studies. Malar J **8:**189.
304. **Singh, R., and K. Mukhopadhyay.** 2011. Survival analysis in clinical trials: Basics and must know areas. Perspect Clin Res **2:**145-148.
305. **Sisowath, C., P. E. Ferreira, L. Y. Bustamante, S. Dahlström, A. Mårtensson, A. Björkman, S. Krishna, and J. P. Gil.** 2007. The role of *pfmdr1* in *Plasmodium falciparum* tolerance to artemether-lumefantrine in Africa. Tropical Medicine & International Health **12:**736-742.
306. **Sisowath, C., I. Petersen, M. I. Veiga, A. Mårtensson, Z. Premji, A. Björkman, D. A. Fidock, and J. P. Gil.** 2009. *In vivo* selection of *Plasmodium falciparum* parasites carrying the chloroquine-susceptible pfcrt K76 allele after treatment with artemether-lumefantrine in Africa. J Infect Dis **199:**750-757.
307. **Sisowath, C., J. Strömberg, A. Mårtensson, M. Msellem, C. Obondo, A. Björkman, and J. P. Gil.** 2005. *In vivo* selection of *Plasmodium falciparum pfmdr1* 86N coding alleles by artemether-lumefantrine (Coartem). J Infect Dis **191:**1014-1017.
308. **Slater, M., M. Kiggundu, C. Dokomajilar, M. R. Kamya, N. Bakyaita, A. Talisuna, P. J. Rosenthal, and G. Dorsey.** 2005. Distinguishing recrudescences from new infections in antimalarial clinical trials: major impact of interpretation of genotyping results on estimates of drug efficacy. The American journal of tropical medicine and hygiene **73:**256-262.
309. **Smith, T., G. Killeen, N. Maire, A. Ross, L. Molineaux, F. Tediosi, G. Hutton, J. U. Dietz, and M. Tanner.** 2006. Mathematical modeling of the impact of malaria vaccines on the clinical epidemiology and natural history of

Plasmodium falciparum malaria: Overview. Am. J. Trop. Med. Hyg. **75 (Suppl 2):**1-10.

310. **Smith, T., N. Maire, K. Dietz, G. F. Killeen, P. Vounatsou, L. Molineaux, and M. Tanner.** 2006. Relationship between the entomologic inoculation rate and the force of infection for *Plasmodium falciparum* malaria. Am J Trop Med Hyg **75 (Suppl 2):**11-18.

311. **Smith, T., Maire, N., Ross, A., Penny, M., Chitnis, N., Schapira, A., Studer, A., Genton, B., Lengeler, C., Tediosi, F. and others.** 2008. Towards a comprehensive simulation model of malaria epidemiology and control. Parasitology **135:**1507-1516.

312. **Smith, T., A. Ross, N. Maire, N. Chitnis, A. Studer, D. Hardy, A. Brooks, M. Penny, and M. Tanner.** 2012. Ensemble modeling of the likely public health impact of a pre-erythrocytic malaria vaccine. PLoS Med **9:**e1001157.

313. **Smith, T., A. Ross, N. Maire, C. Rogier, J.-F. Trape, and L. Molineaux.** 2006. An epidemiologic model of the incidence of acute illness in *Plasmodium falciparum* malaria. Am J Trop Med Hyg **75 (Suppl 2):**56-62.

314. **Smith, T. A., N. Chitnis, O. J. T. Briët, and M. Tanner.** 2011. Uses of mosquito-stage transmission-blocking vaccines against *Plasmodium falciparum*. Trends Parasitol **27:**190-196.

315. **Snounou, G., and H. P. Beck.** 1998. The use of PCR genotyping in the assessment of recrudescence or reinfection after antimalarial drug treatment. Parasitol Today (Redul Ed) **14:**462-467.

316. **Sowunmi, A., E. O. Adewoye, G. O. Gbotsho, C. T. Happi, A. Sijuade, O. A. Folarin, T. M. Okuboyejo, and O. S. Michael.** 2010. Factors contributing to delay in parasite clearance in uncomplicated falciparum malaria in children. Malar J **9:**1-11.

317. **Sowunmi, A., T. Balogun, G. O. Gbotosho, C. T. Happi, A. A. Adedeji, and F. A. Fehintola.** 2007. Activities of amodiaquine, artesunate, and artesunate-amodiaquine against asexual- and sexual-stage parasites in falciparum malaria in children. Antimicrob Agents Chemother **51:**1694-1699.

318. **Staehli Hodel, E., K. Kay, D. Hayes, A. Terlouw, and I. Hastings.** 2012. An *in silico* drug treatment model to assess the robustness of regional age-based dosing regimens for artemisinin-based combination therapies. Malar J **11:**P91.

319. **Stepniewska, K., R. N. Price, C. J. Sutherland, C. J. Drakeley, L. von Seidlein, F. Nosten, and N. J. White.** 2008. *Plasmodium falciparum* gametocyte dynamics in areas of different malaria endemicity. Malar J **7:**249.

320. **Stepniewska, K., W. Taylor, S. B. Sirima, E. B. Ouedraogo, A. Ouedraogo, A. Gansané, J. A. Simpson, C. C. Morgan, N. J. White, and J.-R. Kiechel.** 2009. Population pharmacokinetics of artesunate and amodiaquine in African children. Malar J **8:**200.

321. **Stepniewska, K., and N. J. White.** 2008. Pharmacokinetic determinants of the window of selection for antimalarial drug resistance. Antimicrob Agents **52:**1589-1596.

322. **Stepniewska, K., and N. J. White.** 2006. Some considerations in the design and interpretation of antimalarial drug trials in uncomplicated falciparum malaria. Malar J **5:**1475-2875.

323. **Stoute, J. A., M. Slaoui, D. G. Heppner, P. Momin, K. E. Kester, P. Desmons, B. T. Wellde, N. Garçon, U. Krzych, and M. Marchand.** 1997. A preliminary evaluation of a recombinant circumsporozoite protein vaccine against *Plasmodium falciparum* malaria. RTS,S Malaria Vaccine Evaluation Group. N Engl J Med **336:**86-91.

324. **Sullivan, D. J., H. Matile, R. G. Ridley, and D. E. Goldberg.** 1998. A common mechanism for blockade of heme polymerization by antimalarial quinolines. J Biol Chem **273:**31103-31107.

325. **Talisuna, A. O., P. Langi, N. Bakyaita, T. Egwang, T. K. Mutabingwa, W. Watkins, E. V. Marck, and U. D'Alessandro.** 2002. Intensity of malaria transmission, antimalarial-drug use and resistance in Uganda: what is the relationship between these three factors? Trans R Soc Trop Med Hyg **96:**310-317.

326. **Tan, B., H. Naik, I.-J. Jang, K.-S. Yu, L. E. Kirsch, C.-S. Shin, J. Craft, and L. Fleckenstein.** 2009. Population pharmacokinetics of artesunate and dihydroartemisinin following single- and multiple-dosing of oral artesunate in healthy subjects. Malar J **8**.

327. **Targett, G., C. Drakeley, M. Jawara, L. v. Seidlein, R. Coleman, J. Deen, M. Pinder, T. Doherty, C. Sutherland, G. Walraven, and P. Milligan.** 2001. Artesunate reduces but does not prevent posttreatment transmission of *Plasmodium falciparum* to *Anopheles gambiae*. J Infect Dis **183:**1254-1259.

328. **Tarning, J.** 2007. Piperaquine: Bioanalysis, drug metabolism and pharmacokinetics. Sahlgrenska Academy at Goteborg University, Goteborg.

329. **Tarning, J., N. Lindegardh, S. Sandberg, N. J. P. Day, N. J. White, and M. Ashton.** 2008. Pharmacokinetics and metabolism of the antimalarial piperaquine after intravenous and oral single doses to the rat. J Pharm Sci **97:**3400-3410.

330. **Taylor, W., D. J. Terlouw, P. Olliaro, N. J. White, P. Brasseur, and F. O. ter Kuile.** 2006. Use of weight-for-age-data to optimize tablet strength and dosing regimens for a new fixed-dose artesunate-amodiaquine combination for treating falciparum malaria. Bulletin of the World Health Organization **84:**956-964.

331. **Tediosi, F., N. Maire, M. Penny, A. Studer, and T. A. Smith.** 2009. Simulation of the cost-effectiveness of malaria vaccines. Malar J **8:**127.

332. **ter Kuile, F., N. J. White, P. Holloway, G. Pasvol, and S. Krishna.** 1993. *Plasmodium falciparum*: *in vitro* studies of the pharmacodynamic properties of drugs used for the treatment of severe malaria. Exp Parasitol **76:**85-95.

333. **Teuscher, F., Michelle L. Gatton, N. Chen, J. Peters, Dennis E. Kyle, and Q. Cheng.** 2010. Artemisinin-Induced Dormancy in *Plasmodium falciparum*: Duration, Recovery Rates, and Implications in Treatment Failure. J Infect Dis **202:**1362-1368.

334. **Thanh, N. V., A. F. Cowman, D. Hipgrave, T. B. Kim, B. Q. Phuc, L. D. Cong, and B. A. Biggs.** 2001. Assessment of susceptibility of *Plasmodium falciparum* to chloroquine, quinine, mefloquine, sulfadoxine-pyrimethamine and artemisinin in southern Viet Nam. Trans R Soc Trop Med Hyg **95:**513-517.

335. **The malERA Consultative Group on Drugs.** 2011. A Research Agenda for Malaria Eradication: Drugs PLoS Med **8:**15-23.

336. **The malERA Consultative Group on Modeling.** 2011. A research Agenda for Malaria Eradication: Modeling. PLoS Med **8:**70-78.

337. **The Roll Back Malaria Partnership.** 2008. The Global Malaria Action Plan.1-274.

338. **The RTSS Clinical Trials Partnership.** 2011. First results of phase 3 trial of RTS,S/AS01 malaria vaccine in African children. N Engl J Med **365:**1863-1875.

339. **TJC, A., S. XZ, and B. M. e. al.** 1999. Twelve microsatellite markers for characterization of *Plasmodium falciparum* from finger-prick blood samples. Parasitology **119:**113-125.

340. **Uhlemann, A. C., Y. Yuthavong, and D. A. Fidock.** 2005. Mechanisms of antimalarial drug action and resistance. Washington: ASM Press.

341. **Ursing, J., P. E. Kofoed, A. Rodrigues, Y. Bergqvist, and L. Rombo.** 2008. Chloroquine Is Grossly Overdosed and Overused but Well Tolerated in Guinea-Bissau. Antimicrob Agents **53:**180-185.

342. **Valderramos, S. G., J.-C. Valderramos, L. Musset, L. A. Purcell, O. Mercereau-Puijalon, E. Legrand, and D. A. Fidock.** 2010. Identification of a mutant *PfCRT*-mediated chloroquine tolerance phenotype in *Plasmodium falciparum*. PLoS Pathogens **6:**e1000887.

343. **Valecha, N., P. Srivastava, S. S. Mohanty, P. Mittra, S. K. Sharma, P. K. Tyagi, K. Pradhan, V. Dev, R. Singh, A. P. Dash, and Y. D. Sharma.** 2009. Therapeutic efficacy of artemether-lumefantrine in uncomplicated falciparum malaria in India. Malar J **8:**1475-2875.

344. **van Buuren, S., D. J. Hayes, D. M. Stasinopoulos, R. A. Rigby, F. O. ter Kuile, and D. J. Terlouw.** 2009. Estimating regional centile curves from mixed data sources and countries. Stat Med **28:**2891-2911.

345. **vanAgtmael, M. A., S. Cheng-Qi, J. X. Qing, R. Mull, and C. J. v. Boxtel.** 1999. Multiple dose pharmacokinetics of artemether in Chinese patients with uncomplicated falciparum malaria. Int J Antimicrob Agents **12:**151-158.

346. **Veiga, M. I., P. E. Ferreira, L. Jörnhagen, M. Malmberg, A. Kone, B. A. Schmidt, M. Petzold, A. Björkman, F. Nosten, and J. P. Gil.** 2011. Novel polymorphisms in *Plasmodium falciparum* ABC transporter genes are associated with major ACT antimalarial drug resistance. PLoS One **6:**e20212.

347. **Vekemans, J., A. Leach, and J. Cohen.** 2009. Development of the RTS,S/AS malaria candidate vaccine. Vaccine **27:**G67-G71.

348. **Walton, G. A.** 1947. On the control of malaria in Freetown, Sierra Leone. I. *Plasmodium falciparum* and *Anopheles gambiae* in relation to malaria occurring in infants. Ann Trop Med Parasitol **41:**380-407.

349. **Wang, X., J. Mu, G. Li, P. Chen, X. Guo, L. Fu, L. Chen, X. Su, and T. E. Wellems.** 2005. Decreased prevalence of the *Plasmodium falciparum* chloroquine resistance transporter 76T marker associated with cessation of

chloroquine use against *P. falciparum* malaria in Hainan, People's Republic of China. Am J Trop Med Hyg **72:**410-414.

350. **Ward, S., E. Sevene, I. Hastings, and F. Nosten.** 2007. Antimalarial drugs and pregnancy: safety, pharmacokinetics, and pharmacovigilance. Lancet Infect Dis **7:**136-144.

351. **Wargo, A. R., S. Huijben, J. C. de Roode, J. Shepherd, and A. F. Read.** 2007. Competitive release and facilitation of drug-resistant parasites after therapeutic chemotherapy in a rodent malaria model. Proceedings of the National Academy of Sciences **104:**19914-19919.

352. **Watkins, W. M., and M. Mosobo.** 1993. Treatment of *Plasmodium falciparum* malaria with pyrimethamine-sulfadoxine: selective pressure for resistance is a function of long elimination half-life. Trans R Soc Trop Med Hyg **87:**75-78.

353. **Wellems, T. E., and C. V. Plowe.** 2001. Chloroquine-resistant malaria. J Infect Dis **184:**770-776.

354. **White, N.** 1999. Antimalarial drug resistance and combination chemotherapy. Philos Trans R Soc Lond B Biol Sci **354:**739-749.

355. **White, N.** 1997. Assessment of the pharmacodynamic properties of antimalarial drugs *in vivo*. Antimicrob Agents **41:**1413-1422.

356. **White, N., P. Chanthavanich, S. Krishna, C. Bunch, and K. Silamut.** 1983. Quinine disposition kinetics. Br J clin Pharmac **16:**399-403.

357. **White, N., S. Looareesuwan, D. A. Warrell, M. J. Warrell, D. Bunnag, and T. Harinasuta.** 1982. Quinine pharmacokinetics and toxicity in cerebral and uncomplicated falciparum malaria. Am J Cardiol **73:**564-572.

358. **White, N., M. V. Vugt, and F. Ezzet.** 1999 Clinical pharmacokinetics and pharmacodynamics of artemether-lumefantrine. Clin Pharmacokinet **37:**105-125.

359. **White, N. J.** 1992. Antimalarial pharmacokinetics and treatment regimens. Br J clin Pharmac **34:**1-10.

360. **White, N. J.** 1997. Assessment of the pharmacodynamic properties of antimalarial drugs in vivo. Antimicrob Agents **41:**1413-1422.

361. **White, N. J.** 1994. Clinical pharmacokinetics and pharmacodynamics of artemisinin and derivatives. Trans R Soc Trop Med Hyg **88:**S41-43.

362. **White, N. J., K. Stepniewska, K. Barnes, R. N. Price, and J. Simpson.** 2008. Simplified antimalarial therapeutic monitoring: using the day-7 drug level? Trends in Parasitology **24:**159-163.

363. **Winter, K., and I. M. Hastings.** 2011. Development, evaluation and application of an *in silico* model for antimalarial drug treatment and failure. Antimicrob. Agents Chemother. **55:**3380-3392.

364. **Winter, K., and I. M. Hastings.** 2011. Development, evaluation and application of an *in silico* model for antimalarial drug treatment failure. Antimicrob Agents **55:**3380-3392.

365. **Wongsrichanalai, C., and S. R. Meshnick.** 2008. Declining artesunate-mefloquine efficacy against falciparum malaria on the Cambodia-Thailand border. Emerging Infect Dis **14:**716-719.

366. **Wongsrichanalai, C., A. L. Pickard, W. H. Wernsdorfer, and S. R. Meshnick.** 2002. Epidemiology of drug-resistant malaria. Lancet Infect Dis **2:**209-218.

367. **Wongsrichanalai, C., J. Sirichaisinthop, J. J. Karwacki, K. Congpuong, R. S. Miller, L. Pang, and K. Thimasarn.** 2001. Drug resistant malaria on the Thai-Myanmar and Thai-Cambodian borders. Southeast Asian J Trop Med Public Health **32:**41-49.

368. **World Health Organisation.** 2003. Assessment and monitoring of antimalarial drug efficacy for the treatment of uncomplicated falciparum malaria. n WHO/TDR/RBM SO WHO, Geneva, Switzerland**:**1-68.

369. **World Health Organisation.** 1967. Chemotherapy of Malaria. Report of WHO scientific group.1-92.

370. **World Health Organisation.** 2012. Eradicating polio in the African region: Annual report.1-49.

371. **World Health Organisation.** 1957. Expert committee on Malaria, Sixth Report.

372. **World Health Organisation.** 2008. The global burden of disease (2004 update).1-160.

373. **World Health Organisation.** 2008. Global malaria action plan - Part 1: Malaria today.1-39.

374. **World Health Organisation.** 2009. Global Malaria Control and Elimination: report of a meeting on containment of artemisinin tolerance.1-38.

375. **World Health Organisation.** 1993. Global malaria control. WHO malaria unit. Bull World Health Organ **71:**281-284.
376. **World Health Organisation.** 2012. Global measles and rubella: Strategic plan 2012-2020.1-44.
377. **World Health Organisation.** 2011. Global plan for artemisinin resistance containment.1-88.
378. **World Health Organisation.** 2010. Global report on antimalarial drug efficacy and drug resistance: 2000-2010.1-124.
379. **World Health Organisation.** 2006. Guidelines for the treatment of malaria.
380. **World Health Organisation.** 2010. Guidelines for the treatment of malaria (second edition).
381. **World Health Organisation.** 2006. Indoor residual spraying. Use of indoor residual spraying for scaling up global malaria control and elimination.**:**1-16.
382. **World Health Organisation.** 2011. Intermittent preventive treatment for infants using sulfadoxine- pyrimethamine (SP-IPTi) for malaria control in Africa: Implementation Field Guide.1-68.
383. **World Health Organisation.** 2006. Malaria vector control and personal protection: report of a WHO study group.**:**1-72.
384. **World Health Organisation.** 2010. Mathematical modelling to support malaria control and elimination. Roll Back Malaria: Progress & Impact Series **5:**1-48.
385. **World Health Organisation.** 2011. Methods and techniques for assessing exposure to antimalarial drugs in clinical field studies.1-165.
386. **World Health Organisation.** 2007. Methods and techniques for clinical trials on antimalarial drug efficacy: genotyping to identify parasite populations.
387. **World Health Organisation.** 2009. Methods for surveillance of antimalarial drug efficacy.1-90.
388. **World Health Organisation.** 1965. Resistance of malaria parasites to drugs. . W.H.O. Tech. Rep. Ser. **296:**1-65.
389. **World Health Organisation.** 2004. A strategic framework for malaria prevention and control during pregnancy in the African region.1-39.
390. **World Health Organisation.** 2007. Technical expert group meeting on intermittent preventive treatment in pregnancy (IPTp).1-15.

391. **World Health Organisation.** 2006. WHO briefing on Malaria Treatment Guidelines and artemisinin monotherapies.1-28.
392. **World Health Organisation.** 2012. WHO Evidence review group: The safety and effectiveness of single dose primaquine as a *P. falciparum* gametocytocide.1-19.
393. **World Health Organisation.** 2007. WHO informal consultation with manufacturers of artemisinin-based pharmaceutical products in use for the treatment of malaria.1-33.
394. **World Health Organisation.** 2010. WHO Policy recommendation on Intermittent Preventive Treatment during infancy with sulphadoxine-pyrimethamine (SP-IPTi) for *Plasmodium falciparum* malaria control in Africa.1-3.
395. **World Health Organisation.** 2011. World Malaria Report.1-278.
396. **Yang, H., D. Liu, K. Huang, Y. Yang, P. Yang, M. Liao, and C. Zhang.** 1999. Assay of sensitivity of *Plasmodium falciparum* to chloroquine, amodiaquine, piperaquine, mefloquine and quinine in Yunnan province. Zhongguo Ji Sheng Chong Xue Yu Ji Sheng Chong Bing Za Zhi (Chinese journal of parasitology & parasitic diseases) **17:**43-45.
397. **Yu, V. L., T. C. Merigan, and S. L. Barriere.** 2002. Antimicrobial Therapy and Vaccines, Volume II Antimicrobial Agents. New York: Apple Tree Productions.
398. **Zaloumis, S., A. Humberstone, S. Charman, R. Price, J. Moehrle, J. Gamo-Benito, J. McCaw, K. Jamsen, K. Smith, and J. Simpson.** 2012. Assessing the utility of an anti-malarial pharmacokinetic-pharmacodynamic model for aiding drug clinical development. Malaria J **11:**303.
399. **Zaloumis, S., A. Humberstone, S. A. Charman, R. N. Price, J. Moehrle, J. Gamo-Benito, J. McCaw, K. M. Jamsen, K. Smith, and J. A. Simpson.** 2012. Assessing the utility of an anti-malarial pharmacokinetic-pharmacodynamic model for aiding drug clinical development. Malaria Journal **11:**303.